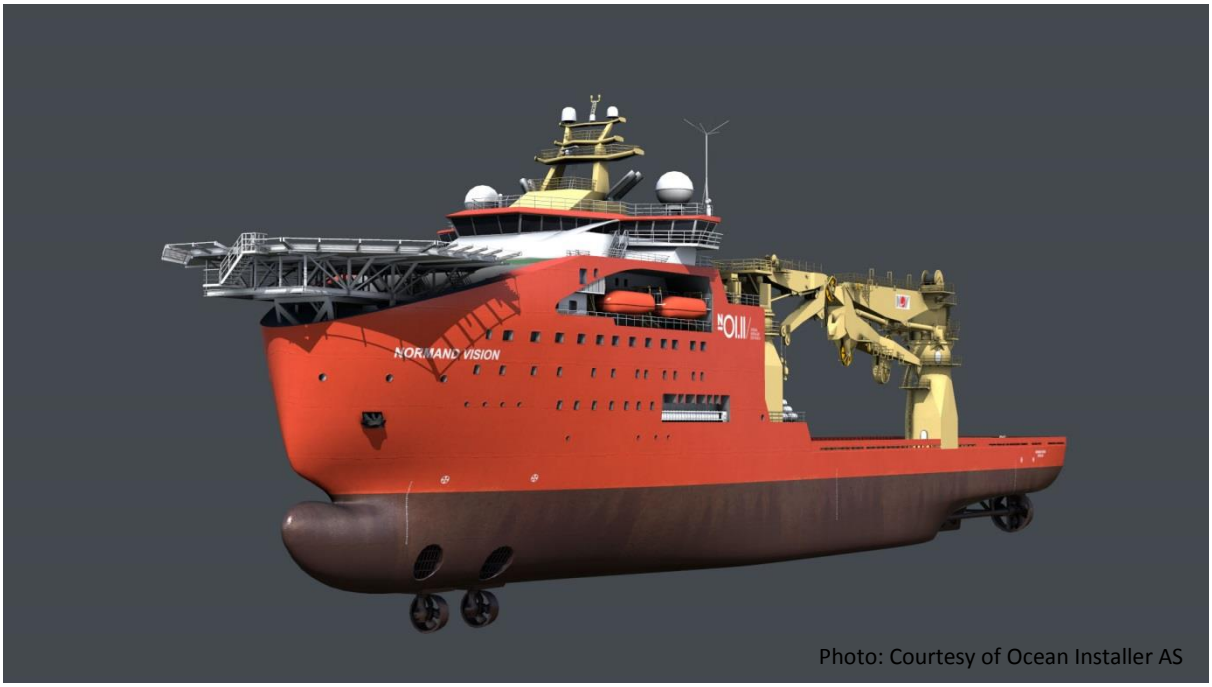

Photo: Courtesy of Ocean Installer AS

Study of Vessel Performance in Extreme Loading Conditions for a new built Offshore Construction Vessel during Installation of Flexible Flowline

Master's thesis at

University of Stavanger

Spring 2014

by

Kristian Lindaas Sørensen

…This Page Intentionally Left Blank…

University of Stavanger

Faculty of Science and Technology

MASTER'S THESIS

Study program / Specialization: Offshore Technology / Marine and Subsea Technology	Spring semester, 2014 ~~Open~~ / Restricted access
Writer: Kristian Lindaas Sørensen	…… (Writer's signature)

Faculty supervisor: Professor Ove Tobias Gudmestad

External supervisor: Joel Ireland, Technical Manager, Ocean Installer AS

Thesis title: Study of Vessel Performance in Extreme Loading Conditions for a new built Offshore Construction Vessel during Installation of Flexible Flowline

Credits (ECTS): 30

Key words: Offshore Construction Vessel, OrcaFlex, dynamic analysis, vessel motions, RAO, parametric roll resonance, flexible flowline, helideck, North Sea conditions,	Pages: 146 + Enclosure: 73 Stavanger, June 16th 2014

…This Page Intentionally Left Blank…

Abstract/Summary

A new built vessel need to carry out extensive sea trials before being put in what could be considered as "normal operation". This is done to make sure the capabilities of the vessel are known to the vessel's crew, captain, client and other interested parties before any real operations takes place.

Prior to the sea trials one may have some knowledge about how the vessel will behave. This is generally based on experience of ship designers, captain, as well as experience from somewhat similar vessels (e.g. sister ships), if available. Model tests are also important, and used to confirm various parameters. In addition preliminary hydrodynamic analyses can be of great advantage.

This is the starting point for my master thesis in "Marine and Subsea Technology" at the University of Stavanger. The focus has been to carry out a study investigating vessel performance/capabilities and motion characteristics for mainly two extreme loading conditions for Solstad Offshore ASA's new built, Offshore Subsea Construction Vessel (OSCV) To Be Named (TBN) "Normand Vision". This ship is to be long term chartered by Ocean Installer AS.
The study is based on an installation operation of a flexible flowline in the North Sea at 350 meters water depth. The motivation is to learn the vessel's performance/capacities when working under different loading conditions and sea states based on available knowledge and data.

To investigate this, a dynamic analysis was carried out with use of the popular hydrodynamic analysis software "OrcaFlex", with help of Microsoft Excel for making of scripts and processing of results.
A number of environmental parameters and data regarding the vessel and the flowline were used in order to get a somewhat precise analysis. Wave heights, directions and periods were determined and a suitable wave model was chosen.

Relevant limits and criteria for various operational aspects were defined according to product data, standards/regulations, certification requirements and other relevant literature. The maximum/minimum values for the different parameters were of interest as these covers the whole range of outcomes one could expect.

The results from the analysis showed to be quite OK for the smallest waves and head seas. The analysis also revealed that the larger waves and more unfavourable wave headings gave more divergent results and challenges for certain parameters.
The results for the various parameters and sea states are outlined and discussed. The different parameters are presented with the limits that apply for the actual parameter.

In addition some spot checking with some more recently defined loading conditions was carried out. Also some highlights especially with respect to roll motions, and landing of helicopters on monohull vessels were looked into.

…This Page Intentionally Left Blank…

Preface

The last two years of my studies are now about to end with the delivery of this thesis. These years can be summarized as, exciting, challenging, confusing and enlightening, though not all at once, fortunately. During these years have gained more "ballast" working as an engineer and I feel that I have learned stuff I could not have been without.
There have been some struggles during the work towards this degree.
This thesis was no exception. As always when working with this type of project, I have once more learned what I did not know. Now I look forward to start working in the industry and learn even more within the field of engineering and science.
These years at the University of Stavanger has brought a whole lot of new experiences both academically and outside of school, which I bring with me.

Acknowledgement

First of all I would like to express my gratitude to Professor Ove Tobias Gudmestad for his inspiring lectures, vast knowledge and guidance throughout the master programme at the University of Stavanger. Also I would like to thank for his useful comments, input, discussions and guidance during the work with this master thesis.

Furthermore I would like to thank Ocean Installer AS who gave me the opportunity to write a thesis in co-operation with them. They gave me a warm welcome and the opportunity to work with their senior engineers. The learning outcome from the work with the thesis was boosted when having knowledgeable and experienced engineers to discuss with.
From Ocean Installer I would especially like to thank my supervisor, Joel Ireland, as well as Abdilahi Qayre, Jin Ping Zhan, Espen Haugseth Svendsen, Shiva Gowda, Henrik Worren and Jørn Waalen for good discussions and guidance.

- Thank you all!

Stavanger, June 15th 2014

- Kristian Lindaas Sørensen

Table of Contents

List of Figures

List of Tables

Abbreviation list

Abbreviation:	Full name/description:
ABS	American Bureau of Shipping
AHC	Active Heave Compensation
ARC	Active Roll Compensation
CAA	Civil Aviation Authority
CESOS	CEntre for Ships and Ocean Structures
CoB	Centre of Buoyancy
CoG	Center of Gravity (centre of weight)
DAF	Dynamic Amplification Factor
DOF	Degrees Of Freedom
DP	Dynamic Positioning
DPS	Differential Positioning Sensor
DWT	Deadweight Tonnage
EPCI	Engineering, Procurement, Construction and Installation
FEM	Finite Element Method
FPSO	Floating Production, Storage and Offloading
GoM	Gulf of Mexico
HAZOP	HAZard and OPerability study (the most common abbreviation)
HMS	Helideck Monitoring System
IMO	International Maritime Organization
L.L.P.	Length between perpendiculars
LC	Load Case
MBR	Minimum Bending Radius
MDPE	Medium Density Polyethylene
MRU	Motion Reference Unit
N/A	Not Applicable
NGI	Norges Geotekniske Institutt
NMD	Norwegian Maritime Directorate
NOV	National Oilwell Varco
NTNU	Norges Teknisk-Naturvitenskapelige Universitet
OSCV	Offshore Subsea Construction Vessel
PGS	Petroleum Geo-Services
QTF	Quadratic Transfer Function
RAO	Response Amplitude Operator
SNAME	the Society of Naval Architects & Marine Engineers
SPS	Special Purpose Ship
STF	Storm factor
SURF	Subsea Umbilical, Risers and Flowlines
TBN	To Be Named
TDP	Touch Down Point
VERES	VEssel RESponse (software from Marintek)
VIV	Vortex Induced Vibrations
VLS	Vertical Lay System
WoW	Waiting on Weather

List of symbols

Symbol:	Description:
Δ	Displacement mass of vessel
Δ_k	Non-dimensional roughness (= k_r/D)
∇	Displacement volume of vessel
μ	Friction coefficient
μ	Angle between approaching waves and vessel heading
μ_F	Friction coefficient with seabed (lateral or axial)
A	Water plane area of vessel
A_c	Cross-sectional area
A_i	Internal cross-sectional stress areas of the pipe
A_{MP}	Cross-sectional area of moonpool
A_o	External cross-sectional stress areas of the
B	Width (breadth) of vessel
c	Damping coefficient
C_A	Added mass coefficients (ref. Appendix H)
C_{crit}	The critical damping value for a segment
C_{DS}	Drag coefficient for steady flow
D	Outer diameter of pipe/flowline
d	Water depth
$D_{draught}$	Draught of vessel
dL/dt	Rate of increase of length
E	Young's modulus
F_R	Soil resistance, in lateral or axial direction
F_S	Undrained shear strength of the soil
g	Acceleration of gravity (considered constant = 9.81 m/s^2)
GM (GM_0)	(Transverse) metacentre height
GM_a	Average metacentre height
GM_L	Longitudinal metacentre height
H and H_{max}	Maximum wave height
H_D	Design wave height
H_S	Significant wave height
H_W	Wave height for design wave recommended by ABS (ABS, 2008)
k	Wave number
K	Water plane stiffness
K_C	Keulegan-Carpenter number
k_r	Surface roughness
L	Instantaneous length of segment
L_0	Unstretched length of segment
L_V	Length of vessel
L_W	Wave length
M	Segment mass, including contents
m_a	Added mass
m_{added}	Added mass of vessel
m_{vessel}	Total displacement mass of vessel
OP_{LIM}	Operational environmental limiting criteria for a certain parameter

OP_{WF}	Forecasted (monitored) operational criteria for a certain parameter
p	Parameter of susceptibility criterion (ABS, 2008)
P_i	Internal pressure
P_o	External pressure
q	Parameter of susceptibility criterion (ABS, 2008)
s	Undrained shear strength gradient
S(ω)	Wave spectrum
T	Wave period or period of structural oscillation
t	Time
T_e	Effective tension
T_E	Encounter period
T_{heave}	Eigen (natural) period in heave
T_P	Peak period
T_{pitch}	Eigen period (natural) in pitch
T_{POP}	Planned operation time
T_{roll}	Eigen period (natural) in roll
T_w	Wall tension
T_{WA}	Wave period corresponding to L_W (in relation to parametric roll resonance)
T_Z	Mean zero up-crossing period
V	Forward vessel speed
v_c	Current velocity
v_m	Maximum orbital particle velocity or wave particle velocity
V_{pr}	Forward speed most likely for development of parametric roll resonance (ABS, 2008)
V_{sr}	Vessel's maximum service speed (ABS, 2008)
W_{pipe}	Submerged pipe weight when filled with water/MEG mix.
x, x_0	Direction of wave propagation
z	Depth below mean still water line
β	Relative frequency or frequency ratio
γ	Non-dimensional peak shape parameter
ζ	Wave profile
ζ_a	Wave amplitude
λ	Relative damping
λ_a	Target axial damping
λ_e	Expansion factor of segment
ν	Poisson ratio
ϕ	Wave velocity potential
φ	Phase angle
ω	Wave frequency
ω_E	Encounter frequency
ω_{vessel}	Eigen/natural frequency of vessel
α	Alpha factor
ε	Total average axial strain
θ	Defined angle for estimation of added mass
κ	Parameter for moonpool calculations (ref. Appendix H)
ρ	Sea water density (often taken as 1025 kg/m^3)

1 Introduction

1.1 Background for the thesis

The thesis is written in cooperation with Ocean Installer AS which is an international offshore contractor currently based in Aberdeen, Houston and with headquarters in Stavanger, Norway. They deliver various EPCI (Engineering, Procurement, Construction and Installation) services, related to marine and subsea operations for the oil and gas industry. Main segments are (Ocean Installer AS, 2014):

- SURF (Subsea Umbilicals, Risers and Flowlines)
- Inspection, Maintenance and Repair (IMR)
- Various surveys
- Diving operations
- Trenching and rock dumping

The company currently has two chartered OSCVs and a third one, TBN “Normand Vision”, is under construction when this is written with estimated delivery second quarter (most likely June) 2014.
This is a brand new state-of the-art vessel. A description of the vessel is included in chapter 2. The vessel will hereafter be referred to as “Normand Vision”.

The thesis contains analysis of the vessel’s motions/response when exposed to various Load Cases considered quite extreme compared to actual operational conditions. The reason for this is that the input data used are extreme in the way that they reflect near-design-limit capacity usage of the vessel. These are normally not applicable conditions when doing real operations, but give a good indication of the vessel’s capabilities before it is completed and ready for thorough testing.
To clarify; analysis is here used when talking of the “whole analysis”, consisting of several simulations depending on the environmental conditions (various wave heights, headings, periods) and the Load Case considered.

The motivation for this is to get theoretical knowledge about the vessel’s performance/capabilities actual parameters before the sea trials takes place.
So an “early” analysis like this will help the marine crew understand some of the vessel’s limits in the testing phase.

In order to carry out a somewhat accurate analysis a number of relevant parameters must be specified and fed into the software.
The environmental conditions used for the analysis are taken from the Tampen area in the North Sea and are mainly based on metocean data. However, some assumptions have also been stated when necessary due to lack of available data.

1.2 Description of scope of work and objective

There are mainly two loading cases (referred to as Load Cases) to be considered, where one case is more extreme than the other. The analysis is based on these two cases which are represented by displacement RAOs (Response Amplitude Operators) prepared by the vessel manufacturer STX OSV, now VARD (changed name in 2013).

The scope of work is to:

- Present a foundation for what the analysis are based on taking into account limitations and assumptions
- Do the analysis based on relevant input data
- Compare the results for the different Load Cases
- Spot check of the extreme loading conditions with newer and more precisely defined conditions for flexible pipeline installation
- Discuss and interpret the results and what impact they may have on the vessel's utilization
- Look at some highlights related to the vessel motions

The objective is to achieve results for various relevant parameters with respect to operational purposes to check the vessel's performance for the actual load cases. The parameters of interest in this study are specified in chapter 7.

As the cases to be analysed are mainly based on theory, there has not been done a particular environment/site survey to base these cases on. So some challenges/limitations are:

- Limited available data for the seabed, like seabed profile (inclines, trenches cliffs etc.) and soil density
- No measurements of the ocean currents at the actual location have been conducted
- No measurements of waves and wind have been conducted

However, proper assumptions will be made and explained, and relevant data will be used if applicable (and available) to get a somewhat realistic environmental basis for the analysis.

1.3 Approach / Method

The approach of the thesis will be to first investigate some of the most important background theory, as well as the input parameters for the analysis. Then use the supplied RAOs to perform the computer analysis and look into the outcomes.

There will as mentioned, due to limited available data, be stated some limitations and assumptions the analysis will depend upon. The hydrodynamic analysis software OrcaFlex from Orcina Ltd. will be used for the analysis.

The OrcaFlex simulations will be executed as partially defined case studies, in the sense that the loading conditions for the vessel are already defined by the yard, VARD, while a number of environmental parameters have to be determined or estimated based on relevant data and assumptions.

In addition there will be some limitations within the software itself.

As the goal is to assess the vessel's capabilities, the analysis will be carried out with a conservative approach. This is considered as "sound engineering practice" when there are a number of uncertainties related to the analysis (Orcina Ltd., 2013).

2 Normand Vision

2.1 Specifications

The vessel NB 811 (TBN "Normand Vision") is a state-of-the-art offshore subsea construction and maintenance vessel. The design is the OSCV 06L design by STX OSV with some minor changes compared to the existing vessels having this design.
The vessel does not have any direct sister ships, but most of the design is similar to that of the following vessels (Waalen, 2014a):

- Lewek Connector (EMAS)
- Normand Oceanic (Subsea 7)
- Skandi Acergy (Subsea 7)
- Skandi Aker (Aker Solutions)
- Skandi Arctic (Technip)
- Skandi Wayfarer (Aker Solutions)

What distinguishes Normand Vision from these vessels is mainly a new bow design. The bow is now more optimized with respect to better float through the waves, with the goal of lowering fuel consumption and pitch motions (Waalen, 2014a).
The vessel was initially planned to be owned by Ocean Installer AS and Solstad Offshore ASA (70/30) through a joint company called Ocean Solstad AS (Næss, 2013). However, in a press release 10th of April 2014 it was announced that Ocean Installer will sell their shares in the vessel which gives Solstad Offshore ASA the full ownership of the vessel.
The reason for this is that Ocean Installer then would have more room for making further investments in organization and assets in the future (OffshoreEnergyToday.com, 2014).

Ocean Installer AS will still be the vessel operator. The vessel manufacturer is VARD, earlier STX OSV. The name was changed in 2013 after the Italian shipbuilding company Fincantieri bought the majorities of the shares in STX OSV (Rosbach, 2013). The hull is made in Tulcea (Romania) and the outfitting of the topside equipment started in Søviknes (Norway) in January 2014. See animated illustration of the vessel in Figure 2.1 and when it is arriving at VARD Søviknes in Figure 2.2.
Figure 2.3 shows a picture of the vessel after the cranes and the VLS was installed.

Normand Vision is a quite large vessel which will give a higher operational window compared to shorter and narrower ships (Ocean Installer AS, 2013).

Figure 2.1: Animated illustration of Normand Vision (STX OSV, 2013b)

Some key data about the vessel (STX OSV, 2013d):

- Length (overall): 156.7 meters
- Length between perpendiculars: ≈ 144.6 meters
- Width: 27 meters
- Draught: Maximum (amidships) 8.5 meters
- Lightship weight: 13541.6 tonnes (calculated from NAPA software, not given (STX OSV, 2013d))
- Maximum deadweight (including cargo, crew, fuel, water, stores and provisions): 12000 tonnes

The maximum deadweight is the limit for when the vessel could be said to ride dangerously low in the sea. In other words the deadweight limitation is related to the minimum freeboard accepted. In the analysis the different Load Cases' deadweight are assumed to include all relevant loads, like crew, fuel, cargo, water, stores, provisions, extra equipment needed for the particular operation and more.

Figure 2.2: Normand Vision arriving at VARD's yard in Søviknes for further outfitting of the topside January 23rd, 2014 (Solstad Offshore ASA, 2014)

Figure 2.3: Cranes and parts of VLS installed on Normand Vision (Waalen, 2014b)

2.2 Areas of use

The vessel is mainly to be used for SURF EPCI operations in the North Sea, but will also be capable of handling global operations. Ocean Installer has been closely involved in the development of the vessel as it will be a crucial tool in the engineers' toolbox (Waalen & Sarhan, 2013). The vessel will be conducting installations of flexible pipelines/flowlines, risers and umbilicals as well as various subsea lifting and installation operations, e.g. various pipeline tees, end terminations and other construction work.

2.3 Features and equipment

The vessel is very well equipped for the tasks it will undertake. Ocean Installer has been heavily involved in the selection of the equipment.

The vessel has three moonpools; two of them are designated ROV deployment moonpools (5.6 by 4 meters) located in hangars at starboard and port side of the vessel in the superstructure.
In these moonpools air can be injected into the water column to lower the impact forces from the moving water on the ROVs. Slamming from the waves on the ROVs is one of the main reasons for why more and more ROVs now are launched from moonpools in recently built vessels. By having the ROVs launched from enclosed moonpools, closer to the centre of the vessel (compared to over the side), are quite favourable as it increases the weather window for launching of the ROVs.

However, a challenge with these moonpools may be during recovery of the ROVs. If the currents in the sea are large enough to cause the ROVs to "drift off" along the hull one will get some trouble taking them up through the moonpool. In the worst case scenario the vessel's thrusters can then hit the ROV and crush it (Hagen, 2014). Moonpools generally give some structural strength challenges, especially in the hull's longitudinal direction. The buoyancy is also decreased the more moonpools that are present.

The main moonpool is located amidships at the centre of the vessel and is measuring 7.2 by 7.2 meters and has the Vertical Lay System (VLS) located above.
The main deck area of the vessel is huge, 2100 m^2, and accommodates the 150 Te VLS with two 75 Te retractable tensioners, as well as a 400 Te main crane and a 70 Te auxiliary crane (both operating to 3000 meter). The main deck is located 12 meters above the baseline of the vessel. A permanently installed 3000 Te carousel (24.3 meters in diameter) for flexible products is placed beneath the main deck (see Figs. 2.4 and 2.5). Not very many vessels have this, except of Normand Vision's "sister ships". This means that one often does not need extra reels on deck, giving more storage and work space. Because of this configuration the diesel engines are placed more in front of the vessel (see Fig. 2.4). The diesel engines drive the generators which in turn supply the electric engines with power (i.e. diesel-electric propulsion). Also, when not having extra reels on deck, it will be more favourable with respect to the intact stability and motion characteristics of the vessel. The Centre of Gravity (CoG) will be lower if no extra reels are carried on deck.
The umbilical/flowline on the under-deck-reel will be loaded and unloaded trough hatches in the main deck.

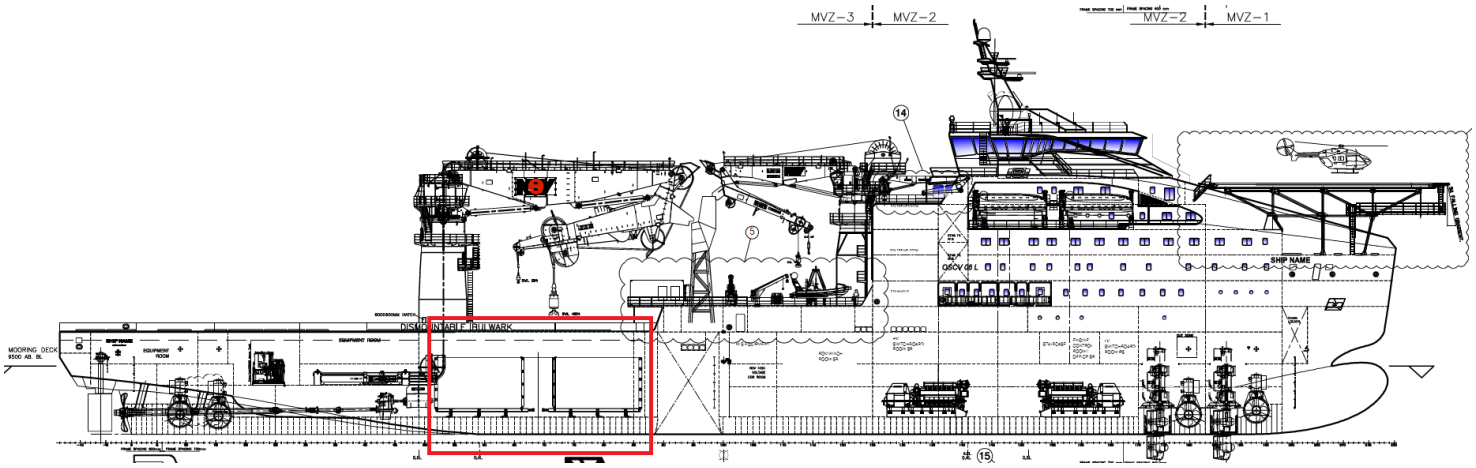

Figure 2.4: Drawing of Normand Vision seen from the starboard side, the VLS does not show on this drawing. Location of the 3000 Te carousel under main deck is shown by the red square (STX OSV Design AS, 2012)

The VLS consists of two 75 Te track tensioners each engaging two or four tracks. Each tensioner can provide a maximum squeeze force of 610 kN/meter per track for pipes with an outer diameter up to 400 mm. This capacity is limited by the drive system. The tensioners are delivered with pads, with a 140° opening angle, which are a trade-off between squeeze force and a wide range of pipe diameters. The pads are relatively easy interchangeable with e.g. 160° pads which allow for other diameters versus squeeze relations. Each track tensioner provides a contact length of 4.4 meters (Huisman, 2013a).

Figure 2.5: Picture from the carousel room looking towards the bow (STX OSV, 2013b)

Normand Vision is a DP (Dynamic Positioning) class 3 vessel according to the Norwegian Maritime Directorate's (NMD) and International Maritime Organization's (IMO) classification (Røkeberg, 1997). This is equivalent to DNV's DYNPOS-AUTRO DPS-3 classification.

The DP class 3 means that the vessel has a fully redundant DP system, and can in emergency situations seal off the DP systems from each other by water tight and fireproof doors, e.g. in case of water ingress or need for flooding due to e.g. fire/explosion (Gudmestad, 2013b).
The vessel's maximum transit speed is 16 knots (Waalen & Sarhan, 2013). See Figure 2.6 for an animated illustration of Normand Vision in transit.

Figure 2.6: Illustration of Normand Vision in transit seen from starboard side (STX OSV, 2013b)

A nice time-lapse compilation video of some of the outfitting at VARD's yard in Søviknes could be found in the following link (http://vimeo.com/93656983) (VARD 811 "Normand Vision" time-lapse compilation, 2014).

3 The vessel model

In this chapter theory about how the vessel is modelled is in focus. However, the chapters 3.1 to 3.4 will also be quite general with respect to background theory regarding vessel motions.

3.1 About vessel motions and some features on Normand Vision

A vessel's motion characteristics are dependent on a number of factors and parameters. Some of the most important are:

- Geometry of the vessel (height, length, width)
- The hull shape
- Weight/displacement (lightship weight plus allowed deadweight)
- Cargo and equipment (their geometry and weight)
- The vessel's velocity
- External factors (wind, waves and current conditions and their direction relative to the vessel)

However, a vessel's motions in general can be influenced by use of various features (both passive and active) in the vessel, like for example:

- Water ballast tanks
- Bilge keels (sometimes referred to as twin keel, e.g. for sailboats)
- Stabilizer fins (active or passive, normally used on larger ships like cruise liners)
- Outriggers
- Internal gyroscopic stabilizers
- Roll reduction tanks active or passive (also known as anti-roll tanks)
- Paravanes
- Anti-heeling tanks (to compensate when CoG and buoyancy centre are not located at same vertical line when looking at the cross-section of the ship from aft or bow)

The vessel motions are described by six Degrees of Freedom (DOF) as shown in Figure 3.1. This figure is an example and does not comply with the sign convention used for the data supplied for the analysis.

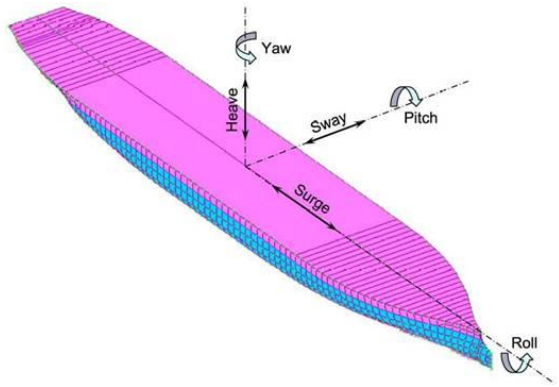

Figure 3.1: The six degrees of freedom for a vessel (Salvador, 2011)

What is positive and negative direction can be defined differently in various cases and must hence be specified each time one carries out an analysis in OrcaFlex. The input regarding the vessel's motion characteristics is based on reports supplied by STX OSV. This is further looked into later in this chapter. In the analysis the surge, sway and yaw motions have been given low priority as they normally not are that important when analysing and planning marine operations.

The roll motion is often considered as the most problematic because it affects operations due to contributions to both horizontal and vertical accelerations, which can grow quite large. A number of phenomena related to the roll motions can be experienced, e.g. (Benedict, et al., 2014):

- Synchronous rolling motion
- Parametric rolling motion/parametric roll resonance
- Reduction of intact stability caused by riding on the wave crest amidships, especially in high waves (this is related to parametric roll resonance)
- Surf-riding
- Combination of phenomena listed above

Normand Vision has numerous water ballast tanks, 6 anti-heeling tanks, as well as 2 roll reduction tanks (lower and upper). The water ballast tanks are of the type "double bottom". This has to do with requirements that fuel oil should not leak out if the hull is damaged.
Normand Vision is also categorized as a SPS (Special Purpose Ship), after the International Maritime Organization's (IMO's) 2008 SPS Code. This means that the vessel normally will have much people on-board and the water ballast tanks has to be many and small so that the vessel can still have some intact stability in damaged condition and, if it sinks, it should sink on more or less even keel (Worren, 2014).

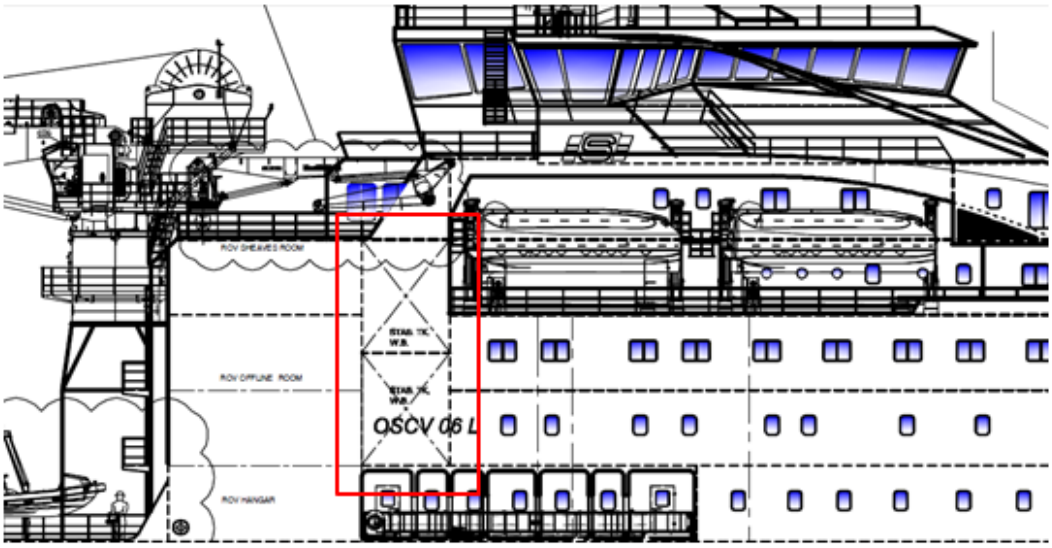

Figure 3.2: Excerpt of drawing of Normand Vision seen from the starboard side with the anti-roll tanks in the red rectangle (STX OSV Design AS, 2012)

The roll reduction tanks (see Fig. 3.2) are located quite high in the vessel (about 18 to 27 meters above the keel) and goes over the whole width of the vessel (27 meters). These are passive tanks where the water moves back and forth as the vessel rolls. Some sort of grating makes up different sections in the tanks. The purpose of this grating is to "disturb" the water so that it moves with another natural period than the vessel. This prevents the water getting in resonance with the vessel and helps reducing the rolling effects.

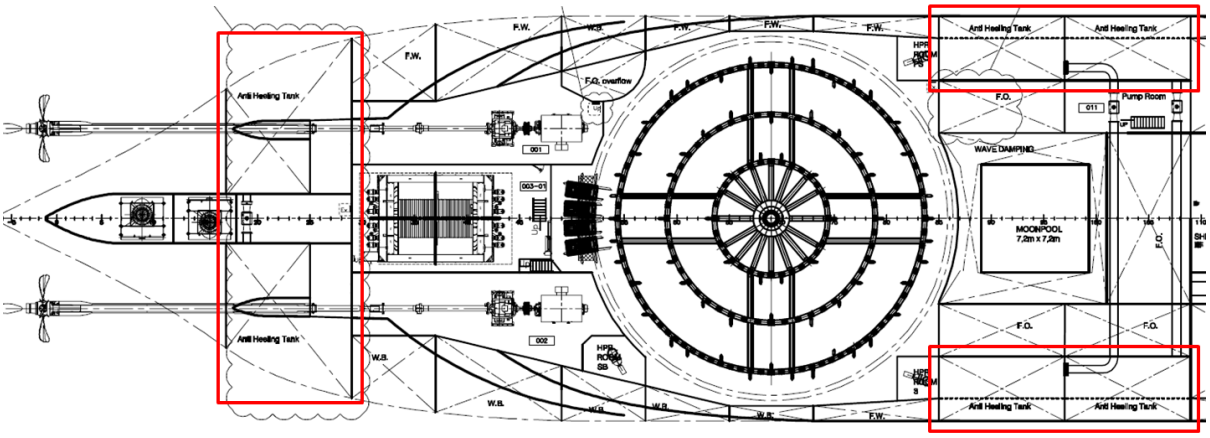

Figure 3.3: Excerpt of drawing of Normand Vision seen from above with the anti-heel tanks in the red rectangles, many water ballast tanks can also be seen (STX OSV Design AS, 2012)

The anti-heeling tanks (see Fig. 3.3) are normally only used when doing crane operations over the side of the vessel. These tanks can then be filled with water to compensate for the moment from the crane and the lifted load. A computer system feeling on the vessel's motions will calculate how much water should be pumped between the different anti-heeling tanks to best compensate for the heeling. Because of this the vessel will not heel that much and be a more stable lifting platform.

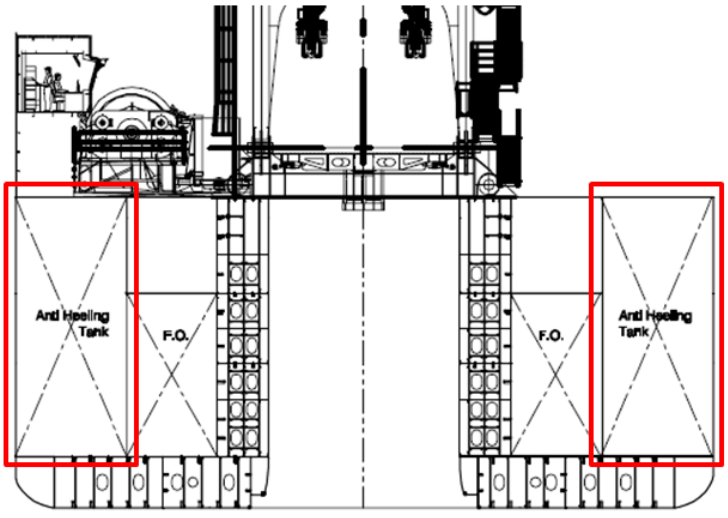

Figure 3.4: Excerpt of drawing of Normand Vision seen from aft with two of the anti-heel tanks in the red rectangles (STX OSV Design AS, 2012)

The anti-heeling tanks are located as shown by the red rectangles in Figures 3.3 and 3.4. They are going from the fuel oil's tank top up to the main deck which is about 8.4 meters (Waalen, 2014a).
The water ballast tanks are used to trim the vessel so that the vessel has enough stability and is on even keel, meaning that the deck is as horizontal as possible. The ballast tanks are also used during lifting.

Normand Vision also has bilge keels to improve its motion characteristics with respect to roll. See also sub-chapter 3.4 and 10.1.

A vessel's motions are described by a set of equations for the translations of the CoG (Centre of Gravity) for the vessel, along the x, y and z axis and the rotation about them (ref. Figs. 3.1 and 3.5).

Figure 3.5 shows a coordinate system $S(x_0,y_0,z_0)$ fixed in space with a moving vessel with the coordinate system $O(x,y,z)$ at constant speed V. Both the (x,y) and (x_0,y_0)-plane lies in the still water surface. The waves with phase velocity c move in the x_0-direction, which is the wave propagation direction. The moving coordinate system $O(x,y,z)$ with origin O, will be in different positions at different points in time as the vessel moves along. This will cause the origin O to be located above or below the time-averaged CoG, here named G. Another coordinate system is located at the vessel's center of gravity: $G(x_b,y_b,z_b)$. The waves travel in the positive x_0-direction and hence with an angle, μ, relative to the vessel's speed vector V, going in the x-direction. The wave profile can then be described as in equation 1 (Journèe & Adegeest, 2003).

$$\zeta = \zeta_a \cos(kx_0 - \omega t) \quad or \quad \zeta = \zeta_a \cos(\omega t - kx_0) \quad [m] \qquad \text{(Eq. 1)}$$

Where:

- x_0 is the wave propagation [m]
- ζ_a is the wave amplitude [m]
- k is the wave number [m^{-1}]
- ω is the wave frequency [s^{-1}]
- t is the time interval one looks at [s]

When then looking at the coordinate system $O(x,y,z)$ moving with a constant speed V with the vessel one can find that the wave propagation, x_0, can be described by equation 2:

$$x_0 = V \cdot t \cdot \cos\mu + x \cdot \cos\mu + y \cdot \sin\mu \quad [m] \qquad \text{(Eq. 2)}$$

If the vessel is <u>not moving</u> the waves will approach the ship with a frequency equal to the wave's frequency, ω. When the vessel <u>is moving</u> with a forward speed V the waves will approach the vessel with an encounter frequency, ω_e, which take into account both the waves' and ship's frequency at that certain speed. For the case in the coordinate system in Figure 3.5 the expression for such an encounter frequency could be written as shown in equation 3 (Journèe & Adegeest, 2003).

$$\omega_e = \omega - k \cdot V \cdot \cos\mu \quad [s^{-1}] \qquad \text{(Eq. 3)}$$

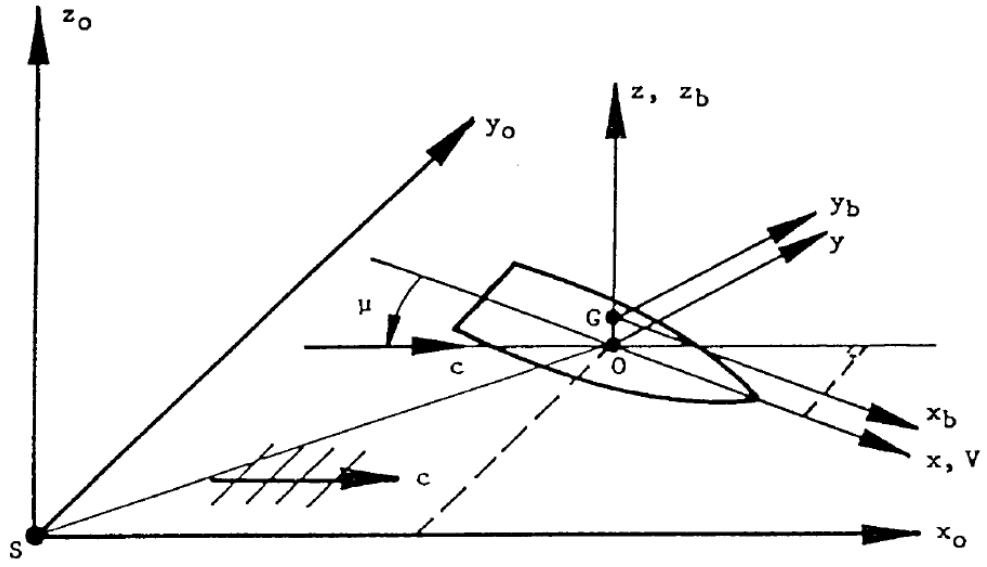

Figure 3.5: Coordinate system for a vessel in waves (Journèe & Adegeest, 2003)

Then, by combining the wave propagation (eq. 2) and the encounter frequency (eq. 3) with the wave profile (eq. 1) one obtain the updated equation for the wave profile, see equation 4.

$$\zeta = \zeta_a \cos\left(\omega_e t - k \cdot x \cdot cos\mu - k \cdot y \cdot sin\mu\right) \quad [\text{m}] \qquad \text{(Eq. 4)}$$

The resulting six ship motions (or degrees of freedom) for the vessel's coordinate system *O*(x,y,z,) can then be described by a set of equations where the sine and cosine parts of equation 4 has been added together and referred to as the phase angle, φ. The motions are described by the three displacements of the vessel's CoG in the x, y, and z-axes directions and the rotations about them, see equations 5 to 10 (Journèe & Adegeest, 2003):

- Heave: $z = z_a \cdot \cos\left(\omega_e t + \varphi_{z\zeta}\right)$ [*m*] (Eq. 5)
- Surge: $x = x_a \cdot \cos\left(\omega_e t + \varphi_{x\zeta}\right)$ [*m*] (Eq. 6)
- Sway: $y = y_a \cdot \cos\left(\omega_e t + \varphi_{y\zeta}\right)$ [*m*] (Eq. 7)
- Pitch: $\theta = \theta_a \cdot \cos\left(\omega_e t + \varphi_{\theta\zeta}\right)$ [*° or rad*] (Eq. 8)
- Roll: $\phi = \phi_a \cdot \cos\left(\omega_e t + \varphi_{\phi\zeta}\right)$ [*° or rad*] (Eq. 9)
- Yaw: $\psi = \psi_a \cdot \cos\left(\omega_e t + \varphi_{\psi\zeta}\right)$ [*° or rad*] (Eq. 10)

Where:

- Ship displacements: $x_a, y_a, z_a = [m]$
- Ship rotations: $\phi_a, \theta_a, \psi_a = [° \; or \; rad]$
- Phase angles: $\varphi_{x\zeta}, \varphi_{y\zeta}, \varphi_{z\zeta}, \varphi_{\phi\zeta}, \varphi_{\theta\zeta}, \varphi_{\psi\zeta} = [° \; or \; rad]$

From these equations one could also find the different velocities and accelerations by taking the first and second derivatives (w.r.t the time) respectively.

The phase angles of the vessel motions are related to the harmonic wave elevation of the vessel's origin (coordinate system *O*(x,y,z)). This means in practice that the average elevation/vertical positions of the vessel's CoG could be given as in equation 11 below.

$$\zeta = \zeta_a \cos(\omega_e t) \quad [m] \qquad \text{(Eq. 11)}$$

The phase is most easily explained as the relation between the vessel motion and the wave. The phase angles provide information of where the maximum harmonic response/motion occurs compared to the maximum wave elevation at the vessel's longitudinal CoG (STX OSV, 2013a).
A positive phase angle means that the motion travels in lead/"in front of" the wave, while a negative value means that the motions lags/"moves behind" the wave propagation, see Figure 3.6.

In other words; the vessel responds to the waves with its maximum motion either before (lead phase) or after (lag phase) the maximum wave elevation occurs. If the waves are in phase with the vessel's motions the phase angle is equal to zero, while an angle of ±180 degrees means that the vessel motion is totally opposite of the waves' maximum elevation. If the vessel amplitude/rotation is zero, the phase angle is irrelevant.

The rotational motions (roll, pitch and yaw angles) are the same for all points on the vessel while the translational motions (heave, surge and sway) are coupled, i.e. depending on the motions of the other degrees of freedom. For example is the heave motion of the helideck dependent on both the heave at the CoG (Centre of Gravity) of the vessel as well as the pitch and roll-induced heave at the actual location. The heave motion alone is equal all over the vessel, while the vertical component of roll and pitch depends on the location on the vessel, with the least deflection on the longitudinal and transverse centrelines (going through the CoG) respectively.

This means in practice for the analysis that roll, pitch and yaw angles are not found for certain locations as they will remain the same wherever one is on the vessel. The maximum, average and minimum values for the angles of these motions are consistent for all locations on the vessel.

However, the contribution from roll and pitch in vertical and horizontal directions are taken into account for the heave, sway and surge (displacements, velocities and accelerations) in OrcaFlex.

So because of the contributions from roll and pitch the heave needs to be measured from specified locations on the vessel, and the magnitude depends on the location. For example, the largest heave motions are located at the bow and stern, as the pitch contributes the most here.
Also, sway and surge will have a horizontal contribution from pitch and roll. These however, are not very large compared to the heave contributions.

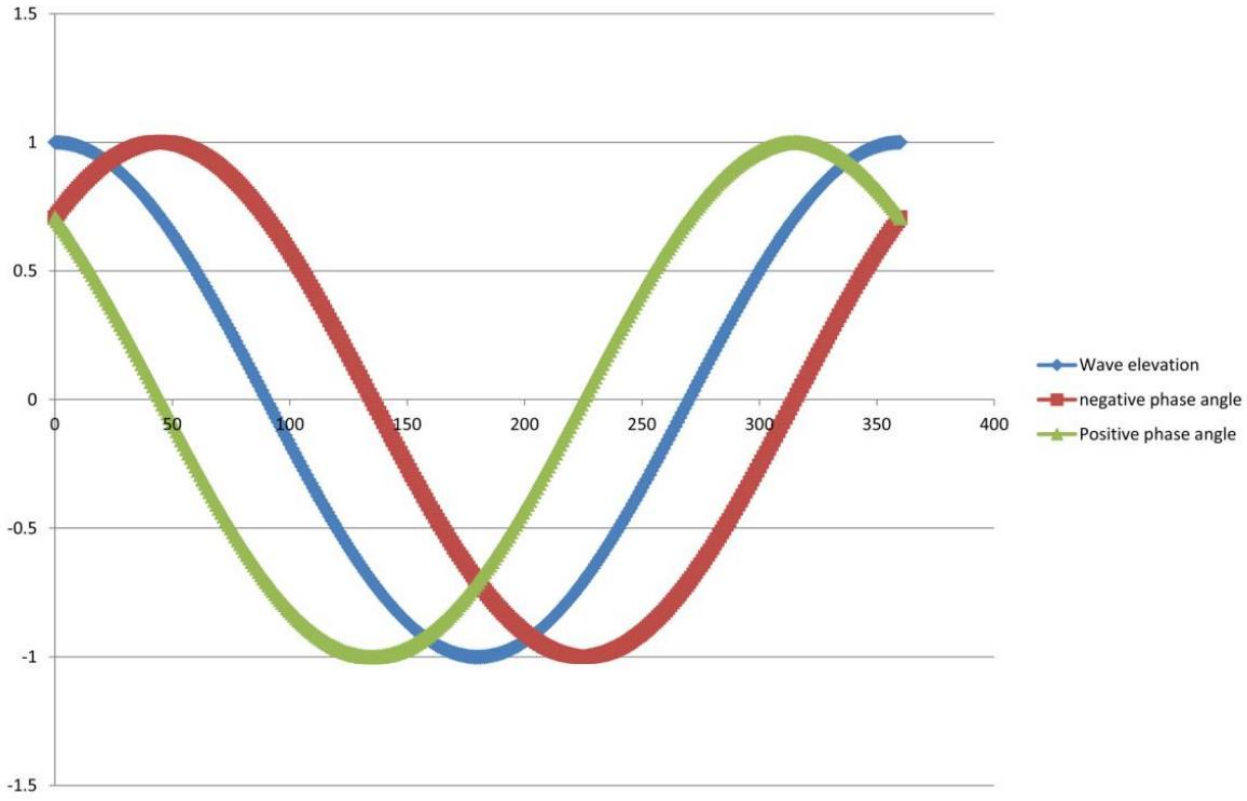

Figure 3.6: Illustration of positive and negative phase angle vs. the wave elevation, the wave here travels from right to left, the horizontal axis represents the time scale, the vertical axis represents the amplitude (STX OSV, 2013a)

3.2 Vessel's response to waves

Dynamic vessel response is normally calculated by the use of Finite Element Method analysis (FEM analysis) on a computer. Such computations can be done in software like e.g. Seaway (Delft University of Technology), MOSES (Ultramarine Inc.) and ShipX/VERES (Marintek).

3.2.1 Linear strip theory

The approach used for analysing motion response on vessels is called (linear) strip theory. In this approach the vessel is divided into many two-dimensional strips along the longitudinal axis of the vessel, see Figure 3.7.

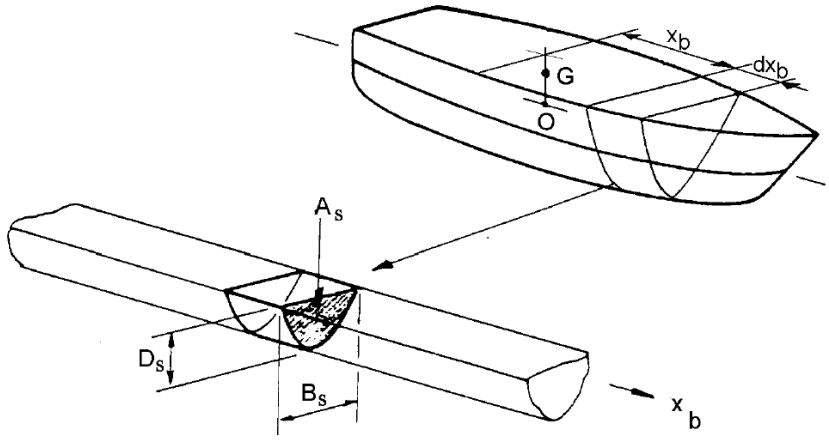

Figure 3.7: Strip theory shown with cross-sections (Journèe & Adegeest, 2003)

The hydrodynamic loads (hydromechanics and exciting wave forces) on each strip are calculated and the total hydrodynamic load effects are found by integrating the strips over the entire length of the vessel $\left(\int_0^L dx_b\right)$. The smaller the strips (intervals) are the more accurate the results are likely to be. All six DOF are considered in such an analysis.
The results show how hydrodynamic forces affect the motion of the vessel (Zhan, 2014).

In order to use the FEM analysis one need to put in a number of parameters to get the desired outcome. The parameters can somewhat vary, but usually the following parameters are paramount when vessel responses due to waves are sought (Journèe & Adegeest, 2003):

- Information about the vessel (dimensions, displacement, draught, trim)
- Loading conditions (giving metacentre height, both longitudinal and transverse are needed)
- Centre of Gravity (longitudinal and transverse)
- Longitudinal weight distribution of the vessel (to look at wave induced shear, moments and torsion)
- The vessel's velocity in the water (if applicable)
- Hull "attachments" (e.g. rudder, bilge keel, paravanes, stabilizer fins etc.)
- The radius of gyration (for the rotational degrees of freedom, roll, pitch, yaw and sometimes roll-yaw)
- Wave specific parameters (wave height, period, regular or irregular waves)
- Type of wave spectra

If the information is fed into suitable software as e.g. Seaway or VERES one will be able to get out data about the vessel's response (displacements, velocities and accelerations).

Since the strip theory is based on a number of assumptions and limitations the results may not always be very accurate compared to what happens in reality.

There are some assumptions and limitations with use of the linear strip theory to be aware of that will affect the outcomes (Journèe & Adegeest, 2003):

- The ship is considered to be a rigid body, floating in the surface of an ideal fluid.

- The ideal fluid is considered to be homogeneous, incompressible, free of surface tension, irrotational and inviscid. That the fluid is considered inviscid will pose a significant problem when looking at roll damping motions. The viscous roll damping effects must then in practice be based on empirical formulas found by model tests (this is done in the VERES software).

- Unsteady divergent wave systems are neglected; hence will the strip theory not be accurate for high-speed vessels and extreme sea state conditions.

- No interaction between the different strips are considered, i.e. the three dimensional effects is neglected.

- Since the strip theory is based on linearity, the ship motions should be small compared to the cross-sectional dimensions of the vessel. This means only the hydrodynamic effects of the hull under the still water line are taken into account. So, if parts of the hull move out of or into the water, one should expect inaccuracies. These inaccuracies in the motions strongly influence the wave's resistance on the ship (which is proportional to the relative motions squared), which again affect the vessel motions. This gives a bad loop of inaccuracy in the motions.
  Also, the strip theory does not distinguish between different hull shapes (and their effects) above the still water line.

- Wave loads at low frequency of encounter in following seas will give a large deviation between calculated and experimental data using strip theory, because of how the forced motions problems are solved. Such problems can be solved by making the wave loads go to zero.

Despite these limitations and simplifications, linear strip theory is considered to be the most successful tool for calculation of wave induced motions on a ship, at least in the early design stages of a ship.
The strip theory is a slender structure theory and gives fairly good results for ships with length to width ratios down to approximately three (Journèe & Adegeest, 2003). This ratio for Normand Vision is calculated in equation 12.

$$\frac{Length\ overall}{Width} = \frac{156.7\ m}{27\ m} \approx 5.80 \rightarrow\ 5.80 > 3\ \rightarrow OK \qquad \text{(Eq. 12)}$$

As the ratio is approximately 5.80 the use of strip theory should be applicable on Normand Vision.

3.2.2 Model testing of Normand Vision

One typically use strip theory in the early phases of the vessel design when there is scarce with information about the motion characteristics.
Then the strip theory can be used to give a feeling of how the vessel will behave, typically through displacement RAOs. These data are then used to further optimize the design of the vessel. In the later design exact models are made and tested in a wave tank. The models are typically in the scale between 1:10 and 1:100, depending on the vessel and tank size.

The model for Normand Vision was in the scale 1:25.438, made and tested by Marintek in their wave tank in Trondheim (Marintek , 2012). A picture of the model towed in Marintek's wave tank is shown in Figure 3.8. The tests performed by Marintek were referred to as "calm water performance tests".

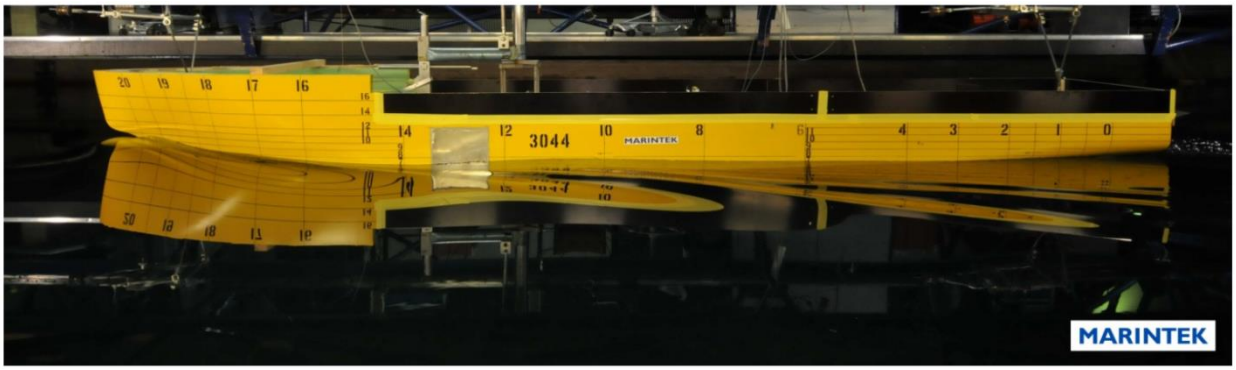

Figure 3.8: Picture of the Normand Vision model in a propulsion test (16 knots) in Marintek's wave tank (Marintek , 2012)

The main focus was resistance and propulsion tests to look at the wave profiles generated by the vessel. Such empirical tests give more realistic motion characteristics as one during the test is able to measure the motions quite exact for different wave conditions. Also, at this stage, more sophisticated software can be used as more information is progressing. When the vessel construction is finished it will be doing sea trials, which often proves that the model tests are quite good (Qayre, 2014).

3.3 Transfer functions and RAOs

To be able to describe a vessel's response to external loads one will need some information about how the various degrees of freedom are affected by wind, waves and currents.

This response is calculated by use of transfer functions based on the relation between the waves' amplitude and the vessel's motion amplitude. These transfer functions basically give a measure of the proportion of wave amplitude "transferred through the ship system" into vessel motions.
In the industry these transfer functions are normally referred to as Response Amplitude Operators (RAOs).

From the FEM analysis of the vessel's response the output from the transfer functions are usually considered as most important. These transfer functions use the provided input and transfer it into vessel response describing the displacements in all the DOF for the vessel. As mentioned, some of the motions from the different DOF are affecting each other.

It is possible to sum the different responses linearly to get the final response; however this may not be very precise, especially for the viscous roll damping motion which is best described with a non-linear approach, where empirical formulas from model testing normally are used (Journèe & Adegeest, 2003).

The transfer functions are obtained by dividing the various motion equations (equations 5 to 10) by the wave amplitude on both sides of the equations. Then two sets of coupled equations, both sine and cosines components, come out as presented in equations 13 to 18 at time equals to zero (Journèe & Adegeest, 2003).

The coupled motions functions for the vertical plane motions:

- Heave: $\frac{z_a}{\zeta_a} \cdot \cos(\varphi_{z\zeta})$ and $\frac{z_a}{\zeta_a} \cdot \sin(\varphi_{z\zeta})$ [-] (Eq. 13)
- Pitch: $\frac{\theta_a}{\zeta_a} \cdot \cos(\varphi_{\theta\zeta})$ and $\frac{\theta_a}{\zeta_a} \cdot \sin(\varphi_{\theta\zeta})$ [-] (Eq. 14)
- Surge: $\frac{x_a}{\zeta_a} \cdot \cos(\varphi_{x\zeta})$ and $\frac{x_a}{\zeta_a} \cdot \sin(\varphi_{x\zeta})$ [-] (Eq. 15)

The coupled motion functions for the horizontal plane motions:

- Sway: $\frac{y_a}{\zeta_a} \cdot \cos(\varphi_{y\zeta})$ and $\frac{y_a}{\zeta_a} \cdot \sin(\varphi_{y\zeta})$ [-] (Eq. 16)
- Roll: $\frac{\phi_a}{\zeta_a} \cdot \cos(\varphi_{\phi\zeta})$ and $\frac{\phi_a}{\zeta_a} \cdot \sin(\varphi_{\phi\zeta})$ [-] (Eq. 17)
- Yaw: $\frac{\psi_a}{\zeta_a} \cdot \cos(\varphi_{\psi\zeta})$ and $\frac{\psi_a}{\zeta_a} \cdot \sin(\varphi_{\psi\zeta})$ [-] (Eq. 18)

These equations are solved numerically and the outcomes are called the transfer functions of the motions. These are more commonly referred to as the Response Amplitude Operators (RAOs).
In practice one then set the sine/cosine part of the equation equal to its maximum value (= 1) as one often is interested in the maximum response the vessel will undertake. So the RAOs are actually peeled down to be the ratios of the amplitude of the vessel's motions to the wave amplitude as shown in equations 19 to 24.

- Surge RAO $\frac{x_a}{\zeta_a}$ [*m/m or* -] (Eq. 19)
- Sway RAO $\frac{y_a}{\zeta_a}$ [*m/m or* -] (Eq. 20)
- Heave RAO $\frac{z_a}{\zeta_a}$ [*m/m or* -] (Eq. 21)

- Pitch RAO $\frac{\theta_a}{\zeta_a}$ [*deg./m or rad./m*] (Eq. 22)
- Roll RAO $\frac{\phi_a}{\zeta_a}$ [*deg./m or rad./m*] (Eq. 23)
- Yaw RAO $\frac{\psi_a}{\zeta_a}$ [*deg./m or rad./m*] (Eq. 24)

One could make the pitch, roll and yaw RAOs dimensionless by also dividing them by the wave number, *k* [m^{-1}]. The corresponding phase angles are specified in equations 25 to 30.

- Surge phase $\varphi_{x\zeta}$ [*rad. or °*] (Eq. 25)
- Sway phase $\varphi_{y\zeta}$ [*rad. or °*] (Eq. 26)
- Heave phase $\varphi_{z\zeta}$ [*rad. or °*] (Eq. 27)
- Pitch phase $\varphi_{\theta\zeta}$ [*rad. or °*] (Eq. 28)
- Roll phase $\varphi_{\phi\zeta}$ [*rad. or °*] (Eq. 29)
- Yaw phase $\varphi_{\psi\zeta}$ [*rad. or °*] (Eq. 30)

The RAOs are normally visually presented as graphs for the different DOF showing how the response of the vessel varies with the frequency (period) of the waves. The waves are normally applied for a set of different headings. Normally angles between 0° and 180° are considered with certain intervals, e.g. 15° or 30°. The values will be the same for the opposite angles. The RAOs provided for Normand Vision are described from 0° to 180° with 15° intervals.

Different wave periods and headings will give different RAO values. The ship's speed will also affect the RAOs. The heights of the incoming waves are multiplied with the RAOs to get the response. The peaks in RAO graphs show where resonance between the vessel and waves will occur. See Figures 3.9 (Load Case 1) and 3.10 (Load Case 2) for a visual representation of roll RAOs for Normand Vision. The various line colours in the figures represent the different wave headings.
The RAOs are helpful when determining what wave periods and wave headings will give the most unfavourable motions and resonance with the vessel, which one of course wants to avoid.

From Figures 3.9 and 3.10 one can observe that the vessel in these cases will have very large roll motions and be in resonance with the waves with periods of about 13 seconds for Load Case 1, and 16.5 seconds for Load Case 2.

The highest responses occur when the wave heading is 90°, i.e. unfavourable beam seas when talking of roll. These peaks indicate where resonance will occur between the vessel's Eigen frequency in roll and the waves' excitation frequency.

The maximum RAO values in Figures 3.9 and 3.10 are about 10.5°/m for Load Case 1 and about 9°/m for Load Case 2. This means if the waves are coming in beam seas with a wave height of 1.0 meter, the vessel will roll to an angle of (max.) 10.5° or 9° relative to the vertical plane (see Fig. 3.11). Before up-righting itself again the vessel will experience some more deflections from side to side which will eventually decrease and come to a halt after some time as they are dampened, if the incoming waves were "removed". If the waves are sustained the motions will cause the ship to keep on rolling.
The same will apply for the other rotational DOF, pitch and yaw, but the maximum deflection angle per meter of incoming wave height will usually be much smaller.

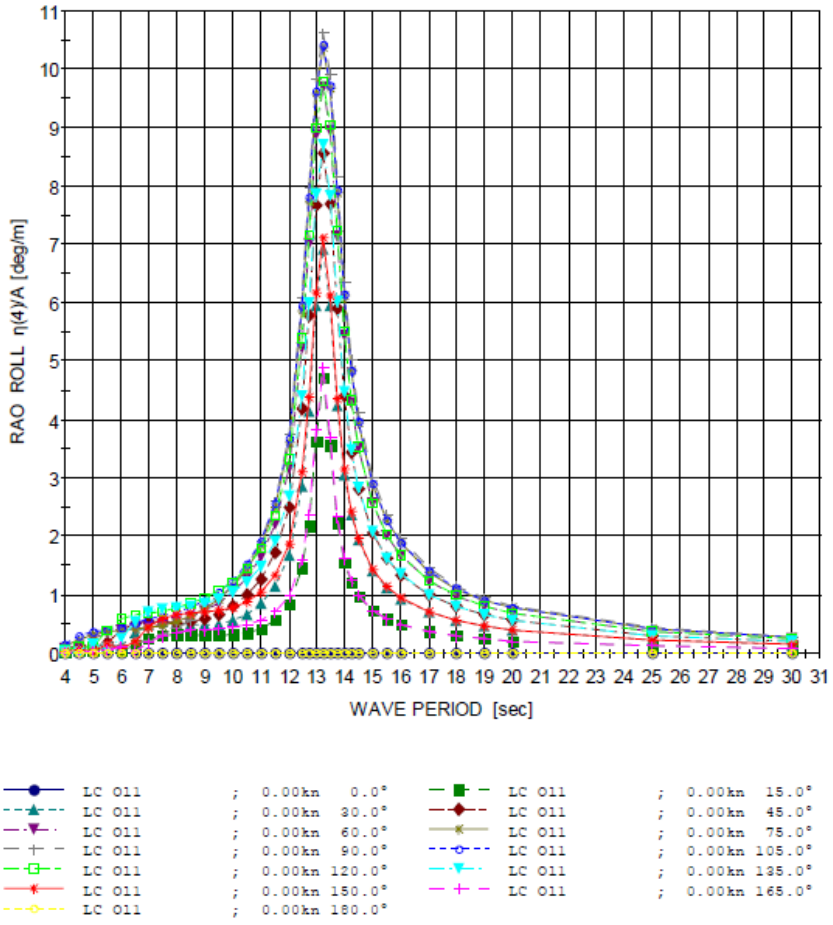

Figure 3.9: Displacement RAOs for roll motion for a range of different wave periods for Load Case 1. Wave headings from 0° to 180° with 15° intervals. Based on VERES simulations of Normand Vision (STX OSV, 2013a)

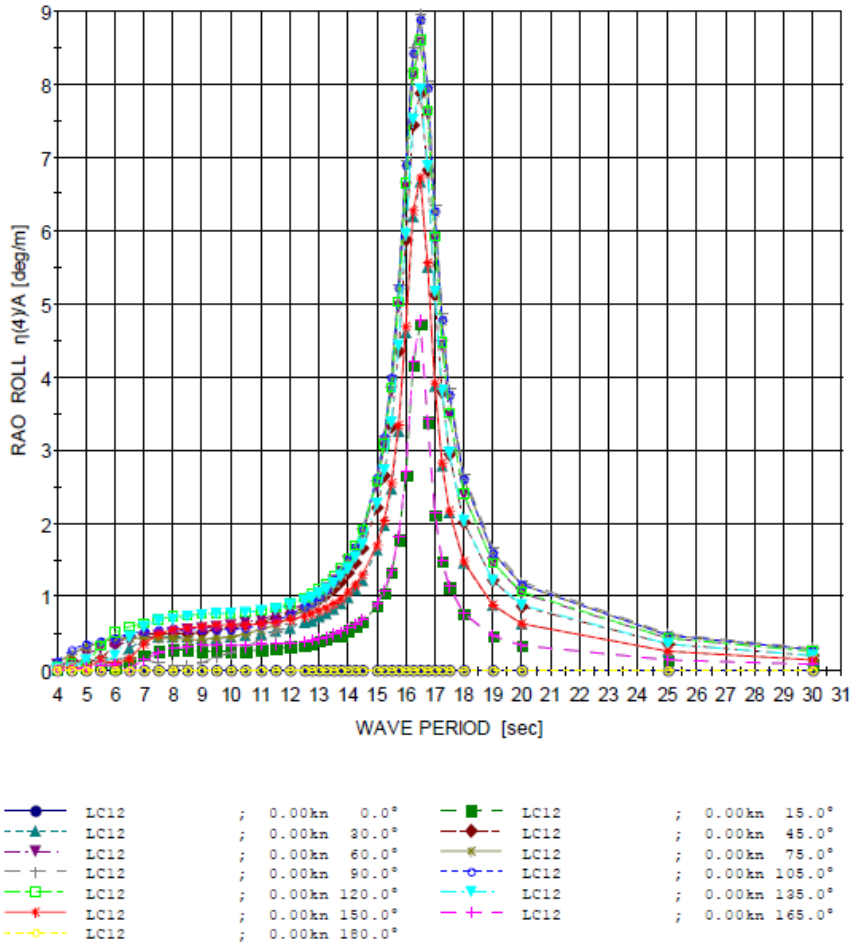

Figure 3.10: Displacement RAOs for roll motion for a range of different wave periods for Load Case 2. Wave headings from 0° to 180° with 15° intervals. Based on VERES simulations of Normand Vision (STX OSV, 2013a)

When the RAO is translational (heave, surge and sway), resonance will occur when the RAO is equal to one. However, for surge and sway one will not in practice get resonance, but the motions can be quite large and move towards a RAO of one when the wave period is getting really large and the wave heading is head seas (0°) or following seas/waves towards the stern (180°) for surge, and beam seas (90°) for sway. The viscous effects and the inertia in the sea will cause the vessel to not get in resonance with the waves for surge and sway. The translational RAOs are dimensionless or have the unit meter per meter, which represent the translational deflections in meter per meter of incoming wave height.

In ship design RAO calculations are usually carried out with many different Load Cases and various external effects (e.g. wind, waves, currents) to get a good picture of the vessel's capabilities.

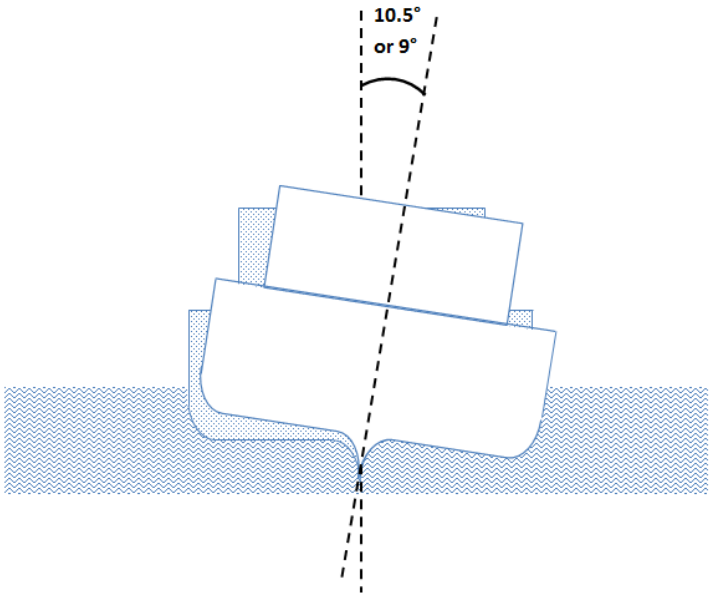

Figure 3.11: Illustration of roll RAO of 10.5 or 9 degrees per meter of incoming wave height for Load Case 1 and 2 respectively

3.3.1 RAO checks in OrcaFlex

In order to ensure that the RAOs and phase angles that are fed into OrcaFlex makes sense, there are a feature called "RAO quality check" in OrcaFlex. This feature helps to avoid wrong input of these parameters. The RAO data to be used for the analysis in OrcaFlex comes from simulations in VERES, which again uses data based on the Load Cases.

Even RAO data and phases from respected companies are prone to errors and it is important to check them. This is done in the way that one has a quite clear interpretation of how the motions should look like for very short and very long wave periods. For example in very short wave periods the vessel's inertia suppresses the waves' power to move the vessel and the expected displacement RAO is approximately zero and the phase is neglected.
In very long wave periods (typically above 20 seconds for ships) the vessel will behave like a raft or dinghy in the waves. Then the different displacement RAOs' amplitudes will be equal to one or zero for the various wave headings and with different phases. With the use of this knowledge one could then be quite sure about the quality of the data provided for the OrcaFlex analysis. The methodology for checking this is either to look at the RAO graphs OrcaFlex provides after the RAOs are imported to OrcaFlex, or to run simple simulations with only the vessel model and check if the motions seem reasonable (Orcina Ltd., 2013).

3.4 Damping of vessel motions

Of the six different DOF, only the roll motion can be relatively easy dampened. This is done with various anti-roll and anti-heeling tanks (to restrict the movement of the vessel), stabilizer fins, bilge keels and more. The principle to avoid or reduce the roll motions are to generate oppositely directed and equally large forces to resist the roll motion forces induced by the waves (Samoilescu & Radu, 2002).

A ship could be seen as a damped mass elastic system. The ocean represents the stiffness, K, and makes up the friction in the system which dampens the mass elastic system, the mass being the vessel's displacement.
When talking of a ship's inherent damping of the roll motion it will in many cases consist of the viscous roll damping and optionally bilge keel damping, if the vessel has bilge keels (Samoilescu & Radu, 2002). The viscous roll damping is made up of two different viscous effects; the skin friction (drag from the water along "the wet area" of the hull) and the viscous effects due to the pressure distribution around the vessel. The skin friction is of minor concern for real sized vessels and can be neglected, but not for vessels in model scale. This is because when vessels e.g. have bilge keels, the damping effects from the bilge keels are much more important than the water's friction with the hull (the wet area).
The pressure distribution effects around the vessel is often associated with the making of eddies, and therefore often referred to as eddy-making damping in literature. When one have bilge keels as on Normand Vision, the bilge keel damping comes in addition. This damping force can be quite large and represent as much as 50% of the total roll damping. Both the eddy-making damping and the bilge keel damping are actually non-linear, but are linearized for practical calculation purposes when e.g. determining roll amplitudes (Faltinsen, 1990).

In the VERES software, which the displacements RAOs used in Orcaflex depends on the viscous roll damping has already been taken into account with the use of empirical formulas. These empirical formulas are based on model tests as the software assumes the fluid to be homogeneous, non-viscous and incompressible (STX OSV, 2013a). This means that OrcaFlex uses the displacement RAOs where the damping is already accounted for.

3.4.1 Damping of one degree of freedom systems

In reality a vessel is damped by the interaction of several degrees of freedom, but the damping is more easily explained by considering one degree at the time. Ship motions can be considered as a simple spring system, so the equation of motion for a vessel in calm water exposed to a disturbance in roll (or e.g. pitch or heave) will be similar to the equations of motion of a mass-spring system (Gudmestad, 2013d).

The forces moving the vessel in waves can be seen as forced oscillations. The impact from forced oscillations can be described by the sum of a homogenous and particular solution of the dynamic equation of equilibrium or more commonly; the equation of motion.
The homogeneous solution can initially have rather large amplitude or deflection, but this motion is damped fully out after a while. The movement caused by the particular solution on the other hand, is lasting as long as there is an external loading (here the wave forces). Therefore the particular solution of the equation of motion will be considered here.

So when damping the movement, one has to dampen the impact from the particular solution.
The damping itself is normally referred to as c, as shown in equation 31 for a one degree of freedom system which is critically damped. If the damping formula is to express oscillating damping it has to be $(c) < 2m\omega_0$ (Gudmestad, 2013a).

$$c = 2 \cdot m \cdot \omega_0 \qquad \text{[kg/s]} \qquad \text{(Eq. 31)}$$

Here:

- ω_0 is the vessel's Eigen/natural frequency [s^{-1}]
- *m* is the vessel's mass (displacement) [kg]

Also the damping could be referred to as the relative damping (coefficient), λ, see equation 32 (Gudmestad, 2013a).

$$\lambda = \frac{c}{2m\omega_0} \qquad \text{[-]} \qquad \text{(Eq. 32)}$$

When the expression in equation 32 is one (λ = 1), the damping is critical ($c = 2m\omega_0$).
When the relative damping has a value below one (λ < 1), one say that the damping is under critical. This is the most normal case in nature and is explaining the natural damping.

The particular solution of the motion (response) can be expressed by harmonic loading as this is what applies for wave loading. The harmonic loading is expressed in equation 33 (Gudmestad, 2013a).

$$Q(t) = Q_0 \cdot \sin(\omega t) \qquad \text{[N]} \qquad \text{(Eq. 33)}$$

The particular solution of motion can then be written as the response shown in equation 34 (Gudmestad, 2013a). This motion will last as long as there are external loads on the system.
φ is the phase angle.

$$u_{particular}(t) = u_0 \cdot \sin(\omega t - \varphi) \qquad \text{[m]} \qquad \text{(Eq. 34)}$$

The amplitude, u_0, is given by equation 35 (Gudmestad, 2013a).

$$u_0 = \frac{Q_0}{m\omega_0^2} \cdot \text{DAF} = \frac{Q_0}{K} \cdot \text{DAF} \qquad \text{[m]} \qquad \text{(Eq. 35)}$$

In the formulas:

- ω is the incoming wave frequency [s^{-1}]
- Q_0 is the static loading [N]
- *DAF* is the Dynamic Amplification Factor [-]
- *K* is the water plane stiffness [kg/s^2]

The dynamic amplification states how large the dynamic motion response is compared to the static motion response caused by the static loading, Q_0.

The ratio between wave and vessel frequency is represented by beta. This is known as the relative frequency and is shown in equation 36.

$$\beta = \frac{\omega}{\omega_0} \qquad \text{[-]} \qquad \text{(Eq. 36)}$$

When the vessel get in resonance with the waves (i.e. $\omega = \omega_0$) the relative frequency is equal to one.

The phase angle between the harmonic loading, *Q(t)*, and the harmonic motion response, $u_{particular}(t)$, is given in equation 37.

$$\varphi = \tan^{-1}\left(\frac{2\lambda\beta}{1-\beta^2}\right) \quad \text{[deg.]} \qquad \text{(Eq. 37)}$$

The dynamic amplification is normally referred to with the Dynamic Amplification Factor (DAF). The DAF is used in structural design and marine operations to take into account the dynamic effects. If the damping is reduced, the DAF also reduces (Gudmestad, 2013a).
The DAF takes into account the damping of the system (here vessel) as well as the relative frequency between the waves and vessel, see equation 38.

$$DAF = \frac{1}{\sqrt{(1-\beta^2)^2 + (2\lambda\beta)^2}} \qquad \text{(Eq. 38)}$$

The DAF explains the relationship between the vessel's motions without any damping features and with damping features. In other words the DAF is limited by the inherent damping of the ship, which in case of the roll will be the viscous damping and the bilge keel damping as mentioned earlier.

When there is resonance the relative frequency is equal to one. Then the formula for the DAF can be simplified. See equation 39 (Gudmestad, 2013a).

$$DAF = \frac{1}{\sqrt{(1-\beta^2)^2 + (2\lambda\beta)^2}} \xrightarrow{\beta=1} \frac{1}{2\lambda} \qquad \text{(Eq. 39)}$$

Equation 39 represents the maximum value for the DAF and the smaller the damping is, the larger the DAF will be. So the lower the DAF is, the more efficient the system is damped. For example when having damping features like bilge keels as shown in Figure 3.12. At resonance ($\beta = 1$) the DAF is only determined by the damping coefficient of the system. Typically this is well below 0.20 for ships.

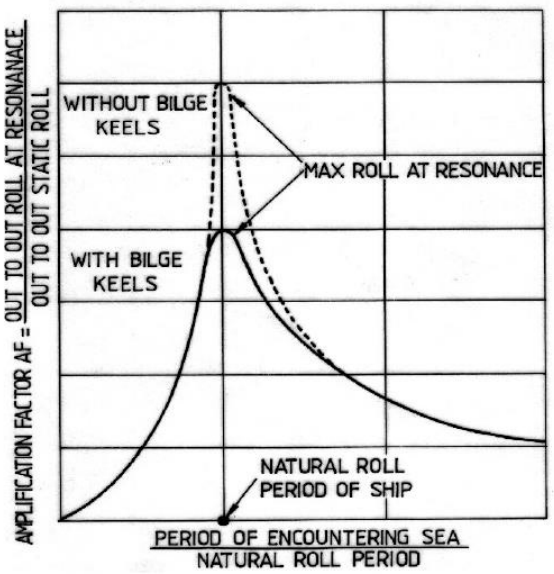

Figure 3.12: Illustration of dynamic amplification, showing motion response with and without bilge keels at resonance for roll (Samoilescu & Radu, 2002)

3.5 Vessel speed

The displacement RAOs provided by STX is based on a stationary vessel, i.e. zero knots (nautical miles/hour), so this must be applied in the analysis. One may assume in the analysis that the vessel, during this operation, mostly will be operating on DP, hence there is not much vessel velocity (≈ 0 knots).

3.6 Modelling of the moonpools

In order to create a proper analysis of Normand Vision's vessel motions, one will need to take into account the three moonpools in the vessel. When the hydrodynamic analysis of the vessel was done in VERES, the vessel's three moonpools was taken into account (STX OSV, 2013a).
This means that the moonpools are included in the displacement RAOs used in OrcaFlex and hence affect the motions of the vessel. So the moonpools are already "modelled" through the RAOs, however, they will be modelled visually to show their location for easier reference in the analysis. This is needed in order to check how the flexible flowline is going through the main moonpool with respect to clashing and deviation angle from the vertical before leaving the vessel at the very bottom of the hull.

3.7 Length and mass of vessel

The length of the vessel that Orcaflex requires for the analysis is the length between perpendiculars, which is the distance from where the bow is in contact with the water, and all the way back to the location where the shaft of the rudder is located.
The specified length between perpendiculars (often abbreviated L.L.P.) for Normand Vision was calculated by VERES to be 144.510 meters for the two Load Cases the RAOs are based on. Therefore this value was used in the OrcaFlex analysis.

The mass of the vessel, the total displacement, was set to 23017.36 and 23637.86 tonnes (based on the VERES calculations) for Load Case 1 and 2 respectively (shown in Table 3.1 in sub-chapter 3.9). The various masses are described somewhat further in the Load Case presentations in chapter 6.

The moment of inertia and added mass are already incorporated in the displacement RAOs as it is based on the total displacement of the vessel and how submerged it is, i.e. the geometry of the hull and the draft (the wet area).

The displacement RAOs are of course the basis for the most calculations done by OrcaFlex, especially when considering uncoupled motions. For example, when only looking at the vessel, the total vessel motion could be seen as "uncoupled"/unrestricted, as only the environment (wind, currents, waves/water in contact with the hull) affects the vessel.
When e.g. attaching a flexible flowline during a pipe lay operations, the vessel's motions will actually in theory be coupled.
However, this coupled motion will in most engineering aspects be considered as negligible as the flowline's effect on the vessel will be very, very small. But in practice when a flowline is suspended from the vessel, it will of course pose some extra load (weight) on the vessel. This extra load will increase the water plane stiffness as the weight of the flowline will make the vessel float slightly lower in the sea (larger draft, less freeboard), because of the added weight (see Fig. 3.13).

This will cause the water plane area, which contribute dictating the water plane stiffness (ref. equation 40), to increase as the draft increases. Hence will also the buoyancy force (or pressure) on the vessel increase.

$$K = \rho g A \qquad \left[\frac{kg}{s^2}\right] \qquad \text{(Eq. 40)}$$

Here:

- K = Water plane stiffness [kg/s^2]
- ρ = Density of sea water [kg/m^3]
- g = Gravitational constant [m/s^2]
- A = Water plane area [m^2]

Put simply; larger water plane stiffness will cause the vessel to be more stable.
This means that the vessel will be dampening its heave motions more quickly because of a larger contact area between the hull and the water. If the attached load (weight) to a vessel is smaller than typically 5-10% of the vessel's total mass (displacement) it will normally not be considered to affect the vessel when doing analysis (Zhan, 2014).

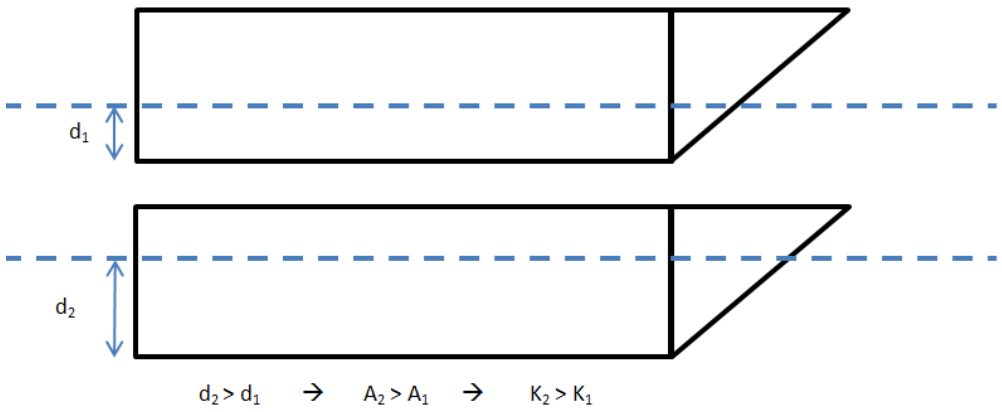

Figure 3.13: Figure showing how the water plane stiffness (K) increase when the draft (d) and water plane area (A) increases

As an example of the magnitude in this particular case one could consider 540 meters of the 8 inch flexible flowline going from the vessel to the touch down point.
This flowline have a submerged weight, including the freshwater inside used during the installation (density ≈ 1000 kg/m^3), of ≈ 78.3 kg/meter.
This makes up a total submerged weight of the flowline similar to ≈ 42.282 tonnes.

If this is compared to Normand Vision's displacement (both for Load Case 1 and 2) it can be observed that this corresponds to less than 0.184% of the vessel's displacement and will practically speaking not affect the vessel at all.

3.8 Layout model of the vessel

In OrcaFlex the standard set up for a layout model of a vessel is a shown in Figure 3.14.
Here the CoG is set to be in the exact center of the vessel. This goes for longitudinal, vertical and transverse point for the CoG. This model is very simple as it does not show the shape or any features of the vessel to be analysed.

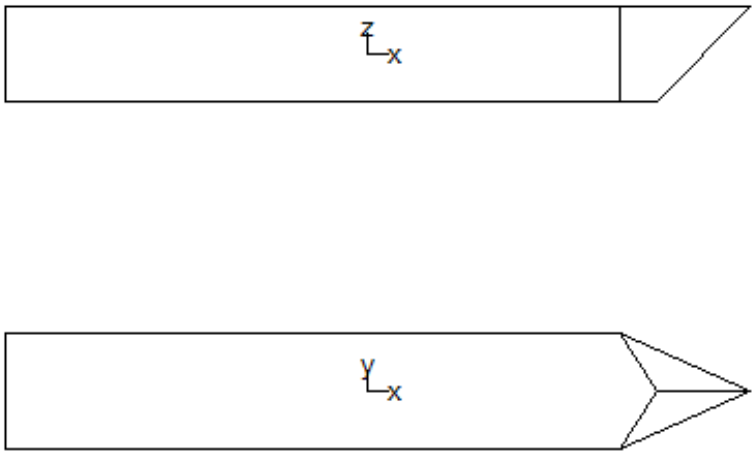

Figure 3.14: Standard layout model of vessel in OrcaFlex

To get a better looking and much more representative layout model of the vessel in question, a layout model of Normand Vision was constructed based on drawings of the general arrangement of the vessel. The model consists of 294 nodes and 465 edges. Microsoft Excel was used for the purpose of making the model. In this model it was favourable to place the origin for the local coordinate system of the vessel in the very centre of the work/main moonpool, as the activities that are to be analysed takes place here. Then it is much easier to specify out from this origin other points of interest on the vessel.
The positive directions of the axes can be seen in Figure 3.15. The VLS was attached as an object and is not part of this layout model and is therefore not showing in Figure 3.15.

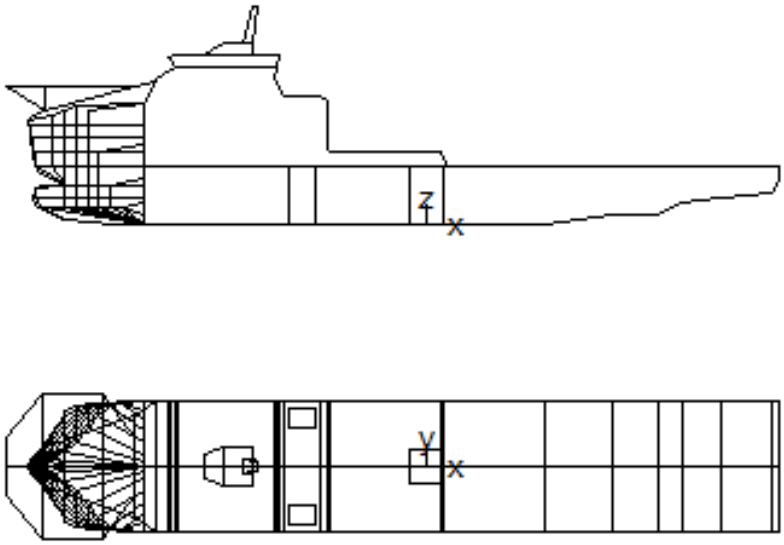

Figure 3.15: The OrcaFlex layout model made of Normand Vision

3.9 RAO and phase angle conventions in the analysis

To obtain good and reliable results from the analysis one of the most important things is to get the sign convention right. From the RAO-report provided by STX OSV the sign convention for the translational and rotational displacement, for all six DOF, are given as follows (STX OSV, 2013a):

- Surge is positive aft
- Sway is positive to starboard
- Heave is positive upwards
- Roll is positive with starboard side upwards
- Pitch is positive with bow upwards
- Yaw is positive with bow to port side

So this was also used in OrcaFlex. See also Figure 3.16 for a visual description of the coordinate system.

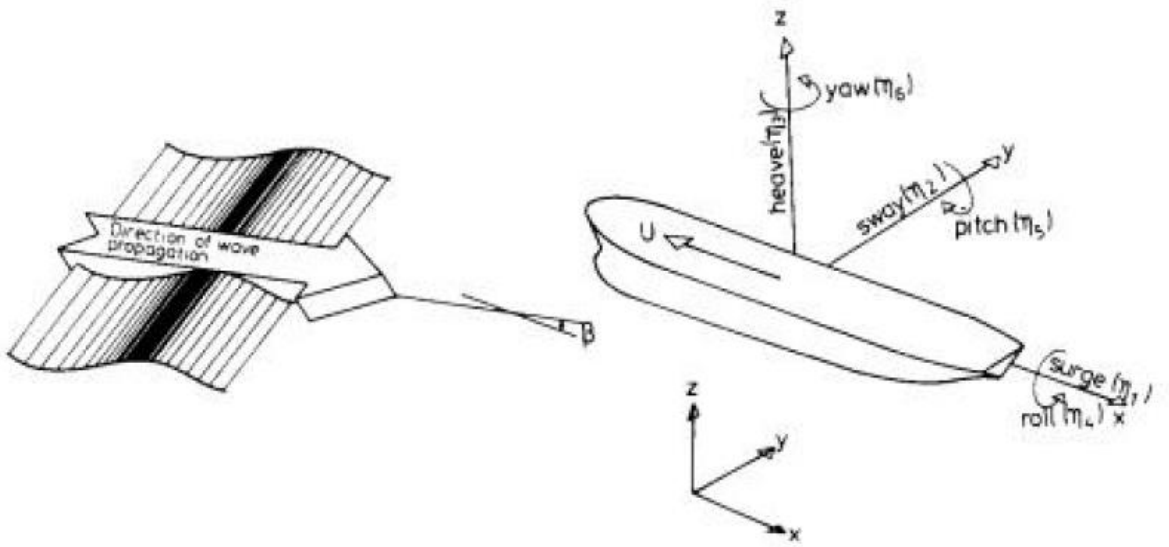

Figure 3.16: Visual presentation of the coordinate system which the vessel's displacements are based upon (STX OSV, 2013a)

The displacement RAOs provided by STX OSV is given in meter per meter of incoming wave height for the translational displacements, and as degrees per meter of incoming wave height for the rotational displacements.

As earlier mentioned the phase angles of the RAOs tell when the maximum vessel response occurs compared to the maximum wave elevation. Also the phase has to be defined in OrcaFlex either in degrees or in radians. The phase angles supplied by STX OSV were in degrees, so this was used in OrcaFlex. The phase angles were set as leads and negative phase angles was corrected for.

When it comes to the location of the "point of motion" for the RAO calculations it can be specified with help of the Centre of Gravity (CoG). This "point of motion" is the origin of where the RAOs are calculated. For simplicity the RAO origin is often set equal to the CoG for analysis purposes (Zhan, 2014).

By specifying the CoG in OrcaFlex, the software will also calculate the Centre of Buoyancy (CoB) based on the vessel's total mass (displacement) and the displaced water volume.

Normally, for all sort of monohull vessels, the CoG and CoB are located along the same vertical line. The CoB is always located in the geometrical centre of the submerged part of the hull.
When OrcaFlex calculates the CoB it will be located at the same vertical line as the CoG.

In the hydrodynamic calculations in VERES the vertical and longitudinal CoG was calculated as shown in Table 3.1 (STX OSV, 2013a). These two locations of the longitudinal CoG gravity were observed to be in the front part of the moonpool. The center of the moonpool is located at a distance of about 65.2 meters from the "zero-frame".

The CoG for the two Load Cases was presented in the following coordinate system, see also Figure 3.17:

- The baseline of the vessel (keel/bottom of the hull) defines Z = 0
  - Positive Z direction is upwards
- The "zero-frame" (just in front of the propeller, see Fig. 3.17) is defining X = 0
  - Positive X direction is towards the bow
- The longitudinal centreline of the vessel defines Y = 0
  - Positive Y direction is towards starboard

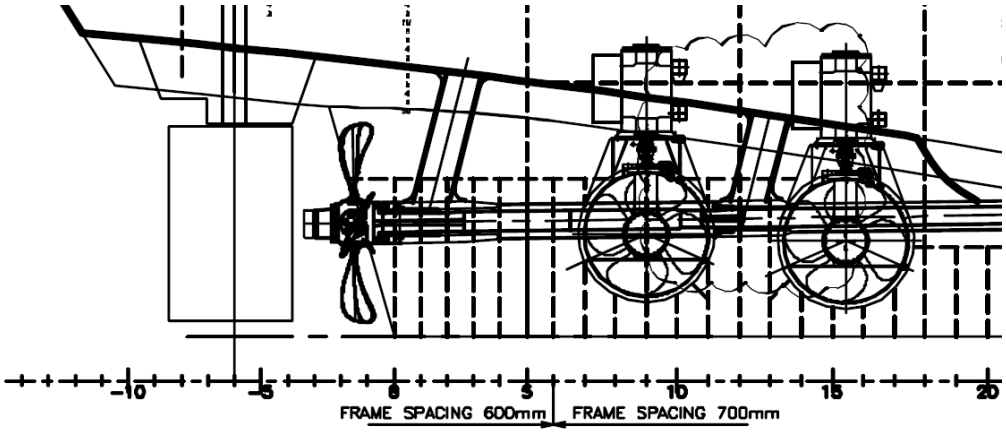

Figure 3.17: Extract from drawings of Normand Vision showing the "zero-frame", centre of the rudder is located at the -6 frame (STX OSV Design AS, 2012)

For convenience the vessel's local coordinate system was adjusted to be in the center of the moonpool, as shown in the layout model (ref. Fig. 3.15). So then the longitudinal CoG has to be specified in OrcaFlex from this origin instead, which gives a "new/corrected" longitudinal CoG presented in Table 3.1.

Table 3.1: Overview over the different CoG and CoB calculated in VERES, "new" longitudinal CoG, as well as the draught and displacement for the two Load Cases (STX OSV, 2013a)

Parameter:	CoG, Load Case 1	CoB, Load Case 1	CoG, Load Case 2	CoB, Load Case 2
Longitudinal [m]	67.808	67.808	66.804	66.804
"New" longitudinal [m]	2.608*	N/A	1.604*	N/A
Transverse [m]	0.000*	0.000	0.000*	0.000
Vertical [m]	10.080*	4.507	11.130*	4.589
Mean draught [m]	8.171*		8.303*	
Displacement [tonnes]	23017.36*		23637.86*	

*Used as input in the OrcaFlex model of the vessel

4 Modelling of the environmental conditions

In this chapter the background for the various input parameters and data used in the modelling of the environment is described as the environmental conditions used in the analysis will affect the outcome.

4.1 Water depth and location

The analysis will be based on a case study for a location in the North Sea. A water depth of 350 meters will be used in the analysis. This is a typical water depth in certain parts of the Northern North Sea (in the Tampen area), e.g. on the Snorre and Visund fields.

4.2 Sea state and weather conditions

4.2.1 Wave models

For waves to be treated by using a linear model (use of linear potential theory for waves) one must assume that the water surface slope is very small, which means that any steepness squared terms in the equations of motions are ignored. The profile of such a wave with small steepness will then look like a sine or cosine wave. Then the velocity potential (see equation 41) can be written as a linear equation with an unknown function of *P(z)* to be determined (Journèe & Adegeest, 2003).

$$\Phi_w(x_0, z, t) = P(z) \cdot \sin(kx_0 - \omega t) \quad [m/s] \qquad \text{(Eq. 41)}$$

Here:

- x_0 is the wave propagation [m]
- ω is the wave amplitude [s^{-1}]
- k is the wave number [m^{-1}]

In order to be applicable to harmonic waves this wave velocity potential must satisfy four fluid dynamical requirements:

- The continuity condition/Laplace equation for a homogeneous and incompressible fluid
- Seabed boundary condition, no vertical velocity of water particles at the seabed and that the bottom is flat
- Free surface dynamic boundary condition, the pressure at the free water surface (still water surface) is equal to the atmospheric pressure
- Free surface kinematic boundary condition, which means the vertical velocity of a water particle in the free surface of the fluid is identical to the vertical velocity of the free surface itself)

With help of these four requirements one can derive the final wave velocity potential equation by determining P(z). The derivation will not be carried out in detail here, but the most used result is stated in equation 42 (Journèe & Adegeest, 2003).

$$\Phi_w(x_0, z, t) = \frac{-\zeta_a \cdot g}{\omega} \cdot \frac{cosh[k(h+z)]}{\cosh[kh]} \cdot \sin(\omega t - kx_0) \quad [m/s] \qquad \text{(Eq. 42)}$$

Here:

- g is the acceleration of gravity [m/s^2]
- h is the distance from the water surface to the seabed, i.e. h is the water depth [m]
- z is the actual level of interest, positive upwards, zero at still water level

The formula presented in equation 42 is applicable for any water depth, and is the velocity potential model for linear waves also used for linear waves modelling in OrcaFlex.

The formula (eq. 42) can also be simplified if it is to be applied only for deep water for example. This deep water approximation can be used when the water depth is considered as deep. What is considered deep can vary, but here the following definition presented in equation 43 will be used (Gudmestad, 2013c).

$$\frac{\text{Water depth}}{\text{Wave length}} > 0.5 \rightarrow \ Deep\ water\ appoximation\ OK \qquad [-] \qquad \text{(Eq. 43)}$$

If this inequality, "the deep water approximation" (eq. 43), is fulfilled the simplifications shown in equation 44 can be used. Equation 42 is then simplified if the water depth is "deep" and this makes some of the terms very small so that they can be set equal to zero as shown in equation 44.

$$\frac{\cosh\big(k(h+z)\big)}{\cosh(h+z)} = \frac{\frac{e^{k(h+z)} + \overbrace{e^{-k(h+z)}}^{\approx 0}}{2}}{\frac{e^{kh} + \overbrace{e^{-kh}}^{\approx 0}}{2}} \approx \frac{e^{k(h+z)}}{e^{kh}} = \frac{e^{kh} \cdot e^{kz}}{e^{kh}} = e^{kz} \qquad \text{(Eq. 44)}$$

With this simplification the velocity potential equation (eq. 42) can be written <u>for deep water</u> as in equation 45.

$$\Phi_w(x_0, z, t) = \frac{-\zeta_a \cdot g}{\omega} \cdot e^{kz} \cdot \sin(\omega t - k x_0) \quad [m/s] \qquad \text{(Eq. 45)}$$

4.2.2 Wind seas and swells

Generally the wave conditions in a sea state are divided into two parts; wind seas and swell. Wind seas are locally generated by wind blowing over the ocean giving birth to local waves. How large the created waves are depends on the velocity of the wind and the fetch length/fetch area. The swell waves have no relationship to the local wind seas, but are generated elsewhere and has travelled out of the areas where they were generated. Normally sea states in open areas (as offshore) are composed of both wind seas and swells (DNV, 2011).

4.2.3 Random (irregular) waves

Real ocean waves (composed of wind seas and swells) are irregular and random in shape, height, length and propagation speed. Therefore a real sea state is best described by random wave models.

A random wave model could be either linear or non-linear. A random linear model is the sum of the contributions of many linear wave components having different amplitude/height, frequency/period and direction. Here each individual wave component has a constant amplitude and frequency. The phases of these different individual components are random with respect to each other.

A random non-linear model allows for non-linear interaction between the individual components with different frequencies and amplitudes within themselves and they come from different directions, a good mixture in other words (DNV, 2011).

The random (irregular) waves are usually modelled stochastically as linear random waves by using wave spectra for determining various parameters as peak period and zero up-crossing periods. The peak period is where the waves have their highest energy potential. Different wave spectra apply for different ocean areas. However, these models can be complex and it is often hard to determine their parameters accurately, and a number of assumptions are normally made (DNV, 2011).

The irregular waves are most easily described by Fourier decomposition. This break down the complex waves into several sine and cosine wave components, which combined represent the real irregular sea state. In other words; by taking the individual sine and cosine wave components and put them "on top of each other" one gets the real irregular sea state.

When doing analysis in software like e.g. OrcaFlex, one is normally interested in what the maximum values are. For example, what is the maximum compression the pipe will see? Or what would the maximum drag forces be?
When an irregular sea state is used in an analysis one will in general get an average wave height and hence average values for various parameters. Then statistical methods are used to calculate what maximum values one could expect. OrcaFlex provides possibilities for calculating such extreme values based on different statistical distributions. In Orcaflex one could choose between Rayleigh, Weibull and Generalised Pareto distributions for this purpose (Orcina Ltd., 2013).

OrcaFlex provide different wave spectra to use for analysis with an irregular sea state, e.g. JONSWAP, Torsethaugen, modified Pierson-Moskowitz/Bretschneider, Ochi-Hubble and Gaussian Swell (Orcina Ltd., 2013).

4.2.4 Regular waves

So-called regular waves have a regular sinusoidal form. They propagate with a permanent shape. Regular waves are recognized as rather long-crested and not very steep (swell-like). Regular linear waves are often referred to as Airy waves. These waves take into account the influence from the seabed on the wavelength.

When linear wave theory is used one simplifies by excluding the higher order terms from the velocity potential to make the calculations easier. This may give a more imprecise description of the waves. There exist other regular wave models adding higher terms to give a more precise description of the behaviour of the waves.

These are e.g. Stokes' 5th order waves (steeper than Airy waves); Dean Stream waves or Cnoidal waves (even steeper). Also these can be modelled in OrcaFlex. See a comparison between these waves in Figure 4.1. A Stokes' 1st order wave coincides with a linear (Airy) wave.

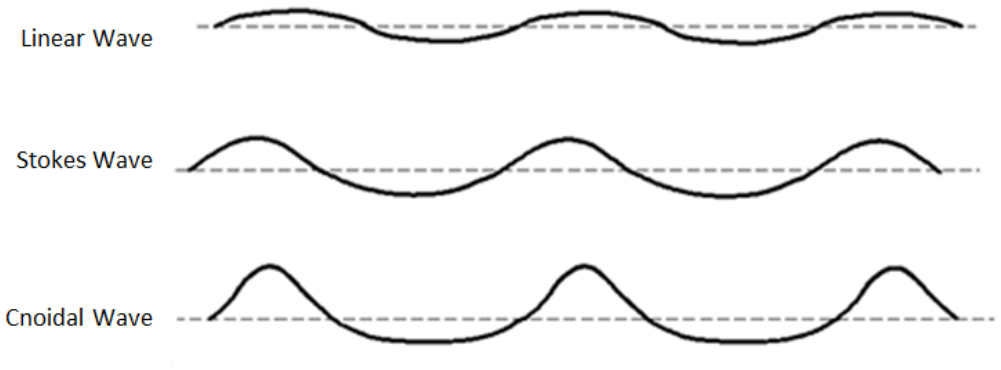

Figure 4.1: Comparison of some regular waves (Flow Science Inc., 2011)

In the OrcaFlex analysis "Stokes' 5th order wave model" was used as wind seas were not taken into account when the RAOs were made (STX OSV, 2013a). These regular waves are considered as a good linear wave model, providing more precise results than e.g. Airy waves.

4.2.5 Waves used in the analysis

Waves used for planning and analysis of marine operations are normally based on metocean data gathered in a metocean design basis. This metocean design basis is often incorporating data from a longer period of time, e.g. observations from the last 30 years or so.
A metocean design basis is often provided by the operator of the actual field in question. The waves one could expect in the North Sea for the Snorre field should be determined from data based on a number of measurements from that particular area. The design waves in the metocean design basis are based on Stokes 5th order theory.

In DNV different methods for defining the design sea state is outlined. Design waves are often regular/linear waves (like e.g. Stokes 5th order waves used in the analysis) used for e.g. load calculations, analysis purposes and more. They are normally determined by deterministic or stochastic methods. Also wave spectra can be used for determining design waves (DNV, 2011b).

In this case, when doing the simulations in OrcaFlex, the vessel can be seen as a quasi-static system because of the large displacement and rather slow motions (e.g. long roll periods). This should be applicable as quasi-static response calculations often are used in early design stages (Buannic, et al., 2009). Quasi-static response justifies using deterministic regular waves in the analysis according to DNV-RP-H103. In DNV-RP-H103 it is stated that it can be sufficient to use deterministic regular waves characterized by wave length, period, and height when looking at quasi-static response of structures. These deterministic parameters are best predicted by statistical methods, normally from a metocean design basis (DNV, 2011). In OrcaFlex the waves can be specified in terms of the waves' height, period and direction of propagation (Orcina Ltd., 2013).

First a short summary of some of the most important wave parameters will be presented.

- **Significant wave height.** Probably the most used reference to real waves is the so-called significant wave height (H_S). This parameter is used for the random/irregular/real sea state and defined as the average distance (height) between the wave troughs and crests of the one-third highest waves in an indicated time interval. The significant wave height is also often denoted as $H_{1/3}$. The period considered is normally between 20 minutes and 3 hours.

- **Peak Period.** Related to the significant wave height is peak period (T_P). This is representing the wave period determined by taking the inverse of the frequency (f^{-1}) at which a wave energy spectrum has its maximum value, see Figure 4.2 for visualization of a JONSWAP wave spectrum. The peak period represents inverse frequency of the highest energy of the spectrum, i.e. the highest peak. The peak depends on the peak shape parameter, γ, which relates to the type of spectrum used. This parameter can also be generally determined from DNV with the use of peak period and significant wave height (DNV, 2011).

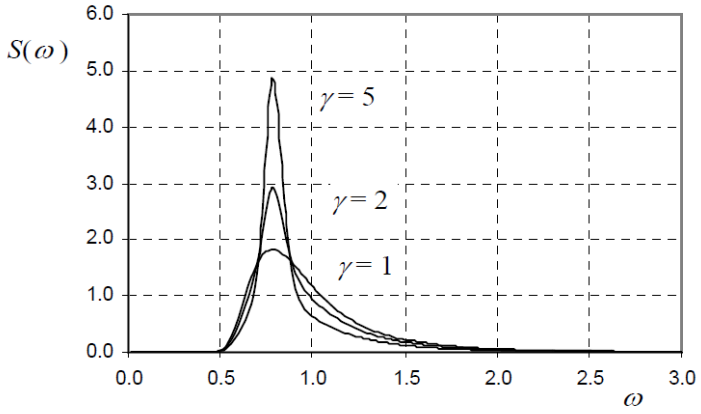

Figure 4.2: JONSWAP wave spectrum for Hs = 4 m, Tp = 8 sec. and for three different peak shape parameters (γ)

- **Zero up-crossing period.** The zero-up-crossing period (T_Z) is the average time interval between two successive up-crossings through the mean still water line.

An important aspect with design waves is where they are to be used. Are they to be used for design of structures or for load calculations related to marine operations for example? This is a relevant question because an installation operation is much shorter than e.g. the life of a platform, so the platform is therefore designed to handle much larger waves. Normally a 100 or 10000 year wave is used as the upper limit, depending on what limit state is considered. These waves have an annual probability of exceedance of 10^{-2} and 10^{-4} respectively (1% and 0.01% probability of being exceeded per year respectively).

If the same safety margin was used for an installation operation as for structural design it would not reflect the reality. However when doing analysis it should generally be looked into the probabilities of encountering large/unacceptable wave heights in the given installation window. For marine operations one would consider the weather window needed for the operation.

This would be the basis for how large the largest waves could be as well as which range of periods to consider. This has to do with the probability of seeing certain waves reflected by return periods.

However, when looking at weather restricted, short duration operations (< 72 hours) the approach of determining the design waves is simplified, as the waves are selected independent of statistical data. DNV then state that significant wave heights and periods generally should be based on (DNV, 2011b):

- Feasibility and safety of the planned operation
- Typical weather conditions at the site
- Operation period
- Uncertainties in weather forecasts

The general recommendation according to DNV is to use two times the significant wave height as the maximum design wave. This factor of two is by DNV called STF (storm factor). The value of STF should in general not be lower than two, but lower values can be acceptable (DNV, 2011b).

As the environmental conditions used in the analysis are based on a metocean design basis, the STF was determined by use of the statistical data presented in the metocean design basis. The maximum wave heights and significant wave heights with the annual probability of exceedance of 0.63, 10^{-1} and 10^{-2} were used to determine the factor to multiply the H_S with. The wave data used was the average of all months and wave directions. The factor was taken as the average. See Table 4.1.

Table 4.1: Determination of "design"/STF factor for the waves used in the analysis (Mathiesen & Kvingedal, 2010)

Annual probability of exceedance	H_{max} [m]	H_S [m]	STF ($=H_{max}/H_S$)	Average STF used
0.63	22.0	11.2	1.96	≈ 1.90
10^{-1}	25.9	13.5	1.92	
10^{-2}	29.8	15.5	1.92	

From the table one could see that an average value of 1.90 was used. This was assumed to be OK as it is based on measured statistical data, despite it was below DNV's recommended STF value.

To investigate the vessel motions and the effects on the flexible product the analysis will be executed for a range of different headings, wave heights and periods. Since the waves used in the analysis are linear their wave height is described by the design wave height (H_D) which is equal to the maximum wave height (H) so, $H_D = H$. The design wave height is based on the value of the significant wave height (H_S). The design wave is taken to be the H_S multiplied by the average "design"/STF factor as shown in Table 4.1. So the design wave height used is: $H_D = 1.9 \cdot H_S$.

Generally for analyses this factor is typically taken to be between 1.8 and 2 when using linear waves (Qayre, 2014). According to NORSOK N-003 this factor for design waves can be set to 1.9 for an annual probability of exceedance of 10^{-2} (long term statistics, 100 year wave) and a sea state duration of 3 hours (OLF and The Federation of Norwegian Industry, 2007).

The analysis will contain several simulations. The following wave heights and periods (T) will be considered:

- H_S = 2 meters → H_D = 3.8 meters, T = 6 to 18 seconds
- H_S = 3 meters → H_D = 5.7 meters, T = 6 to 18 seconds
- H_S = 4 meters → H_D = 7.6 meters, T = 6 to 18 seconds

The reasoning behind these wave heights (H_S of 2 to 4 meters) is that they represent typical North Sea (summer) conditions, which are the area in question. The range of periods (6 to 18 seconds) is taken to be sure to capture the periods where extensive roll motion will occur (especially Eigen periods in roll). These periods can be quite large (ref. Figs. 3.9 and 3.10). This range is also covering a large amount of the North Sea waves.
See Appendix G for details regarding metocean data.

Regarding the wave heights, it is usually not feasible or possible to operate in larger wave height than 4 meters H_S due to increased risk for damaging the product and/or people involved in the operation. The design wave heights may be considered as quite conservative, but they are representing the highest waves that can occur for the various significant wave heights during this rather short marine operation. Therefore the peak values regarding the vessels capabilities are captured. These regular waves approaching the vessel have the same magnitude (amplitude) during the whole analysis. In reality one would generally only have seen some peaks with this large wave height in a sea state.

From the metocean design basis the expected 100 years scatter diagram (regarding H_S and T_P) show that these conditions will be quite representative for a large portion of the time for this actual area, see Table 9.6 and the figures in Appendix G. Duration of the sea state is 3 hours. The scatter diagram is included as Table G.0.1 in Appendix G and its distribution of peak periods and significant wave heights are presented in Figures G.0.4 and G.0.5.
As can be seen from the NORSOK map in Figure 4.3 the maximum peak period and significant wave height one will experience with a 10^{-2} probability of exceedance for 3 hours duration at the Snorre field are:

- $T_P \approx 16.5$ seconds
- $H_S \approx 15$ meters

This coincides fairly well with the information in the metocean design basis, which states an extreme H_S of 15.5 meters for the 100 years wave (ref. Table 4.1). The peak period (T_P) for the 100 years wave also coincide quite well with the metocean design basis, as it operates with a peak period of 17.5 seconds (Mathiesen & Kvingedal, 2010).

Significant wave heights and peak periods of this magnitude are of course rare events, but these conditions can be present for some time once in a while. However, for a pipe installation operation as considered here it should of course not happen, as it is a very short operation planned to be carried out in a much more favourable sea state according to best practice and based on weather forecasts.

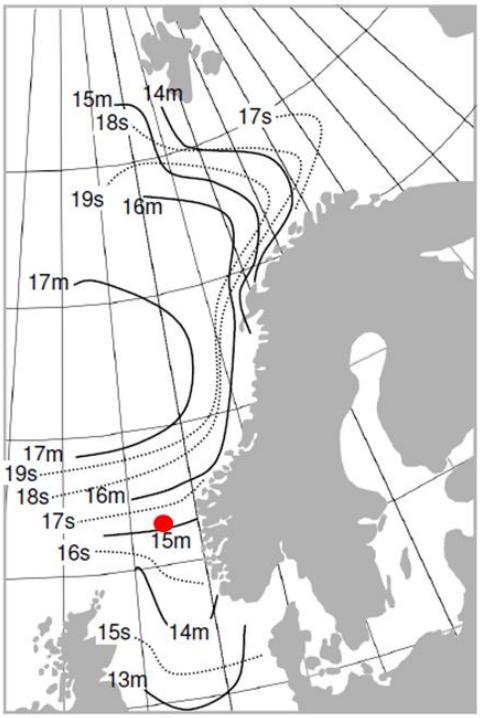

Figure 4.3: Significant wave height H_S and related maximum peak period T_P with annual probability of exceedance of 10^{-2} for sea-states of 3 hours duration. ISO-curves for wave heights are indicated with solid lines while wave period lines are dotted. The red point marks the approximate position of the Snorre field (OLF and The Federation of Norwegian Industry, 2007)

4.2.6 Weather conditions related to marine operations

Marine operations may be delayed due to e.g. the significant wave height exceeding a prescribed operational limit leading to a possible increase in the duration of the operation. Commonly delays caused by weather are generally referred to as Waiting on Weather (WoW).
Marine operations can hence be divided into critical and non-critical operations, where the critical operations have to be executed from start till end without being halted. A pipe lay operation can be considered critical as there may be no room for an easy and quick disconnect if it should be necessary, e.g. due to bad weather coming up. This could also be referred to as a weather restricted operation, which is the term used by DNV. According to DNV all marine operations planned to last less than 72 hours should be considered as weather restricted (DNV, 2011b).

In this analysis the operation will be considered carried out during the summer season (May to August) when the waves are most “cooperative”. As the flowline to be installed is considered to be rather short, 540 meters (ref. chapter 5) the operation is considered to be completed within a short period of time, e.g. less than 24 hours. The surveying (before and after), preparations and tie-in will probably take much more time than the out reeling installation of the flowline.

Some diagrams showing the expected duration for an operation planned to be completed within 24 hours for the different significant wave heights are included in Appendix G (ref. Figs. G.0.1, G.0.2 and G.0.3).

From these figures it can be observed that the average <u>total</u> expected duration (T_R) of a 24 hours summer operation, including delays/waiting time (T_{C1}), are about 2 days, 1.2 days and 1.0 day if one should not see waves equal to or larger than H_S 2, 3 and 4 meters respectively (for May to August). Because of such delays the need of a larger weather window should be planned for. How much delays that could be accepted due to WoW are often a discussion when putting up obligations in contracts. Often the client has to take the largest risk here.
According to DNV this expected delay time may be referred to as the "estimated contingency time", T_C. This contingency time is mainly included to cover uncertainty in the planned operation time (T_{POP}) and possible unforeseen delays, meaning it will take longer time to complete the operation than first anticipated. See equation 46 for the relation of the contingency time and planned operation time to the total operation reference period, T_R (DNV, 2011b).

$$T_R = T_{POP} + T_C \quad \text{(Eq. 46)}$$

Weather forecasts are used to find suitable conditions for operations with respect to wind and waves. From DNVs recommendations this type of installation operation would require a level B weather forecast. This requires the weather forecasts to come from at least two independent sources every 12 hours, and the most severe one is to be used. Level B does not require a meteorologist on site during the operations, but it should be conferred with one if the weather situation is unstable or close to the operational limits (DNV, 2011b).

Due to uncertainties in both monitoring and forecasting of environmental conditions DNV recommends to include a factor to account for this known as the "alpha factor" (α). The factor is generally used as shown in equation 47 (DNV, 2011b).

$$OP_{WF} = \alpha \cdot OP_{LIM} \quad \text{(Eq. 47)}$$

Where:

- OP_{WF} = Forecasted (monitored) operational criteria for a certain parameter
- OP_{LIM} = Operational environmental limiting criteria for a certain parameter

This alpha factor can be used in relation with the limits for various parameters. The operational criteria to be used are then defined by OP_{WF}.

It could be interesting to check the weather window with respect to the estimated contingency time (T_{C1}) from the metocean design basis, to see if it is in accordance with DNVs recommendations. The check is presented in Table 4.2.

Table 4.2: Check of weather window for a marine operation planned to be completed within 24 hours (= T_{POP})

H_S [m]	H_D [m]	T_{C1}* [days]	T_R* [days]	α factor	T_{C2} [days]***	Weather window****
2	3.8	1.025	2.025	≈ 0.80**	1.25	2.25
3	5.7	0.2	1.2	≈ 0.82**	1.22	2.22
4	7.6	0.025	1	0.82	1.25	2.25

*Based on the average of "mean expected duration" (May-August), ref. Figures G.0.1, G.0.2 and G.0.3 (in Appendix G)
**Interpolated, based on DNV-OS-H101 (DNV, 2011b)
***Calculations based on DNVs recommended alpha factors (DNV, 2011b)
****Based on the T_{C2} calculated in accordance with DNV

From Table 4.2 it could be observed that the estimated expected durations including delays (T_R) are in accordance with the weather windows calculated based on DNVs recommendations.

4.2.7 Wave directions considered

The regular waves are in the analysis applied from 3 different directions. The displacement RAOs for the different DOF are given in increments of 15 degrees. However, not all directions are applicable to consider in this analysis. Here the following 3 wave headings are assumed to be representative:

- 0° (head seas, bow right towards the waves)
- 45° (waves in between head and beam seas, normally known as bow quartering seas)
- 90° (beam seas, waves directly towards the beam/side of the ship)

The orientation of the wave directions used in relation to the vessel is shown in Figure 4.4.
Zero degrees heading is head seas and 90 degrees are beam seas toward port side of the ship.

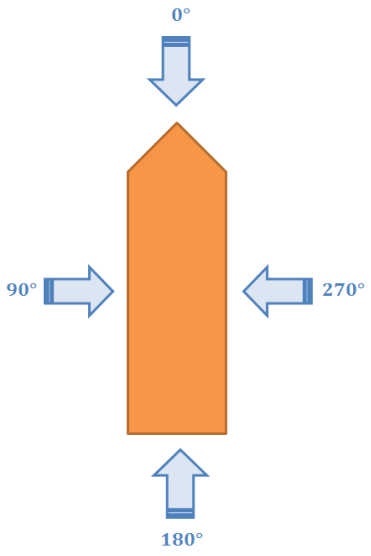

Figure 4.4: Illustration of wave directions towards the vessel

In general marine operations should be planned with the goal of having the most favourable wave heading for the vessel on the actual location, if it is possible.

Sometimes the operations are heading restricted e.g. when installing pipe on an already existing field with a lot of pipes and umbilicals on the sea bed to consider.

A wave rose for the actual location would be of great help when planning operations, to check from which directions one could expect the largest, and most of the waves to come from. Such wave roses (and normally also wind and current roses) are normally included in the metocean design basis for a field.

See Figure 4.5 for a wave rose from the Snorre field. From this wave rose it could be observed that the most and largest waves approaches from West, closely followed by waves coming from North. If a pipe is to be installed in the North-South direction this could e.g. mean that it has to be done while experiencing unfavourable beam seas on the vessel.

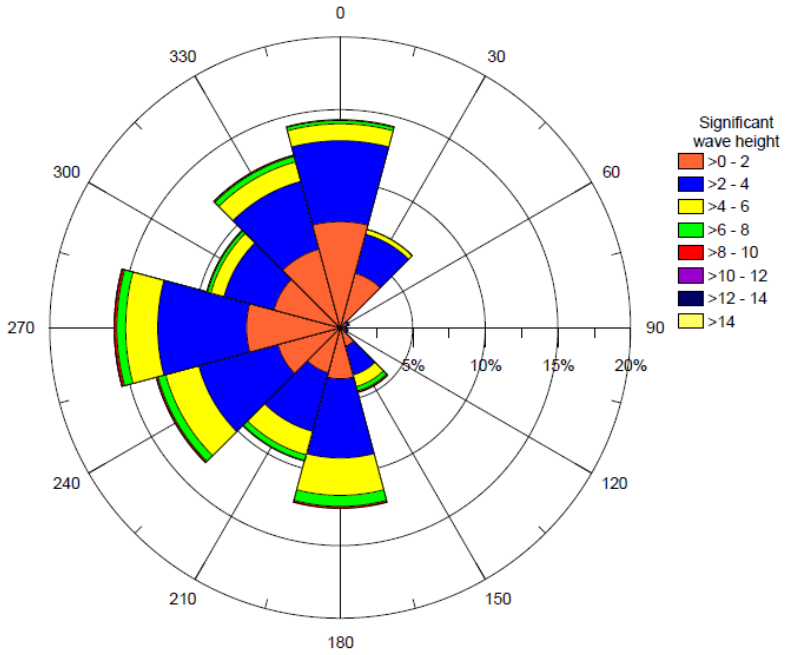

Figure 4.5: All-year wave rose from the Snorre field, based on the period 1958-2008, North = 0° (Mathiesen & Kvingedal, 2010)

4.3 Current

At the location where the flexible flowline is considered to be installed, in the Tampen area in the Northern North Sea, the Atlantic Ocean's currents originating from the West are dominating, see Figure 4.6.

These currents will give rise to hydrodynamic drag and inertia forces on the flowline. These forces can also give Vortex Induced Vibration (VIV) which could result in damages.
It could be especially severe if e.g. a riser starts to vibrate when experiencing lock-in cross-flow effect when the vortex shedding frequency is two times the natural frequency of the riser. This can give quite violent motions which are highly unfavourable and will increase the stress and risk for damages. However, this is more likely to happen to permanently installed structures like e.g. hybrid risers (Subsea 7, 2013). As the flowline here is not permanently installed and rather "free to move" it is assumed that VIV will not be an issue during installation.

The ocean currents' effects on a vessel of this magnitude are normally very small considering the vessel's response. In the OrcaFlex analysis the vessel is operating at zero knots as the displacement RAOs used was captured considering a stationary vessel.
Since the vessel's motions are described by the displacement RAOs not considering any current, it will not be applicable to include current that will affect the vessel response (Orcina Ltd., 2013).

The flexible flowline considered here will be subjected to some currents as it is hanging from the vessel's VLS tower through the water column. For the analysis the focus will be on the installation of a flexible pipeline, i.e. a temporary condition. During such an installation task the vessel will in reality be moving both relatively to the water, the seabed and the flexible pipe during the pipe installation.

From metocean data the largest average current at only 5 meters water depth, and most unfavourable heading, showed to be only 0.25 m/s. The current was smaller for all larger water depths. The wave induced bottom currents, for both JONSWAP and Torsethaugen wave spectra, was zero for wave heights up to 5 meters H_S (Mathiesen & Kvingedal, 2010). So the currents seems to be rather small at this location and it was decided to not include current in the analysis as it was tested to only have a small impact on the results.

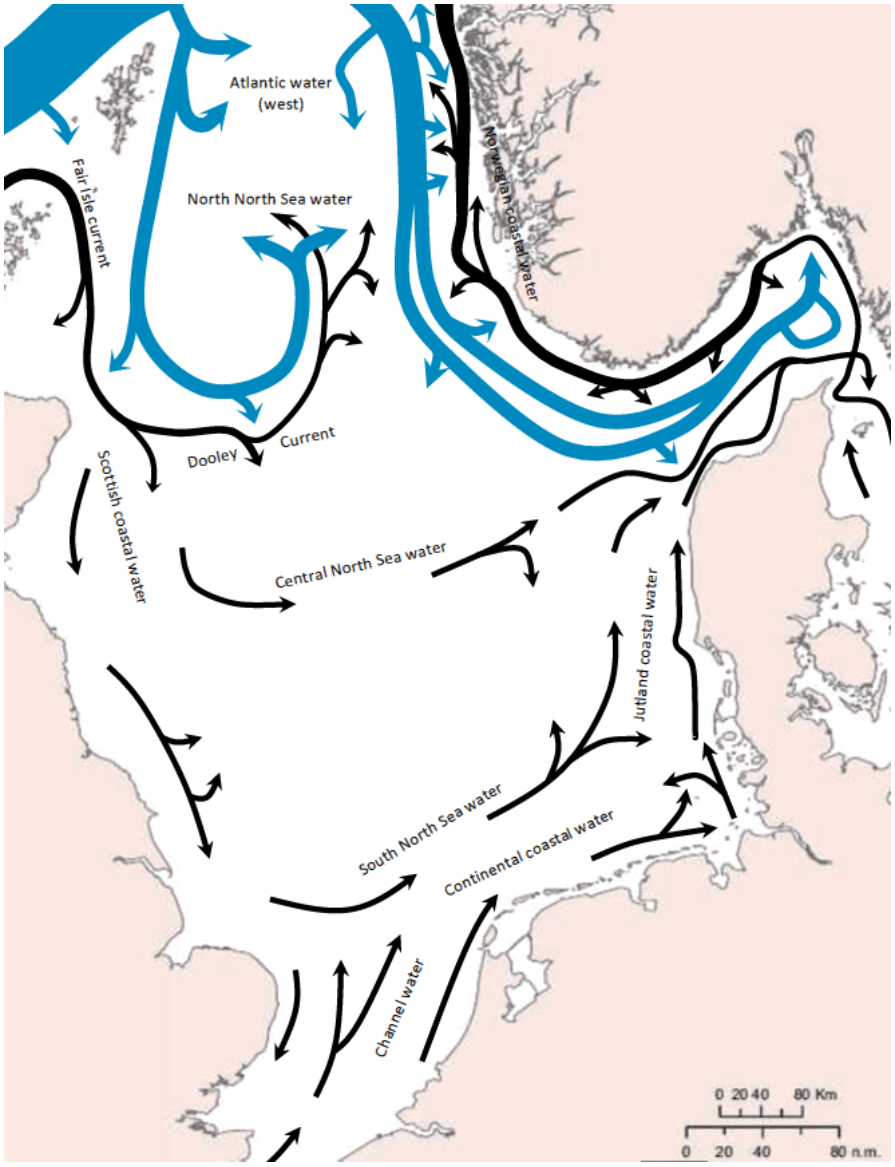

Figure 4.6: Currents in the North Sea (MEFEPO, 2009)

4.4 Wind

The wave model used (Stokes 5th order) is a regular wave model and it does not take into account wind seas and could hence be seen as pure sinusoidal waves. However, if the wind seas are to be taken into account a wave spectrum like Pierson-Moskowitz or JONSWAP would be applicable (DNV, 2011). A combination of both wind seas and swells are described in two-peaked spectra like e.g. Torsethaugen (best for North Sea conditions) or Ochi-Hubble where the largest peaks corresponds to swell waves (Orcina Ltd., 2013).

The vessel's motions are described through a set of displacement RAOs and wind effects were not taken into account when these RAOs were made, so it would not be applicable to include the wind's effect on the vessel response. This is why a regular wave model was chosen for the analysis.

Normally it is not easy to include wind effects on the vessel in this type of analysis as winds have an unpredictable nature. It does not e.g. come from one direction all the time, wind shifts may occur several times per hour and the wind may be "boosting" for periods.
To check for impact from wind on the vessel in OrcaFlex one will normally need the quadratic transfer functions (QTFs) and load RAOs for the vessel, instead of the displacement RAOs (Orcina Ltd., 2013).
Strong winds will of course affect the vessel's behaviour e.g. if one got winds directly on the side of the ship, but one will not be doing operations in such strong winds as the waves also grow to be quite large in such a situation (Svendsen, 2014).
Operating envelopes regarding wind will be shown in the vessel's capability/"DP plot". See Figure 4.7. The capability plot (envelope), here represented by the green lines, will be narrower as the vessel's capability will be reduced if some thrusters are failing or other damages occur.

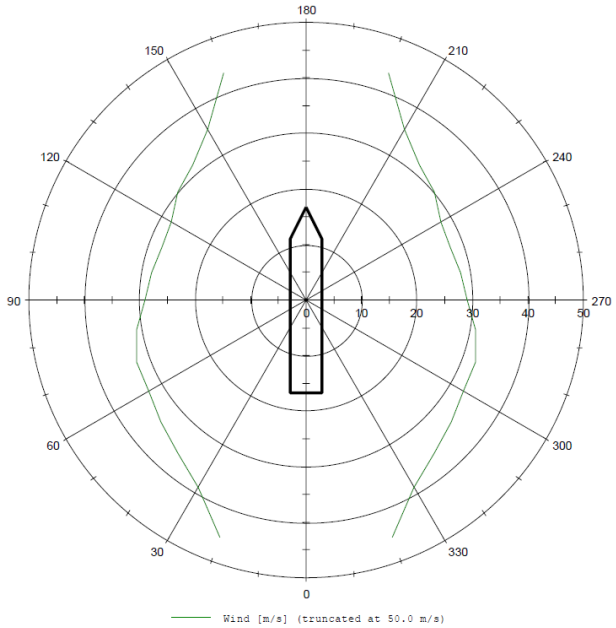

Figure 4.7: Capability plot for Normand Vision (STX OSV, 2013e)

4.5 Soil conditions

The soil conditions in the North Sea are varying between mud, clay, fine sand, coarse sand, gravels and pebbles depending on the location, see Figure 4.8. For the petroleum fields in the Tampen area the soil is mostly consisting of fine sand. However, when going down into the "Norwegian trench" (Norskerenna) one could experience varying degrees of clayish soil. Therefore a sand and clay "mixture" of the soil may be representative for the analysis (MEFEPO, 2009).

To get a realistic picture of the seabed/soil with clay and sand, geological data from the Dagny/Eirin field is used. This area is located close to the Sleipner field, south-west in the central North Sea. Dagny is located about 30 km North of Sleipner and Eirin about 9 km from Dagny (Statoil ASA, 2012).
However, the soil here is assumed to be quite similar as for the Snorre field, with a soil mix of sand and clay.

The soil data is based on a survey and laboratory tests performed by Norges Geotekniske Institutt (NGI) for the area.

Here the soil is said to consist of sand which is medium dense to dense, fine, silty and with thin layers of clay. A few shell fragments may also be found (NGI, 2012).

In OrcaFlex one can choose whether to apply a linear or a non-linear soil model. In this case it would be most realistic to use a non-linear model. The soil model used in OrcaFlex has been developed in collaboration with Professor Mark Randolph at the University of Western Australia (Orcina Ltd., 2013). For this model to be valid, data regarding the shear strength and density of the soil is required. The soil's shear stiffness is calculated based on this, see equation 48.

The soil density contains the largest amount of water at the mud line as the soil is least consolidated here. The amount at the mud line was here ≈ 27% water. The saturated soil density is taken at the mud line to be 20.3 kN/m^3 or ≈ 2069.3 kg/m^3. The undrained shear strength of the soil (F_S) at the mud line is approximately 7 kPa. The undrained shear strength gradient, s, is 10.3 kPa/m (NGI, 2012).

The soil's shear stiffness is then calculated by OrcaFlex and is hence set as default based on the formula shown in equation 48. The diameter is here the outer diameter (D) of the flexible product (ref. chapter 5). All these relevant parameters are then inserted in the OrcaFlex soil model.

$$Soil'shear\ stiffness = \left(\frac{20}{D}\right) \cdot \left(F_S + s(0.5D)\right) \qquad \text{(Eq. 48)}$$

$$= \left(\frac{20}{0.3510\ m}\right) \cdot \left(7\frac{kN}{m^2} + 10.3\frac{kN}{m^2 \cdot m}(0.5 \cdot 0.3510\ m)\right) \approx 501.9\ \frac{kN}{m^3}$$

A survey of the topography of the seabed is not carried out, so a 3D model of the seabed will not be applied. Such 3D models are also quite demanding and will cause simulations in OrcaFlex to run much more slowly.
So the seabed is assumed to be flat. Often it is sufficient to assume that the seabed is flat, as it in most cases gives satisfying results from the analysis (Gowda, 2014).

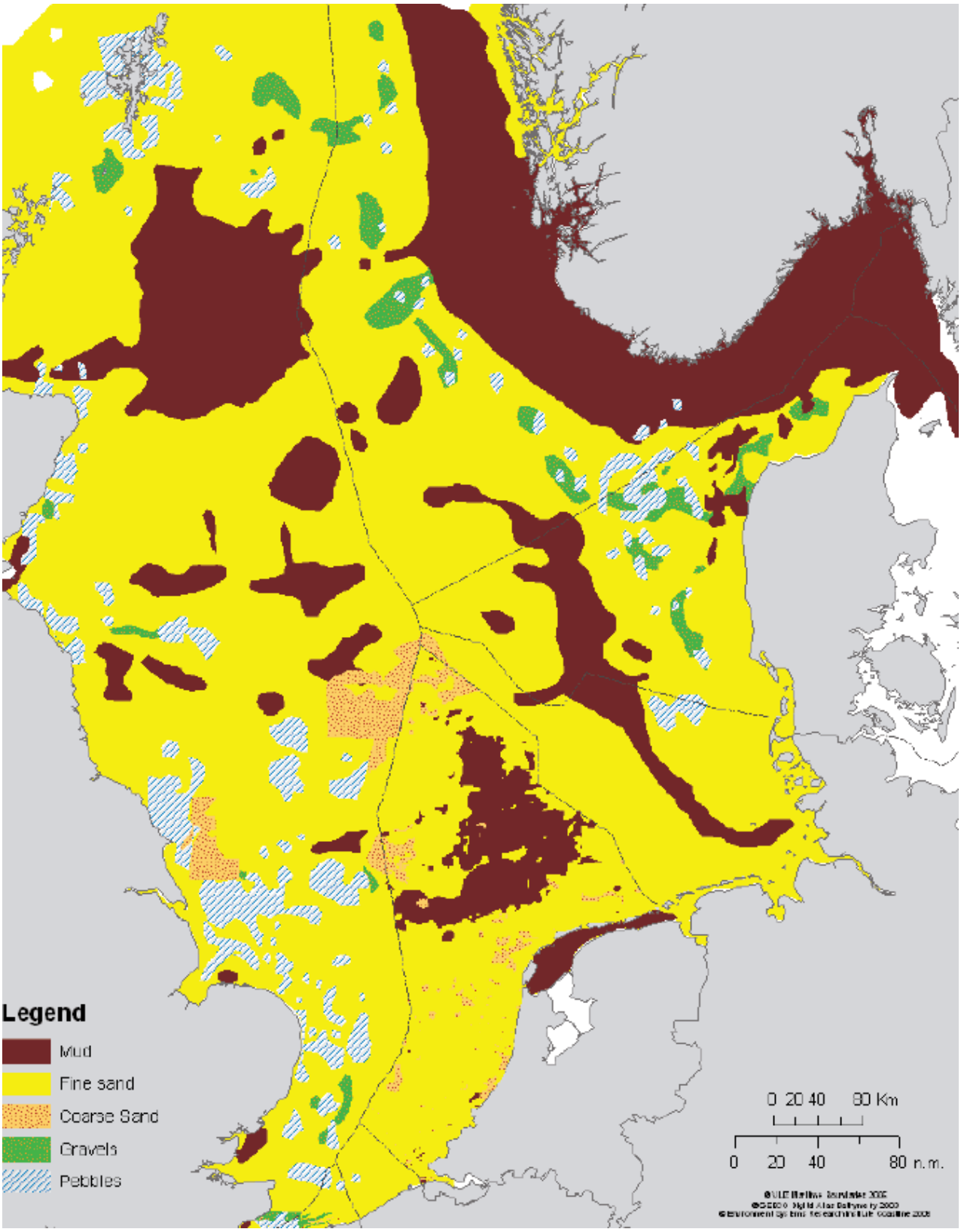

Figure 4.8: Soil conditions in the North Sea (MEFEPO, 2009)

4.6 Icing

The displacement/stability effects from icing are not included in the analysis. As most of the operations with Normand Vision will be executed out of the winter season and south of the Barents Sea, the atmospheric icing (precipitation and snow), and ice accretion by sea spray will be of small concern. If the vessel is to be used in cold climate/arctic regions, it would most likely have to go through some modifications/outfitting in order to be winterized and better prepared for the conditions it will face in such winter operations.

4.7 Sea water density, temperature and viscosity

In general the sea water is assumed to be homogeneous, non-viscous and incompressible in the OrcaFlex analysis.
The kinematic viscosity and sea water temperature can be specified if lines (representing risers, pipes and similar) are set to have lift and drag coefficients varying with the Reynolds number. The Reynolds number is used for calculation of the drag and lift coefficients of objects/lines.

Sea water density will be set to 1025 kg/m^3 and is assumed to be constant in the vertical direction of the water column. This is the most important sea water parameter as it will affect the analysis most.

Values for the sea water temperature and viscosity was specified based on metocean data, but was eventually not used by OrcaFlex, as the drag and lift coefficients was considered as constant, i.e. no need for calculations of the Reynolds number.

5 Modelling of the flexible product

In the analysis the focus will be on the use of Normand Vision during installation of a flexible product when loaded as specified in chapter 6. A typical operation that is to be performed by Normand Vision is the installation of an 8 inch flexible flowline with the use of the VLS (see Fig. 5.1), making the installation method reeled lay/J-lay, i.e. the pipe have a catenary-like shape when approaching the seabed. The same specifications for the flexible pipe are used for all Load Cases during the analysis.

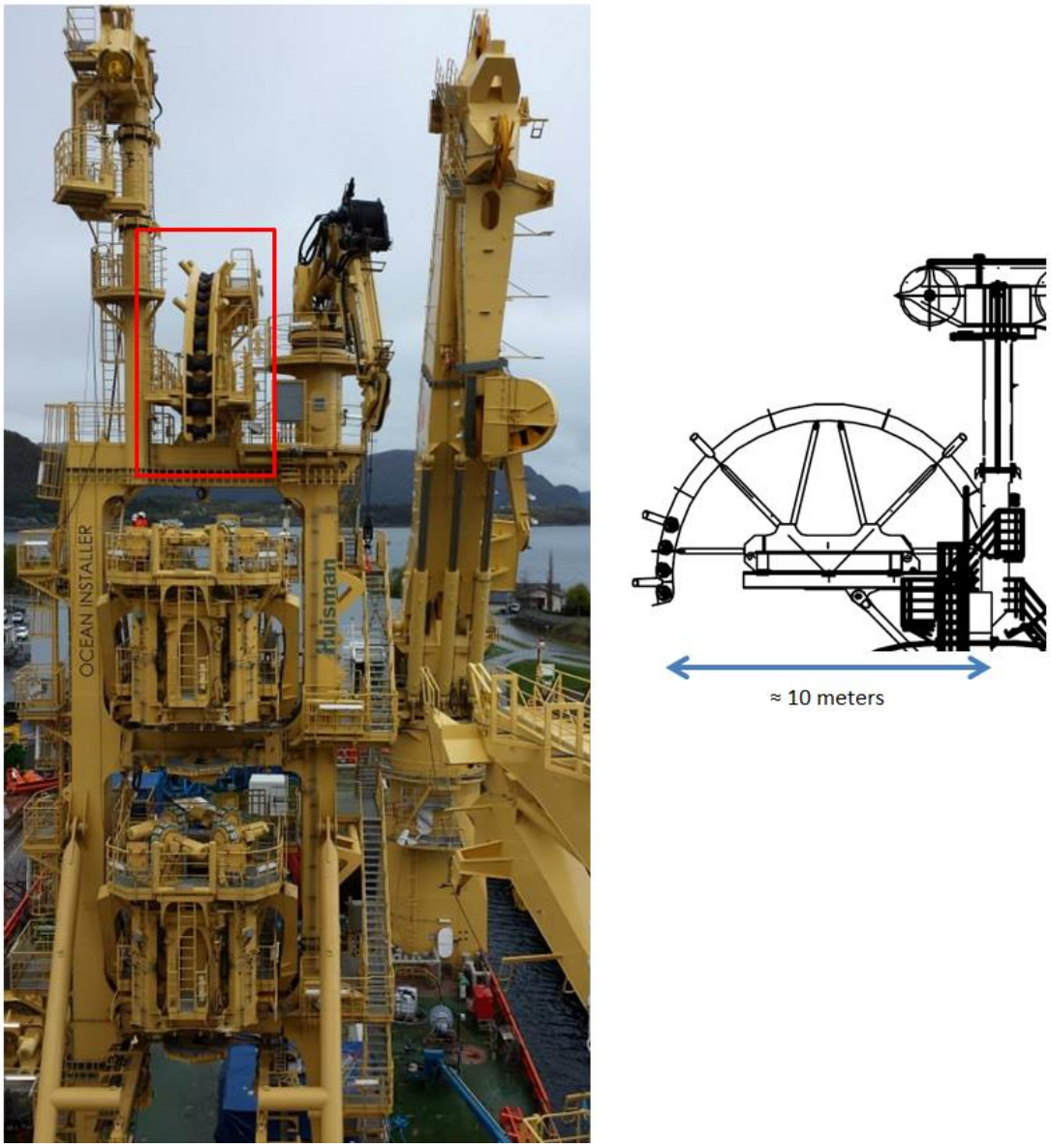

Figure 5.1: Picture of the VLS installed, the chute is marked in red box with the two tensioners located directly below, drawing of chute seen from starboard side, left: (Solstad Offshore ASA, 2014), right: (STX OSV Design AS, 2012)

The flowline is passing over a chute with a diameter of approximately 10 meters before going through the tensioners (ref. Fig. 5.1). The track tensioners are providing 4.4 meters of contact length each, so 8.8 meters in total (Huisman, 2013a).

5.1 Specifications of the flexible product

The flexible flowline to be used in the analysis will be an 8 inch production flowline for oil and associated gas. The data is obtained for a standard 8 inch production flowline from NKT Flexibles, now part of NOV. The flowline consists of 14 layers, amongst others Duplex 2101 steel carcass, sour grade steel, several layers of polyester and other plastic materials. The outer sheath is made of Medium Density Polyethylene (MDPE).

Table 5.1: Some basic properties for 8" flexible flowline used for input for the analysis (NKT Flexibles, 2011)

Parameter	Value
Inner diameter	0.2032 m (8 inch)
Outer diameter (D)	0.3510 m (≈13.8 inch)
Design (operating) pressure	220 bar
MBR (Minimum Bending Radius) at storage, no safety factor	2.28 m
MBR in service, no safety factor	2.28 m
MBR during installation at installation tension	4.69 m
Maximum allowable installation tension	382 kN
Maximum allowable axial compression during installation	50 kN
Maximum allowable axial compression when installed	10 kN
Damaging pull	2012 kN
Burst pressure	450 bar
Carcass collapse pressure	55 bar
Bending stiffness at 20 °C	223 kNm²
Axial tensile stiffness	474 MN
Torsional stiffness	57 kNm²/deg.
Buoyancy in seawater	99.2 kg/m
Mass (weight) of pipe in air, empty	139.2 kg/m (1.366 kN/m)
Weight of pipe submerged, fresh water/MEG filled	0.768 kN/m

Most of the data in Table 5.1 are used in OrcaFlex to define the flowline. The flowline is to be filled with a certain "installation fluid". In this case the flowline will be assumed filled with fresh water with added corrosion inhibitor and MEG, giving a density of approximately 1097 kg/m^3, and a submerged weight of 0.768 kN/meter of pipe. As the mass of the pipe in OrcaFlex is specified when it is empty in air, OrcaFlex will calculate the submerged weight of the pipe with its fluid content, if specified.

5.2 Input parameters used for the flexible product in the analysis

The installation of the flexible product is to be carried out in a water depth of 350 meters, with the wave descriptions given in chapter 4.

5.2.1 Lift and drag coefficient of the flowline

The lift coefficient of the flowline is assumed to be zero as it should be of minor concern as the flowline is quite slender and installed with a small layback, hence will the projected area in the vertical direction be quite small. The drag is more important. The coefficients were set to be constant.

The drag forces could be quite large in deep water with current, especially if the diameter of the product is somewhat large as well. This will pose some extra tension on the flowline. In this analysis the vessel have zero velocity as it is considered to be perfectly still on DP. No current is applied. This means the only factor affecting the drag coefficient is the approaching waves' velocity (horizontal water particle velocity) and the roughness of the flowline. The flow from the waves is considered steady. According to DNV-RP-C205 (Environmental Conditions and Environmental Loads), the Keulegan-Carpenter (K_C) number should be specified from the formula shown in equation 49 (DNV, 2010).

$$K_C = (v_m + v_c) \cdot \frac{T}{D} \quad [-] \qquad \text{(Eq. 49)}$$

Here is;

- v_m = Maximum orbital particle velocity or wave particle velocity [m/s]
- v_c = Current velocity [m/s]
- D = Outer diameter of flowline [m]
- T = Wave period or period of structural oscillation [s]

According to DNV the significant wave induced velocity should be used instead of the maximum orbital particle velocity in a general sea state (DNV, 2010). As no current is considered $v_c = 0$, the maximum wave particle velocity will vary with the water depth and wave period. The largest water particle velocity on the flowline will be right below the moonpool/at the keel (≈ 8 meters below the still water line). See Figure 5.2 for illustration of wave velocity profile.
The formula for the (horizontal) wave particle velocity simplified for deep water is shown in equation 50 (Gudmestad, 2013c).

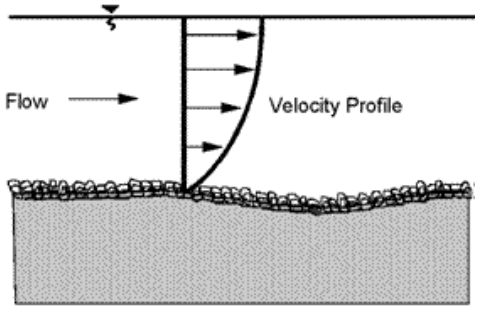

Figure 5.2: Typical illustration of wave velocity profile varying with water depth (FHWA, 2013)

$$v_m = \frac{\zeta_a \cdot k \cdot g}{\omega} \cdot e^{k \cdot z} \cdot \sin(\omega \cdot t - k \cdot x) \quad [\text{m/s}] \qquad \text{(Eq. 50)}$$

Where:

- ζ_a = Wave amplitude [m]
- k = Wave number ($= 2\pi/L_W$) [m^{-1}]
- ω = Wave frequency ($= 2\pi/T$) [s^{-1}]
- x = Direction of wave propagation [m]
- z = Depth below mean still water line [m]
- t = Time [s]

As the different simulations in the analysis will be carried out for different wave periods and wave heights it would not be applicable to calculate all the different Keulegan-Carpenter numbers. However, one could observe that the K_C number is going to be quite large ($K_C > 3$) for most wave periods. For high Reynolds number (>10^6) and large K_C number, which is assumed to applicable, the drag coefficient depends on the relative roughness of the flowline which may be taken as presented in equation 51.

$$\Delta_k = \frac{k_r}{D} \approx 1.425 \cdot 10^{-5} \quad [-] \qquad \text{(Eq. 51)}$$

By assuming that the surface roughness of the flexible flowline is the same as for a painted steel pipe ($k_r \approx 5 \cdot 10^{-6}$), which is considered as a smooth pipe, the drag coefficient for steady flow (C_{DS}) will be 0.65 according to DNV (DNV, 2010). This is assumed to be okay and $C_{DS} = 0.65$ is assumed to be constant through the analysis for all wave heights and periods.
Sometimes also a drag coefficient of about 0.8 is used for smooth cylinders for analysis purposes, but this is typically for larger velocities (Reynolds number) than in this case (DNV, 2010).

5.2.2 Added mass of flowline

Added mass of the flowline must be taken into account and is also calculated in accordance with DNV-RP-C205. The added mass coefficient (C_A) for cylindrical structures is specified with formulas with either the Keulegan-Carpenter number (K_C) or the drag coefficient for steady flow (C_{DS}). See equations 52 and 53 (DNV, 2010).

$$C_A = 1 - 0.044(K_C - 3) \quad [-] \qquad \text{(Eq. 52)}$$

$$C_A = 0.6 - (C_{DS} - 0.65) \quad [-] \qquad \text{(Eq. 53)}$$

According to DNV-RP-C205 this will give an added mass coefficient of 0.60 (given $C_{DS} = 0.65$) if equation 53 is used. This could be used, but after a discussion with an analysis engineer it was decided to raise it to 1.0, as this would cover more uncertainties and is a bit more conservative (Qayre, 2014). So this was applied in the analysis for all simulations.

5.2.3 Friction at the seabed

As the flexible flowline approaches the seabed at the Touch Down Point (TDP, ref. Fig 5.4) it will eventually be fully in contact with the seabed. Then the flowline will experience a certain friction with the seabed. This friction is an important feature as a certain friction is needed when installing pipes as they then are easier to control. However, it need to be a balance between too much and too little friction, as too much friction could cause large stresses to occur in the pipe, especially in the sag bend. This is not a very large issue for flexible flowlines.

The sag bend is the lower part of the flowline where it bends the most before approaching the sea bed, Figure 5.4 somewhat shows this. In the sag bend there will be compression "inside the arc" and tension "on the back of the arc" (ref. Fig. 5.4).

Pipes are usually tested for their friction and these types of tests give an upper and lower soil resistance (friction) value and a best estimate. Some values are presented in Table 5.2. These are from an area with clayish sea bed in the Norwegian Sea for an 8 inch flexible production flowline. It is assumed that the values are representative also for the area in question here.

Table 5.2: Temporary peak conditions for soil/pipe resistance (F_R) during installation (JP Kenny Norge AS, 2014)

Direction of resistance	Lower boundary [kN/m]	Best estimate [kN/m]	Upper boundary [kN/m]
Lateral soil resistance, F_{RL}	0.60	1.05	1.50
Axial soil resistance, F_{RA}	0.40	0.61	0.82

From the soil resistance it is possible to calculate the friction coefficients between the pipe and soil when the undrained shear strength of the soil and the contact area is known. The soil-pipe resistance could be defined as shown in equation 54.

$$F_R = \left(W_{pipe} - F_S \cdot D\right) \cdot \mu_F \quad \text{[N/m]} \qquad \text{(Eq. 54)}$$

Here:

- F_R = Soil resistance, in lateral or axial direction [N/m]
- W_{pipe} = The submerged pipe weight when filled with a water/MEG mixture (with density of 1097 kg/m^3) [N]
- F_S = Undrained shear strength of soil [Pa]
- μ_F = Friction coefficient with seabed (lateral or axial) [-]
- D = The pipe's outer diameter [m]

The friction coefficients can then be calculated by use of equation 54 solved with respect to the friction coefficient, which gives equation 55 for the lateral friction coefficient. The best estimate values for the soil/pipe resistance (F_R) from Table 5.2 are used.

$$\mu_{F,lateral} = \frac{F_{RL}}{W_{pipe} - F_S \cdot D} = \frac{1.05\ kN/m}{0.768\frac{kN}{m} - 7\frac{kN}{m^2} \cdot 0.352\ m} \approx 0.62 \qquad \text{(Eq. 55)}$$

In equation 55 only the calculation of the lateral friction coefficient is shown, however the calculation will be similar for the axial coefficient (only with axial soil resistance best estimate = 0.61), which turned out to be approximately 0.36.
So 0.62 for the lateral and 0.36 for the axial friction coefficients seems reasonable and were used in the OrcaFlex simulations.

Since the vessel will be holding its initial position and heading through the simulations, torsion on the flexible product is not considered, and hence neglected.

5.2.4 Flowline model description

The flowline is modelled to be 540 meters, where one end (End A, ref. Fig. 5.3) is attached in the VLS, and the other end (End B, ref. Fig. 5.3) is considered anchored at the sea bottom.
In reality, when sufficient length of a flowline is laid, it will be so heavy that it could be seen as "anchored". The reason why choosing it as anchored with a length of 540 meters is that it would take a significant amount of flowline before it could be seen as "anchored" in reality. To model this in OrcaFlex will slow down the simulations significantly because of a very long flowline must be modelled. So to set the lower end of the flowline as anchored and allow for bending (and torsion, if applicable) is a lot faster and is assumed to produce the somewhat same results in this case.

The flowline is modelled in OrcaFlex with the help of a number of segments and nodes. The segments are connected to each other by nodes. Different sections of the pipe consist of a number of segments and nodes where the stresses are distributed (ref. Fig 5.3). The more segments and nodes one use in an analysis, the more precise the outcome should be. The number of nodes and segments are defined by the segment length.
The flowline was divided into 3 sections with different segment lengths to get a more precise picture of the forces in the flowline.

- Section 1: 0 - 60 meters, segment length = 0.10 meters
- Section 2: 60 – 260 meters, segment length = 1.00 meters
- Section 3: 260 – 540 meters, segment length = 0.50 meters

The number of segments (here totally 1360) should be a trade-off between need of accuracy from the results versus the simulation time, as more segments increases the duration of the simulations.
Section 1 and 3 has a higher number of segments than section 2, as it is here the pipe is anticipated to see the peaks for compression/tension and bending. The number of nodes was determined from a sensitivity check, where several "check-simulations" with different number of segments were carried out, until the results did not change much. When the results did not change with more segments added, it was considered accurate enough for describing the flowline fairly well.

It is hard to determine the layback distance (ref. Fig. 5.4) right away for a flexible flowline as one also must take into account the possibility of clashing with the moonpool. Clashing poses the risk of the pipe being damaged. After some "check-simulations", a compromise between layback distances versus clashing was determined.

The trade-off was made to make sure that no clashing occurred in the moonpool and that the bending radius did not get too low, which could result in too high compression in the pipe (in the sag bend). The worst case with respect to this situation was extensively tested with waves of 7.6 meters (H_D) and period of 18 seconds from different directions. Even if the pipe does not clash into the moonpool's walls it could still move around more than allowed (from the installation procedure). These limits for the pipe are presented in chapter 8.3. After the "check-simulations" the layback distance was initially set to be ≈ 25 meters. To check the impact on the results from the layback distance a sensitivity check was carried out with other layback distances. This is presented in sub-chapter 9.2.3.

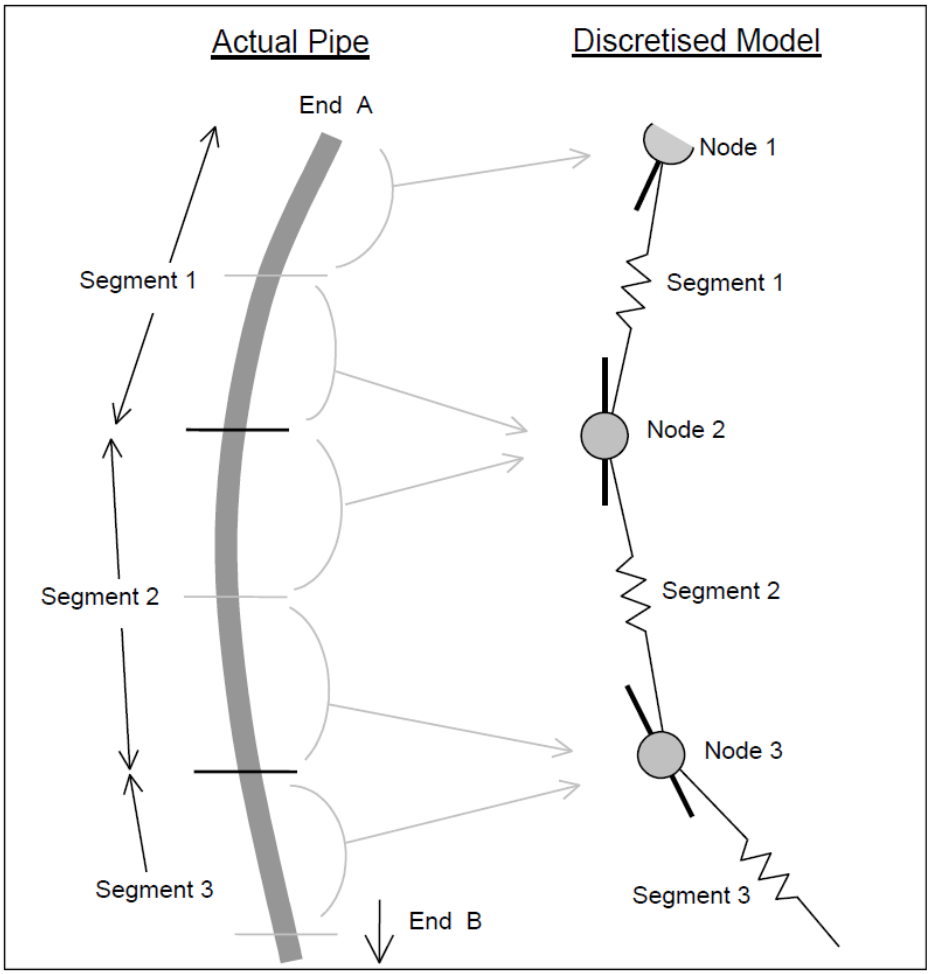

Figure 5.3: Illustration of how a pipe is modelled in OrcaFlex (Orcina Ltd., 2013)

To reduce the possibility of clashing the pipe with the moonpool's walls a "centralizer with a slightly "flared"/tapered hole is placed over the moonpool during this type of operation. This keeps the pipe going more vertical until it is clear of the moonpool. The centralizer can be adjusted to fit a series of pipes with different outer diameter. More about this centralizer is presented in sub-chapter 8.3.

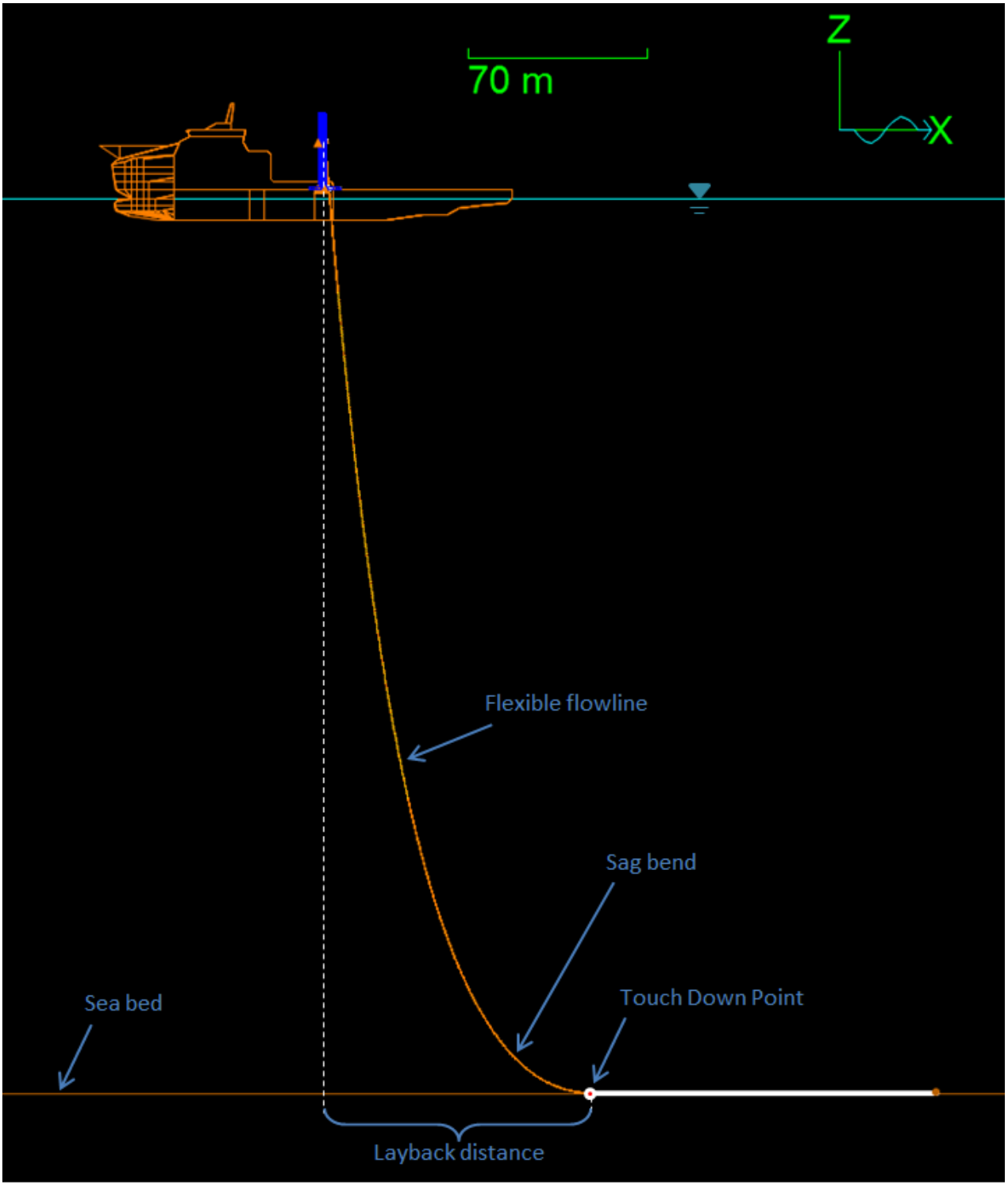

Figure 5.4: Screenshot from OrcaFlex showing the setup with the flowline, End A is in the VLS on the vessel (shown by the blue "pole"), and End B is in the right end of the white line

6 Load Cases to be analysed

In this chapter the two different extreme Load Cases to be analysed are described. For easier reference they will be referred to as Load Case (LC) 1 and 2. Both Load Cases look at the vessel loaded and prepared for departure, hence representing the loads the ship is exposed to before any pipeline is installed. The Load Cases are prepared by STX OSV Design AS. The total allowed deadweight of the vessel is 12000 tonnes making the maximum possible (design) displacement in the order of 25541.6 tonnes, as the lightship weight is 13541.6 tonnes (calculated).
The two Load Cases presented are coming rather close to this design limit which is why they are considered to be sort of extreme.

6.1 Load Case 1 (Construction Mode, 150T VLS)

This Load Case is the least extreme of the two cases to be considered in terms of total displacement. This load condition looks at a construction mode with some deck load.
For easier reference the loads could be divided into various categories. Two main categories are liquid and dry loads. These loads combined make up the total deadweight for the vessel.
The liquid loads are distributed as follows (STX OSV, 2013c):

- 12 fuel oil tanks are 98% full, one is 45.4% full
- 8 fresh water tanks are 98% full, one is 31% full
- 28 miscellaneous liquid load tanks are all 50% full
- 27 of 34 water ballast tanks are full (100%), the last seven tanks are between 25% and 87% full

So, most of the tanks are approximately totally full which will not be the case in a real operation. The only benefits one get from such full tanks are that the sloshing effects due to free water surface is limited. However, anti-roll tanks and other motion enhancing devices are in place to limit such effects even if tanks are not full.
Figure 6.1 shows a general overview of where the loads are located in the vessel from main deck and downwards to the lower decks.
For a summary of the loads, see Tables 6.1 and 6.2. The density of the “miscellaneous liquid loads” has for simplicity been approximated to have the same density as the sea water.

Table 6.1: Overview of liquid loads for Load Case 1 (STX OSV, 2013c)

Liquid loads for Load Case 1	Load value (in tonnes)
Fuel oil (density 850 kg/m^3)	1317.5
Fresh water (density 1000 kg/m^3)	1125.4
Miscellaneous (lubrication, drain and thruster oil, sewage etc., density 1025 kg/m^3)	327.6
Water ballast (density 1025 kg/m^3)	4248.4
Total liquid loads	*7018.9*

Table 6.2: Overview of dry loads for Load Case 1 (STX OSV, 2013c)

Dry loads for Load Case 1	Load value (in tonnes)
Crew and stores	50.0
Deck load	1600.0
Load out tower	70.0
Total dry loads	*1720.0*

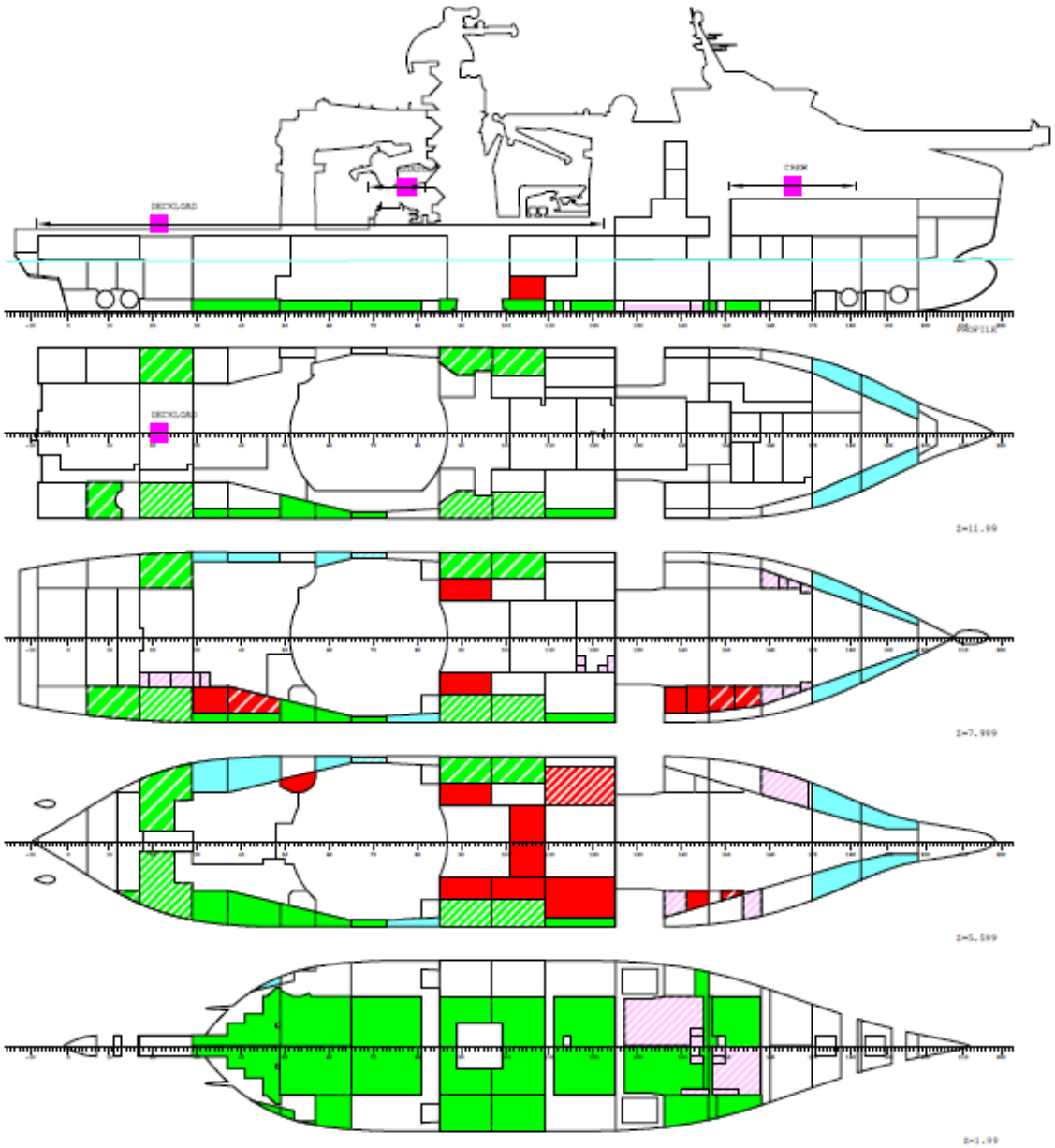

Figure 6.1: General overview over the load locations on Normand Vision for Load Case 1 (STX OSV, 2013a)

The total weight of all loads is then 8738.9 tonnes. So with this deadweight the total displacement of the vessel is ≈ 22280.5 tonnes (as the lightship weight is set to 13541.6 tonnes). The calculated value for the total displacement from VERES is however 23017.36 tonnes which is what the RAOs are based on, and is therefore the value that will be used in OrcaFlex.

A rough hand calculation, using displacement = 23017.36 tonnes, shows a total displacement volume (∇) of ≈ 22456 m^3 due to Archimedes' principle (equation 56). This loading gives the vessel a mean draught of 8.171 meters with a corresponding estimated freeboard (to main deck) of about 3.8 meters.

$$mg = \nabla \cdot \rho \cdot g \ \rightarrow m = \nabla \cdot \rho \rightarrow \nabla = \frac{m}{\rho} \qquad \text{(Eq. 56)}$$

Here:

- g = gravitational acceleration [m/s^2]
- m = structural mass (total displacement) of the vessel [kg]
- ∇ = displacement volume [m^3]
- ρ = density of the sea water [kg/m^3]

The same principle is used in OrcaFlex for calculation of the displacement volume (Orcina Ltd., 2013).

For information about the Centres of Gravity for this Load Case, the reader is referred to Table 3.1.

Prior to STX OSV carrying out the analysis in VERES the stability of the vessel for the actual Load Case was checked using NAPA software. These results show that all specified parameters for intact stability are satisfied both for the operation and for accidental load drop during the operation. Some key data with respect to initial stability based on these results, compared with DNV's Rules for Classification of Ships, are presented in Appendix A.

6.2 Load Case 2 (Flex lay mode, 150T VLS, 4500T deck load)

This Load Case is the most extreme of the two cases to be considered in terms of total displacement, even if less liquid loads are involved. On the other side, the deck load in this case is enormous, 4500 tonnes. As for Load Case 1, coarse categories are used also here for easier reference. The two main categories are liquid and dry loads.
The liquid loads are distributed as follows (STX OSV, 2013d):

- 7 fuel oil tanks are 98% full
- 3 fresh water tanks are 98% full
- 28 miscellaneous liquid load tanks are all 50% full (similar as for Load Case 1)
- 22 out of 25 water ballast tanks are full (100%), the last three tanks is between 10% and 55% full

Figure 6.2 shows a general overview of where the loads are located on the vessel from main deck and downwards to the lower decks. For a summary of the loads, see Tables 6.3 and 6.4. The density of the "miscellaneous liquid loads" has for simplicity been approximated to have the same density as the sea water.

Table 6.3: Overview of liquid loads for Load Case 2 (STX OSV, 2013d)

Liquid loads for Load Case 2	Load value (in tonnes)
Fuel oil (density 850 kg/m^3)	617.2
Fresh water (density 1000 kg/m^3)	396.1
Miscellaneous (lubrication, drain and thruster oil, sewage etc., density 1025 kg/m^3)	327.6
Water ballast (density 1025 kg/m^3)	3193.4
Total liquid loads	*4534.3*

Table 6.4: Overview of dry loads for Load Case 2 (STX OSV, 2013d)

Dry loads for Load Case 2	Load value (in tonnes)
Crew and stores	100.0
Deck load	4500.0
Tower tension	185.0
Total dry loads	*4785.0*

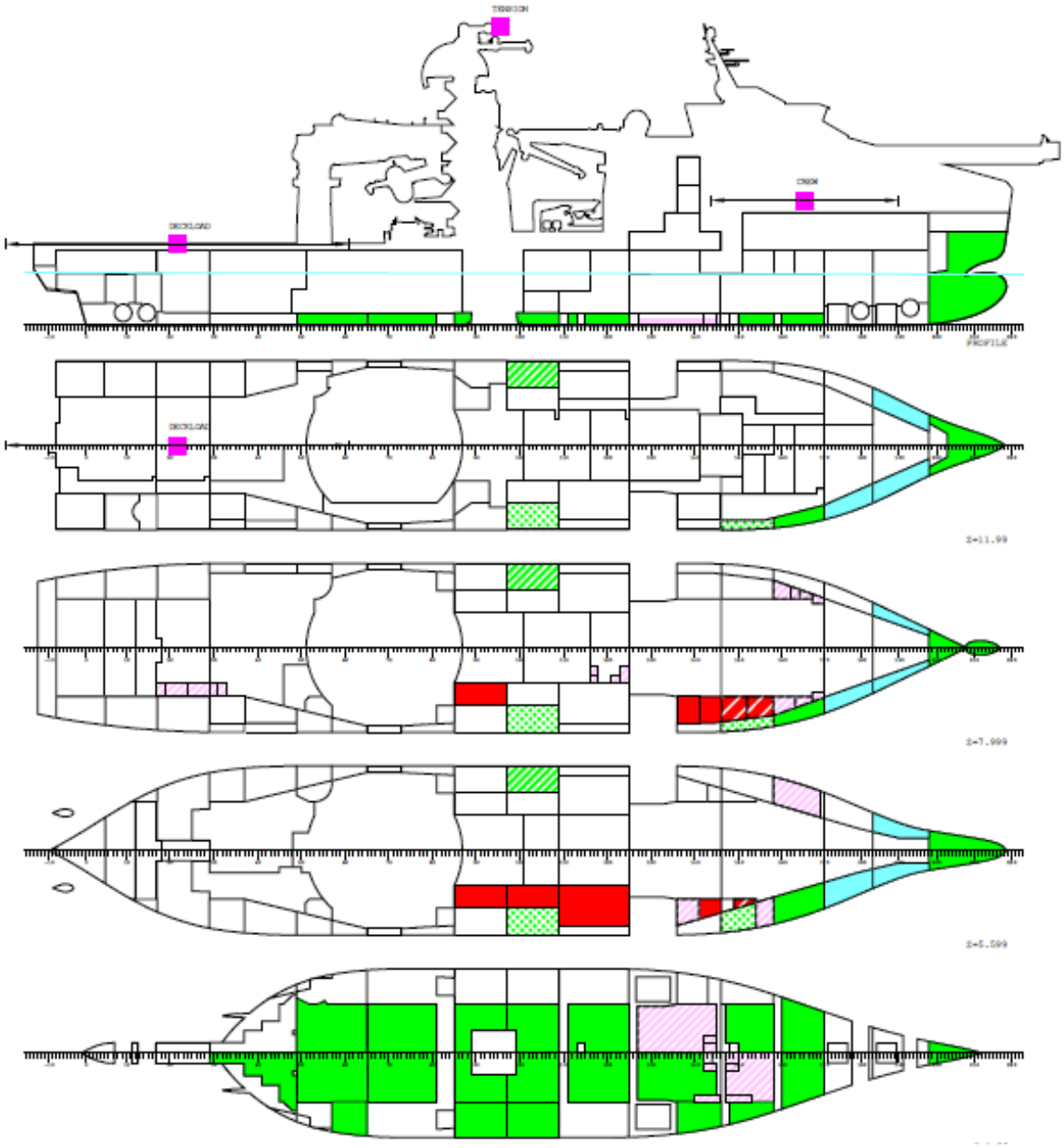

Figure 6.2: General overview over the load locations on Normand Vision for Load Case 2 (STX OSV, 2013a)

The total weight of all loads is then 9319.3 tonnes. So with this deadweight the total displacement of the vessel is ≈ 22861 tonnes (as the lightship weight is set to 13541.6 tonnes). The calculated value for the total displacement from VERES is however 23637.86 tonnes, which is what the RAOs are based on, and is therefore the value that will be used in OrcaFlex.

A rough hand calculation, using displacement = 23637.86 tonnes, shows a total displacement volume (∇) of ≈ 23061 m^3 due to Archimedes' principle (ref. equation 56). This loading gives the vessel a mean draught of 8.303 meters with a corresponding estimated freeboard (to main deck) of about 3.7 meters.

For information about the Centres of Gravity for this Load Case, the reader is referred to Table 3.1.

Prior to STX OSV carrying out the analysis in VERES the stability of the vessel for the actual Load Case was checked using NAPA software. These results show that all specified parameters for intact stability are satisfied both for the operation and for accidental load drop during the operation. Some key data with respect to initial stability based on these results, compared with DNV's Rules for Classification of Ships, are presented in Appendix A.

7 OrcaFlex analysis

7.1 About the analysis

The parameters to be checked in the analysis will be determined by OrcaFlex based on the displacement RAOs as well as assumptions and specified parameters for the flowline, soil, waves and more specified in the previous chapters 3, 4 and 5.

With the two different Load Cases presented in chapter 6, three different wave headings, three different wave heights and 13 different wave periods, a total of (2·3·3·13=) 234 simulations are to be carried out.

Relevant limits and criteria for various operational aspects are defined according to product data, procedures, standards/regulations, certification requirements and other relevant literature as presented in chapter 8.

The maximum/minimum values for the different parameters were of interest as this cover the whole range of what outcomes one could expect. The maximum/minimum values may not reflect the conditions as they really are most of the time (thinking of average values). But they cover the peak values, which are crucial to know about as they actually may occur during an operation.

The reason why different wave heights are considered is because of the interest in the operational window for the vessel, i.e. where the restrictions for operation under the different wave conditions are. If the vessel is capable of operating in higher waves, it will give a much larger utilization of the vessel, which benefits all parties, as this can mean enormous economical savings for the vessel owners/charterers and eventually the customers.
Vessels of the size of Normand Vision may have a day rate of several million NOK. As it in most contracts will be the customer, typically an operator, who has to pay for Waiting on Weather (WoW) a larger weather window will of course be very favourable for the customer.

7.2 What to look at?

As mentioned above there are certain parameters from the analysis which are of interest. OrcaFlex can produce heaps of results based on the input data. As it is too extensive to consider absolutely all relevant parameters, it was necessary to pick out some that were of most interest. The parameters of interest are based on the three following areas:

1. The flexible product's tolerances
    a. Top tension in tensioners
    b. The flowline's deflection angle with the vertical when going through the moonpool
    c. Compression in the sag bend
    d. Bending radius in the sag bend

2. Limitations for doing manual work on main deck

3. Limitations of movements of the helideck for landing of helicopters

Based on these three areas it was in this study focused especially on the following parameters:

- Maximum heave acceleration on main deck
- Maximum lateral acceleration on main deck
- Maximum roll rotation of vessel
- Maximum pitch rotation of vessel
- Maximum top tension in flexible flowline
- The flowline's maximum deflection angle with the vertical from the tensioners and down to the bottom of the hull
- Maximum compression in the sag bend
- Bending radius of the flexible flowline in the sag bend (minimum values)
- Conditions for landing of helicopters in daylight and at night, based on:
    - Maximum pitch and roll motion
    - Maximum helideck inclination relative to the horizontal
    - Maximum heave rate (heave velocity)

All parameters are obtained for all the relevant wave periods (6 to 18 seconds). The resulting limitations for these parameters will be presented in chapter 8.

7.3 Description of some geometries

Some of the parameters to be checked need to be outlined with respect to the vessels geometry which is done in this sub-chapter.
Regarding the different velocities and accelerations these are chosen for some specific points of interest on the vessel:

- "Main deck" means a point just aft (≈ 2.4 m) of the moonpool's aft end on the longitudinal centreline (Y = 0), on main deck which is 12 meters from the baseline/keel. This point is chosen because it is close to the moonpool, where manual work often is carried out. The reason for choosing the point to be at the longitudinal centreline is because the motions should be at the minimum here. If the limits for motions and accelerations are breached here they should also be breached closer to port side or starboard side of the vessel.
- The term "helideck" means a point approximately in the center of the helideck about 76.8 meters in front of the moonpool's center (the origin of the vessel's local coordinate system) and 29.5 meters above the baseline/keel.

See Figure 7.1 for approximate location of these two points.

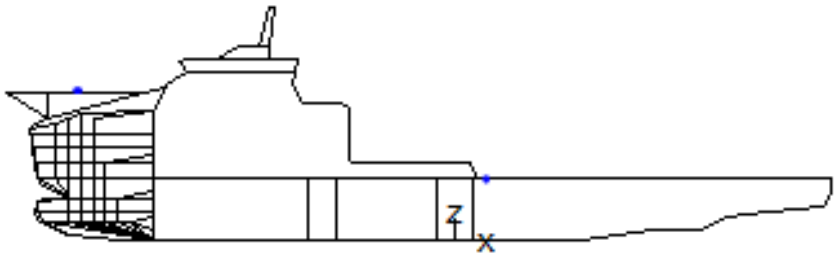

Figure 7.1: Points of interest on the vessel marked by blue dots

The top tension is taken to be in the lower part of the lower tensioner in the VLS, which is where the flowline leaves the tensioner, approximately 19.5 meters above the main deck. This connection point is located about 0.6 meters aft of the moonpool's center. See Figure 7.2.

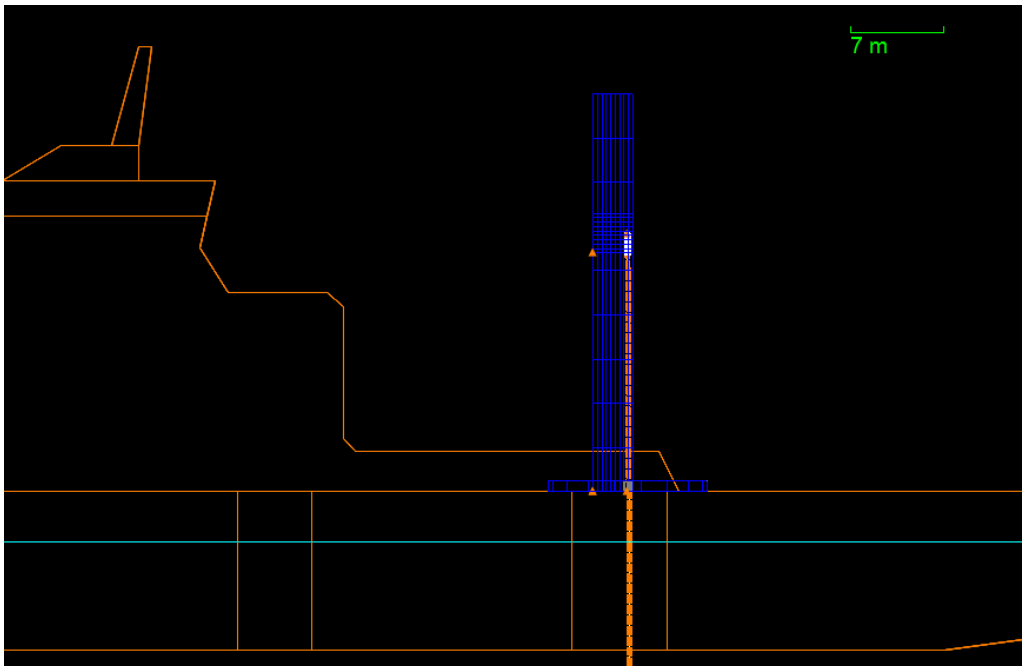

Figure 7.2: Connection point between lower tensioner and the flexible flowline, screenshot from OrcaFlex

When it comes to the flowline's deflection angle with the vertical, this is taken to be the largest angle occurring between the flowline's connection point (in the lower tensioner) and the bottom of the hull (baseline/keel). This distance is approximately 31.5 meters (ref. Fig. 7.2).

The compression in the flowline is taken for a section including the sag bend which is located at some distance above the touchdown point (ref. Fig. 5.4). This is because the largest compression is normally located in this area during installation of pipes, as it is here the pipe will bend the most if not taking into account when it goes over the chute.

But when going over the chute one have control on the bending and it is easier to monitor the forces. To be sure to capture the largest compression the length of the pipe to be examined was specified to be in the interval of 250 to 540 meters (from 250 meters till End B).

Regarding the bending radius one is here interested in where the smallest bending radius occurs, as this is most critical to the flowline. This is related to the compression. The smaller the bending radius is, the higher the compression gets. Hence a too small bending radius could damage the product. Also the bending radius is examined in the interval of 250 to 540 meters.

For the landing of helicopters on the helideck, there are mainly three parameters that need to be considered in order for the pilots to conduct a safe landing. These are the heave rate, pitch rotation and roll rotation on the helideck. The limitations are stated in chapter 8. The pitch and roll will propagate through the vessel. As the helideck is located at the very front of the vessel and high above the baseline it is expected it will see quite large motions from the rotation angles, especially pitch. The heave rate is taken at the point somewhat in the center of the helideck (ref. Fig. 7.1) which is where the pilot will aim when the helicopter is approaching for landing.

8 Results from the analysis

8.1 About the actual results

The results for the various simulations are obtained for three different wave headings (0°, 45°and 90°) and for the different wave periods (6 to 18 seconds) and the various design wave heights (3.8, 5.7, and 7.6 meters) as outlined in sub-chapter 4.2.
However, not all of these combinations are just as critical with respect to given limitations. So in order not to have a too excessive amount of results to relate to, certain combinations are omitted. For instance is there very little compression in the sag bend with a design wave height of 3.8 meters in head seas. Therefore this case is not presented. However, only the results for the parameters where one sees some significant values will be presented. For a complete list of what combinations that are included the reader is referred to sub-chapter 8.6.

As earlier mentioned the three areas considered are the following:

1. The flexible product's tolerances
    a. Top tension in tensioners
    b. The flowline's deflection angle with the vertical when going through the moonpool
    c. Compression in the sag bend
    d. Bending radius in the sag bend

2. Limitations for doing manual work on main deck

3. Limitations of movements of the helideck for landing of helicopters

The limitations with respect to capabilities and tolerances relevant for this installation operation will be considered. There are many aspects that are important when carrying out such an operation. It is e.g. important that it is safe for the personnel (marine crew) to work on deck, that the product is installed within allowable limits and that it is possible to do a crew change. Of course it is not always necessary to have a crew change during a flowline installation. That will of course depend on the scope for the installation operation, but in order to keep up the vessel utilization it is desirable to have the vessel out on the sea operating as much as possible when not mobilizing/demobilizing.

The basis for what limitations the results are compared against are presented in the next sub-chapters 8.3, 8.4 and 8.5.

The results themselves are presented in Appendix C.

8.2 Quality check of RAOs

As mentioned, there exists a method for checking the quality of the RAOs put into OrcaFlex. It is important that the input RAOs are correct with respect to sign convention and phases in order to represent the vessel's motions correctly.
The quality check can be done in mainly two different ways:

- Comparison of RAO graphs provided from the RAO data basis versus the graphs in OrcaFlex after the data has been imported (see Appendix B for comparison). When comparing the graphs directly like this it is easier to spot errors. There are also some confident observations that can be done which say if the interpretation of the RAOs is correct in OrcaFlex. For example if very long waves are coming towards port side, the RAO values presented in Table 8.1 should apply. Such tables with expected RAO values also apply for very long waves coming from ahead, astern and towards the starboard side.

Table 8.1: Expected RAOs when very long waves approaches from port side (Orcina Ltd., 2013)

Degree of Freedom	Amplitude	Phase [°]
Surge	0	N/A
Sway	1	-90
Heave	1	0
Roll	1	-90
Pitch	0	N/A
Yaw	0	N/A

It was checked if the RAOs were converging towards these values when the waves grew long and came from the different directions (0°, 90°, 180° and 270°), which they did. Also the RAO graphs looked to coincide fairly well (ref. Appendix B), hence this check was concluded to be positive.

- Also OrcaFlex provides another quality check method of the RAO data. This is more a visual and practical check as one then looks into a short dynamic simulation of the vessel in large regular waves, e.g. waves with a height of 20 meters and a period of 10 seconds could be used. With such large waves the vessel should behave more like a raft riding on the waves and hence it is fairly easy to see if the movement of the vessel is sensible and natural/realistic for these big waves. The vessel should for example (Orcina Ltd., 2013):
    - Be at maximum heave on the wave crest and minimum heave in wave trough.
    - When the wave slope is at its maximum (steepest) and the wave crest approaches, the ship should be at maximum surge (forward into the wave), as well as the pitch angle with the bow up should be at its maximum.

If there then is something wrong with the interpretation of the sign convention, e.g. phase angles have been read as lags when they are leads or vice versa, the motion will obviously be wrong and easy to detect. However, also this quality check of the RAOs was positive, and it could be concluded that the RAO data was confirmed to be understood correctly by OrcaFlex.

8.3 The product's tolerances

The 8 inch flexible flowline has the following limitations for the parameters of interests, see Table 8.2.

Table 8.2: Installation limitations for the 8 inch flexible flowline, ref. Table 5.1 (NKT Flexibles, 2011)

Parameter	Value
Maximum allowed tension during installation	382 kN
Maximum allowed compression during installation	50 kN
Minimum bending radius allowed during installation	4.69 m

In order of having the tension/compression quite steady in the sense to avoid sudden (unexpected) peaks, one must avoid that the flowline gets too slack (too little layback and tension, or too much compression), so that one could get snap loads in the flowline when the vessel moves from a wave trough to a wave crest. This may give very large tension peaks, which absolutely are unfavourable as it can damage the pipe due to large stretch forces.

In addition to the parameters in Table 8.2, it is also important to prevent the flowline from colliding with the hull when going through the moonpool. The "centralizer" over the moonpool (used for this type of operations) provides lateral support to reduce the possibility of clashing. This means the pipe is going practically speaking vertical until leaving the centralizer, see Figures 8.1 and 8.2.

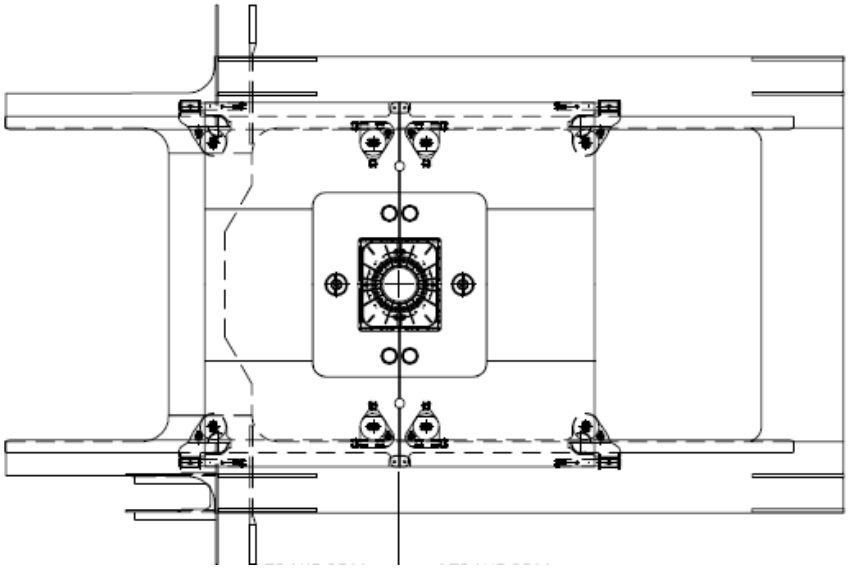

Figure 8.1: Centralizing "grillage" seen from above, centre point indicates where the flowline passes through. The Grillage can be adapted to flowlines of different diameters (Huisman, 2013b)

A maximum deflection angle from the vertical when going through the moonpool has been set to be 7.3° from the center of the centralizer to the centre of the flowline, giving a "safety distance" of about 1125 mm (when ≈ 600 mm outer diameter pipe) before it hits the edge of the moonpool, at the baseline (see Fig. 8.2).

As we in this case look at an 8 inch pipe with a 13.8 inch (351 mm) outer diameter this “safety distance” will be about 124.5 mm larger. However, the limit for the deflection angle is still taken to be 7.3° for conservatism and because the angle will be only a little larger (≈ 8.1°) for the 8 inch pipe considered.

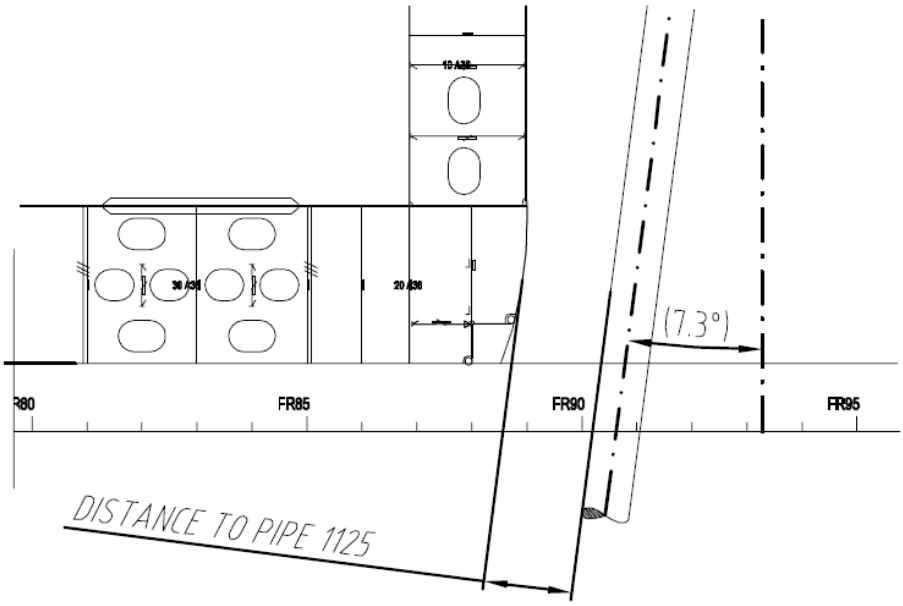

Figure 8.2: Excerpt of drawing showing the maximum allowable deflection angle of the pipe with the vertical during installation (Huisman, 2013b)

The deflection angle is set by the VLS supplier and the users of the vessel. There will be a significant increase in the risk of clashing the flowline into the hull if this limit is breached.

The maximum allowable installation tension and compression must be seen in relation with the bending radius as the product can be damaged anyway if the bending radius is less than the MBR (4.69 m), even if the tension/compression values are complied with. The tensile armour(s) of a flexible flowline can normally take quite some tension as it is designed for, but have trouble when it comes to bending and compression.
The flowline may also in many cases crash into the hull long before the tension or compression reach unacceptable values. So there are quite some aspects to be aware of and take into account when planning the installation of the flowline.

The tension/compression for the various segments (distance between two nodes, ref. Fig. 5.3) in the flowline is calculated in OrcaFlex by use of the following formula (equation 57), for linear axial stiffness, which is applicable here as the Young’s modulus and cross-sectional area are considered constant (Orcina Ltd., 2013).

$$T_e = T_w + (P_o A_o - P_i A_i) \qquad \text{(Eq. 57)}$$

Here:

- T_e = Effective tension [N]
- T_w = Wall tension [N]
- P_i = Internal pressure [Pa]
- P_o = External pressure [Pa]
- A_i = Internal cross-sectional stress areas of the pipe [m^2]
- A_o = External cross-sectional stress areas of the pipe [m^2]

The wall tension (T_w) is calculated as shown in equation 58 (Orcina Ltd., 2013).

$$T_w = E \cdot A_c \cdot \varepsilon - 2\nu(P_o A_o - P_i A_i) + \frac{E \cdot A_c \cdot C \cdot \left(\frac{dL}{dt}\right)}{L_0} \quad \text{(Eq. 58)}$$

Here:

- E = Young's modulus [N/m^2]
- A_c = Cross-sectional area [m^2]
- ε = Total average axial strain equal to: $(L - \lambda_e L_0)/(\lambda_e L_0)$ [-]
- L = Instantaneous length of segment [m]
- λ_e = Expansion factor of segment [-]
- L_0 = Unstretched length of segment [m]
- ν = Poisson ratio [-]
- C = Damping coefficient equal to: $(\lambda_a/100)\cdot C_{crit}$ [s]
- dL/dt = Rate of increase of length [m/s]
- λ_a = Target axial damping [-]
- C_{crit} = The critical damping value for a segment equal to: $((2\cdot M\cdot L_0)/(E\cdot A_c))^{0.5}$ [s]
- M = Segment mass, including contents [kg]

Description of the formula for the wall tension (equation 58), (Orcina Ltd., 2013):

- The first term is the contribution from the axial stiffness ($E\cdot A_c$)
- The second term is the contribution from external and internal pressure (via the Poisson ratio effect)
- The third term is the axial damping contribution

8.4 Limitations for manual work on deck

During marine operations, there are several tasks to be performed on the main deck and it is favourable not to have big movements and accelerations. Regarding manual work on-board a vessel one could categorize the work as e.g. light and heavy, see Table 8.3. Here the stricter criterion belongs to the heavy manual work. The limitations for the heavy manual work were chosen as it seems like the most descriptive as well as more conservative for this study. However, there also exist other criteria (e.g. in ISO 2631) so some may think of those presented in Table 8.3 as too strict or too gentle.

Table 8.3: Limiting criteria based on accelerations and roll for different situations (Faltinsen, 1990)

Description	Heave (vertical) acceleration [m/s^2]	Lateral (horizontal) acceleration [m/s^2]	Roll [°]
Light manual work	0.20·g ≈ 1.96	0.10·g ≈ 0.98	6.0
Heavy manual work	0.15·g ≈ 1.47	0.07·g ≈ 0.69	4.0
Intellectual work	0.10·g ≈ 0.98	0.05·g ≈ 0.49	3.0
Transit passengers	0.05·g ≈ 0.49	0.04·g ≈ 0.39	2.5
Cruise liner	0.02·g ≈ 0.20	0.03·g ≈ 0.29	2.5

All three criteria (roll, heave and lateral acceleration) should preferably be complied with for heavy manual work on deck. The limitations are shown in the presentation of the results in Appendix C to show the relation to the actual values obtained from the simulations. The pitch could also be considered here, but the pitch motion will mostly be related to the personnel's effectiveness, i.e. decreasing personnel efficiency with increasing pitch motion. Pitch itself is often not considered as the heave also will take into account the vertical components of the pitch motion.

Some comments to the different parameters (Marintek, 2007):

- A vertical acceleration of 0.15·g should be tolerable for the crew for some time. This limit is also often used as limit for heavy manual work on fishing vessels.
- The roll motions are also mostly related to the personnel effectiveness, but issues with respect to comfort and seasickness may also arise with large roll motions.
- In a sea state giving a lateral acceleration of 0.07·g about 99 percent of standing personnel will be able to keep their balance without the need of grabbing hold to something.

It is important to emphasize that these criteria are defined on a general basis and does not reflect the limitations set by e.g. Ocean Installer AS or others for Normand Vision in particular. They are mainly introduced here for a general guidance. In practice the limit for when one choose to do an operation or not, e.g. lift and install a spool piece will be based on the sea state present, experience and what the personnel and captain feel is safe working conditions at that time.

8.5 Helideck movement limitations

It could be interesting to look into how the helideck "will perform" when looking at these rather extreme loading cases. In order to land a helicopter safely on the helideck of Normand Vision, certain limitations with respect to motions must be complied with.

The Helideck Certification Agency (HCA) is the certification body used for certification of the helideck on Normand Vision (Waalen, 2014a). The helideck is especially made for the Sikorsky S-92 helicopter and has a diameter of about 1.25 times the diameter of the S-92's rotors, which is 17.17 m (Ocean Installer AS, 2013). An S-92 is considered a large helicopter with capacity of 19 passengers and two pilots (Bristow, 2013).

HCA's definition of an unstable or moving helideck is as follows (Helideck Certification Agency, 2013): *"Any helideck on a floating unit such as a vessel, floating production unit, semi- submersible or floating jack-up rig shall be considered to be an unstable/moving deck if the pitch or roll exceeds 1° either side of the vertical and/or if the vertical movement of the helideck exceeds 2 metres".*

So the vessel is definitely to be treated as an unstable platform for most situations. From HCA's classification of different helidecks, Normand Vision's helideck will fall into category 3 which comprise helidecks mounted in the bow section, typically at the bow deck or above the bridge superstructure. The aircraft will fall into category A which is for quite large helicopters, see Table 8.4.

Table 8.4: The table shows the operational motion limits for a helideck with respect to the aircraft and helideck category, limits for Normand Vision's helideck in red frame (Helideck Certification Agency, 2013)

		Helideck Category											
Aircraft Category		1				2				3			
		P/R	INC	H/R	H/A	P/R	INC	H/R	H/A	P/R	INC	H/R	H/A
A	DAY	±3	3.5	1.3	5.0	±2	2.5	1.0	3.0	±2	2.5	1.0	3.0
	NT	±3	3.5	1.0	4.0	±2	2.5	0.5	1.5	±1	1.5	0.5	1.5
B	DAY	±4	4.5	1.3	5.0	±3	3.5	1.0	3.0	±3	3.5	1.0	3.0
	NT	±4	4.5	1.0	4.0	±2	2.5	0.5	1.5	±1.5	2.0	0.5	1.5

The red frame in the table indicates what operational limitations that apply for the helideck on Normand Vision. The following key to Table 8.4 is provided (Helideck Certification Agency, 2013):

- P/R = Pitch and roll [deg.]
- INC = Helideck inclination relative to the horizontal [deg.]
- H/R = Heave rate [m/s]
- H/A = Heave amplitude (trough to crest distance) [m]
- DAY = Day(time), NT = Night

It is in the analysis assumed that the helideck follows the exact movement of the vessel with respect to pitch and roll motion. It is hence assumed that one will experience maximum pitch and roll at the helideck.

These motions and the heave rate are measured by the helicopter's Helideck Monitoring System (HMS) with help of one of the vessel's Motion Reference Units (MRU).

Regarding when it is possible to land a helicopter, all of the operational limitations in Table 8.4 must be complied with. However, the heave amplitude is generally not something one relates to when performing landings (Smith, 2014). It was a change in the regulations in 2010 where the use of heave amplitude as a criterion was discontinued from 1st November 2010. It is included in Table 8.4 only for comparison with the heave rate. So the parameters considered by the pilots are pitch, roll, the inclination of the helideck and the heave rate. The pilots do not have any particular preferences when landing as long as the motions are within the operational limits (Smith, 2014).

In this study the inclination of the helideck with the horizontal is best described by assuming it to be the same as whatever is largest of roll and pitch. The roll motion is generally larger and worse than the pitch when it comes to the landing of a helicopter. This is naturally due to the width versus the length of the vessel. The length of Normand Vision is over five times the width. This means that the roll to a large extent takes part in restricting when the helicopters can land. However, in the analysis it turned out that basically it is the heave rate that mostly is the determining factor whether the conditions are acceptable for landing or not. This is discussed in sub-chapter 9.4.

What is important to be aware of regarding these operational limits is that they are made by HCA which is a certification agency based in UK and which focuses on the conditions in the North Atlantic Ocean, especially in the North Sea and the Norwegian Sea. In generally calmer waters, as e.g. the Gulf of Mexico (GoM), other criteria would be governing and the helideck may be "over-certified" for such an area.

8.6 Presentation of results

The results are presented in Appendix C with the respective wave heights. As earlier mentioned not all combinations of wave heights and wave directions are considered for the different parameters. The results are presented graphically because it then is easier to visualize how well the results comply with the limitations for the different parameters. Both Load Cases are presented in the same graph for the different parameters. For each wave height and wave direction considered there is one graph. The actual wave height and direction in question are stated.

The graphs in Appendix C also show the limits (as a horizontal line) for the actual parameter, such as maximum allowable installation tension and compression, maximum heave and lateral accelerations, maximum allowable roll motion, MBR and more.

The results presented for the different parameters are for all wave heights, but only for some wave headings. The wave headings studied are stated in the list presented below. The order of the parameters in the list below reflects the order of how the results are presented in Appendix C.

- Maximum heave acceleration on main deck for 90° wave heading
- Maximum lateral acceleration on main deck for 45° and 90° wave headings
- Maximum roll rotation of vessel for 45° and 90° wave headings
- Maximum pitch rotation of vessel for 0° and 45° wave headings
- Maximum top tension on flexible flowline for 0°, 45° and 90° wave headings
- The flowline's maximum deflection angle with the vertical from the tensioners and down to the bottom of the hull for 0°, 45° and 90° wave headings
- Maximum compression in the sag bend for 90° wave heading
- The smallest bending radius of the flexible flowline in the sag bend for 0°, 45° and 90° wave headings
- OK, and not OK periods for landing of helicopters at helideck in daylight for 0°, 45° and 90° wave headings, being based on;
    - Maximum pitch and roll motion
    - Maximum helideck inclination relative to the horizontal
    - Maximum heave rate (heave velocity)
- Maximum heave rate of the helideck for 0°, 45° and 90° wave headings

A special case is the landing of helicopters at night, which showed to be quite challenging. During the various simulations in the analysis one could observe that when it came to landing of a helicopter on the helideck at night, the criteria was breached for all actual wave periods, wave heights and wave headings. Therefore no results for this are included in Appendix C. Regarding daytime landing of helicopters the compliance with the criteria are shown in tables where it is indicated which periods are okay, and which are not. The heave rate itself is also shown.

9 Discussion of the results

From the results of the analysis one can see that there are some challenges related to flowline installation with these extreme loading conditions. The reader is referred to chapter 8 and Appendix C for presentation of the results. The figures in Appendix C are presented with both Load Cases in the same graph for the various wave heights and directions. In the beginning of Appendix C a list of how the different results are presented are shown (it is in the same order as the list in sub-chapter 8.6).

9.1 Discussion of the vessel's motions

9.1.1 Heave

The heave motion of the vessel is becoming larger as the waves grow larger. This is because the waves considered are regular, i.e. the waves' propagation shape is not changing. So when the wave height is increased it gives larger amplitude. So the largest heave motion is experienced for the design waves of 7.6 meters (H_S = 4 m). The wave heading giving the largest heave values is beam seas (90°).

The heave amplitude must be considered when it comes to displacement length of compensating equipment, landing of helicopters and lifting especially. Normally the vessel can measure the heave (amplitude, velocity and acceleration) from a MRU (Motion Reference Unit). This is necessary e.g. to be able to have Active Heave Compensation (AHC) on winches and other equipment.
The heave will get some contribution from the vertical components of roll and pitch. The heave velocity is important to know with respect to lifting operations and landing of helicopters. The heave accelerations are important with respect to what vertical forces one could experience as well as seasickness of the personnel and sea fastening of cargo and equipment (Gudmestad, 2013d). In the analysis the heave rate was in the spotlight for the landing requirements of the helideck. The heave accelerations were looked into due to the criteria for manual work on deck. The heave accelerations and heave rate are discussed later in this chapter.

The vessel's Eigen period in heave can be found from the total mass of the vessel (included added mass) and the vessel's water plane area, see equation 59. From the heave accelerations on main deck presented in Figures C.0.1 – C.0.3 it could be seen that the differences between Load Case 1 (LC1) and Load Case 2 (LC2) are marginal. This relates to equation 59, as all variable parameters relates to the displacement of the vessel. The added mass only relates to the geometry of the hull and will therefore not change much as the draft of the vessel is not very different for LC1 and LC2. The same goes for the water plane area. The draft is determined by the displacements which are 23017.36 tonnes (Load Case 1) and 23637.86 tonnes for (Load Case 2). As the difference is this small (≈ 2.6%) it will not have any significant impact.
From equation 59 one could observe that the denominator is the water plane stiffness which has an important role for the damping of the heave motion. A rough estimate of the value of the Eigen period could be made using an approximate water plane area for the vessel (see Figure H.0.1 in Appendix H). Based on the measurements in this figure Normand Vision is estimated to have a water plane area of ≈ 2755 m^2 (see Appendix H for calculation).

The added mass of the vessel was calculated (ref. Appendix H) to be $36.24 \cdot 10^6$ kg when taking into account the added mass also from the heaving water plugs in in the moonpools. With these values applied for Load Case 2, which have a total vessel displacement of about 23638 tonnes, the Eigen period in heave was calculated to be ≈ 9.2 seconds (see equation 59) which seems to be an okay estimate when compared to the first peak in beam seas for the heave RAO curve (for LC2) in Figure 9.1. This first peak indicates approximately where the Eigen period is located.

$$T_{heave} = 2\pi \cdot \sqrt{\frac{m_{vessel} + m_{added}}{\rho g A}} = 2\pi \cdot \sqrt{\frac{23638 \cdot 10^3 + 36.24 \cdot 10^6}{1025 \frac{kg}{m^3} \cdot 9.81 \frac{m}{s^2} \cdot 2755 m^2}} \approx 9.2\ s \qquad \text{(Eq. 59)}$$

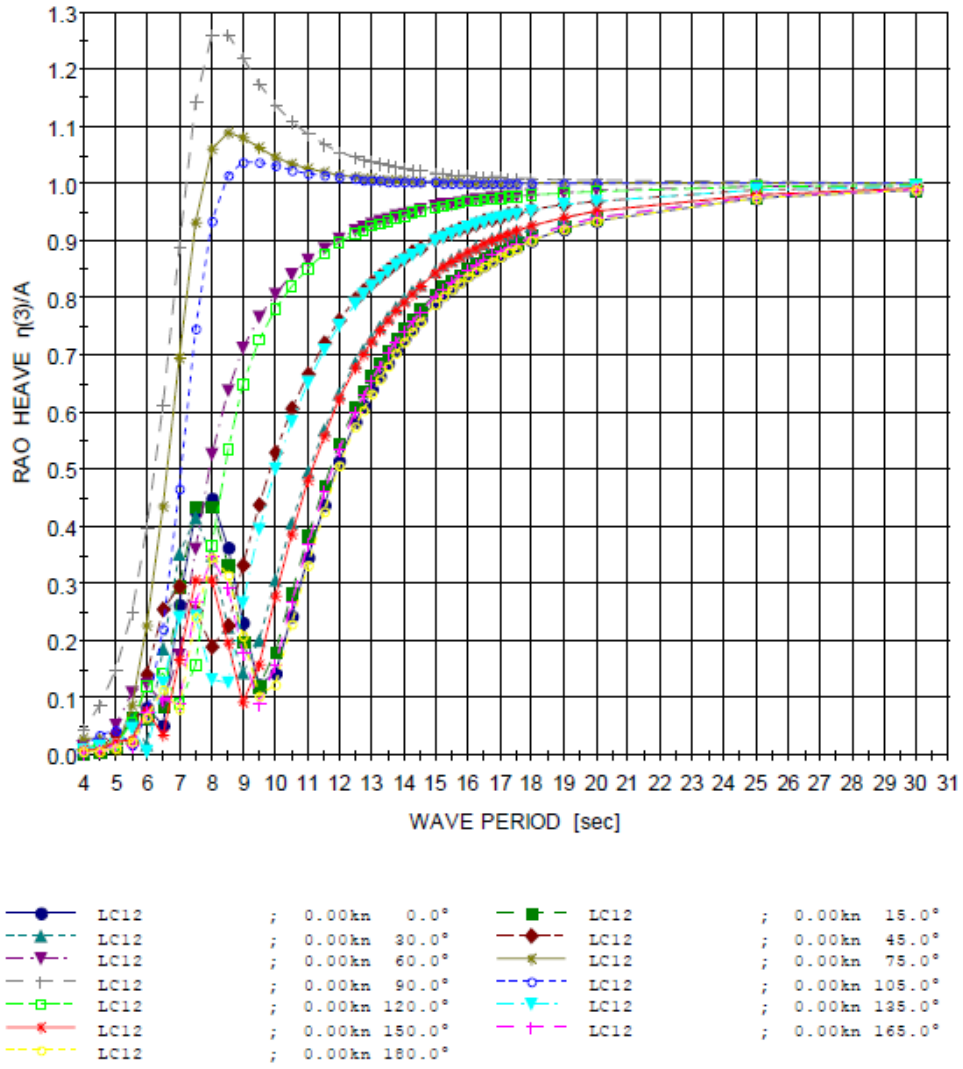

Figure 9.1: Displacement RAOs for heave motion (LC2) for a range of different wave periods. Wave headings from 0° to 180° with 15° intervals. Based on VERES simulations of Normand Vision (STX OSV, 2013a)

The heave RAO graph for is very similar also for Load Case 1 (LC1).

For the heave acceleration on main deck there is no significant difference between LC1 and LC2 as mentioned (ref. Figs. C.0.1 – C.0.3). However, it can be noticed that there is a tiny plateau at about 13 seconds wave period for LC1. The descending acceleration stops a bit at this point, which may be due to the vessel's roll period of about 13 seconds for LC1.
Only the 90° wave direction is here considered as the heave acceleration is well below the limit for the other wave headings independent of wave height. The peak values for the heave acceleration at main deck are located at about 7 - 8 seconds, which looks to coincide fairly well with where the most heave displacement is located (ref. Fig. 9.1). Also the peak values are quite similar for the same wave heights for both Load Cases. The limit for manual work is breached for every wave height with the 90° wave direction. It is quite narrow for the 3.8 meters H_D but is of course wider the higher the wave height is.

9.1.2 Roll

As can be seen from the roll result graphs in Appendix C there seems to be a recurring peak value of about 13 seconds wave period for LC1 (ref. Figs. C.0.10 – C.0.15). For LC2 the peak values seem to be located at higher periods around 16 seconds. The limit is for the heavy manual work on main deck.
To check the vessel's Eigen period in roll a rough estimate for ships could be found from equation 60 (Norwegian Maritime Directorate, 2008):

$$T_{roll} = 0.8 \cdot \frac{B}{\sqrt{GM}} \qquad \text{(Eq. 60)}$$

For the two Load Cases this formula gives the periods shown in Table 9.1. Here the width (B) is equal to 27 meters. The metacentre height (GM) is taken from Table 9.1. The estimates give about 13 and 16 seconds which coincide perfectly well with the anticipated values based on the Eigen periods in roll from the RAO graphs (ref. Figs. 3.9 and 3.10).

Table 9.1: Values for Eigen period in roll for LC1 and LC2 (ref. Appendix A for the GMs)

Load Case	GM [m]	T_{roll} [s]
#1	2.83	≈ 13
#2	1.83	≈ 16

For LC1 the peaks of the roll motions are quite distinctive and have large values (15°-37°). For LC2 the peak values are not that large and occur around 16 seconds (ref. Fig. C.0.15).

From the roll motion for LC1 it is clear that a wave period of about 13 seconds causes very large motions as the waves then comes in resonance with the vessel's roll period. The same is the case for LC2. The reason why the peak values are somewhat lower for LC2 relates to its larger displacement. A larger displacement means larger draft, water plane area and therefore also water plane stiffness. This will have an effect on the vessel's vertical component of the roll and pitch motions to be damped more efficiently.

"Everything" is affected by the roll period. The roll motion affects the comfort of the personnel, handling of cargo and sea fastening. So it is one of the major issues for the lateral acceleration on deck as well as the landing of helicopters which will be discussed later in this chapter. The dangerous roll period and roll angle are different from one ship to another. However, if the vessel is rolling so much that it experiences much water on the deck it is generally considered as unfavourable as water can penetrate into the vessel and affect the vessel's stability. When the roll angle is above 25°-30° it could be considered as large. The vertical component of the roll (motion, velocity and acceleration) also contributes to the heave (motion, velocity and acceleration).

9.1.3 Pitch

The pitch motion is also important to consider as pitch's vertical component also contribute to the heave. The pitch motions are in the analysis particularly important when it comes to the landing of helicopters as the helideck is located in the front. The vessel will experience much larger pitch in the bow and stern regions than e.g. amidships. Long wave period and large wave height in head seas can cause the pitch to be quite high and together with the heave it can give big challenges with respect to vertical motions in certain areas of the vessel.
An advantage with Normand Vision is its length of 154.7 meters, as this is favourable when it comes to reducing pitch motions compared to a shorter vessel. The vessel will better float on top of the wave crests rather than plunge into them which could be the case for a shorter vessel, say e.g. ≈ 100 meters long, in the same waves (in terms of wave length). The maximum pitch occurs at a wave period of about 9-11 seconds and head seas for both Load Cases with the largest value of approximately 4.5° (ref. Figs C.0.16 – C.0.21). This is reasonable as the Eigen period in pitch for a ship is lower than the Eigen period in roll for example.
It also coincides fairly well with the provided RAO graph for pitch for LC2, see Figure 9.2 (the pitch RAO graph for LC1 is practically speaking indistinguishable). And as can be seen from Figures C.0.16 – C.0.21, the pitch motions is practically speaking identical for both load cases. This relates to the small difference in displacement, meaning that the longitudinal metacentre height is almost identical for both Load Cases. So the pitch of the vessel itself may not be very critical, but affects the helicopter landings which will be discussed later in this chapter. Pitch motions combined with heave will result in the largest heave motions, velocities and accelerations.

The limit for the pitch motion is not included in these figures as it is not used directly but indirectly to check the helicopter landing criteria. The limits are however ±2° and ±1° for day and night landing of helicopters, respectively.

The Eigen period in pitch for a ship could be found from equation 61 (Gudmestad, 2013d). The Eigen period for pitch is located approximately at the top of the first peak in head seas in the RAO graph (ref. Fig. 9.2). A rough estimate has here been calculated based on a longitudinal metacentre height assumed to be about 200 meters for Normand Vision and the displacement for Load Case 2. This assumption is based on the longitudinal metacentre height of about 273 meters for another Load Case (Load Case 3 which is to be described later), with smaller displacement for Normand Vision. And for a heavier vessel a smaller GM_L will be applicable.
The estimate presented in equation 61 gave an Eigen period in pitch of about 5.90 seconds.

If the estimated Eigen period is compared to Figure 9.2 it seems like a period of 5.90 seconds is not too bad as this is a very rough estimate/"guestimate".

$$T_{pitch} = \frac{2\pi}{\sqrt{12 \cdot g}} \cdot \frac{L_V}{\sqrt{GM_L}} = \frac{2\pi}{\sqrt{12 \cdot 9.81 \frac{m}{s^2}}} \cdot \frac{144.51\ m}{\sqrt{200\ m}} \approx 5.90\ s \qquad \text{(Eq. 61)}$$

Here:

- L_V = L.L.P. for the vessel [m]
- GM_L = The longitudinal metacentre height [m]

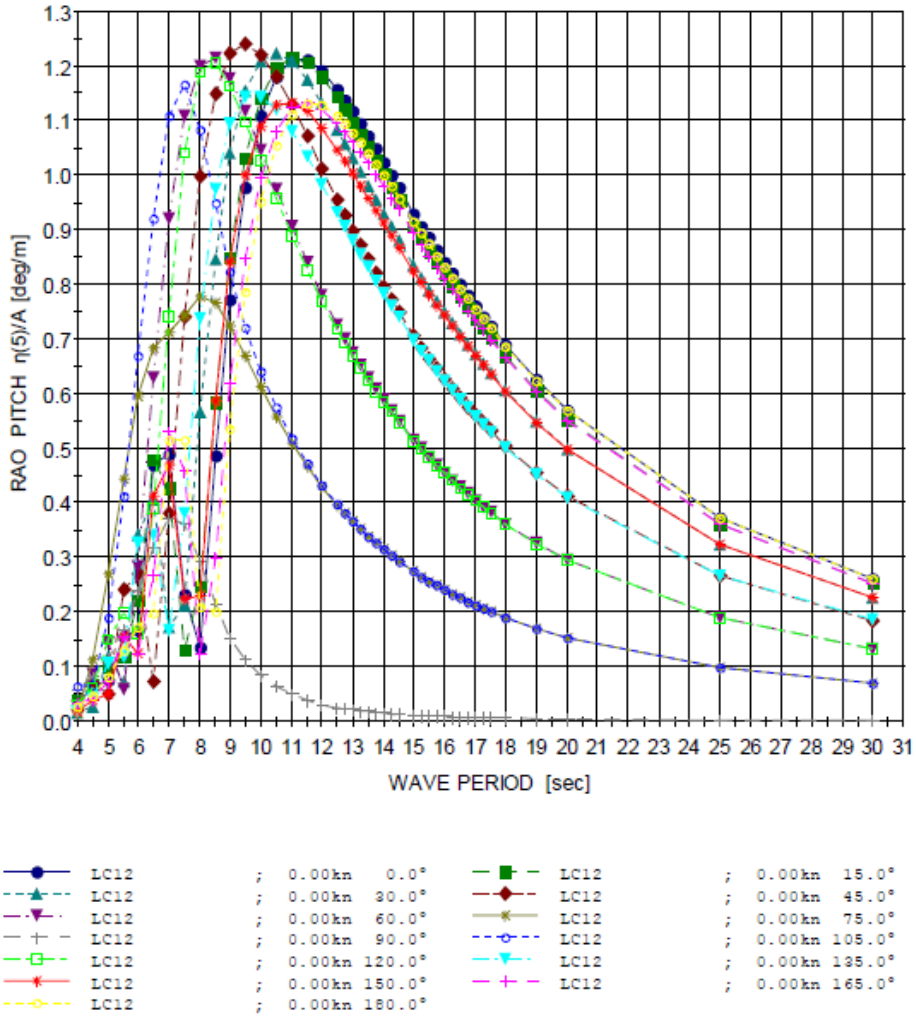

Figure 9.2: Displacement RAOs for pitch motion (LC2) for wave headings from 0° to 180° with 15° intervals. Based on VERES simulations of Normand Vision (STX OSV, 2013a)

9.2 Discussion of the product's capabilities

9.2.1 Top tension in the flowline

Based on the OrcaFlex analysis the capabilities of the product are one of the most challenging areas. The top tension is of most concern. As can be seen from the results presented in Appendix C, the flowline will see too large top tension when the wave direction gets unfavourable (45°, 90°) and the wave height increases (5.7 and 7.6 meters H_D). This applies for both Load Cases (ref. Figs. C.0.22 – C.0.30). Generally the peak value for the top tension is located around two different wave periods of about 7 – 8 and 12 – 17 seconds, depending on Load Case and wave heading.

For easier overview over what wave periods causes dangerous tension in the flowline, the periods causing the allowable tension limit to be breached are presented in Table 9.2. This gives an approximate presentation of which wave periods will cause problems. Approximate presentation means; if there is a tiny operational window with tension just below the allowable limit for say only 12 – 15 seconds, this is in Table 9.2 considered as "limit breached" because the values are close to the limit so one would probably not use the window from a practical point of view. The rest of the periods (those not mentioned in Table 9.2 or any of the following tables) are not breaking their respective limits.
For the full details regarding what periods are breached and not, please see the graphs in Appendix C.

Table 9.2: Approximate presentation of wave periods causing the allowable tension limit to be breached

Periods where allowable installation tension (top tension) is breached for both Load Cases (LC1 and 2)			
H_D [m]	**0°**	**45°**	**90°**
3.8	None	12 – 14 sec. for LC1	12 – 14 sec. for LC1 and < 9 sec. for LC2
5.7	None	12 – 14 sec. for LC1	< 15 sec for LC1 and 6 - 11 and > 15 sec. for LC2
7.6	None	12 – 15 sec. for LC1	< 16 sec. for LC1 and all periods for LC2

For Load Case 1 (LC1) and H_D of 3.8 meters, the largest top tension is seen at peaks of about 13 seconds for 45° and 90° wave headings. The interval for breaking the limit is here very narrow compared to the larger wave heights. Reference is made to Figures C.0.23 and C.0.24.
When H_D is 5.7 and 7.6 meters, the top tension peaks occurs both at 7 – 8 and 12 – 14 seconds with 90° wave heading. They break the tension limit with peak values much over 400 kN.
For the 45° heading the peak is about 13 seconds and breaks the limit for both wave heights. Reference is made to Figures C.0.26 – C.0.27 and C.0.29 – C.0.30.
From these results one could see that the vessel from a practical point of view is not of much use for pipe installation with H_D equal to 5.7 or 7.6 meters and beam seas (90°).

For Load Case 2 (LC2) the results are somewhat different. One difference is that there are no particularly high values around 13 seconds wave period. The peak values for LC2 are located at 7 – 8 and 16 – 17 seconds wave period. For H_D of 3.8 meters only 90° wave heading breaks the limit from 6 – 9 seconds wave period (ref. Fig. C.0.24).

Actually for LC2, none of the wave heights breaks the tension limit for 0° and 45° wave headings. For H_D of 5.7 meters the limit is breached for 6 – 11 and 15 – 17 seconds wave period. And for H_D of 7.6 meters the limit is breached for 6 – 12 and 15 – 17 seconds wave period.
Despite that LC2 has the largest total mass of the Load Cases it mostly gives a lower tension in the flowline. This can relate to the larger draft of LC2, which causes the vessel to gain larger water plane area and water plane stiffness which may help giving the vessel better damping capabilities. This again gives rise to a more limited tension in the flowline as the vessel does not move that much around, as could be seen from the values for the roll rotation.

To sum up, the flowline faces too large tension for some periods with wave heading 45° and 90° for LC1 and for wave heading 90° for LC2. Based on this it will most likely not be possible to install the flowline in the largest waves (H_D = 7.6 m) as this will most likely damage the product. For the smaller waves (H_D = 5.7 m) there are no problems for LC2. There is a good operational window for wave periods less than 12 seconds for LC1, which are typical North Sea conditions. The smallest waves (H_D = 3.8 m) sees no challenges with respect to the top tension.

9.2.2 Deflection angle of pipe with the vertical when going through the moonpool

The deflection angle with the vertical is an important parameter to consider so that the flowline does not clash into the sides of the moonpool during installation. An approximate presentation of the wave periods which will cause the limit for the deflection angle to be breached is presented in Table 9.3.

Table 9.3: Approximate presentation of wave periods causing the limit for deflection angle to be breached

Periods where maximum deflection angle in moonpool is breached for both Load Cases (LC1 and 2)			
H_D [m]	**0°**	**45°**	**90°**
3.8	None	12 – 14 sec. for LC1 and 15 – 17 sec. for LC2	12 – 15 sec. for LC1 and 15 – 18 sec. for LC2
5.7	None	11 – 15 sec. for LC1 and 14 – 18 sec. for LC2	11 – 16 sec. for LC1 and 15 – 18 sec. for LC2
7.6	11.5 – 18 sec. for LC1 and 11.5 – 18 sec. for LC2	9 – 18 sec. for LC1 and 9 – 18 sec. for LC2	All periods for both LC1 and LC2

The smallest waves (H_D = 3.8 and 5.7 m) does not cause the deflection limit to be breached for any of the Load Cases in head seas (ref. Figs. C.0.31 and C.0.34).
However, for the bow quartering (45°) and beam seas (90°) there are certain intervals where the deflection angle grows too large (ref. Figs. C.0.32 – C.0.33 and C.0.35 – C.0.36), see Table 9.3. The peaks are also here located close to the Eigen periods in roll located at approximately 13 (LC1) and 16 seconds (LC2). These peaks reflect the effects of the roll motion which gives large deflections of the pipe in the moonpool when closing in on the Eigen periods.
The lowest periods where one will break the limit for these wave heights are for waves with 11 seconds period for LC1 and 14 seconds period for LC2. So LC2 is more favourable regarding the deflection angle than LC1. Waves over 13 seconds are rather long and might not be of very critical concern for operating in the North Sea periods (ref Fig. G.0.4).

But when the wave height is increased to (H_D = 7.6 m) there are quite some challenges as most of the periods gives a too large deflection for all three headings, see Figures C.0.37 – C.0.39 and Table 9.3.

One thing that could help for avoid the flowline to clash into the moonpool is to have a higher weight of the pipe. One could e.g. have a more dense fluid inside the pipe during installation, but this may not be feasible due to increase in top tension.
In most cases a flexible flowline would not have any additional weight attached to it during installation. However, in some cases there will be a need for bend stiffeners/bend restrictors. These will pose an additional weight to the flowline helping to straighten it more and somewhat reduce the deflection angle.

9.2.3 Compression and bending radius in the sag bend

The compression and the bending radius in the sag bend are closely related and therefore discussed together. As the compression in OrcaFlex is presented as negative tension, the compression results are presented with negative y-axis, see Figures C.0.40 – C.0.42.

Compression

The compression in the sag bend seems to be of minor concern as there in practice are only in beams seas one sees any compression at all, which is why only these results are shown.

For Load Case 1 (LC1) one could observe that the compression is rather linear except of an increase in the compression of around 13 seconds. As it is beam seas which is considered this is related once again to the vessel's Eigen period in roll. This could also be observed for Load Case 2 (LC2) for the higher waves (H_D = 5.7 and 7.6 m).
For LC2 the compression is even more linear than for LC1 and the compression limit is not breached for any wave heights.
For LC1 the compression peaks grow quite large for the highest waves (H_D = 7.6 m) and the limit (50 kN) is breached with a compression value of above 80 kN (ref. Fig. C.0.42).

Bending radius

Because a too small bending radius can damage the product, the interest is towards the lowest (minimum) values one could see for the bending radius.
Generally the bending radius behaves very well and the Minimum Bending Radius (MBR) limit is not breached for the smallest waves (H_D = 3.8 and 5.7 m) at all. The bending radius is quite linear for almost all the wave periods and headings. But some peaks are located at around 8 seconds period in beam seas. The results are presented in Figures C.0.43 – C.0.51 with the MBR as the red limit line.

Both Load Cases could for the bending radius be considered more or less identical. The only case where the bending radius is getting smaller than the MBR is for the largest waves (H_D = 7.6 m) and beam seas (90°), see Figure C.0.51. But it should be emphasized that the bending radius is not very far away from the MBR limit (4.69 m) for the other cases as well (ref. Figs. C.0.43 – C.0.50), where the bending radius lies in a belt between ≈ 10.3 meters down to ≈ 5.0 meters.

The reason for why the peak values are located at about 8 seconds may be because the wave length for this particular period looks to move the vessel quite a bit as the heave also have a peak for this period in beam seas (ref. Figs. C.0.1 – C.0.3).

If the layback distance and then also the bending radius are becoming very small one will in some cases see quite large compression in the sag bend, however, this is not always the case for flexible flowlines. Some sensitivity checks were carried out by using simulations. The layback was decreased and increased to check the effects (see Table 9.4).

The MBR is generally reached before the compression reaches 50 kN for a flexible flowline when the layback distance is decreased. The reason for having "difficulties" breaking the allowable compression limit during installation may be because of the high flexibility in the flowline, so it moves into the direction where it sees the least resistance, and hence "limits" the compression is it exposed to.

To affect the loads in the flowline one could adjust the layback distance (ref. Fig. 9.3). A shorter layback may work favourably in the sense that the top tension will be reduced, however the compression may increase and the bending radius will certainly be smaller. A longer layback will give a larger top tension as the horizontal force component of the tension will increase. Vice versa a shorter layback will give a decrease in the horizontal force component resulting in a smaller top tension. As can be seen from Table 9.4 the trend is that with a shorter layback distance the top tension is decreasing along with the bending radius. The pipe did not experience any dangerous compression in neither of these cases.

Table 9.4: Test case for change in layback distance. These tests were conducted for Load Case 2, head seas, H_D = 5.7 m (H_S = 3 m) and a wave period of 8 seconds, the values shown are maximum/minimum values

Case	Top tension [kN]	Compression in sag bend [kN]	Bending radius [m]
Test case with new layback of ≈ 15.0 m	≈ 355.3	≈ 3.6	≈ 7.3
Original case with layback of ≈ 25.0 m	≈ 357.6	≈ 2.1	≈ 8.5
Test case with new layback of ≈ 60.0 m	≈ 368.9	Do not see compression	≈ 13.3
Test case with new layback of ≈ 106.0m	≈ 373.4	Do not see compression	≈ 20.1

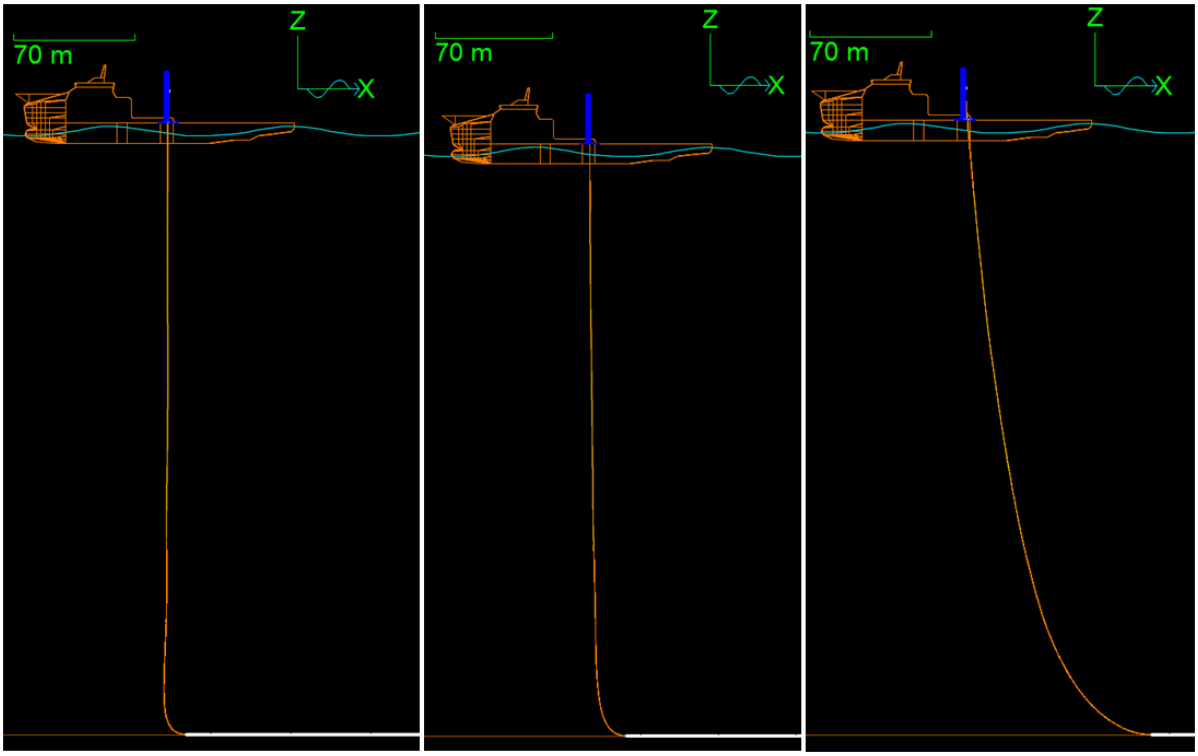

Figure 9.3: Layback distance for some of the test cases presented in Table 9.4 of about 15, 25 and 106 meters

Flexible flowlines are normally not installed with a large layback, compared to e.g. rigid steel pipes, for exactly the reason that they are flexible and can handle smaller bending radiuses and hence gain more favourable top tension values.

As the layback distance was increased, to e.g. 106 meters, it can be seen that the biggest issue is for the top tension, which closes in on the allowable installation tension of 382 kN. For this test case based on LC2 with 5.7 meters H_D and head seas, there are not big concerns regarding the bending radius, but it should of course be closely monitored as it is not very much bending it takes before the MBR is reached when having short laybacks.

Other wave headings may of course be less favourable with respect to the bending radius.
If the bending radius is becoming too small and smaller than the MBR, it will result in too much bending, which will most likely damage the flowline. Therefore it is important to assess the bending radius so a favourable trade-off point between a proper layback, bending radius, compression and top tension can be obtained.

The driving factor regarding layback should be to adjust the layback distance to gain the most favourable top tension values as well as the pipe is not damaged because of too small bending radius or too large compression. This was done before the analysis was started and the trade-off point chosen was to be a layback distance of ≈ 25 meters (“the original layback distance”) shown in Table 9.4.

Another parameter which is important to consider in this case is the deflection angle with the vertical when the pipe goes through the moonpool. When the layback is a bit larger than 106 meters (for LC2 and H_D = 5.7 m) it will break the limit for the deviation angle (7.3°) and there will be a larger risk for the pipe to clash into the moonpool walls. This is important to bear in mind.

So by adjusting the layback distance one could actually fine-tune the parameters to stay within their allowable limits in different sea states, even in the event of the somewhat extreme loading cases considered in this study.

9.3 Discussion of the conditions regarding heavy manual work on deck

Regarding the heavy manual work on deck there are the three limitations; heave acceleration (1.47 m/s^2), lateral acceleration (0.69 m/s^2) and roll motion (4°) to consider if the conditions are satisfactory for work or not. An approximate overview over the results is shown in Table 9.5.

Table 9.5: Periods where the limits for heavy manual work on main deck are breached

Periods where the limits for manual work on main are deck breached for both Load Cases (LC1 and 2)			
H_D [m]	**0°**	**45°**	**90°**
3.8	None	> 11.5 sec. for LC1 and > 13 sec. for LC2	< 9 and > 11 sec. for LC1 and < 9 and > 14.5 sec. for LC2
5.7	None	> 11 sec. for LC1 and > 14 sec. for LC2	All periods for LC1 and < 12 and > 13.5 sec. for LC2
7.6	None	> 10 sec. for LC1 and > 13 sec. for LC2	All periods for both LC1 and LC2

The results for the heavy manual on deck generally show that there are no breached limits ***for head seas (0°)***, independent of wave height. The reason why one sees such positive results for head seas is because the deck crew then will experience minimal roll and lateral accelerations. Also the vertical accelerations are rather small because the measurement point is almost at the center of the vessel, close to the moonpool, and that the length of Normand Vision gives limited pitch even in head seas because of its length.

When the wave heading is changed to bow quartering seas (45°) there are some challenges. As the limit for heavy manual work is composed of three parameters one must consider these three together. ***For 45° wave heading*** reference is therefore given to:

- Figures C.0.10, C.0.12 and C.0.14 for roll rotation
- Figures C.0.4, C.0.6 and C.0.8 for lateral acceleration on main deck
- (Heave acceleration was not a concern for bow quartering seas)

What could be observed from the results is that for bow quartering seas (45°) the roll makes some restrictions while the lateral acceleration not give any problems, apart from being close to the limit for the largest waves for Load Case 1 (LC1), see Figure C.0.8.

As earlier commented the roll has its peak values located around the respective Eigen periods in roll for both Load Cases. The interval for how many periods are breaching the limit is typically wider the higher the wave height is (ref. Table 9.5). LC1 gives larger roll peaks than LC2 and they are located at lower periods which are more unfavourable for the conditions in the North Sea. When having bow quartering seas (45°) the limit for the lateral acceleration is not breached for any Load Case, wave height and period (ref. Figs. C.0.4, C.0.6 and C.0.8).

For beam seas also the heave acceleration causes some more challenges for the manual work on deck and must be considered. ***For 90° wave heading*** reference is given to:

- Figures C.0.11, C.0.13 and C.0.15 for roll rotation
- Figures C.0.5, C.0.7 and C.0.9 for lateral acceleration on main deck
- Figures C.0.1 – C.0.3 for heave acceleration on main deck

The heave acceleration is too large in beam seas for intervals with a peak around a period of 8 seconds, but it do not limit the manual work in total as it is incorporated into the intervals for lateral acceleration. The lateral accelerations are mostly of concern in beams seas as the limit then is breached for some periods for all wave heights. For LC1 and 90° wave heading the values breaking the limit are found in the interval from 6 to about 13.7 seconds when taking into consideration all the wave heights.
The values are steadily descending towards the higher wave periods. At about 13 seconds one could notice a significant drop. What is interesting is that for the 45° heading there is a peak rather than a drop in the lateral acceleration at about 13 seconds. This may reflect that the waves coming from this direction are more likely to increase the horizontal component of the roll acceleration and hence also the lateral acceleration, while the 90° wave heading does not activate this horizontal component of the roll in the same way.
The same comments apply also to LC2, but here the limit is breached from 6 to 14 seconds (all wave heights seen together) and the “drop/peak point” is closer to 16 seconds, which is approximately where the Eigen period in roll for LC2 is located. These points regarding the lateral acceleration could also clearly be seen in the RAO curves for sway for all wave headings (see e.g. Figs. B.0.3 and B.0.15).

The roll rotation for beam seas are even larger than for bow quartering seas and strongly limits the manual work on deck. The problem is that the lateral acceleration and roll in beam seas breaks their limits with overlap for some or all period for the larger waves (H_D = 5.7 and 7.6 m). This strongly limits the possibilities for manual work on deck.

The general recommendation must be that in bow quartering sea the lower wave periods (typically 6 to 10 seconds) are satisfying to carry out work in, while the higher periods give restrictions due to large roll motions. In beam seas, with the limitations mentioned, it will in practice not be feasible to carry out manual work on deck as there are only very narrow windows that are okay for operation. In other words, the opportunities will be very limited.

Since the requirements for the heavy manual work depends on the three underlying parameters the decision to work or not should be assessed in every case based on what work is actually feasible to undertake in the actual conditions. It is also important to remember that the measure point for the vessel's lateral and vertical accelerations are located in the middle of the ship.
The heave acceleration would most certainly change to be more unfavourable if the position was located further out to either starboard or port side of the vessel. So the location of where the work is to be carried out is also important to consider.
But as earlier mentioned, in the end it will be up to the vessel's captain and crew to determine if the working conditions are safe or not.

9.4 Discussion of landing of helicopters

When it comes to the landing of helicopters during the two different Load Cases a proper description would be; challenging.
Firstly the helicopters would not be able to land on the helideck night time based on the certification criteria from HCA. Some general observations regarding landing in daylight:

- One will mostly not be able to land at all during beam seas for the different wave heights considered, except for wave periods >13 seconds and H_D = 3.8 meters for Load Case 2 (ref. Table C.0.2).
- No helicopter can actually land on the helideck regardless of Load Case and wave heading in the largest waves (H_D = 7.6 m), see Tables C.0.5 and C.0.6.
- Also for H_D of 5.7 meters there are very limited landing opportunities. The only window here is for a wave period of 6 seconds in head seas (see Tables C.0.3 and C.0.4).
- For the smallest waves (H_D = 3.8 m) it looks a bit brighter (ref. Table C.0.1 and C.0.2). Here there are some landing windows for 0° and 45° wave heading for some of the shortest and longest periods for Load Case 1.
  For Load Case 2 there is even a wider range of satisfying conditions as also some periods in beam seas (> 13 seconds) are okay.

Generally the pitch and roll motions are considered most critical with respect to helicopter landing by the pilots, as the skids of the helicopter can "take a punch" from the heave motions (Smith, 2014). However, if the heave accelerations become too large there are of course danger of a hard and dangerous collision between the helicopter and the helideck.
If the helicopter has a helideck under its skids before it is fully landed, and the pitch or roll suddenly flicks the helideck out of its position, the skids could slide on the helideck, or worse slide off the helideck. This could result in a number of dangerous scenarios with potentially fatal outcome for those involved. This is why the roll and pitch are considered to be of most concern.

However, from the analysis it is actually the heave rate that is most limiting for landing of helicopters. This is not very surprising since the helideck is placed in the very front of the vessel. This means that the contribution to the heave from the pitch motion will be significant. This is easy to see if comparing the heave rate graphs (ref. Figs. C.0.52 – C.0.60) with the pitch graphs (ref. Figs. C.0.16 – C.0.21).

In addition one also has the vertical component of roll. So the underlying factors for why one get high heave rates on the helideck is actually to a certain degree dictated by the roll and pitch motions of the vessel.

Since the heave rate is the most limiting factor only this is presented in Appendix C with the limit for the heave rate in daylight. For the wave heights of 5.7 and 7.6 meter H_D it could be seen that the heave rate is ruthless for both Load Cases (ref. Figs. C.0.55 – C.0.60).
For the 3.8 meters H_D the heave rate is mostly too high except for a few of the lowest and highest wave periods for the 0° and 45° wave heading for both Load Cases (ref. Figs. C.0.52 – C.0.54).

It could generally be observed that the heave rates have two peaks. The peaks for the lower periods are in the range of 7-9 seconds, where both Load Cases coincide very well. Actually the graphs for H_D = 3.8 meters coincide perfectly.
The other peaks are for periods related to the Eigen periods in roll as the wave heading turns to 45° and 90°. So these peaks are located around 13 seconds for LC1 and 16 seconds for LC2.

As the criteria for the inclination of the helideck is less strict than those for roll and pitch, and the inclination is taken to be equal whatever is largest of pitch and roll it would in practice not be important as it will not limit the landing possibilities (ref. Table 8.4).

The helicopter safety has increased a lot over the years since flying in the petroleum industry first started. From 1968 to 2000 the helicopter traffic in the petroleum industry has taken 50 lives in Norway and 86 in UK. Last time there was a fatal accident involving helicopters in the petroleum industry in Norway was back in 1979, when a helideck crew member was killed at Frigg (HSE, 2001).
When it comes to judging if the landing conditions are safe, it is up to the pilots to take the final decision/last call. The trend nowadays is more towards complying with the helideck's certification limits to be sure that the landing conditions are unified considered as safe (Huse, 2014).
Then one eliminates the different pilots' own judgment of the landing conditions, which could be quite different. So in practice they will not land before they have been given green light (see Appendix D) from the captain or other authority on board the actual vessel/installation.

Green light means that the criteria one is to operate within are complied with for at least 20 minutes, which is when the conditions can be considered as steady. See Figures D.0.1 and D.0.2 for examples of helideck monitoring systems in Appendix D.

So to sum up, there are not very many opportunities to land a helicopter based on the OrcaFlex simulations. In practice it may not happen unless the sea state is very calm and stable (e.g. has been stable for a longer period of time with H_S = 2 m/H_D = 3.8 m).

9.5 Summary with some remarks

Some summaries are made and the main points and some remarks are presented here. These are to some extent based on two "summary tables" (Table I.0.1 and I.0.2) presented in Appendix I. The reader is referred to Appendix I for more details.

The comments in this chapter are based on the assumption that the vessel will operate in the North Sea and the wave periods most likely to encounter are in the range of 6 to 13 seconds with waves from 2 to 4 meters significant wave height.

These conditions should be representative as can be seen from Table 9.6. The percentage says how much of the time the conditions are representative both for wave periods and wave heights. See Table G.0.1 and Figures G.0.4 and G.0.5 in Appendix G for more details.

Table 9.6: Percentage of time the wave conditions are representative, ref. Appendix G (Mathiesen & Kvingedal, 2010)

Wave periods (T_P)	**Percentage**
6 to 13 seconds compared to all periods (for all H_S)	≈ 85.1 %
6 to 13 compared to 6 to 18 seconds (for all H_S)	≈ 89.9 %
6 to 13 seconds compared to all periods (for H_S 2 to 4 m)	≈ 89.1 %
6 to 13 compared to 6 to 18 seconds (for H_S 2 to 4 m)	≈ 90.9 %
Wave heights (H_S)	
2 to 4 meters compared to all heights (for periods 6 – 13 s)	≈ 46.5 %
2 to 4 meters compared to all heights (for periods 6 – 18 s)	≈ 46.0 %
2 to 4 meters compared to all heights (for all periods)	≈ 44.4 %

From Table 9.6 one can observe that the wave conditions should be quite representative as the wave periods are representative over 85% of the time and the wave heights are representative over 44.4 of the time in total. The wave heights have a bit lower percentages as the scatter diagram (Table G.0.1) is not presenting seasonal variations in the wave height. As the summer season here is considered for the installation the wave heights will actually be more favourable (ref. Figs G.0.1 – G.0.3).

Installation of flexible flowline (in waves with period 6 - 13 seconds)

- Flowline installation in 2 meters H_S (H_D = 3.8 m) is unproblematic for head seas. Bow quartering seas will give too large top tension and deviation angle with the vertical for Load Case 1 (LC1) with period > 12 seconds. These periods should be avoided. Load Case 2 (LC2) is unproblematic. Also beam seas will pose problems for LC1 for periods larger than 12 seconds and in the range of 7-9 seconds for LC2. These periods should be avoided.

- For waves of 3 meters H_S (H_D = 5.7 m) there are still possibilities for doing installations. However, for LC1 care should be taken when entering bow quartering seas with period larger than 11 seconds. Such periods should be avoided. LC2 is unproblematic. Installation in 90° heading is not advisable. As the allowable installation tension is breached for most periods for both load cases.

The deviation angle with the vertical is very close to its limit for both load cases and is also breached at about 11.5 seconds for LC1.

- When H_S is equal to 4 meters (H_D = 7.6 m), which is rather rough conditions for this type of operation, it is not advisable to install the pipe for 45° and 90° headings. Some periods may be possible to operate in for 45° heading, if staying below 9 seconds period. This is however a very narrow installation window. There are better possibilities to install in head seas, under close monitoring of the wave period, as there is a danger of clashing the pipe into the moonpool walls when the wave period is larger than 11.5 seconds. Also the tension should be monitored as it is quite close to the limit for certain periods. This applies for both Load Cases.

Manual work on deck

The roll motions are the first to limit the manual work in 45° wave heading. This means that in many cases the roll motion will, at least "on the paper", be too large for manual work to be carried out. For 90° wave heading there will be practically speaking no satisfying conditions for carrying out the work as both the heave accelerations and lateral accelerations also gets very large. What is also important to be aware of is that the measure point in the analysis pretty much was in the middle of the vessel (both transversally and longitudinally) which means that most of the other deck locations gives larger heave contributions from the roll.
So based on this the vessel should be facing the waves at about 0° so that the personnel can execute work on deck under satisfying conditions.

Helicopter landing

The helicopter landings are very limited as there are few wave periods which satisfy the landing criteria for the wave heights considered. There will most likely be many cancellations of crew changes. Based on the analysis it is recommended that the best conditions to land in are when the vessel takes the waves from dead ahead. The lower the wave height, the more favourable the landing conditions are. For the Load Cases considered here there are some "green lights" for H_S of 2 meters, while for 3 and 4 meters it is practically not a chance to land within the helideck criteria from HCA.

From the summaries a general observation is that beam seas should as far as possible should be avoided, especially for H_S of 3 and 4 meters. What could be called the best operational envelope with respect to the wave heading is from head seas to somewhere between head and bow quartering seas (0° and 45° wave heading), as also bow quartering seas causes problems in certain conditions. In heading restricted operations, e.g. operations close to offshore platforms, the wave height should be as small as possible during the operation.

So the performance of the vessel in these rather extreme loading conditions is for pipe installation quite good. There are more challenges related to manual work on deck and especially to landing of helicopters.

It should at the same time be emphasized that the analysis has a conservative approach focusing on peak values and that certain aspects may have been dealt with in a too conservative way compared to reality. This is hard to say before sea trials and/or real operations have been conducted with the vessel.

9.6 Spot checking of results with new Load Cases (RAOs)

During the work with this thesis, some more recently defined Load Cases with corresponding new RAO data arrived. These new Load Cases should be a bit more precisely defined than Load Case 1 (LC1) and Load Case 2 (LC2) in terms of flexible flowline installations. LC1 and LC2 are more preliminary compared to the new ones as the knowledge about the vessel has increased a bit more towards the end of the project. The new Load Cases are named Load Case 3 (LC3) and Load Case 4 (LC4) and are presented in Appendix E.

As a full comparison would be too time consuming and extensive to present, it was chosen to do some "spot checking" of relevant wave conditions and parameters between all the Load Cases. It was chosen to focus on 3 meters H_S (H_D = 5.7 m) as this is sort a limit between 2 meter H_S, which is mostly within the limits for LC1 and LC2, and 4 meters H_S, which often break the limits.

The Eigen period roll for these new Load Cases was found to be about 13.8 seconds for LC3 and 14.1 seconds for LC4 (from equation 60). This looks to coincide fairly well with the RAO graphs provided from VARD (ref. Figs. F.0.3 and F.0.6). From the documentation provided from VARD one could observe that the Eigen periods in heave are about 8 seconds for both Load Cases (ref. Figs. F.0.4 and F.0.7). For pitch the periods seems to be about 6 – 7 seconds for both Load Cases (ref. Figs. F.0.5 and F.0.8).

These new Load Cases were developed by a group of people with extensive knowledge about marine operations which sat down to define some really realistic loading conditions. This group of expertise consisted of the captain, chief officer, lead hydrodynamic designer, analysis engineers and technical/project managers for the Normand Vision construction project from Solstad Offshore ASA, Ocean Installer AS and VARD.

Actually it is quite important in the industry to obtain detailed/fine-tuned Load Cases and RAO data. Because if not one could e.g., based on analyses, limit oneself or the client to do work.
It happens that analyses carried out prior to an offshore operation show to be quite more conservative than necessary due to various assumptions in the analysis or other aspects. This can introduce some challenges during the planning of the operation. Therefore it is important to assess the analyses after the actual operations are carried out, to be able to continuously improve and do more precise analyses in the future.

9.6.1 Results of the spot checking with the new Load Cases

The results from the spot checking analysis are presented in Appendix F for all the parameters and wave directions as presented in sub-chapter 8.6. For an easier comparison with the new Load Cases, all Load Cases are plotted in the same graphs. LC1 and LC2 are shown as black curves, while the new LC3 and LC4 are drawn in colours. The limits are still drawn in red and remain unchanged.

The spot checking will not be discussed in detail, but some main lines will be drawn.

From the spot checking one could in general see that the new Load Cases were less severe than LC1 in most cases, while LC2 actually turned out to not be too bad compared with LC3 and LC4.

LC3 and LC4 have in most cases somewhat similar trends/curves as LC1, but the peak values are typically located at a bit higher wave periods and for some parameters also with higher peak values, as e.g. the top tension in beam seas (ref. Figs. F.0.9 and F.0.10).
The peaks for the different parameters, often dictated by the Eigen periods in roll, are prominent also for LC3 and LC4.
That the peaks are generally located at higher values than LC1 applies to most of the parameters investigated (ref. Figures in Appendix F). This is because the Eigen periods in roll for LC3 and LC4 are a bit higher than for LC1. The higher they are the more out of the interval of the normal (frequent) wave conditions one will face e.g. in the North Sea they are (ref. Fig. G.0.4).

It is easy to see from the results in Appendix F that the new Load Cases are more favourable than LC1 and LC2 as the peak values generally are quite a bit lower in magnitude. This should reflect more how the vessel will behave in reality and is important with respect to planning.

Also what is more favourable with the new Load Cases is that the period ranges for the peak values are more narrow which results in better operational window. See e.g. the results for the roll, top tension, deflection angle and compression in Appendix F.

The overall performance of the vessel with respect to the motion characteristics does not improve very much, so the landing of helicopters also for LC3 and LC4 is a big challenge (ref. Tables F.0.1 and F.0.2).

To sum up the results of the spot checking, one could say that the new Load Cases may better represent the reality when installing flexible flowlines. Also they seem to be more favourable than LC1 and LC2 with respect to peak values and larger operational window.
Generally one could say that it is important to get as good/precise input data (here thinking of RAOs from Load Cases) as possible, so that the planning of operations are based on a foundation as close as possible to the reality. When doing e.g. a HAZOP study in advance of an offshore operation, a somewhat imprecise analysis can limit the operation and result in wrong decisions being taken.

9.7 General improvements for execution of the operation

As can be seen from the discussions there are some possibilities that one will encounter waves with periods that will be unfavourable for one or more of the parameters considered in this study. Based on what was observed in the results, some aspects for improving overall operability of an Offshore Construction Vessel (OCV) during installation of flexible flowline are looked into.

Larger, more stable vessel with better motion characteristics

Longer, wider and hence a heavier vessel means a more stable vessel. This also means more favourable motion characteristics. This can be of great advantage, especially if the areas of operations have long swells as e.g. outside the coast of Western Africa, in the Norwegian Sea and in South-Western Barents Sea. A larger vessel on the other hand is much more expensive as there will be need for more steel, so a trade-off between what is considered as tolerable vessel conditions and how much one will invest should be found.

To get better stability the basic idea will be to lower the CoG which causes the transverse metacentre height to increase. This may be obtained by the use of more ballast (permanent or temporary) strategically located in the vessel. This will however result in a lower freeboard. So this must be taken into account.
The locations of the water ballast tanks also have an effect on how the vessel will behave. The location of these tanks should in general be assessed to gain the most favourable motion characteristics of the vessel without sacrifice of other important equipment and features.

Increase in stability can also be obtained by designing a wider vessel. This will increase the distance between the CoB and the metacentre. This will again affect the metacentre height to be larger which will give a larger natural period in roll (ref. equation 60).
It is mostly of interest to increase the natural roll period for OCVs, i.e. an even wider vessel, as this will move the natural roll period more away from the range of wave periods one will normally see. This is because these types of vessels basically have a quite large period in roll because of their size. A reduction in the natural roll period will therefore in most cases mean that the probability for more unfavourable roll motions and the chance of experiencing roll resonance will increase. A larger vessel will have a larger water plane area, which results in a lower natural period in heave, and vice versa with a decreased water plane area (ref. equation 59). The vessel should be fine-tuned as good as possible with respect to the wave conditions for the area where it is to mostly operate, so that the most frequent range of wave periods are not incorporating the natural period in heave and roll. This gives more favourable vessel motions and could lead to increased operability window.

The best compromise between necessary size (length, width, water plane area, keel, displacement, geometry and more), and the most frequent wave conditions the vessel will meet when operating, should in general be sought when designing an OCV.
In this way one gets the most favourable motion characteristics possible for that particular vessel.

Helideck

When it comes to the helideck it seems to move quite a lot in certain wave conditions. Helidecks on OCVs of this size are normally located in the bow area.
Another location of the helideck, than in the bow, might give better weather window for landing of helicopters. If a helideck was located more amidships and maybe a bit lower, this could be more favourable for landing. This may not give any significant improvements with respect to motions and is difficult to introduce, as OCVs has the need of a large main deck area and space for equipment around the work moonpool. However, if an "active motion compensating helideck" was installed, even at the current location, this might give significant improvements.
As mentioned mostly roll and pitch are of concern for the helicopters when approaching the helideck. This will be further discussed in chapter 10.2.

Flowline

The flowline shows quite good performance for tension/compression and bending radius for the various wave conditions. Still, it could benefit from even smaller motions of the vessel as this will pose less force on the flowline. Less external pressure on the flowline will also give less top tension, which is favourable when the waves are getting tougher. This could be achieved by having longer tensioners for distribution of the same amount of squeeze force. Buoyancy modules may also be an option for decreasing the forces on the flowline, but may give more challenges during installation.

An alternative will be to use a stronger flowline which will be much heavier and more expensive. This may also need to have attached buoyancy modules because of the extra weight, if the tensioners' capacity is close to being reached. Alternatively to the buoyancy modules, the VLS can be upgraded to be stronger with new tensioners to get more squeeze/clamping forces.

A vessel like Normand Vision could in theory install almost all sizes of flexible flowline, also in very deep water. A criterion is however that the wave conditions are okay and that the flowline is not too heavy so too large forces will be seen. Attachment of buoyancy modules will then be necessary.

10 Some highlights with respect to vessel motions

10.1 Parametric roll resonance

The phenomenon of parametrically excited roll motion, also known as parametric roll, has been known to mariners and naval architects since the 1950s. This phenomenon can be quite dangerous if the vessel enters into so-called parametric roll resonance. Parametric roll resonance is unpredictable and can suddenly occur with the result that the vessel suddenly changes its roll rotation from a few degrees to over 30° in a few wave cycles. Roll angles over 50° has been reported (González , et al., n.d.).
Earlier this phenomenon was mostly related to smaller ships in following seas, but is today mostly of concern for large container carriers in head seas (Belenky, et al., 2004). The phenomenon can happen to any type of vessel, small or large, but it depends on vessel geometry and wave length (Zhan, 2014).

The parametric roll resonance may be defined as a dynamic amplification of the roll motions due to periodic changes in a ship's stability in head or following seas. Development of parametric roll resonance can occur when the waves' encounter/excitation frequency (frequency of periodic stability changes) is about twice (typically between 1.8 – 2.1) the Eigen frequency of the vessel, (Hovland, 2007), (Benedict, et al., 2014). Also it is most likely to occur when the wave length is about the same as the waterline length of the vessel.
So the parametric roll resonance can occur both in head seas and following seas. The phenomenon is not yet fully understood and much research is on-going on the topic. In Norway the Centre for Ships and Ocean Structures (CESOS) at NTNU and Marintek is the leading research facilities on this topic.

The phenomenon is quite complex to explain theoretically in detail, as would be too extensive here, therefore only a limited and more practical description follows.
As the parametric roll resonance occurs during head or following seas it is longitudinal waves that causes the problem. The maximum change in stability will occur when the wave length is about the same as the waterline length (L.L.P.), which for Normand Vision is ≈ 144.51 meters. The vessel motions will be more severe/violent and hence more dangerous, the higher the waves are. See Figure 10.1 for a picture of the impact of parametric roll resonance on a container carrier.

Figure 10.1: Container carrier APL China arriving Seattle in October 1998 after having experienced parametric roll resonance, 60% of its cargo was lost at sea or damaged (van Laarhoven, 2009)

A vessel in calm sea without any waves will have a different water plane area, and hence stability than a vessel in waves. However, the water plane area will also be different in waves depending on whether the vessel is located on a wave crest or in a trough.
For example, a vessel in a wave trough will have a much larger average water plane area than it would have in calm water as the bow and stern are more deeply immersed. A more deeply immersed vessel will have a wider water plane, as a larger percentage of the hull will be immersed (see Figs. 10.2 and 10.3). So the draught will be larger which gives the vessel better stability because of increased metacentre height (GM).

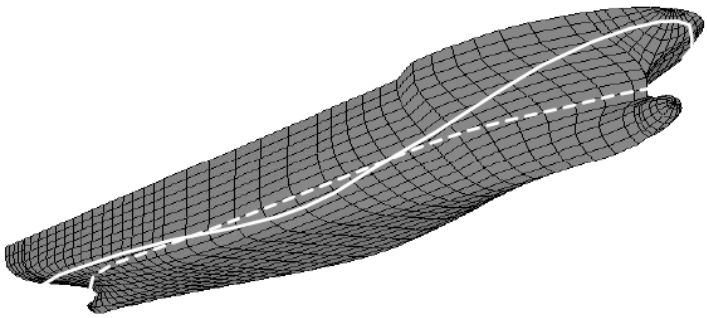

Figure 10.2: Waterline in wave trough (solid line) vs. in calm water (dotted line) (Belenky, et al., 2004)

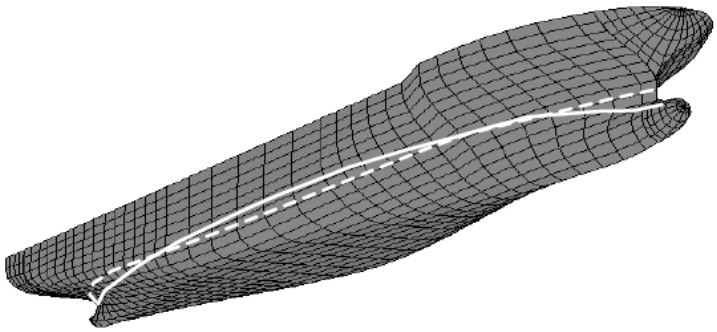

Figure 10.3: Waterline in wave crest (solid line) vs. in calm water (dotted line) (Belenky, et al., 2004)

On the other hand, when the vessel is located with the wave crest amidships the vessel will be less immersed. This means narrower width of the water plane than in calm water, hence smaller draught and water plane area. This means a lower GM and a less stable vessel. See also Figure 10.4.
The change in the stability means the restoring forces (the righting arm/moment) fluctuate between a lower and a higher value as the waves passes along the hull. The pitching motions coupled with roll motions, push the vessel from side to side as it pitches up and down. This eventually results in quite large roll motions over only a few wave cycles.

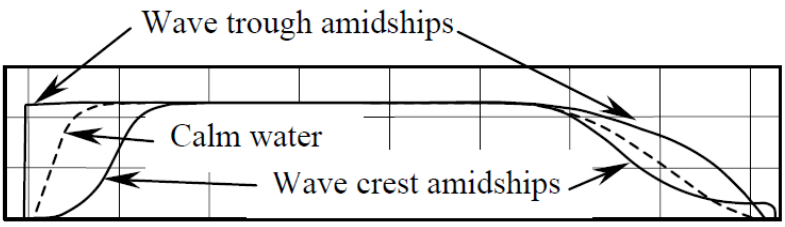

Figure 10.4: One half of a vessel seen from above showing differences in water plane areas (Belenky, et al., 2004)

Theoretically a vessel sailing straight against/from the waves (vessel's longitudinal centreline perpendicular to the waves) is not exposed to any wave-induced heeling moment. So one should believe it was not susceptible to any roll, however, small disturbances from the environment like e.g. wind gusts will set the vessel in an oscillatory roll motion with its natural roll frequency (period).
However, if the vessel then experiences encountering waves with twice the period of its natural roll period it will give rise to the self-reinforcing roll resonance motion known as parametric roll resonance. See Figure 10.5.

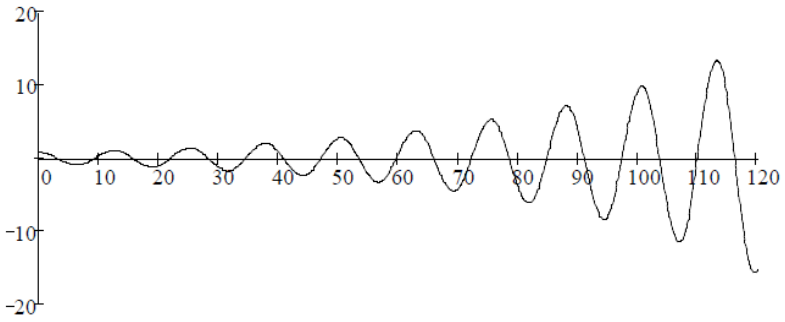

Figure 10.5: Development of parametric roll resonance, time on horizontal axis, roll angle on vertical axis (Belenky, et al., 2004)

There are few warning signs of parametric roll as the real sea states are complex. The only warning tends to be when the roll period closes in on the pitching period (Chen, 2014).

It could be worth investigating if there is any chance of Normand Vision to encounter such resonance in either head or following seas. This will be a rough estimate as not all data was possible to obtain during this study. Only Load Case 2 (LC2) is considered.
In order to do so a method for check of the susceptibility for parametric roll resonance by the American Bureau of Shipping (ABS) is used. The method is described in a guide called: "Guide for the Assessment of Parametric Roll Resonance in the Design of Container Carriers" (ABS, 2008). The guide contains mainly four steps the vessel is to be checked through:

1. Design wave and wave frequency
2. Stability in longitudinal waves
3. Ahead speed
4. Application of susceptibility criteria

In addition one could check the so-called "severity criteria for roll resonance" if the susceptibility test show that the vessel is prone to experience parametric roll resonance. Some of the notation does not coincide with that used by ABS for easier to distinguish between symbols used in this report.

10.1.1 Step 1: Determine the design wave and wave frequency

First the design wave height and wave frequency is checked. Then the design wave length (L_W) is set equal to the length between perpendiculars (L.L.P.) which is 144.51 meters.

By applying linear wave theory, the water depth can be checked whether any simplifications can be made or not, e.g. assuming infinite water depth if the water depth relative to the wavelength is above 0.5 (Gudmestad, 2013c). When using linear wave theory one assumes horizontal seabed and surface of infinite horizontal extent (Faltinsen, 1990). The water depth is still taken to be 350 meters.

Deep water check is shown in equation 62, where *d* is the water depth and L_W is the wave length.

$$\frac{d}{L_W} = \frac{350\ m}{144.5\ m} \approx 2.42 \rightarrow\ 2.42\ > 0.5\ \rightarrow OK \qquad \text{(Eq. 62)}$$

So the water depth is satisfying and linear wave theory can be applied. From the wave length one can then determine the wave's period (T_{WA}) by use of equation 63 for linear wave theory (ABS, 2008).

$$T_{WA} = \sqrt{\frac{2\pi \cdot L_W}{g}} = 0.8\ s \cdot m \cdot \sqrt{L_W} = 0.8 \cdot \sqrt{144.51\ m}\ s \cdot m \approx 9.62\ s \qquad \text{(Eq. 63)}$$

The wave frequency is then calculated from equation 64.

$$\omega_W = \frac{2\pi}{T_{WA}} \approx 0.65\ rad/s \qquad \text{(Eq. 64)}$$

Based on the wave length, ABS gives a recommendation for design wave height in accordance with Table 10.1.

Table 10.1: Wave length and wave heights for design wave according to ABS' guide (ABS, 2008)

Wave length, L_W [m]	50	100	150	200	250	300	350	400	450
Wave height, H_W [m]	5.9	11.6	14.2	15.1	15.2	14.6	13.6	12.0	9.9

The design wave height is found by linear interpolation as L_W = 144.5 meters (eq. 65):

$$H_W = 11.6\ m + \frac{14.2 - 11.6}{150 - 100} \cdot (144.5 - 100)\ m \approx 13.9\ m \qquad \text{(Eq. 65)}$$

This wave height should be used when calculating the transverse metacentre height with the wave crest at different locations along the hull, see next sub-chapter.

10.1.2 Step 2: Stability check in longitudinal waves

Here ABS says that any appropriate method could be used, but the accuracy of the method has to be demonstrated to their satisfaction. In this study ABS' method is used, but because of lack of data some assumptions must be made. This results in a rough estimate.

According to ABS one should calculate the GMs for at least 21 different locations with equally spaced wave crest positions. Then the maximum and minimum GM values are used to calculate the amplitude of stability change in longitudinal seas (GM_a) and mean GM value (GM_m), (ABS, 2008). See equations 66 and 67.

$$GM_a = 0.5 \cdot (GM_{max} - GM_{min}) \quad \text{(Eq. 66)}$$

$$GM_m = 0.5 \cdot (GM_{max} + GM_{min}) \quad \text{(Eq. 67)}$$

Calculations of the metacentre heights for different locations along the hull are normally done in software for calculation of stability. Since such a program was not available during this study the GM_a and GM_m are assumed to be equal a ratio of the metacentre height for Normand Vision in calm water (GM). The ratios are estimated from a sample case for a 262 meters long container carrier presented by ABS (ABS, 2008), see equations 68 and 69.

$$\frac{GM_a}{GM} = \frac{3.77\ m}{2.48\ m} \approx 1.52 \quad \text{(Eq. 68)}$$

and

$$\frac{GM_m}{GM} = \frac{4.52\ m}{2.48\ m} \approx 1.82 \quad \text{(Eq. 69)}$$

If these same ratios are applied on the GM for LC2 obtained from NAPA (ref. Appendix A), one get roughly estimated GM_a and GM_m values. These values are presented in Table 10.2.

Table 10.2: Roughly estimated GM_a and GM_m for LC2

Load Case	GM [m]	GM_a [m]	GM_m [m]
Load Case 2	1.83	≈ 2.78	≈ 3.33

10.1.3 Step 3: Ahead speed

Parametric roll is most likely when the waves' encounter frequency (ω_W) is approximately twice the natural roll frequency in waves (ω_m). If $\omega_W < 2\omega_m$ parametric roll resonance may be expected in head seas. If $\omega_W > 2\omega_m$ the parametric roll may be expected in following seas.
A number of parameters are to be determined in order to check if the vessel is susceptible to parametric roll resonance. These parameters are presented in Table 10.3, where also the proper formula or data source is shown. Not all the symbols used here are included in the general symbol list as they are presented here. The reader is referred to ABS' guide (ABS, 2008) for the full description of the different parameters.

Table 10.3: Parameters for calculation of susceptibility criterion for parametric roll resonance (ABS, 2008)

Value	Symbol	Formula or data source	Result
Minimum GM value [m]	GM_{min}	From calculations	N/A*
Maximum GM value [m]	GM_{max}	From calculations	N/A*
Amplitude of parametric excitation [m]	GM_a	$GM_a = 0.5 \cdot (GM_{max} - GM_{min})$	≈ 2.78*
Mean value of GM [m]	GM_m	$GM_m = 0.5 \cdot (GM_{max} + GM_{min})$	≈ 3.33*
Amplitude of stability change in longitudinal waves expressed in terms of frequency [rad/s]	ω_a	$\omega_a = \left(7.854\sqrt{GM_a}\right)/B$	≈ 0.49
Mean value of stability change in longitudinal waves expressed in terms of frequency [rad/s]	ω_m	$\omega_m = \left(7.854\sqrt{GM_m}\right)/B$	≈ 0.53
Forward speed most likely for development of parametric roll [knots]	V_{pr}	$V_{pr} = \frac{19.06 \cdot \lvert 2\omega_m - \omega_W \rvert}{\omega_W^2}$	≈ 18.5
Encounter frequency, +/- depends on head/following seas [rad/s]	ω_E	$\omega_E = \omega_W +/- 0.0524 \cdot V_S \cdot \omega_W^2$	≈ 1.06
GM value in calm water [m]	GM	From stability calculations	1.83
Natural roll frequency in calm water [rad/s]	ω_0	$\omega_0 = \left(7.854\sqrt{GM}\right)/B$	0.39
Roll damping coefficient expressed as a fraction of critical damping [-]	λ	Normally obtained from model tests	0.03**
Parameter of susceptibility criterion [-]	p	$p = (\omega_m^2 - (\lambda \cdot \omega_0)^2)/\omega_E^2$	≈ 0.25
Parameter of susceptibility criterion [-]	q	$q = \omega_a^2/\omega_E^2$	≈ 0.21

*Assumed value, **Assumption made based on recommendation from ABS' guide (ABS, 2008)

10.1.4 Step 4: Application of susceptibility criteria

As presented in Table 10.3, the susceptibility criteria, *p* and *q*, are determined. The ABS guide uses the following criteria to determine whether a vessel is prone to parametric roll resonance or not, see equation 70 (ABS, 2008). If this inequality is satisfied the ship may be susceptible to parametric roll.

$$0.25 - 0.5 \cdot q - 0.125 \cdot q^2 + 0.03125 \cdot q^3 - \frac{q^4}{384} \leq p \leq 0.25 + 0.5 \cdot q \qquad \text{(Eq. 70)}$$

Put in the value for *q* in the inequality (eq. 70) and obtain the following (eq. 71):

$$0.14 \leq p \leq 0.36 \qquad \text{(Eq. 71)}$$

As the inequality is satisfied with the *p*-value from Table 10.3 further checks are required. Also one could observe from Table 10.3 that parametric roll resonance can happen in head seas as the speed is positive and $\omega_W < 2\omega_m$ is fulfilled.

The "damping criterion of susceptibility" is to be checked, see equation 72 (ABS, 2008):

$$\lambda \frac{\omega_0}{\omega_E} < q \cdot k_1 \cdot k_2 \cdot \sqrt{1 - k_3^2} \qquad \text{(Eq. 72)}$$

The *k*-coefficients are shown in Table 10.4.

Table 10.4: Coefficients for the damping criterion inequality

Value	Symbol	Formula or data source	Result
Coefficient 1 of damping criterion	k_1	$k_1 = 1 - 0.1875q^2$	≈ 1.00
Coefficient 2 of damping criterion	k_2	$k_2 = 1.002p + 0.16q + 0.759$	≈ 1.01
Coefficient 3 of damping criterion	k_3	$k_3 = \frac{q^2 - 16 + \sqrt{q^4 + 352 \cdot q^2 + 1024p}}{16q}$	≈ -0.13

With these results the inequality (eq. 72) yields 0.011 < 0.21, this means that also this damping inequality is satisfied. From here ABS' guide (ABS, 2008) tells you to check the severity criterion of the parametric roll. This check procedure involves numerical integration of the roll equation with a non-linear restoring term taking into account the change in stability in longitudinal waves. Eventually one can find the actual righting arm (GZ) with the wave crest at different positions along the hull. There exists software for doing such rather complex calculations, but this will not be pursued here as we only roughly look into the possibility of experiencing parametric roll resonance.

From Table 10.3, one could see that the most likely forward speed to experience parametric roll resonance is about 18.5 knots. This is actually above Normand Vision's maximum speed. The ABS guide then says that the calculations are to be done for the closest achievable speed, which in this case would be the maximum operational speed, 16 knots (= V_{sr}).
With the use of this speed a new wave frequency is to be used with a corresponding new wave length. This means that a set of new metacentric height values must be determined with a new design wave height. Then new frequencies and susceptibility criteria are to be determined.
This is not done during this study because the results would not be any more precise as this is only a rough estimate, since the GM's are not calculated with the wave crest at different locations along Normand Vision's hull.

Based on the results from this parametric roll check, it looks like Normand Vision could be in danger of experiencing parametric roll resonance in certain conditions. This seems to have been considered to certain degree when the designing the vessel, as one will see from the next sub-chapter.

10.1.5 Mitigation measures for avoiding parametric roll resonance

As the results of parametric roll resonance could be severe, especially with respect to economic losses, it is important to try to avoid it as far as possible. If it occurs, however, one should reduce the vessel's speed and/or change the heading so the waves approach more towards the beam of the vessel. A course change, to break the "parametric roll friendly" frequency condition, has shown to be most efficient to get rid of the resonance since the inertia in the vessel causes a speed change to take quite some time (Chen, 2014).
However, it is of course in best interest to completely avoid parametric roll. In order to do so one should have a certain control over when one may experience the phenomena.

The most convenient way of presenting which conditions are unfavourable with respect to parametric roll resonance, is often by use of a polar diagram, see Figure 10.6. These diagrams show in which vessel headings and velocities one may get problems with parametric roll with respect to wave heading.

What could be dangerous and surprising is that the resonance can occur when encountering certain wave components, even if the average wave period is not equal to the vessel's Eigen/natural period. This may not pose any real threat, at least not for large vessels, but is still something the marine crew on the bridge should be aware of.

The probability of experiencing parametric roll can be reduced with change of the hull design so one gets additional damping in order to distribute the roll energy.

If the parametric roll occurs the impact could be reduced by opposing the roll motions. Measures may include features related to geometry and mass of the vessel. These features can be e.g. bilge keels, anti-roll tanks (movement of fluid mass), stabilizer fins (active or passive), outriggers, gyroscopic internal stabilizers and paravanes. Such features help improve stability with respect to the roll motions.

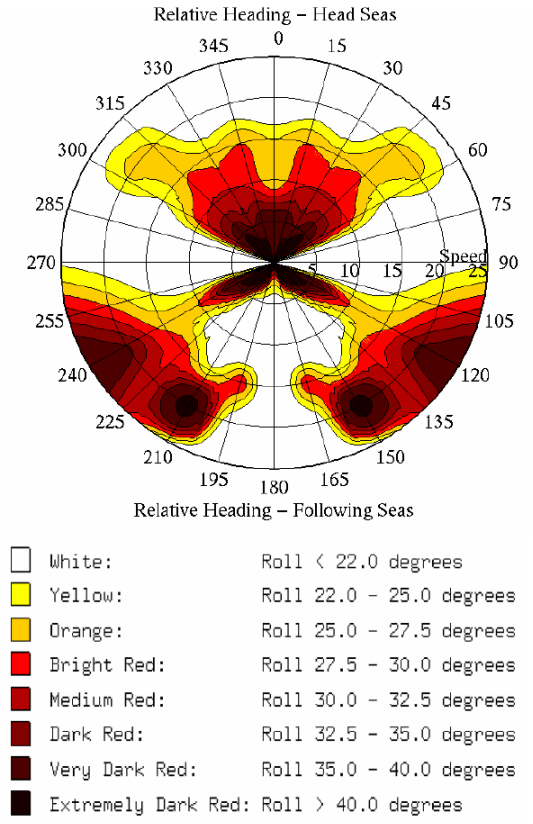

Figure 10.6: Sample polar diagram from ABS also showing possible roll angles (ABS, 2008)

Stabilizer fins can be found in many designs, both retractable and non-retractable. Most of the fins are adjusting themselves automatically as a computer (MRU or similar) registers the vessel's motions and continuously calculate the necessary fin angle. See Figure 10.7 for illustration of a retractable fin.
Bilge keels are also very much used when it comes to coping for roll motions. Bilge keels are normally located approximately amidships, where the vessel is at its widest (see Fig. 10.8). Normand Vision has bilge keels. What the bilge keels mainly does is to increase the added mass of the ship, due to larger projected contact area with the water, which helps gaining better damping of heave and roll motions (ref. sub-chapter 3.4 and Fig. 3.12).

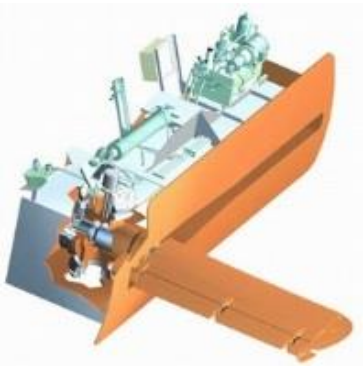

Figure 10.7: Non-retractable stabilizer fin (BVI Marine, 2009)

Figure 10.8: A bilge keel on a ferry (pbase.com, 2005)

Another geometry related anti-roll feature is related to the shape of the vessel's bow section.
Large container ships are often very wide in addition to having large bow flares. Then they are able to carry more containers on deck. Also the stern would normally have a large flare (see Fig. 10.9). The large flares are used because it will then reduce the resistance from the water on the ship's hull. If the bow then is symmetric it looks to be ideal conditions for parametric roll to occur. On such large container carriers it has proved efficient to reduce the possibilities for parametric roll by designing an asymmetric bow (see Fig. 10.10) as the waves then are directed somewhat differently along the hull. Normand Vision has not an asymmetric bow, as it may be unfavourable when doing operations using DP as well as in transit.

Figure 10.9: The stern flare of Gosport Maersk (Kantharia, 2013)

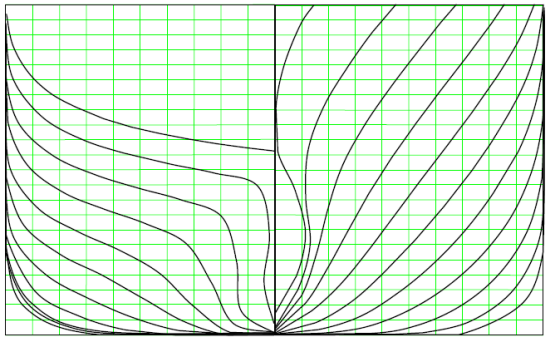

Figure 10.10: Illustration of an asymmetric bow on a containership (ABS, 2008)

A hydraulically operated bow spoiler can also be of help as it can "change the angle of the bow" to reduce pitch and roll motions when a ship is in transit (see Fig. 10.11). Depending on the sea state significant motion reductions can be achieved.

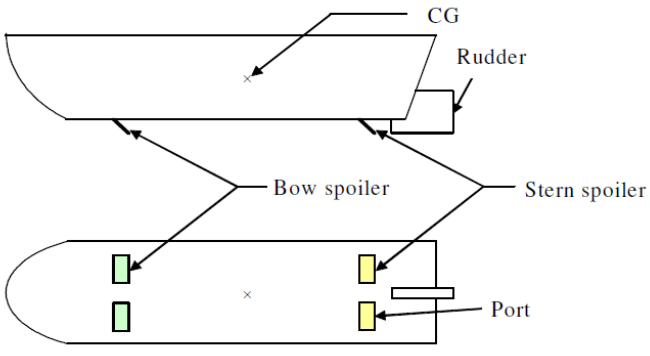

Figure 10.11: Illustration of where spoilers can be located (Djebedjian, et al., 2008)

For example roll reduction by a factor of 2 to 5 and pitch reduction by a factor of 1.2 to 1.5 can be achieved. This will also work favourable as speed efficiency can be gained. The principle of the spoiler is like that of a plane wing. The spoiler obstructs the flow, and two flow fields with different pressures are made on the up- and downstream side of the spoiler. The difference in pressure generates forces on the spoiler which can be used for controlling and reducing the hydrodynamic pitch and roll motions of the vessel (Djebedjian, et al., 2008).

10.2 Improvements of helideck with respect to motions

As have been seen from the analysis, the landing of helicopters on the vessel is quite challenging, even in only 2 meter H_S (H_D = 3.8 m). This is a well-known issue for monohull vessels. When the petroleum industry still was young the safety was not as highly prioritized as today. Nowadays the safety is much better and accidents are very rare. However, the requirements have become stricter and stricter, which often means that the vessel have to go to port for crew changes. This of course depends on the size of the vessel, the time of the year and location with respect to the sea/weather conditions. For example, it is more normal to have to go to port in the Norwegian Sea than in the North Sea because of generally larger and longer waves, hence more movement of the vessel.
This is uneconomically in most cases if a crew change is the only reason for why the vessel goes to port.

As was observed from the analysis, the pitch and roll are quite critical when landing a helicopter as they cause much motion also vertically. A helideck which could somewhat cope for these motions would most likely improve the rate of helicopter landings and crew changes.

Actually there exist at least two Active Roll Compensating helidecks (ARC) today. These are located on-board the PGS' (Petroleum Geo-Services ASA) seismic vessels Ramform Sovereign and Ramform Sterling. See Figure 10.12 for photograph of Ramform Sterling.

Figure 10.12: Picture of Ramform Sterling transiting in calm sea (Ship Portal Korabley, 2013)

The background for placing the ARC helidecks on these vessels was that they are relatively light, and wide, which result in a shorter Eigen period in roll which could be especially challenging when landing a helicopter.

A short Eigen period in roll is unfavourable for monohull vessels in most ocean areas around the globe, as it then is larger possibilities for the vessel to get in roll resonance. The helidecks on the Ramform vessels are mounted with an offset from the longitudinal centrelines of the vessels.

The helidecks are delivered from Uptime International AS (Uptime). The helidecks are mounted on skids so that they can move sideways (in lateral direction) to cope for the roll. The helideck will then stay more or less in the same position below the approaching helicopter. See Figure 10.13 for an animation picture of the helideck. A video of a helicopter landing on the deck can be found on Uptime's homepage.

Figure 10.13: Screenshot from an animation video where a helicopter is approaching the ARC helideck which can move about ±2.60 meters back and forth on the skids (Uptime International AS, 2010)

The helideck was first installed on Ramform Sovereign where it worked satisfactory for a period, until the nylon wheels melted as they did not handle the loads properly. There were also some issues with the hydraulic system on the first helideck. The hydraulic system and the wheels were changed on the second helideck which was mounted on Ramform Sterling. The vessel has shown good performance with these helidecks offshore Tasmania, the Falklands Islands, north of the Shetland Islands and off the Labrador Coast.

During the use of the helidecks it was after a while observed that the wheels started to engrave depressions in the skids so that they wobbled on the skids, first some millimetres then some centimetres. Over time this caused the hydraulic system to lose some of its accuracy. The reason this happened was lack of proper maintenance according to the provided maintenance plan. To repair this, the whole helideck has to be lifted off the vessel as the skids must be replaced. Because this is a costly and time-consuming operation the ARC function on the helidecks are not used today (Huse, 2014).

If an actual vessel has more issues with respect to pitch motions the ARC helideck could be mounted to cope for this instead, i.e. rotated 90°.

Uptime was recently contacted by Stena Drilling regarding a new drill ship that is to be operated West of Shetland, which will face challenging pitch motions with respect to helicopter landing. Uptime had several different projects going, but they are now stopped because of lack of funding (Huse, 2014).
The feedback from the pilots regarding the ARC helidecks is very good and the vessels were able to change crew in conditions that was actually considered as too rough based on the standard limitations for a helideck on this type of vessel.
The incentive for potential customers for having such a helideck is to have more uptime (extended operational window), with respect to crew changes and hence cost savings.
These helidecks on the Ramform vessels was actually upgraded to a better helideck category, from B+ to A+ during daylight, see Table 10.5. This change was issued by HCA. This means an upgrade from helideck category 2 to 1 (aircraft category A) according to HCA's requirements (ref. Table 8.4).

Table 10.5: Table of vessel categories with limitations, Norwegian codes (Huse, 2014)

Category (Appliccable for North Sea Operation)	Landing and planning			
	Pitch, Roll / Helideck Inclination		Max Average Heave Rate	
	Day	Night	Day	Night
A	±3°	±2°	1,0 m/s	0,5 m/s
A+	±3° / 3,5°	±2° / 2,5° (*)	1,3 m/s	1,0 m/s
B	±2°	Not approved	0,5 m/s	Not approved
B+	±2° / 2,5°	±1,5° / 2°	1,0 m/s	0,5 m/s

An issue may be if a vessel already having the best helideck category (category 1, ref. Table 8.4) gets an ARC helideck, as it then would not have a better category to upgrade to. So a better category for certification of helidecks does not exist today. Uptime wants to introduce a category for stabilized helidecks, which HCA so far has been a bit negative to.

The existing regulations only set criteria for the vessel's motions, and not the motions of the helideck itself. Neither is the height of the helideck relative to the sea surface taken into account (Huse, 2014). Wind speed is also absent, but work on "wind speed criteria" for deck stability (after the helicopter has landed) is ongoing. So there is actually a gap in the regulations when it comes to such improvements as a motion compensating helideck.

A helideck which could cope with both pitch and roll simultaneously would be an even better advantage. A company called Stable AS has started to think about the possibilities for this but have no specific projects on-going. They have experience with marine stabilized platforms which so far mainly have been used for pool tables, beds and other features on-board cruise liners, ferries and luxury yachts.
These systems have proved very reliable and are controlled by electrical engines adjusting very quickly.

The principle of the "Stable system" is that a certain point on e.g. the pool table should be at the same location all the time and that the table always is horizontal (Heier, 2014). If this system was to be used for helideck the engines should be hydraulically in order to handle the large weight of the helideck. The Stable system does not have the ability to move back and forth which is a big advantage when the helicopters is above the helideck and about to land. A combination of Stable's and Uptime's system might be a very good solution for future helidecks which need active compensation of vessel motions. Also Ampelmann's technology for access bridges (based on Stewart platform) could be interesting to look into if designing a helideck that could cope for more than one DOF.
Further work on such helidecks could e.g. be to make a small scale prototype which could have been tested e.g. at the University of Agder's six DOF Stewart platform (see video on YouTube; http://www.youtube.com/watch?v=WmKnnp1xTPg). The helideck could then have been placed on top of the Stewart platform, which could be programmed to simulate vessel motions, while executing experiments with a small remotely operated helicopter trying to land on it.

It must anyhow be an emergency possibility of locking the helideck in a "normal position", horizontal to the vessel deck, if e.g. a hydraulic malfunction occurs. A safety problem when compensating for several DOF could be in case a helicopter is about to land when the helideck is compensating e.g. for 7° roll and then suddenly stops working. Then say, the vessel rolls 7° in the opposite direction.
This could be a very dangerous situation so such a helideck must be very reliable. Also there must be carried out extensive risk assessments on this.

There must be a change in the regulations if there should be any point in making such stabilized helidecks as they are quite costly to develop and build. The most recent status for Uptime's proposal of a new "stabilized helideck category" is that the consultancy firm, WS Atkins plc, works on a report for CAA (Civil Aviation Authority, UK) and other parties where this is to be considered. The outcomes of this report may have a large impact on whether HCA will think more positively about making a new certification category or not (Huse, 2014).
An estimate of the return on investment time was carried out with two different scenarios by MARIN. Since the rental prices for vessels and personnel are rather high, the increased operational windows with respect to landing possibilities are important.

The first was for the well intervention vessel "Island Frontier" which has two "sister ships", "Island Wellserver" and "Island Constructor" (Huse, 2014):

- Current conditions: 35% operability, 70 flights, 15 port calls
- New conditions with improved helideck: 50% operability, 100 flights, 5 port calls

The improvement costs for these 3 vessels are of about 14 million Euros, but the return on investment time is only 6 months.
The second scenario is for 3 FPSOs in the North Sea (Huse, 2014):

- Current conditions: 50% operability, 100 flights/year, 50 flights/year with 2 days delay, 10 aborted flights
- New conditions with improved helideck: 75% operability, 100 flights/year, 25 flights/year with 1 day delay, 5 aborted flights

This improvement costs for these 3 FPSOs are of about 14 million Euros. The return on investment time is 2.5 years. So the potential for cost savings can be quite significant over time.

11 Conclusions and recommendations

Based on the analysis there can be drawn a number of concluding remarks with respect to the vessel's capabilities, where most are already highlighted in the discussions. The Load Case with the largest displacement (Load Case 2) showed to be quite favourable, in the sense that the vessel's motions were smoother. It takes more from the nature's side to move the vessel around the higher the displacement is. However, it is important to bear in mind that the freeboard decreases with the increased displacement. So the more favourable motions may not be that favourable if water suddenly enters the deck because of large waves and lower freeboard, as this can affect the initial stability quite much.
Load Case 1 with lower displacement and shorter roll period, with more damping involved (closer to critical damping), gave more "violent" motions, and higher accelerations, and hence larger peak values for the different parameters. These larger accelerations cause more challenges for carrying out the operation, but will also give the crew a more rough/uncomfortable ride. The spot checking with the new Load Cases (3 and 4) showed that these Load Cases have smaller peak values and have the peaks located in (wave) period intervals between the intervals that apply for Load Case 1 and 2.
The largest peaks are for most parameters concentrated around the Eigen period in roll for all Load Cases.

The top tension may be considered the most important parameter which was analysed. The vessel showed in general good performance for head seas. Some of the higher wave periods (typically > 12 seconds) showed to be unfavourable for bow quartering seas (45°), while beam seas (90°) was unfavourable for a much larger number of wave periods. The conclusion here would be that heading restricted flowline operations could be a challenge and must be carried out in very small waves to make sure to not overstress the flowline. These headings (between 45° and 90°) should of course as far as possible be avoided as the operations are to be carried out with minimal risk and in accordance with best practice. Other directions should also be looked into if they are relevant for the operation in question. OrcaFlex is here a very helpful tool to predict what to expect when the waves comes from certain headings.

Regarding the wave height the vessel showed good performance for H_S of 2 meters, and partly for 3 meters, depending on parameter considered and wave heading. The largest waves of 4 meters H_S (H_D = 7.6 m) are very challenging and causes many the various parameters' limits to be breached for some periods in different headings.

It is important to emphasize that the study is carried out with a conservative approach. Most of the values considered are minimums or maximums, and does not represent the average values. This was done to be sure to capture the most dangerous conditions, the large peaks.
However, during most operations in the North Sea the wave period will be far below 16 seconds (the 100 years wave, ref Fig. 4.3). The weather with respect to wave heights and periods one is susceptible to experience should be checked and operations only carried out if the conditions are satisfying.

This should be taken into account when planning the operations and during the making of the procedures. From the typical weather conditions in the North Sea it could be seen that a wave period interval of 6 to 13 seconds are quite representative. Then the vessel performs very well as it almost only break limits for wave periods above 12 seconds. This is favourable for most parameters, but other parameters have their peak values at the lower wave periods (e.g. in the range of 7 – 9 seconds), and can therefore see these peaks under the given conditions.

The conclusion here is to avoid these particular "trouble making" conditions if support systems like e.g. active heave compensation equipment and anti-roll tanks, does not provide enough safety margins for work to be carried out.

Based on the check for the susceptibility of parametric roll resonance it could be concluded and recommended that Ocean Installer, and the vessel's captain, and marine crew on the bridge, should be aware of this danger.

One can from the results see that the vessel performs fairly well for wave headings up to 45 degrees even for the largest waves considered in this analysis. However, the helideck's "motion performances" related to helicopter landing are quite disappointing. This is a well-known challenge to the industry as the criteria for safety and safeguarding of the helicopter transport has been stricter over the years.
The conclusion in most of the conditions analysed will be that the possibilities for landing of helicopters are very limited when the vessel is offshore. This can make the operations more inefficient as the vessel may have to travel to shore for crew changes.

A further scope of work could be to look more into the development of a helideck which could cope for more than one degree of freedom, e.g. both pitch and roll simultaneously, and which still is safe to use. This would clearly improve the operational window of Normand Vision with respect to crew changes.

It was seen from the analysis that how the vessel was loaded (i.e. Load Case) strongly affects how the vessel will behave. It will be interesting to see how the vessel will perform when the sea trials starts in late May until the end of June. One thing is how analyses turn out, based on the theory, data and assumptions. A somewhat different view may come to light when "reality kicks in", and challenges may occur.

So the methodology used in this study, to check the performance of a new built Offshore Construction Vessel in OrcaFlex, in an early phase, can prove quite useful and gives input regarding the vessel's capabilities before the sea trials and operations start.
This input can help prepare for sea trials and can provide interested parties with valuable information about the vessel's capabilities.

References / Bibliography

- ABS, 2008. *Guide for the Assessment of Parametric Roll Resonance in the Design of Container Carriers.* 2nd ed. Houston: American Bureau of Shipping.
- Anon., n.d. [Online]
  Available at: http://www.operatorchan.org/v/3.html
  [Accessed 11 May 2014].
- Belenky, V. L., Paulling, J. R., Lin, W. M. & Shin, Y. S., 2004. *Criteria for Parametric Roll of Large Containerships in Longitudinal.* Washington D.C., SNAME.
- Benedict, K., Baldauf, M. & Kirchhoff, M., 2014. *Schiffahrtsinstitut Warnemünde e.V., Institut an der Hochschule Wismar.* [Online]
  Available at: http://schiw.sf.hs-wismar.de/siw/paper/heft5/beitrag10
  [Accessed 13 May 2014].
- Bristow, 2013. *Helicopter Fleet: Bristow.* [Online]
  Available at: http://www.bristowgroup.com/clients/helicopter-fleet/
  [Accessed 1 April 2014].
- Buannic, N. et al., 2009. *Quasi Static Response (Committe II.1).* Seoul, 17th ISSC (International Ship and offshore Structures Congress).
- BVI Marine, 2009. *Products & Services: Blohm & Voss Industries (China) Ltd..* [Online]
  Available at: http://www.bvi-marine.com/eng/E213/E213.htm
  [Accessed 19th May 2014].
- Chen, H., 2014. *Parametric Roll,* Alameda: Ocean Systems Inc..
- Djebedjian, B., Mostafa, N. H., El-Said, E. M. S. & Rayan, M. A., 2008. *Experimental and Numerical Study of Spoiler Effect on Ship Stability: Effect of Air Injection Position.* Alexandria, Ninth International Congress of Fluid Dynamics & Propulsion.
- DNV, 2010. *Recommended Practice C205 Environmental Conditions and Environmental Loads,* Høvik: Det Norske Veritas AS.
- DNV, 2011b. *DNV-OS-H101 Marine Operations, General,* Høvik: Det Norske Veritas.
- DNV, 2011. *Recommended Practice DNV-RP-H103 Modelling and Analysis of Marine Operations,* Høvik: Det Norske Veritas AS.
- DNV, 2013a. *DNV-OS-H204 Offshore Installation Operations (VMO Standard Part 2-4),* Høvik: Det Norske Veritas AS.

- DNV, 2013b. *Rules for classification of ships, Part 3 Chapter 3, Hull Equipment and Safety,* Høvik: Det Norske Veritas AS.
- Faltinsen, O. M., 1990. *Sea loads on ships and offshore structures.* 1st ed. Cambridge: Cambridge University Press.
- FHWA, 2013. *Engineering: U.S. Dept. of Transportation, Federal Highway Administration.* [Online]
  Available at: http://www.fhwa.dot.gov/engineering/hydraulics/pubs/08090/images/fig4_3.gif
  [Accessed 26th May 2014].
- Flow Science Inc., 2011. *Resources: Flow Science Inc..* [Online]
  Available at: http://www.flow3d.com/resources/news_11/winter/modeling-waves-FLOW-3D-development.html
  [Accessed 22 January 2014].
- González , M. M. et al., n.d. *Prediction of Parametric Roll Resonance by Multilayer Perceptron Neural Network.* Coruña, Lyngby, Trondheim: University A Coruña, Technical Univeristy of Denmark Kgs, NTNU.
- Gowda, S., 2014. *Senior Analysis Engineer, Ocean Installer AS* [Interview] 2014.
- Gudmestad, O. T., 2013a. *14 Dynamic of one degree of freedom systems,* Stavanger: Univeristy of Stavanger.
- Gudmestad, O. T., 2013b. *Lecture in Marine Operations (OFF600) 16.10.13.* Stavanger: University of Stavanger.
- Gudmestad, O. T., 2013c. *2. Linear wave theory,* Stavanger: University of Stavanger.
- Gudmestad, O. T., 2013d. *9 Vessel motions.* Stavanger: University of Stavanger.
- Hagen, A., 2014. *Technical Lead ROV, Ocean Installer AS* [Interview] 2014.
- HCA, Bristow Group, Bond Offshore and CHC, 2010. *Standard Measuring Equipment for Helideck Monitoring System (HMS) and Weather Data,* Aberdeen: HCA.
- Heier, S., 2014. *CEO, Stable AS* [Interview] (10th April 2014).
- Helideck Certification Agency, 2013. *Information HLL Part C: Helideck Certification Agency.* [Online]
  Available at:
  http://www.google.no/url?sa=t&rct=j&q=&esrc=s&frm=1&source=web&cd=1&cad=rja&uact=8&ved=0CCsQFjAA&url=http%3A%2F%2Fwww.helidecks.org%2Fdownload%2520files%2FFSI%2520new%2520pitch%2520roll%2520and%2520heave%2520limits.pdf&ei=Lbs6U_aUCIiIhQf1_YD4

Aw&usg=AFQjCN
[Accessed 30 March 2014].

- Hovland, E., 2007. *Evaluation of Vessel Concepts for Subsea Operations in Northern Seas.* 1st ed. Stavanger: University of Stavanger.
- HSE, 2001. *Helicopter Safety Offshore,* Norwich: Health and Safety Executive.
- Huisman, 2013a. *Huisman technical specification 75 mt tensioner,* Bergen: Huisman Norge AS.
- Huisman, 2013b. *Flare - basic design.* Schiedam: Huisman Equipment b.v..
- Huse, B., 2014. *Managing Director at Uptime AS International* [Interview] (2nd May 2014).
- Journèe, J. M. J. & Adegeest, L. J. M., 2003. *Papers and Reports: shipmotions.nl.* [Online] Available at: http://www.shipmotions.nl/DUT/PapersReports/1370-StripTheory-03.pdf [Accessed 28 January 2014].
- JP Kenny Norge AS, 2014. *Draugen Infill Project ,* Stavanger: JP Kenny Norge AS.
- Kantharia, R., 2013. *marineinsight.com.* [Online] Available at: http://www.marineinsight.com/misc/marine-safety/what-is-extended-dry-docking-of-ships/ [Accessed 20th May 2014].
- Kongsberg Maritime AS, 2013. *MRU 5th generation (datasheet).* Kongsberg: RK Grafisk AS.
- Marintek, 2012. *Model Tests, OSCV06L,* Trondheim: Norwegian Marine Technology Research Institute.
- Marintek, 2007. *Model Test Aker OSCV 06L Seakeeping,* Trondheim: Marintek/Sintef.
- Mathiesen, M. & Kvingedal, B., 2010. *Snorre Field Metocean Design Basis,* Stavanger: Statoil ASA.
- MEFEPO, 2009. *MEFEPO home: University of Liverpool.* [Online] Available at: http://www.liv.ac.uk/media/livacuk/mefepo/documents/wp1/atlases/NS_Atlas_English.pdf [Accessed 23 January 2014].
- NGI, 2012. *Eirin – 2011 Soil Investigation Geotechnical Report,* Oslo: NGI.
- NKT Flexibles, 2011. *8" Production Flowline,* Brøndby: NKT Flexibles .
- Norwegian Maritime Directorate, 2008. *Regulations: Lovdata.* [Online] Available at: http://www.lovdata.no/dokument/SF/forskrift/2007-07-04-854 [Accessed 5 May 2014].

- Næss, A., 2013. *Energi: DN.no.* [Online]
  Available at: http://www.dn.no/energi/article2676235.ece
  [Accessed 21 January 2014].

- Ocean Installer AS, 2013. *Normand Vision: Ocean Installer AS.* [Online]
  Available at: http://www.oceaninstaller.com/wp-content/uploads/2013/10/Vessel-specification-Newbuild-CSV_24102013.pdf
  [Accessed 21 January 2014].

- Ocean Installer AS, 2014. *Services and Expertise: Ocean Installer AS.* [Online]
  Available at: http://www.oceaninstaller.com/fleet-and-operations/services-and-expertise/
  [Accessed 20 January 2014].

- Ocean Installer AS, n.d. *Services and Expertise: Ocean Installer AS.* [Online]
  Available at: http://www.oceaninstaller.com/fleet-and-operations/services-and-expertise/
  [Accessed 20 January 2014].

- OffshoreEnergyToday.com, 2014. *News: OffshoreEnergyToday.* [Online]
  Available at: http://www.offshoreenergytoday.com/ocean-installer-sells-70-pct-share-in-csv-normand-vision/
  [Accessed 11th April 2014].

- OLF and The Federation of Norwegian Industry, 2007. *NORSOK STANDARD N-003: Actions and action effects.* 2nd ed. Lysaker: Standards Norway.

- Orcina Ltd., 2013. *OrcaFlex Documentation: Orcina Ltd..* [Online]
  Available at: http://www.orcina.com/SoftwareProducts/OrcaFlex/Documentation/OrcaFlex.pdf
  [Accessed 22 January 2014].

- pbase.com, 2005. *Queen of Nanaimo: pbase.com.* [Online]
  Available at: http://m5.i.pbase.com/v3/45/387545/1/50702675.DSC_3086z.jpg
  [Accessed 19th May 2014].

- Qayre, A., 2014. *Senior Engineer, Ocean Installer AS* [Interview] 2014.

- Rosbach, M., 2013. *News: Sunnmørsposten.* [Online]
  Available at: http://www.smp.no/naeringsliv/article7201963.ece
  [Accessed 29th January 2014].

- Røkeberg, H., 1997. *Dynamic-Positioning.com.* [Online]
  Available at: http://www.dynamic-positioning.com/dp1997/dpclass_rokeberg.pdf
  [Accessed 11 February 2014].

- Salvador, R., 2011. *Nautico.* [Online]
  Available at: http://salvador-nautico.blogspot.no/2011/09/cabeceio-pitch.html
  [Accessed 24 January 2014].

- Samoilescu, G. & Radu, S., 2002. *Stabilisers and stabilising systems on ships.* Târgu Jiu, Constantin Brâncusi University - Engineering Faculty (8th international Conference).

- Ship Portal Korabley, 2013. *Korabley.net.* [Online]
  Available at: http://korabley.net/_nw/2/71596.jpg
  [Accessed 12th May 2014].

- Smith, C. C., 2014. *Chief Pilot Stavanger, Bristow Norway AS* [Interview] (April 2014).

- Solstad Offshore ASA, 2014. Skudeneshavn: Solstad Offshore ASA.

- Statoil ASA, 2012. *News and media: Statoil ASA.* [Online]
  Available at: http://www.statoil.com/no/NewsAndMedia/News/2012/Pages/17Jan_Dagny.aspx
  [Accessed 4 March 2014].

- STX OSV Design AS, 2012. *OSCV 06 L General Arrangement,* Ålesund: STX OSV.

- STX OSV, 2013a. *811-101-191 RAO calculations,* Ålesund: STX OSV.

- STX OSV, 2013b. *Illustration: Normand Vision.* Søviknes: STX OSV.

- STX OSV, 2013c. *Yard No. 811 Owner loading conditions,* Søviknes: STX OSV.

- STX OSV, 2013d. *Yard No. 811 Stability calculations for design,* Søviknes: STX OSV.

- STX OSV, 2013e. *Capabilty calculations NB 811,* Søviknes : STX OSV .

- Subsea 7, 2013. *Pipeline span and VIV,* Stavanger: Subsea 7.

- Svendsen, E. H., 2014. *Senior Engineer, Ocean Installer AS* [Interview] 2014.

- The bridge of Island Intervention, 2011. *Helideck Report,* s.l.: Island Offshore.

- Uptime International AS, 2010. *Helideck: Uptime.no.* [Online]
  Available at: http://www.uptime.no/?page_id=115
  [Accessed 11 May 2014].

- van Laarhoven, B., 2009. *Stability Analysis of Parametric Roll Resonance,* Eindhoven: Eindhoven University of Technology.

- *VARD 811 "Normand Vision" time-lapse compilation.* 2014. [Film] Directed by Fredrik Bjørnøy. Søviknes: http://vimeo.com/93656983.

- *VARD 811 "Normand Vision" time-lapse compilation.* 2014. [Film] Directed by Fredrik Bjørnøy. Søviknes: s.n.
- VARD, 2014. *Normand Vision RAO Calculation,* Søviknes: VARD .
- Waalen, J., 2014a. *Project Manager / Vessel Superintendent, Ocean Installer AS* [Interview] 2014a.
- Waalen, J., 2014b. *Offshore Cranes and VLS installed on NB 811,* Søviknes: Ocean Installer.
- Waalen, J. & Sarhan, H. B.-H., 2013. Cross-company cooperation in shipbuilding. *DYP - magasinet fra Forening for Fjernstyrt Undervannsteknologi*, Nr. 2, pp. 6-7.
- Worren, H., 2014. *Vessel Superintendent, Ocean Installer AS* [Interview] 2014.
- Zhan, J. P., 2014. *Senior SURF Project Engineer Analysis, Ocean Installer AS* [Interview] 2014.

Appendix A: Intact stability of Normand Vision

Only some of the most important intact stability criteria for the vessel in an undamaged condition are included in Table A.0.1. These are based on data from the stability calculations in NAPA and model tests of the vessel.
The general criteria from DNV's Rules for Classification of Ships (based on IMO 2008 IS Code Part B Ch.2.4.5) are used.

In addition to these general stability criteria DNV also states that vessels with anti-roll devices should satisfy the applicable intact stability criteria with these devices in operation, which applies for Normand Vision (DNV, 2013b).

Table A.0.1: Comparison of stability criteria for Normand Vision according to DNV's Rules for Classification of Ships

General intact stability criteria from DNV (DNV, 2013b)	Intact stability values for Normand Vision
• The maximum righting arm (GZ) should occur at a heel angle ≥ 15°	**Load Case 1:** GZ_{max} at θ_{max} = 28.216° **Load Case 2:** GZ_{max} at θ_{max} = 21.749°
• Area under GZ curve ≥ 0.070 meter-radians (mrad) for heel angles up to 15°, when the maximum righting arm (GZ) occurs at a heel angle of 15° • And the area under GZ curve ≥ 0.055 mrad for heel angles up to 30°, when the maximum righting arm (GZ) occurs at a heel angle of ≥30° • Where the maximum righting arm (GZ) occurs at angles between 15° and 30° heel angle, the corresponding area under the righting arm curve should be: ≥0.055 + 0.001 (30° − θ_{max}) mrad where θ_{max} is the angle of heel in degrees at which the righting arm curve reaches its maximum.	**Load Case 1:** Here the minimum requirement for the minimum area under the GZ curve is ≈0.057 mrad as θ_{max} = 28.216°. The area is 0.325 mrad. **Load Case 2:** Here the minimum requirement for the minimum area under the GZ curve is ≈0.063 mrad as θ_{max} = 21.749°. The area is 0.124 mrad.
• The area under the righting arm (GZ) curve for heeling angles between 30° and 40°, or between 30° and θ_f (flooding angle) and that θ_f is less than 40°, should not be less than 0.030 mrad.	**Load Case 1:** area = 0.178 mrad **Load Case 2:** area = 0.051 mrad
• The righting arm (GZ) ≥ 0.20 m for a heel angle ≥ 30°. The maximum righting arm should not occur at an angle of heel less than 15°	**Load Case 1:** GZ_{min} = 1.094 m **Load Case 2:** GZ_{min} = 0.450 m
• The initial metacentric height (GM) ≥ 0.15 m • (For installation operations from monohull vessels NMD requires GM > 0.50 m (Gudmestad, 2013d), which is satisfied for both Load Cases)	**Load Case 1:** • GM_0 (dry loads, including tanks full of liquid loads which also is treated as they were dry loads due to no free surface effects) ≈ 2.97 m • Free surface correction of 0.14 m, gives corrected GM (for liquid loads with free surface) ≈ 2.83* m **Load Case 2:** • GM_0 (dry loads, including tanks full of liquid loads which also is treated as they were dry loads due to no free surface effects) ≈ 1.92 m • Free surface correction 0.09 m, giving corrected GM (for liquid loads with free surface) ≈ 1.83* m *This is the minimum GM from probabilistic dam calculations

Appendix B: Graphs related to RAO quality check

In this Appendix some of the results from the graphical RAO check in OrcaFlex are presented for comparison between the originally provided RAOs from STX OSV and the RAOs after they have been inserted into OrcaFlex. This is done to check that the RAOs are imported correctly. For easier comparison only one wave direction is shown for each Load Case here in the Appendix, but the comparison was satisfying also for all the other directions (0°-180°). See Figures B.0.1 to B.0.24. If the graphs tend to coincide fairly well it means that the RAOs are correct used in OrcaFlex, as they then represent the vessel well. So the conclusion to this RAO quality check is positive, i.e. the RAOs should represent the Normand Vision's motions correctly.

B.1 RAO comparison Load Case 1 – wave direction 60°

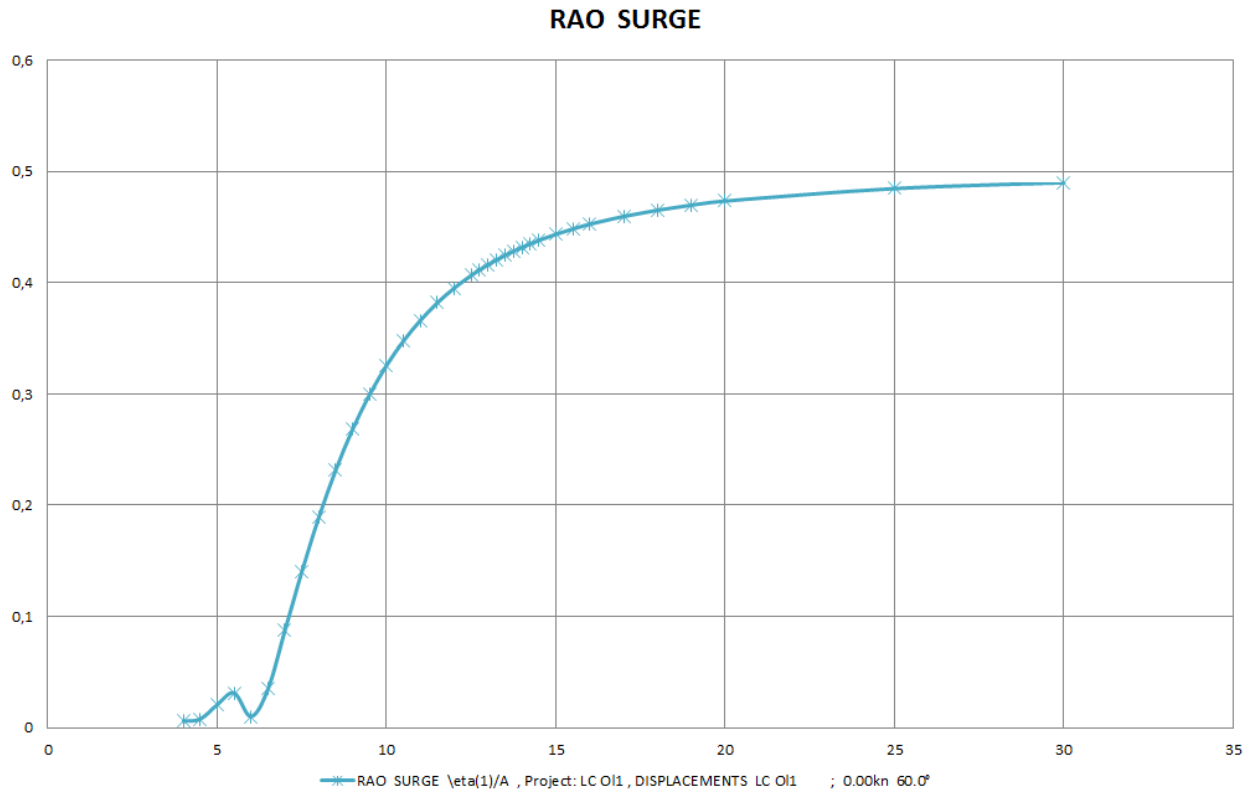

Figure B.0.1: RAO graph Load Case 1 for surge provided by STX OSV (STX OSV, 2013a)

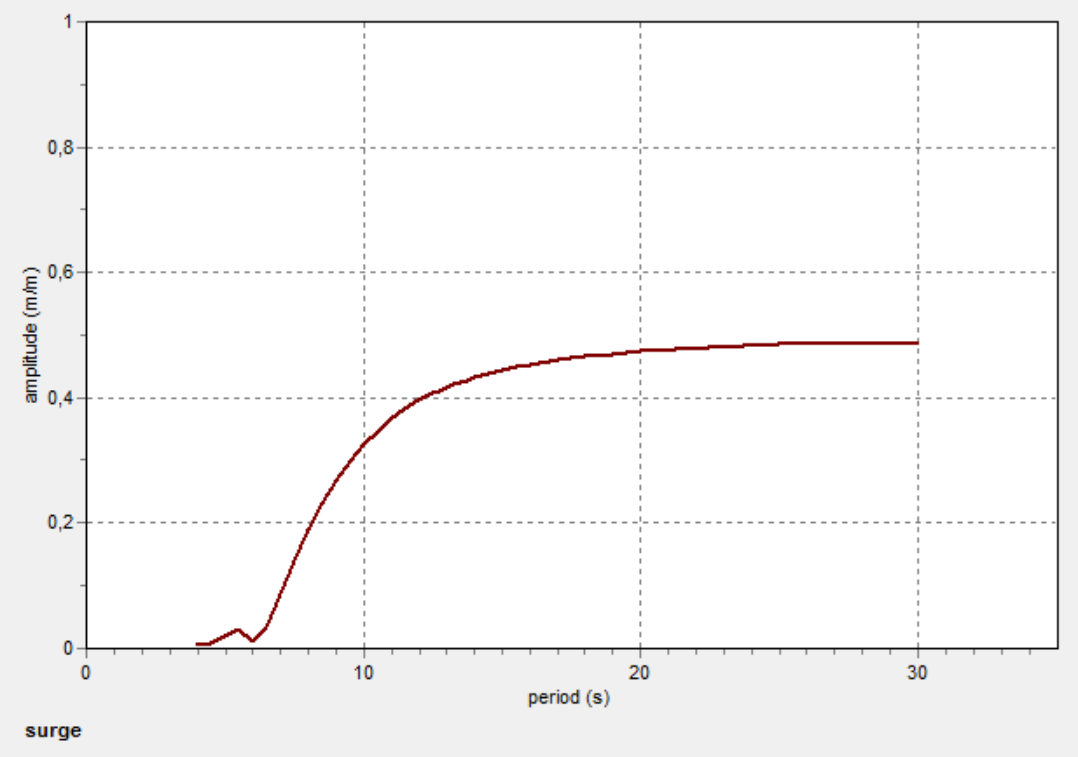

Figure B.0.2: RAO graph Load Case 1 for surge from OrcaFlex

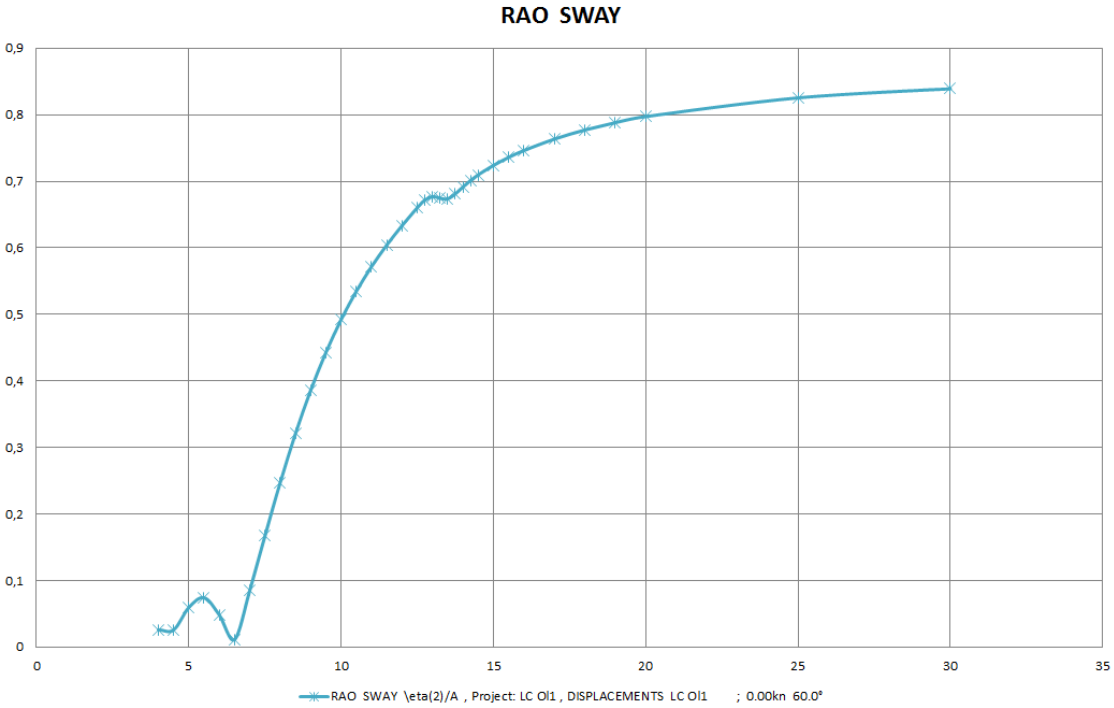

Figure B.0.3: RAO graph Load Case 1 for sway provided by STX OSV (STX OSV, 2013a)

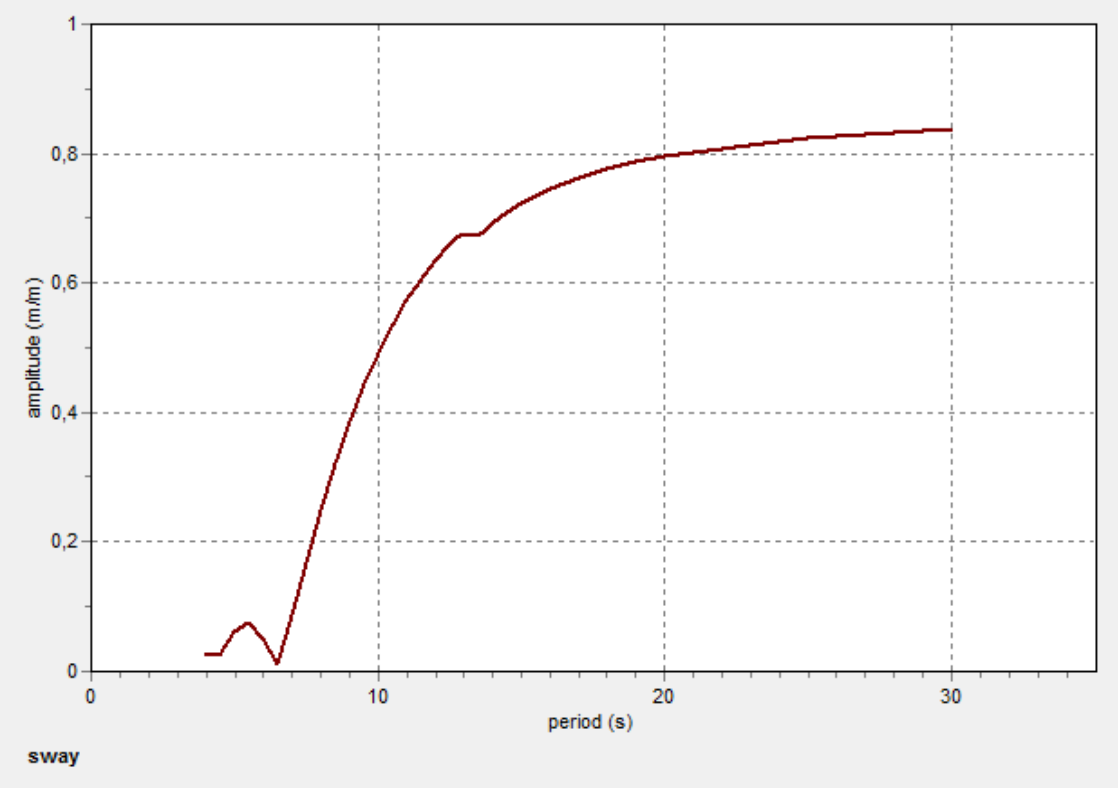

Figure B.0.4: RAO graph Load Case 1 for sway from OrcaFlex

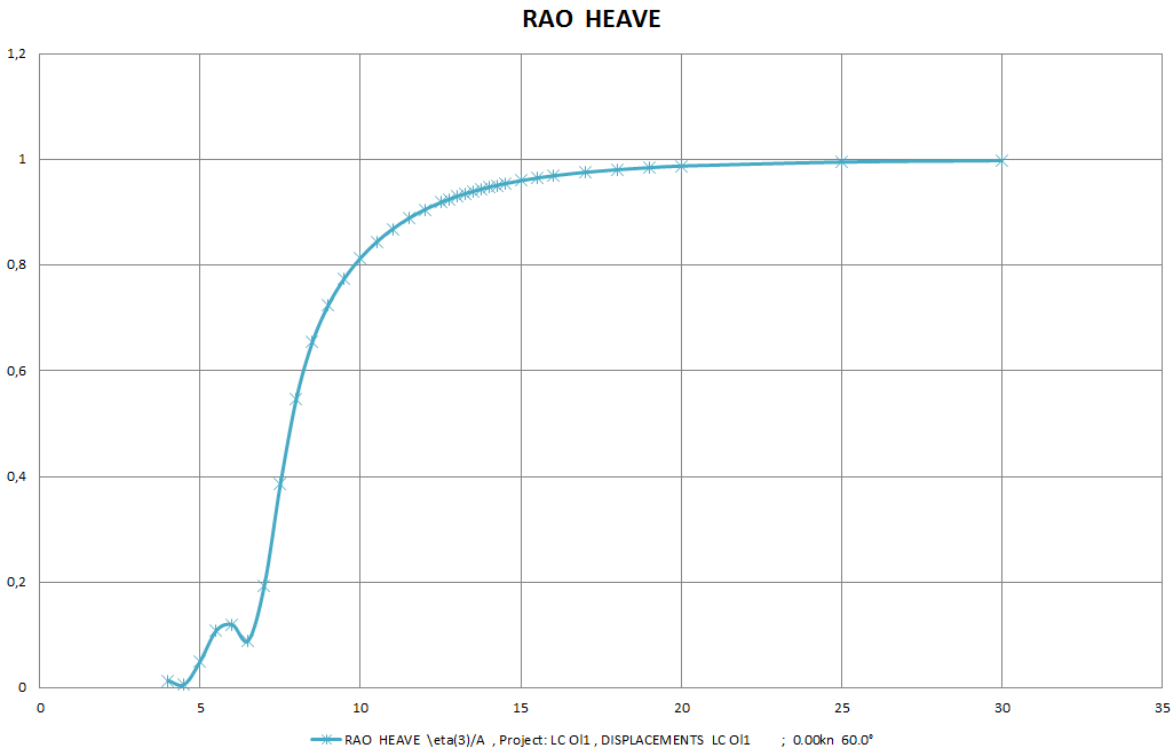

Figure B.0.5: RAO graph Load Case 1 for heave provided by STX OSV (STX OSV, 2013a)

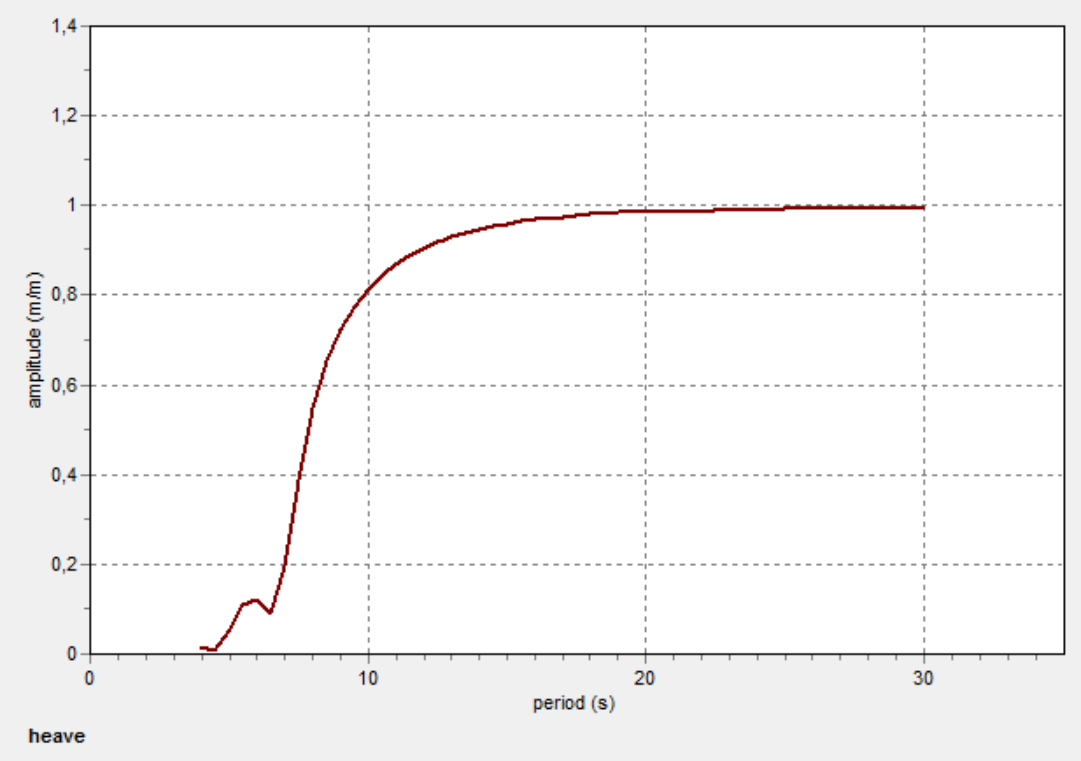

Figure B.0.6: RAO graph Load Case 1 for heave from OrcaFlex

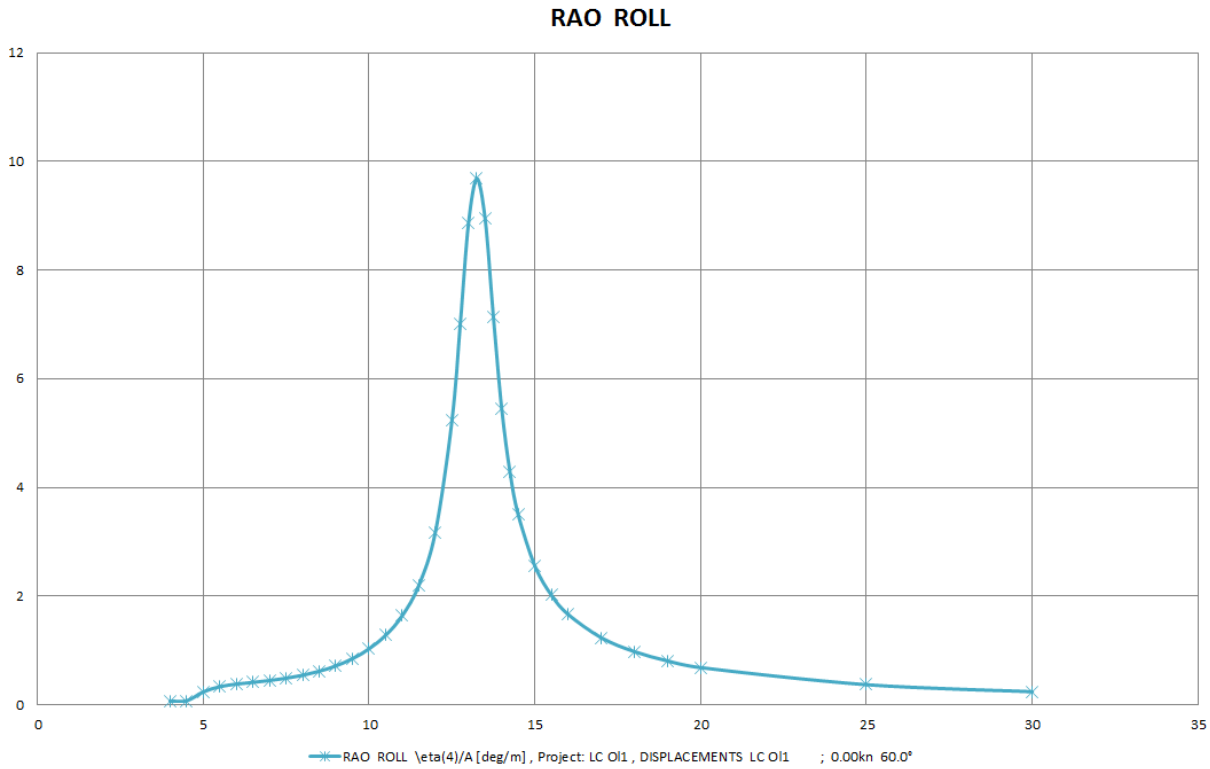

Figure B.0.7: RAO graph Load Case 1 for roll provided by STX OSV (STX OSV, 2013a)

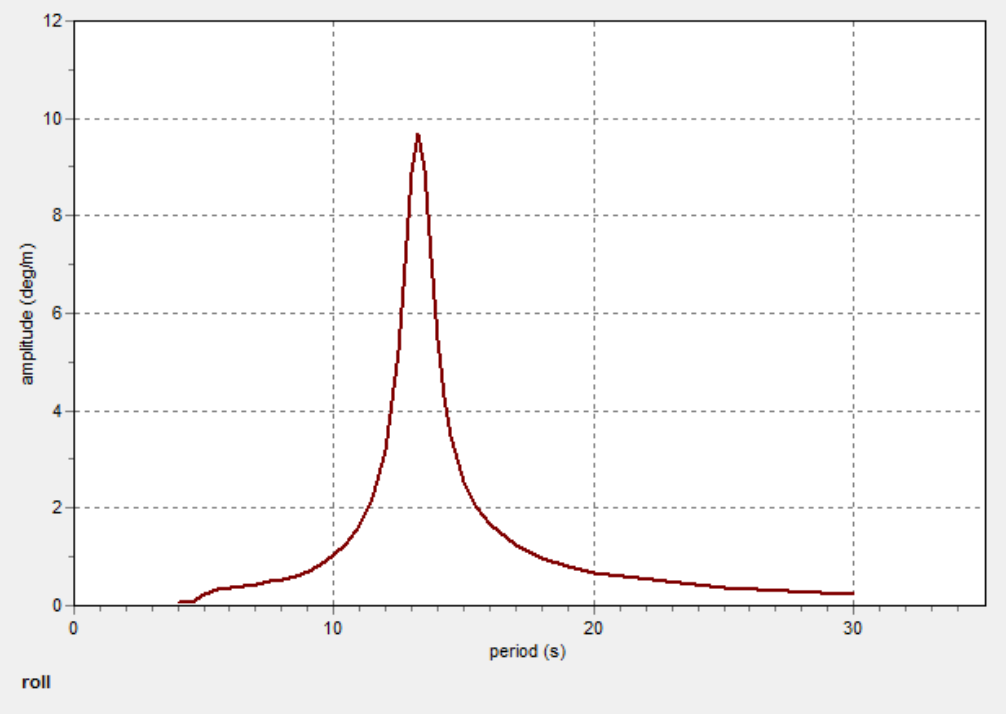

Figure B.0.8: RAO graph Load Case 1 for roll from OrcaFlex

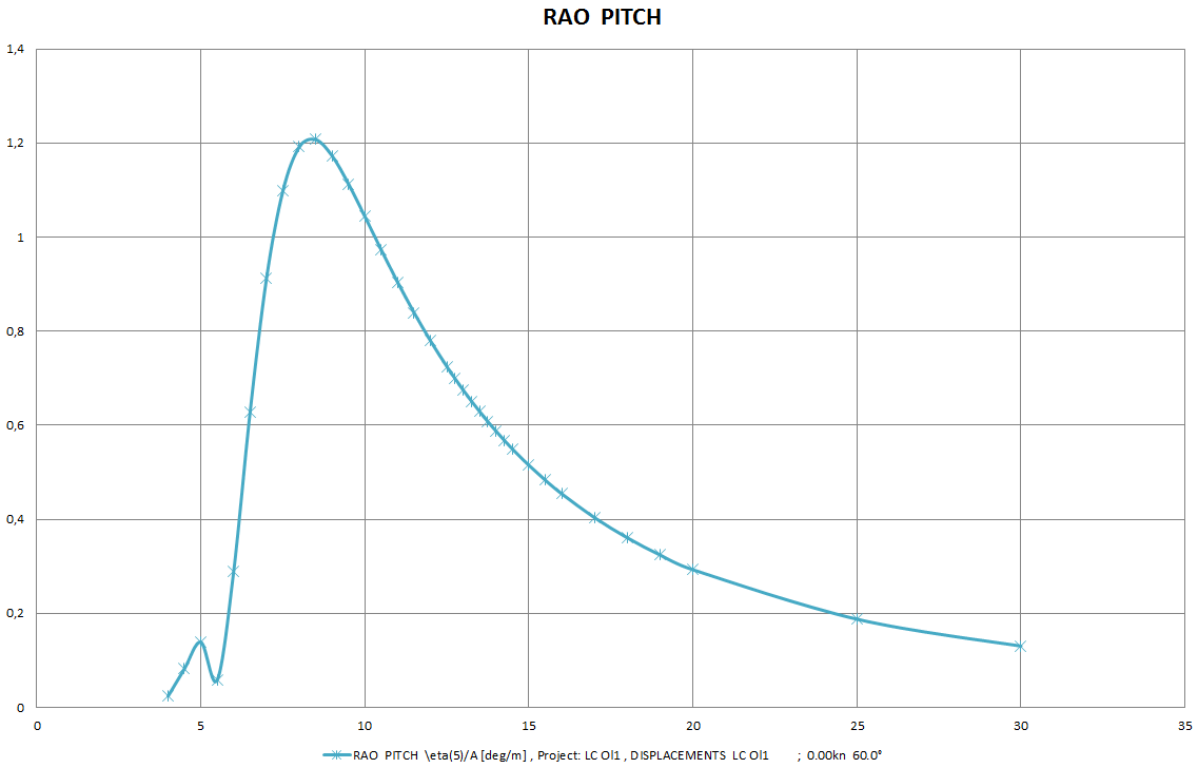

Figure B.0.9: RAO graph Load Case 1 for pitch provided by STX OSV (STX OSV, 2013a)

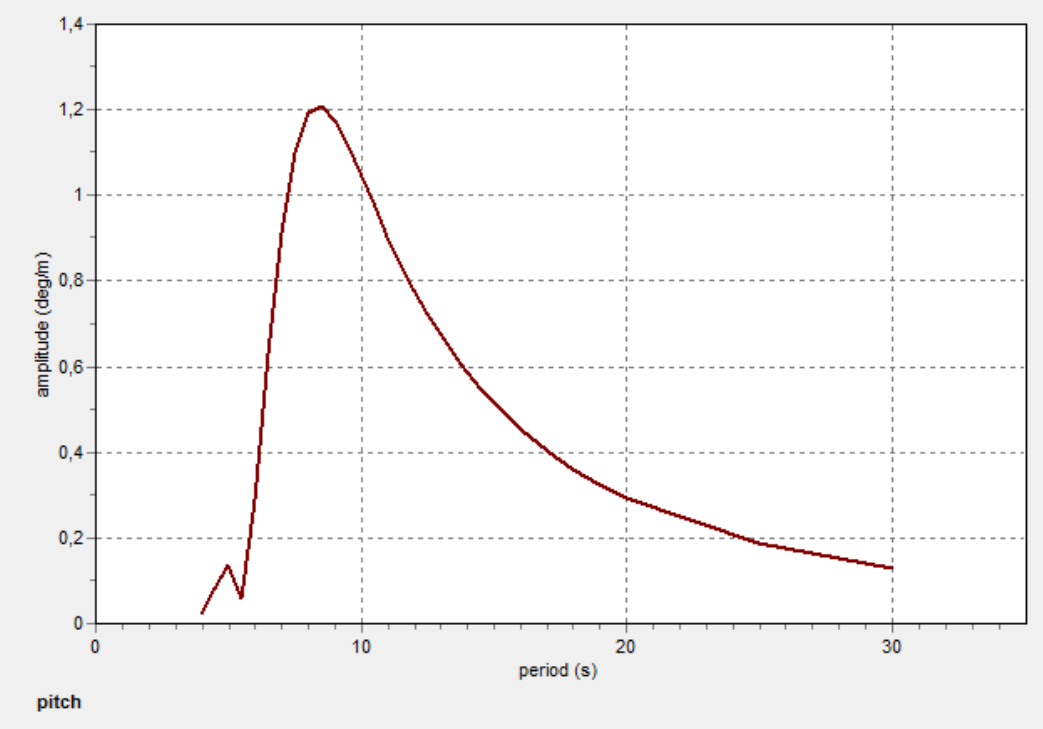

Figure B.0.10: RAO graph Load Case 1 for pitch from OrcaFlex

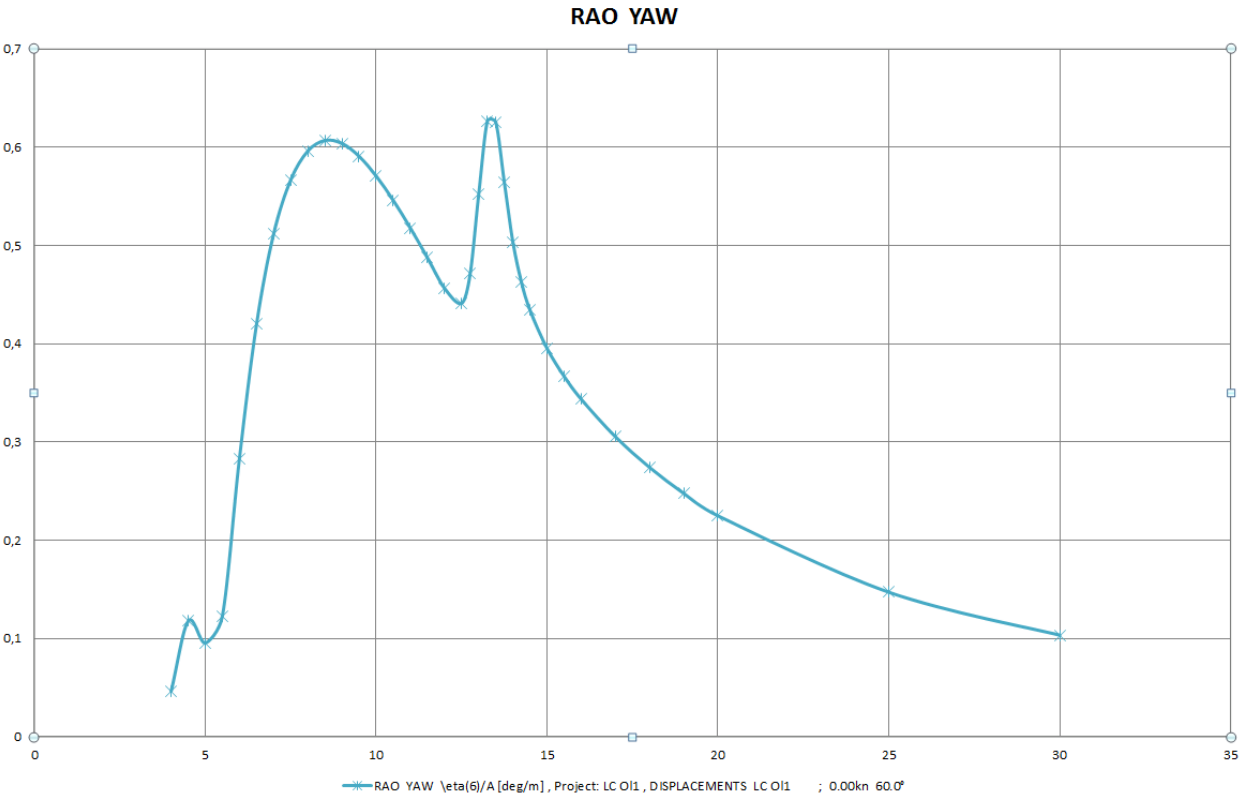

Figure B.0.11: RAO graph Load Case 1 for yaw provided by STX OSV (STX OSV, 2013a)

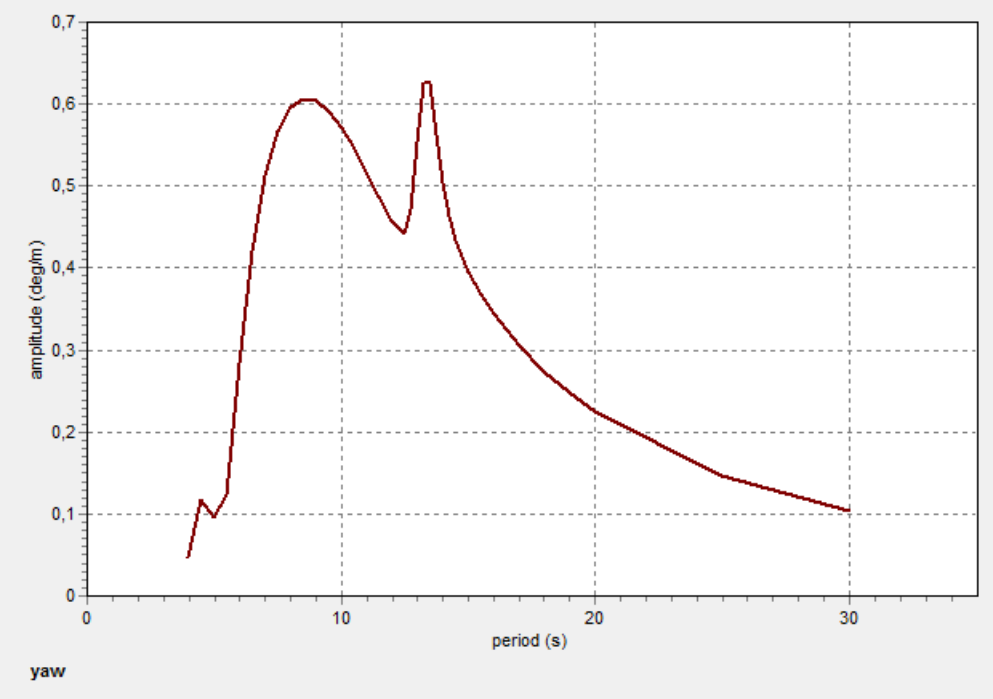

Figure B.0.12: RAO graph Load Case 1 for yaw from OrcaFlex

B.2 RAO comparison Load Case 2 – wave direction 75°

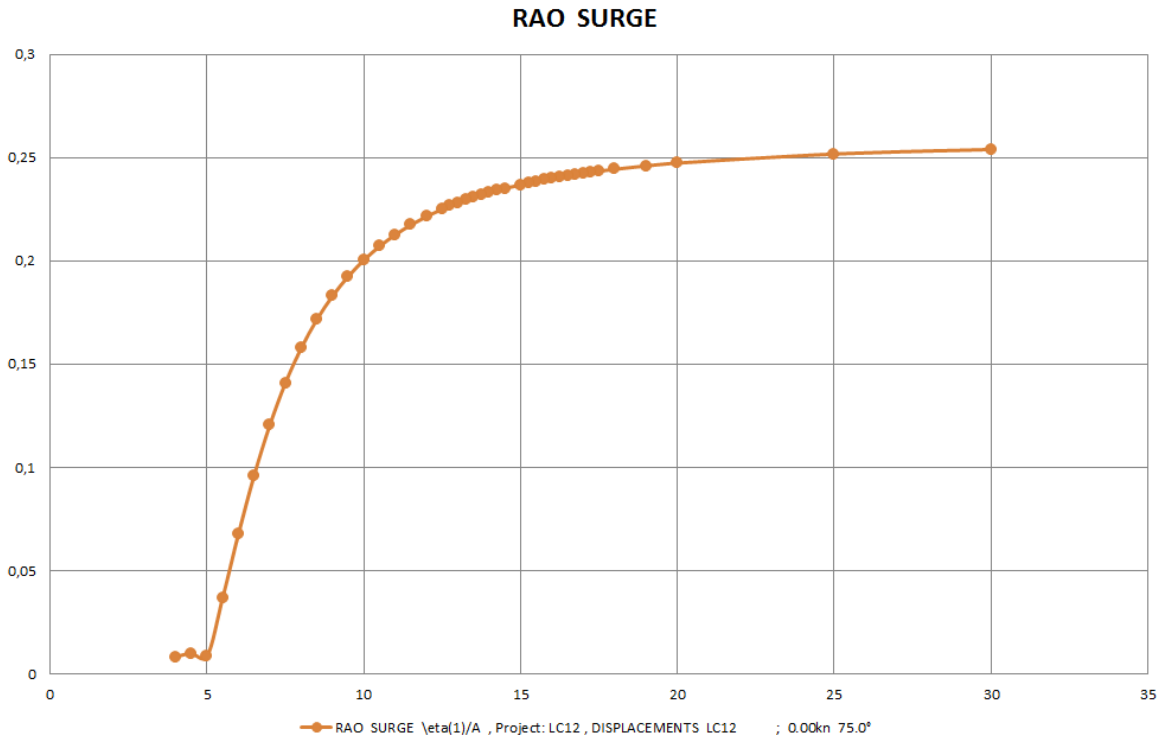

Figure B.0.13: RAO graph Load Case 2 for surge provided by STX OSV (STX OSV, 2013a)

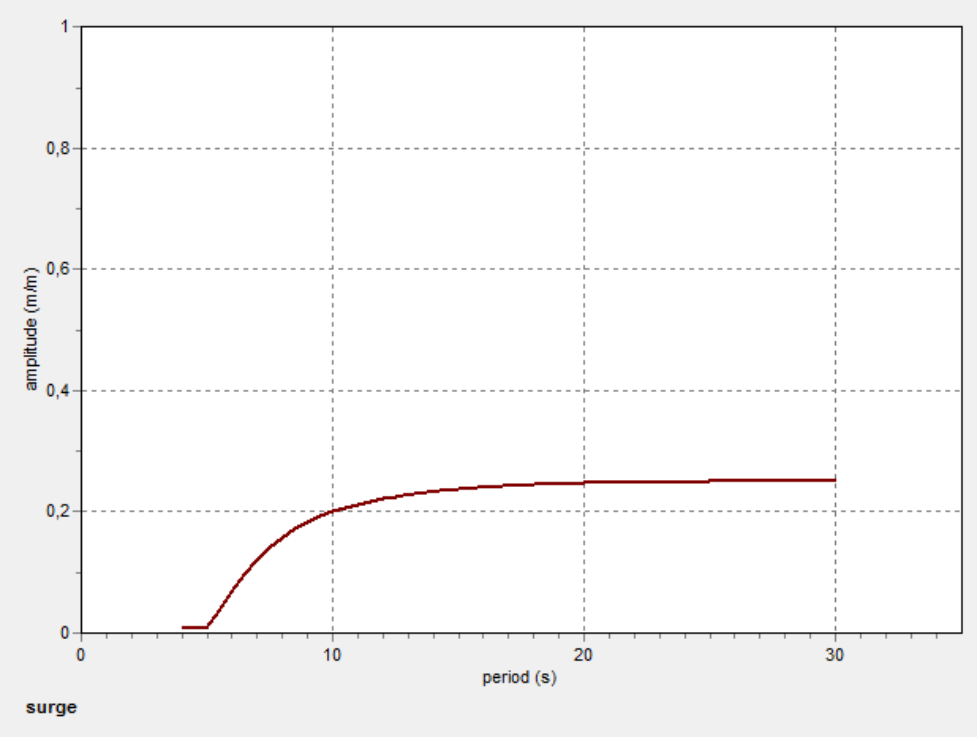

Figure B.0.14: RAO graph Load Case 2 for surge from OrcaFlex

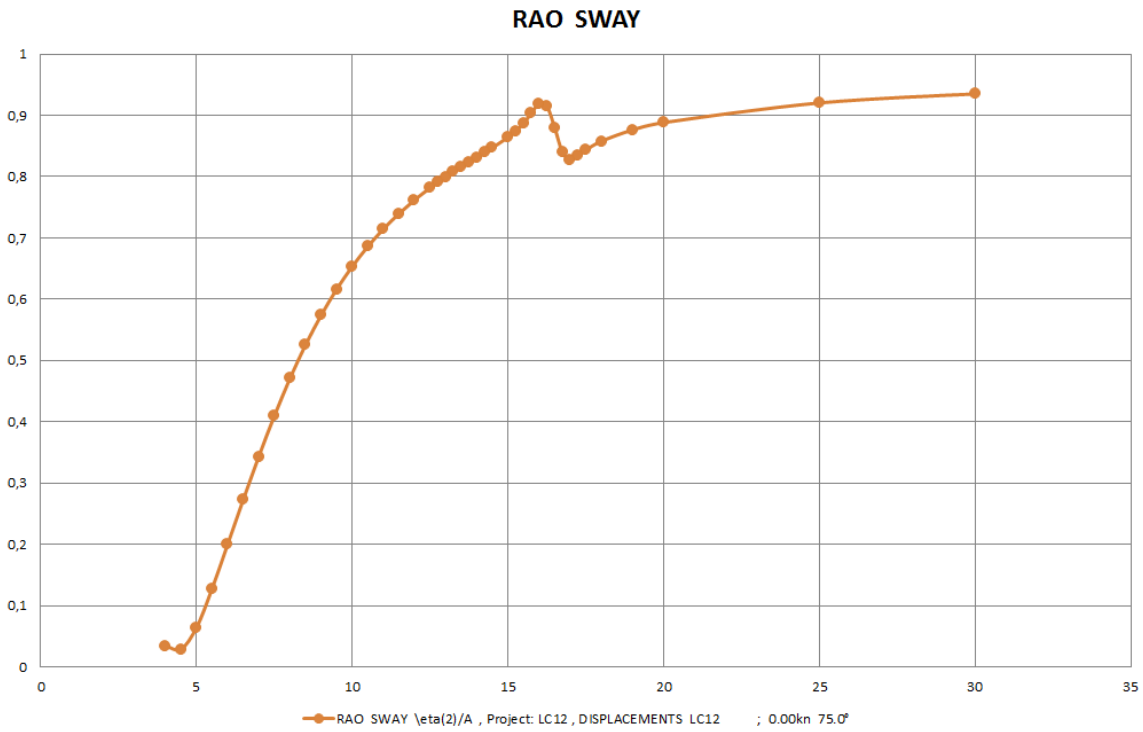

Figure B.0.15: RAO graph Load Case 2 for sway provided by STX OSV (STX OSV, 2013a)

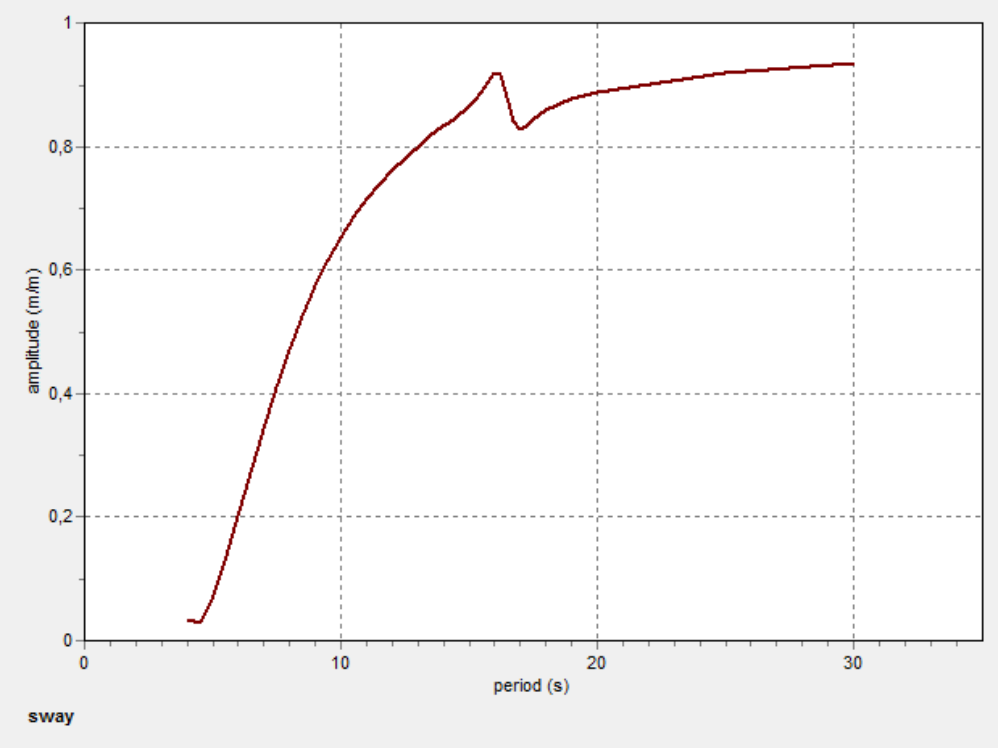

Figure B.0.16: RAO graph Load Case 2 for sway from OrcaFlex

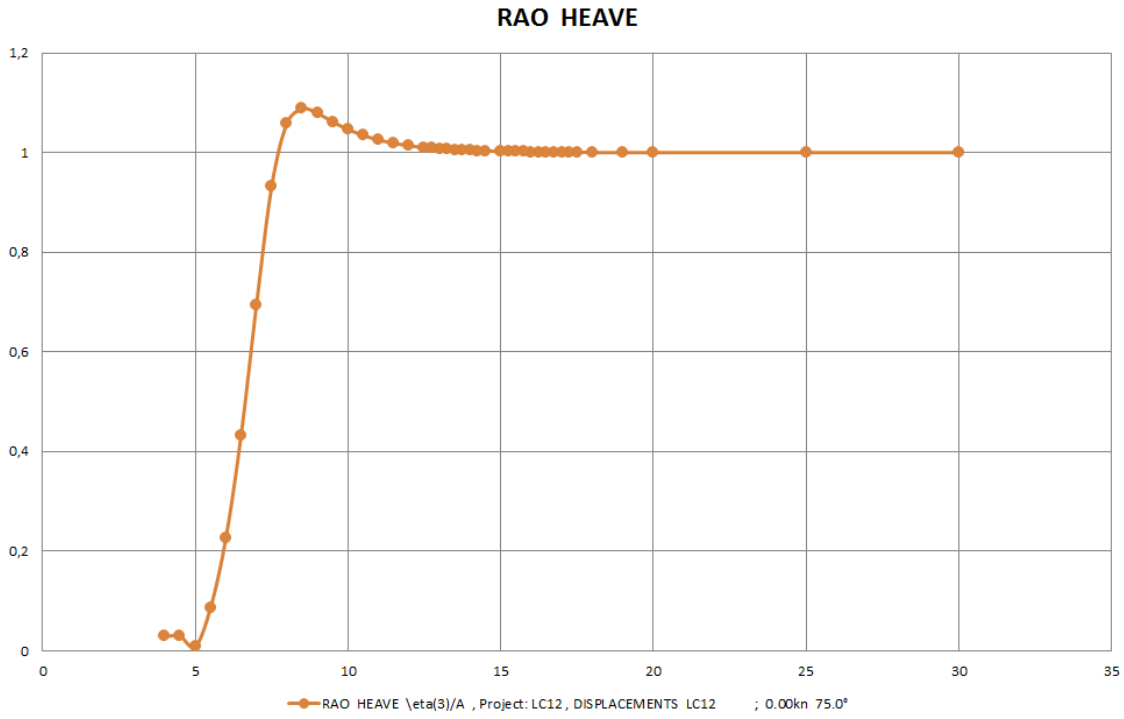

Figure B.0.17: RAO graph Load Case 2 for heave provided by STX OSV (STX OSV, 2013a)

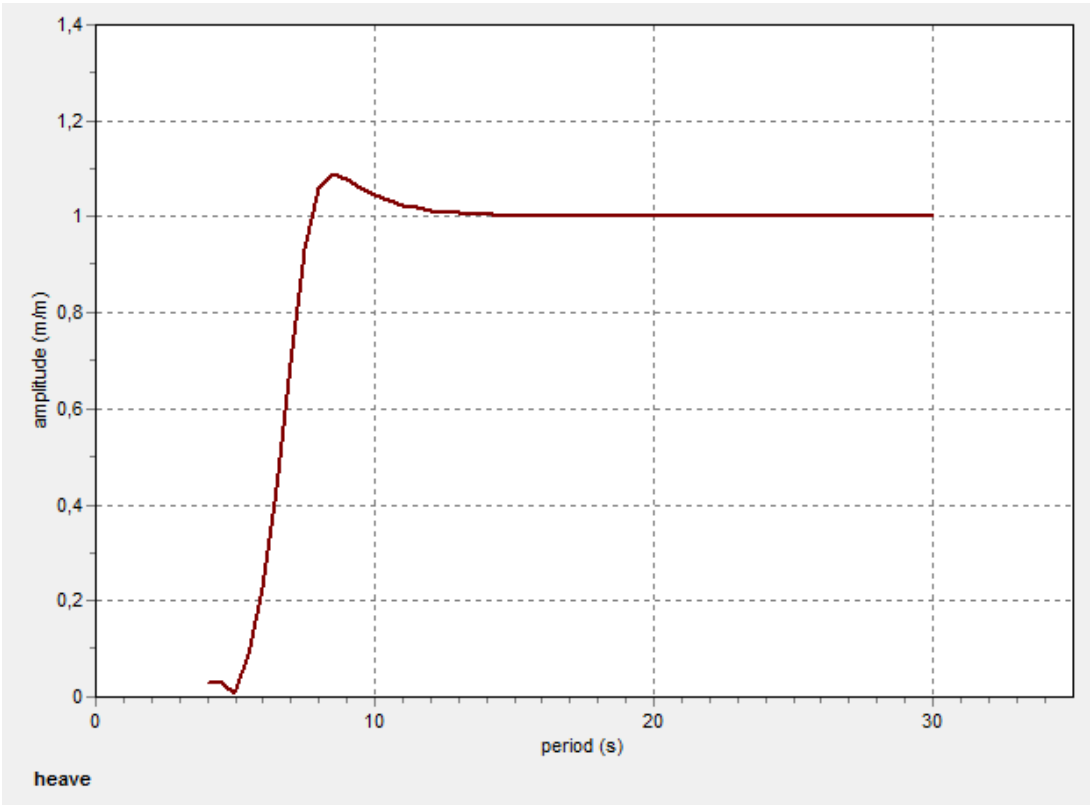

Figure B.0.18: RAO graph Load Case 2 for heave from OrcaFlex

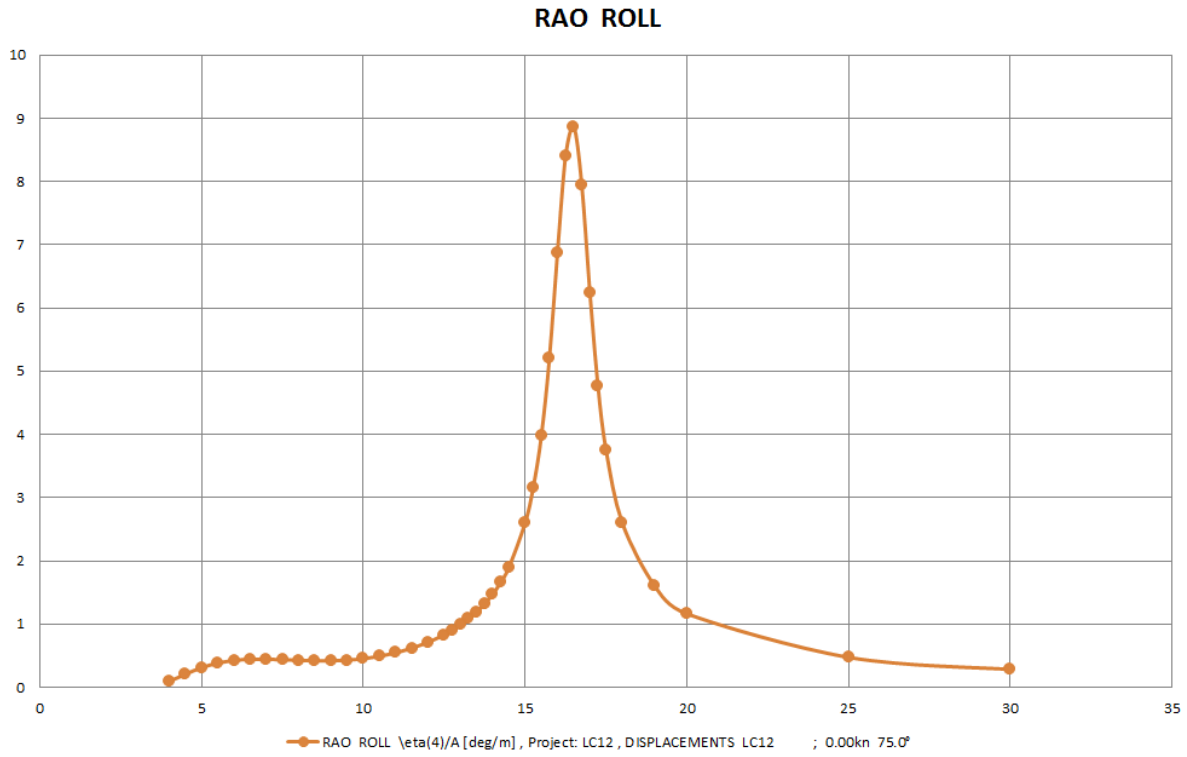

Figure B.0.19: RAO graph Load Case 2 for roll provided by STX OSV (STX OSV, 2013a)

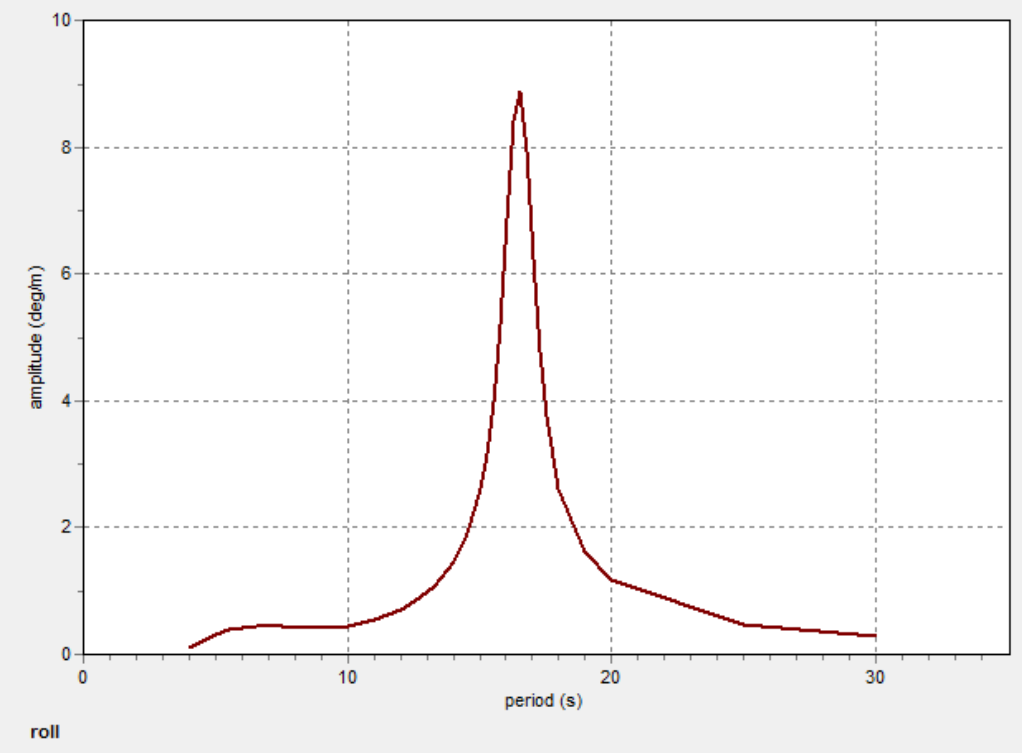

Figure B.0.20: RAO graph Load Case 2 for roll from OrcaFlex

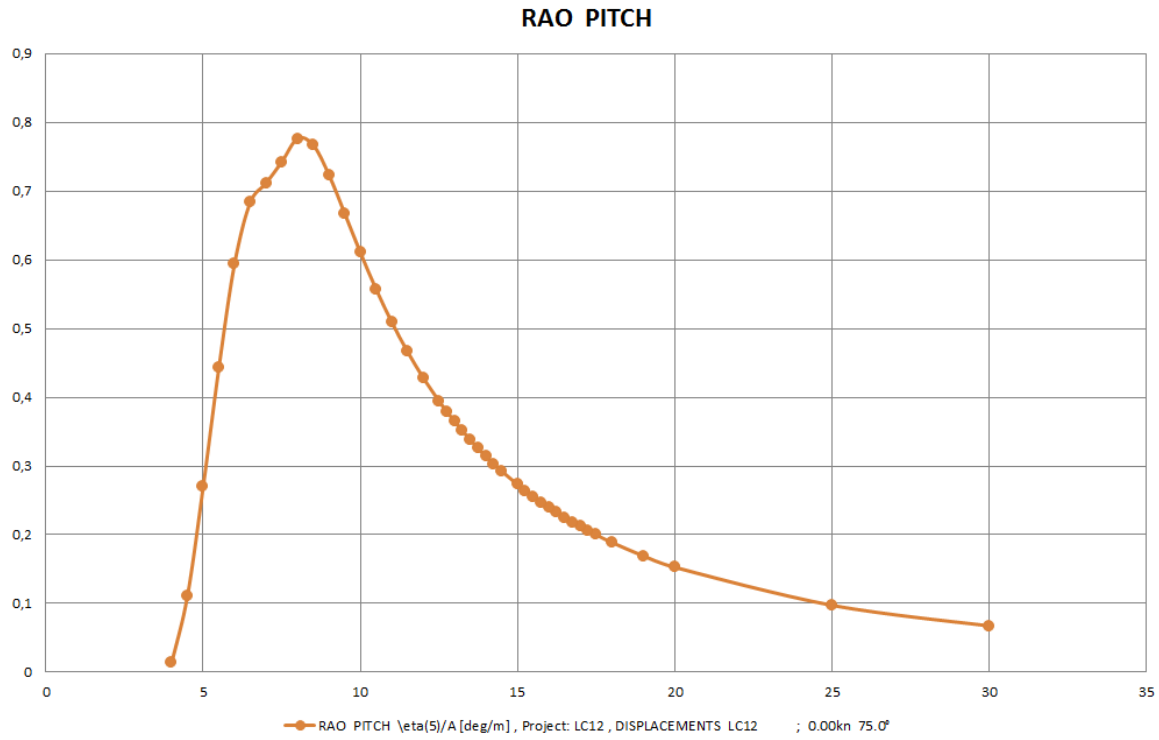

Figure B.0.21: RAO graph Load Case 2 for pitch provided by STX OSV (STX OSV, 2013a)

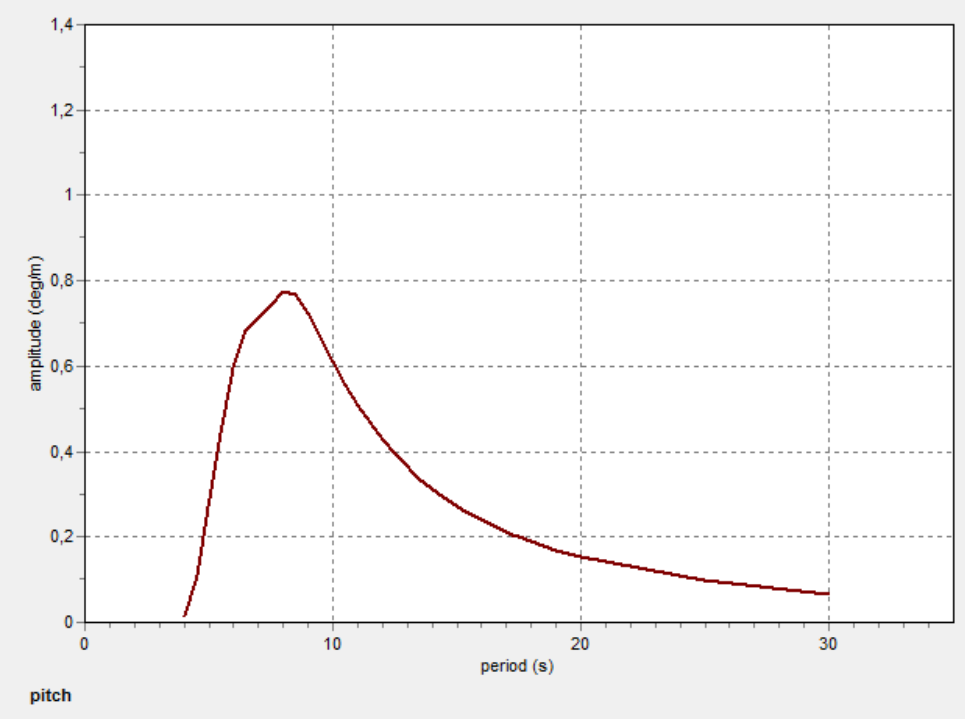

Figure B.0.22: RAO graph Load Case 2 for pitch from OrcaFlex

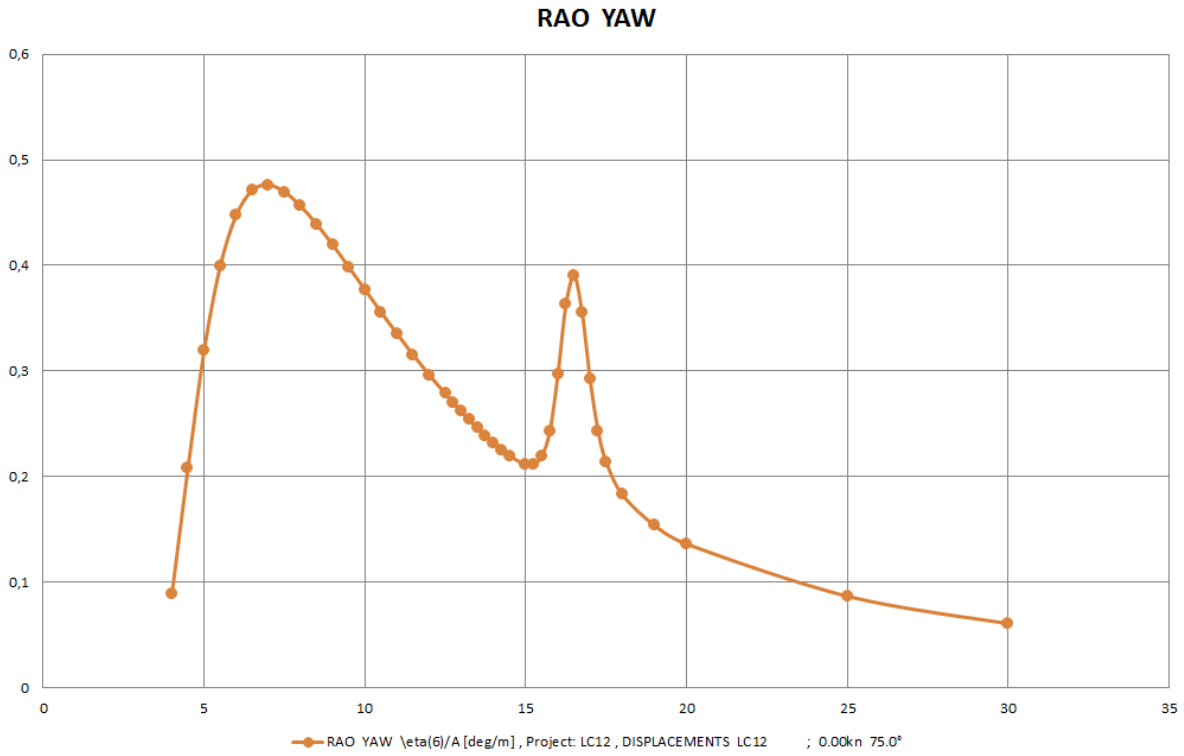

Figure B.0.23: RAO graph Load Case 2 for yaw provided by STX OSV (STX OSV, 2013a)

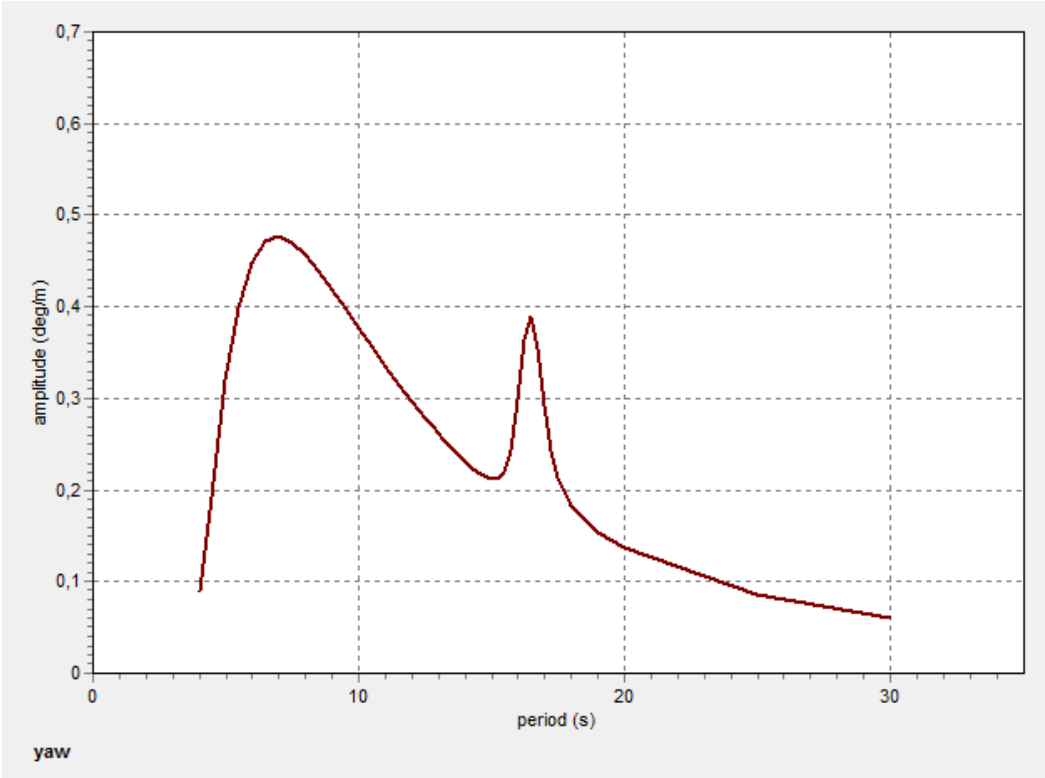

Figure B.0.24: RAO graph Load Case 2 for yaw from OrcaFlex

Appendix C: Results from the OrcaFlex analysis

The results will be presented in relation to the limitations presented in sub-chapters 8.3 to 8.5. The results are commented upon in chapter 9 and in the chapter 11, the concluding chapter.

The results are presented in the following order (see also Table of Contents, for page numbers):

- C.1 Results for heave acceleration on main deck for H_D = 3.8 meters
- C.2 Results for heave acceleration on main deck for H_D = 5.7 meters
- C.3 Results for heave acceleration on main deck for H_D = 7.6 meters
- C.4 Results for lateral acceleration on main deck for H_D = 3.8 meters
- C.5 Results for lateral acceleration on main deck for H_D = 5.7 meters
- C.6 Results for lateral acceleration on main deck for H_D = 7.6 meters
- C.7 Results for roll rotation for H_D = 3.8 meters
- C.8 Results for roll rotation for H_D = 5.7 meters
- C.9 Results for roll rotation for H_D = 7.6 meters
- C.10 Results for pitch rotation for H_D = 3.8 meters
- C.11 Results for pitch rotation for H_D = 5.7 meters
- C.12 Results for pitch rotation for H_D = 7.6 meters
- C.13 Results for top tension for H_D = 3.8 meters
- C.14 Results for top tension for H_D = 5.7 meters
- C.15 Results for top tension for H_D = 7.6 meters
- C.16 Results for the pipe's angle with the vertical for H_D = 3.8 meters
- C.17 Results for the pipe's angle with the vertical for H_D = 5.7 meters
- C.18 Results for the pipe's angle with the vertical for H_D = 7.6 meters
- C.19 Results for compression in sag bend for H_D = 3.8 meters
- C.20 Results for compression in sag bend for H_D = 5.7 meters
- C.21 Results for compression in sag bend for H_D = 7.6 meters
- C.22 Result for bending radius in sag bend for H_D = 3.8 meters
- C.23 Result for bending radius in sag bend for H_D = 5.7 meters
- C.24 Result for bending radius in sag bend for H_D = 7.6 meters
- C.25 Results for landing of helicopters in daylight for H_D = 3.8 meters
- C.26 Results for landing of helicopters in daylight for H_D = 5.7 meters
- C.27 Results for landing of helicopters in daylight for H_D = 7.6 meters
- C.28 Results for heave rate of helideck for H_D = 3.8 meters
- C.29 Results for heave rate of helideck for H_D = 5.7 meters
- C.30 Results for heave rate of helideck for H_D = 7.6 meters

C.1 Results for heave acceleration on main deck for H_D = 3.8 meters

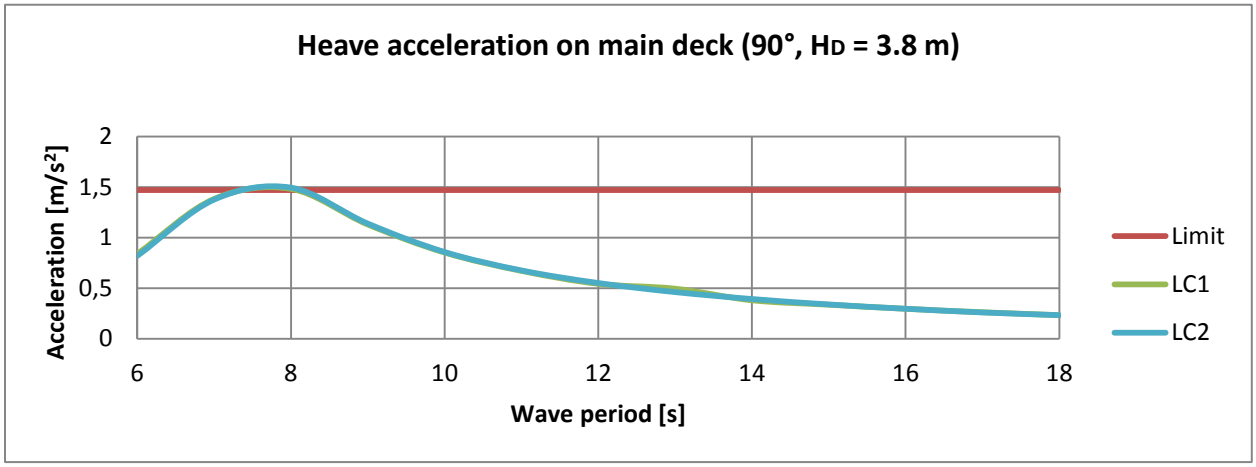

Figure C.0.1: Heave acceleration on main deck for LC1 and LC2, wave direction 90° and H_D = 3.8 m

C.2 Results for heave acceleration on main deck for H_D = 5.7 meters

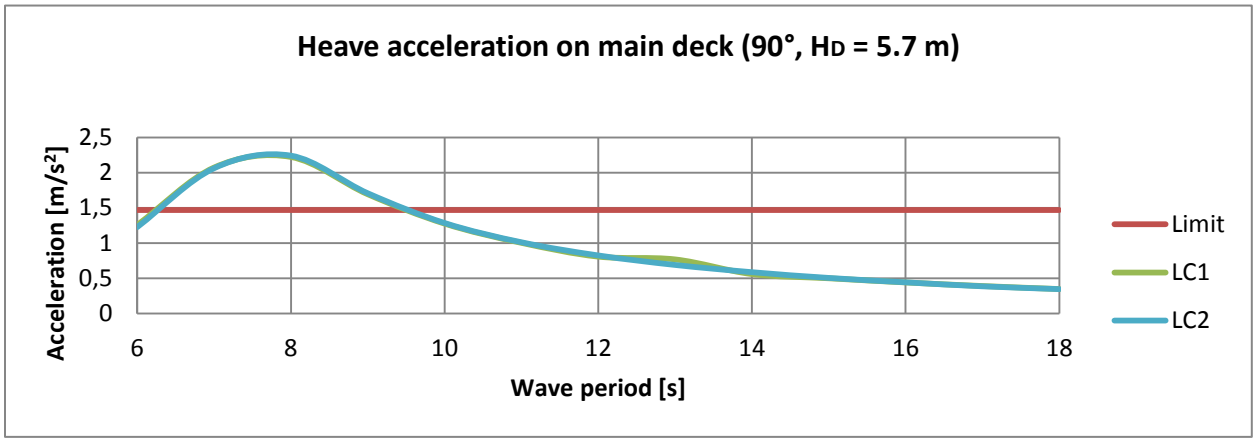

Figure C.0.2: Heave acceleration on main deck for LC1 and LC2, wave direction 90° and H_D = 5.7 m

C.3 Results for heave acceleration on main deck for H_D = 7.6 meters

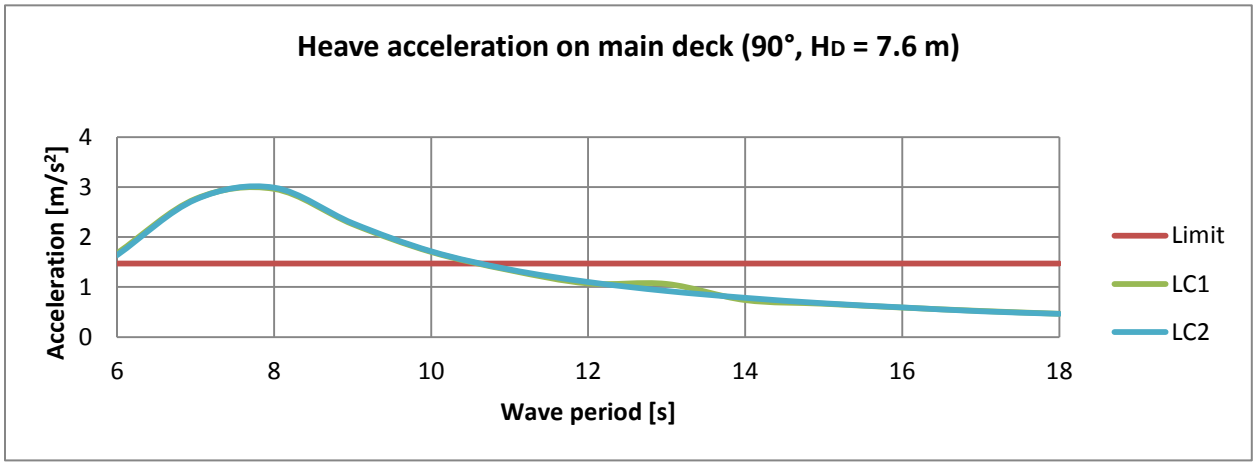

Figure C.0.3: Heave acceleration on main deck for LC1 and LC2, wave direction 90° and H_D = 7.6 m

C.4 Results for lateral acceleration on main deck for H_D = 3.8 meters

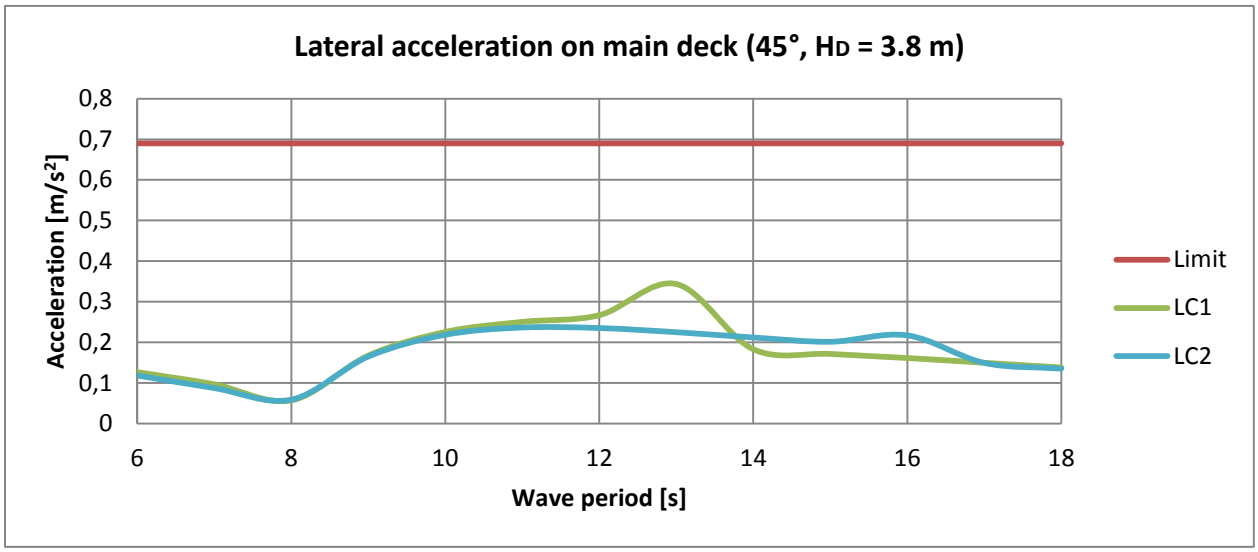

Figure C.0.4: Lateral acceleration on main deck for LC1 and LC2, wave direction 45° and H_D = 3.8 m

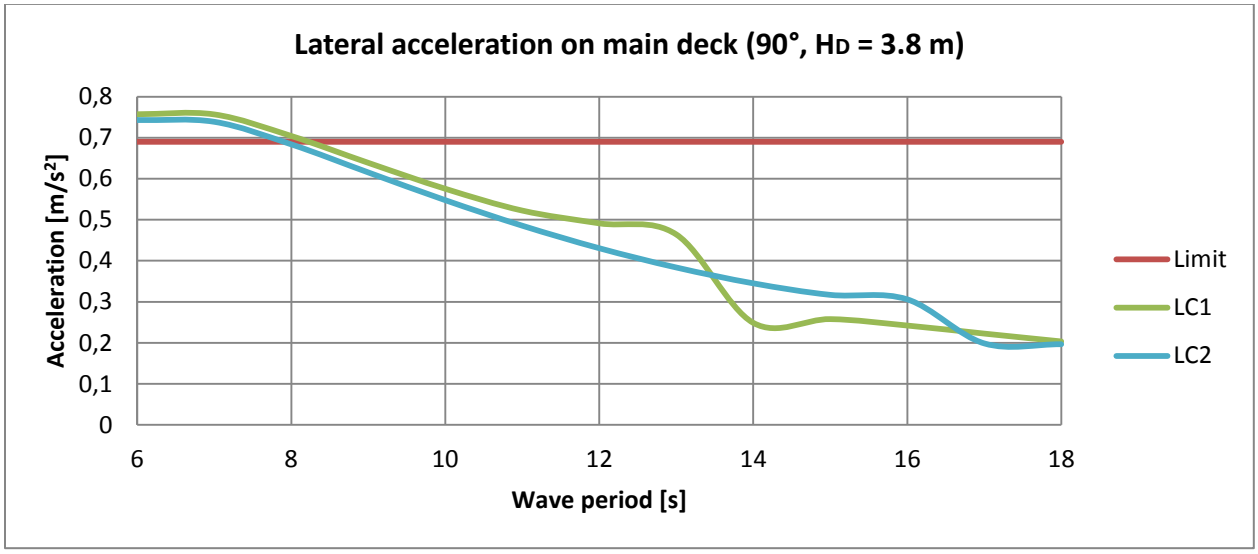

Figure C.0.5: Lateral acceleration on main deck for LC1 and LC2, wave direction 90° and H_D = 3.8 m

C.5 Results for lateral acceleration on main deck for H_D = 5.7 meters

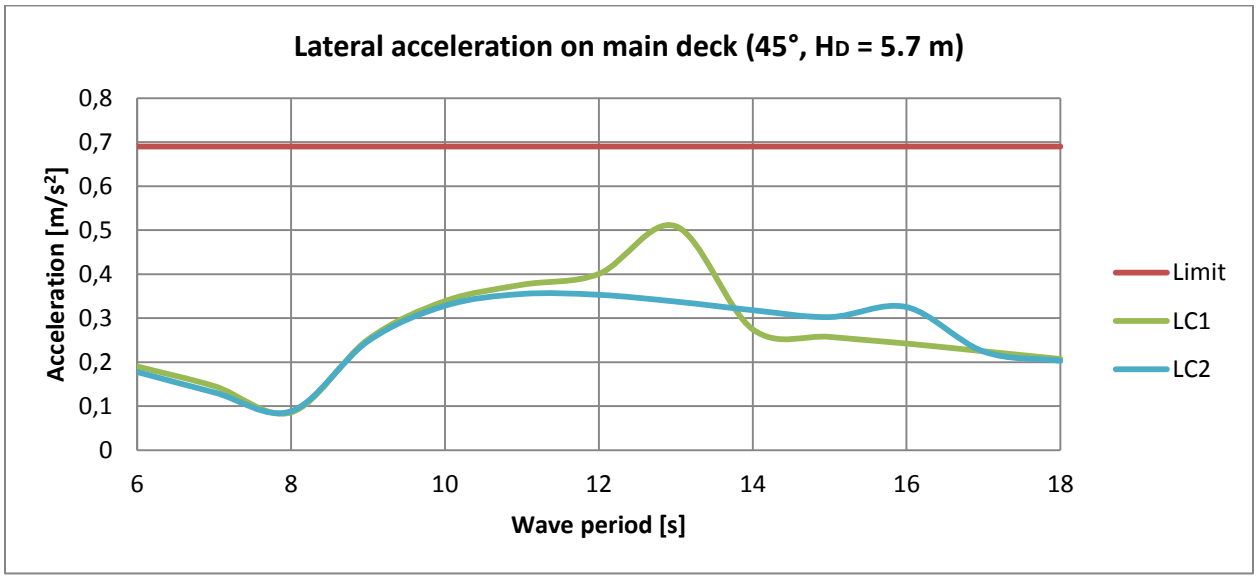

Figure C.0.6: Lateral acceleration on main deck for LC1 and LC2, wave direction 45° and H_D = 5.7 m

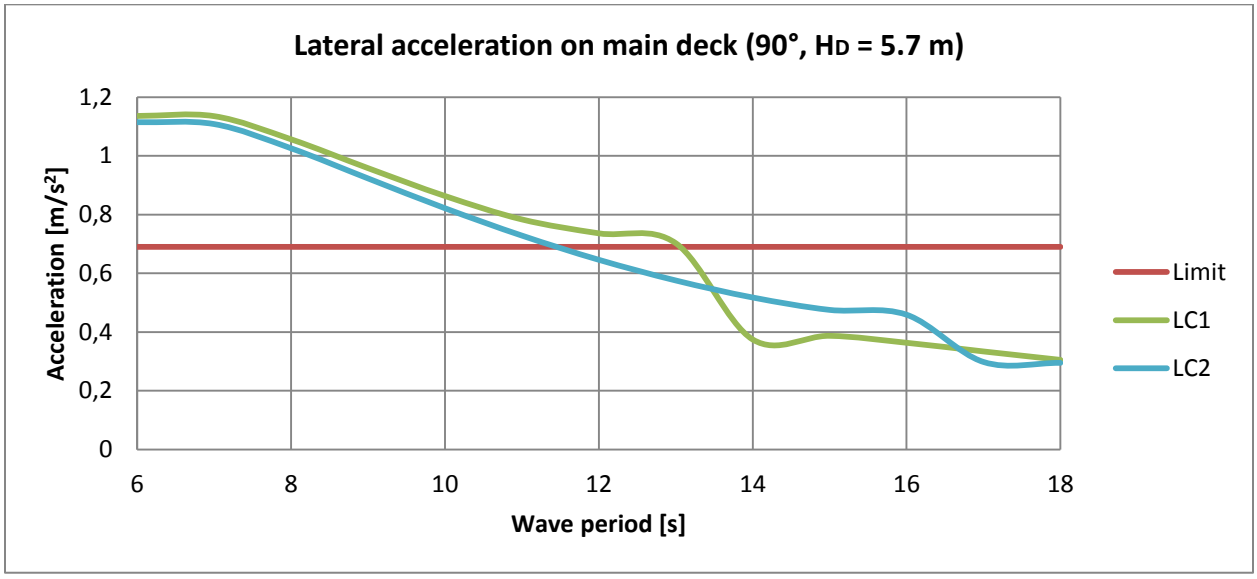

Figure C.0.7: Lateral acceleration on main deck for LC1 and LC2, wave direction 90° and H_D = 5.7 m

C.6 Results for lateral acceleration on main deck for H_D = 7.6 meters

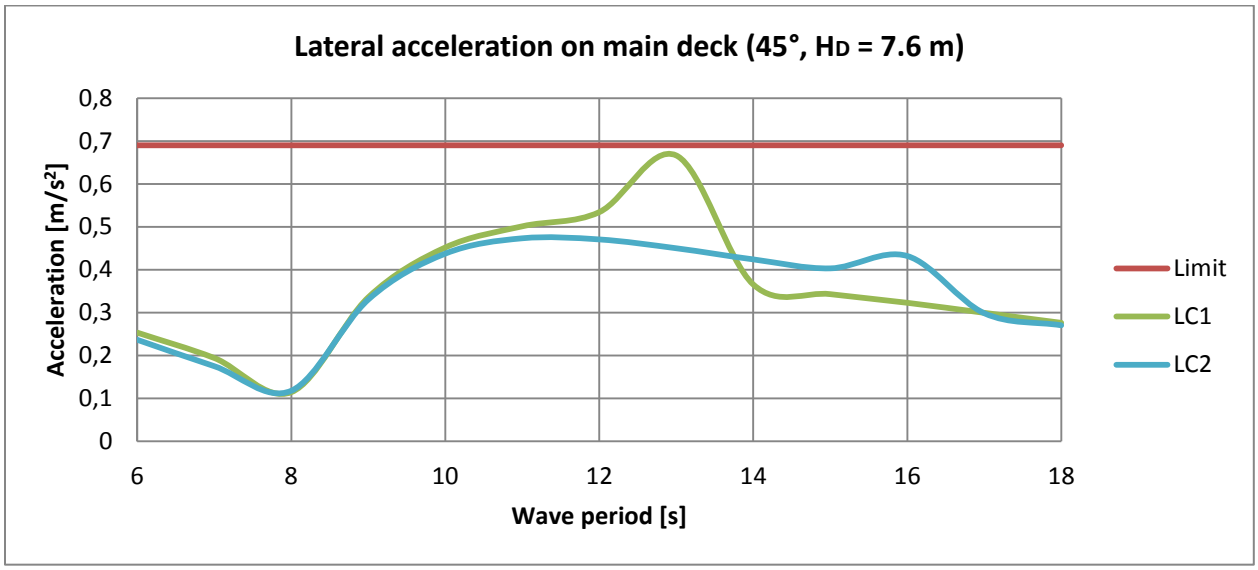

Figure C.0.8: Lateral acceleration on main deck for LC1 and LC2, wave direction 45° and H_D = 7.6 m

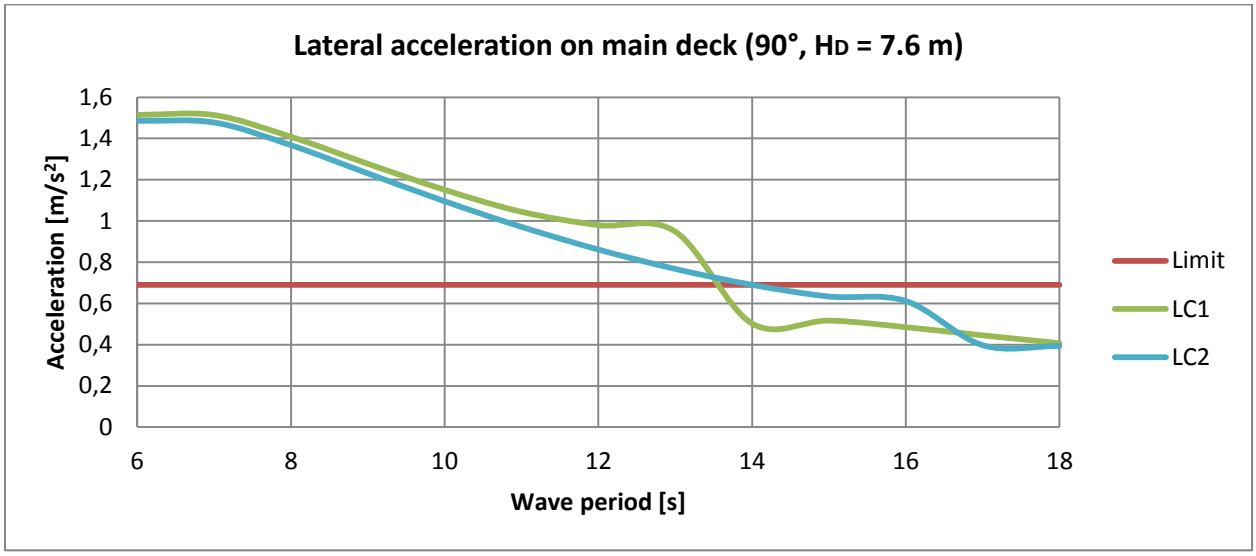

Figure C.0.9: Lateral acceleration on main deck for LC1 and LC2, wave direction 90° and H_D = 7.6 m

C.7 Results for roll rotation for H_D = 3.8 meters

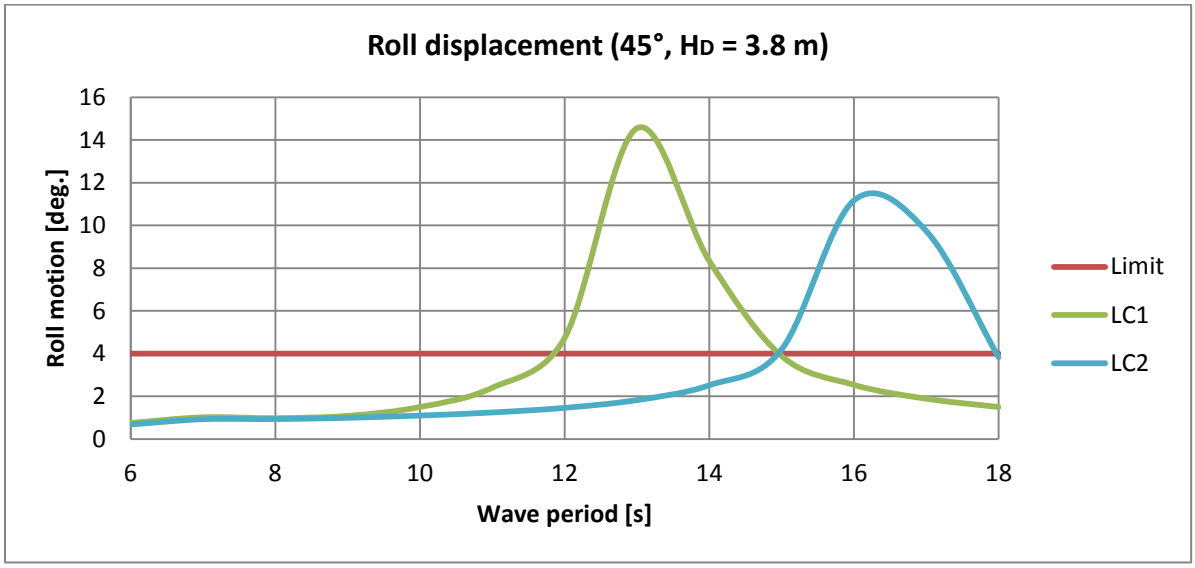

Figure C.0.10: Roll displacement for LC1 and LC2, wave direction 45° and H_D = 3.8 m

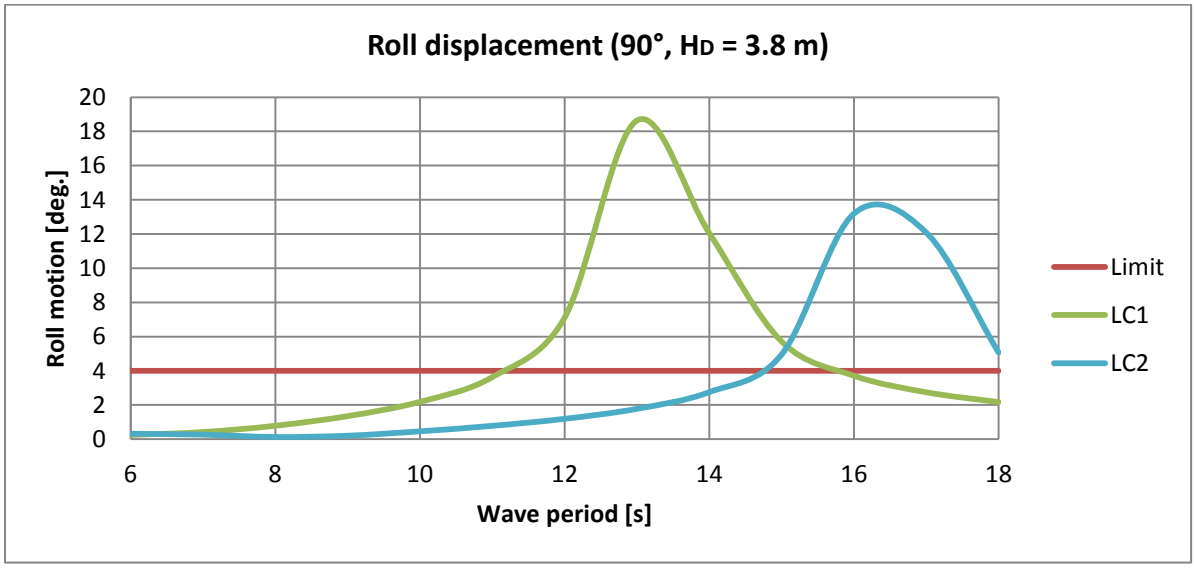

Figure C.0.11: Roll displacement for LC1 and LC2, wave direction 90° and H_D = 3.8 m

C.8 Results for roll rotation for H_D = 5.7 meters

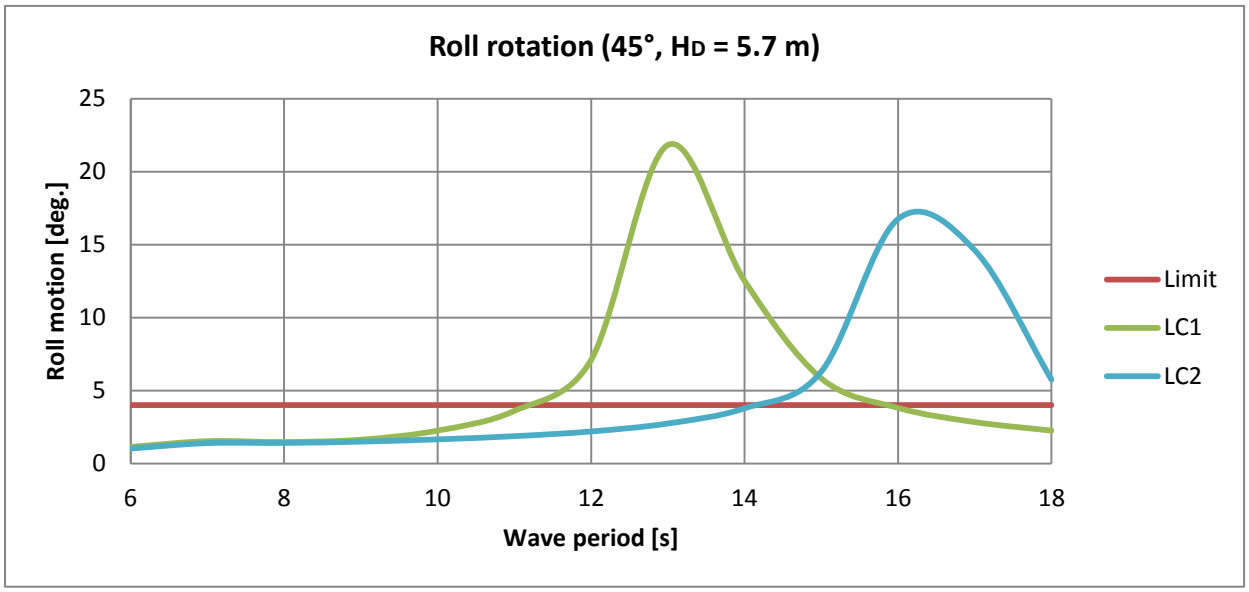

Figure C.0.12: Roll displacement for LC1 and LC2, wave direction 45° and H_D = 5.7 m

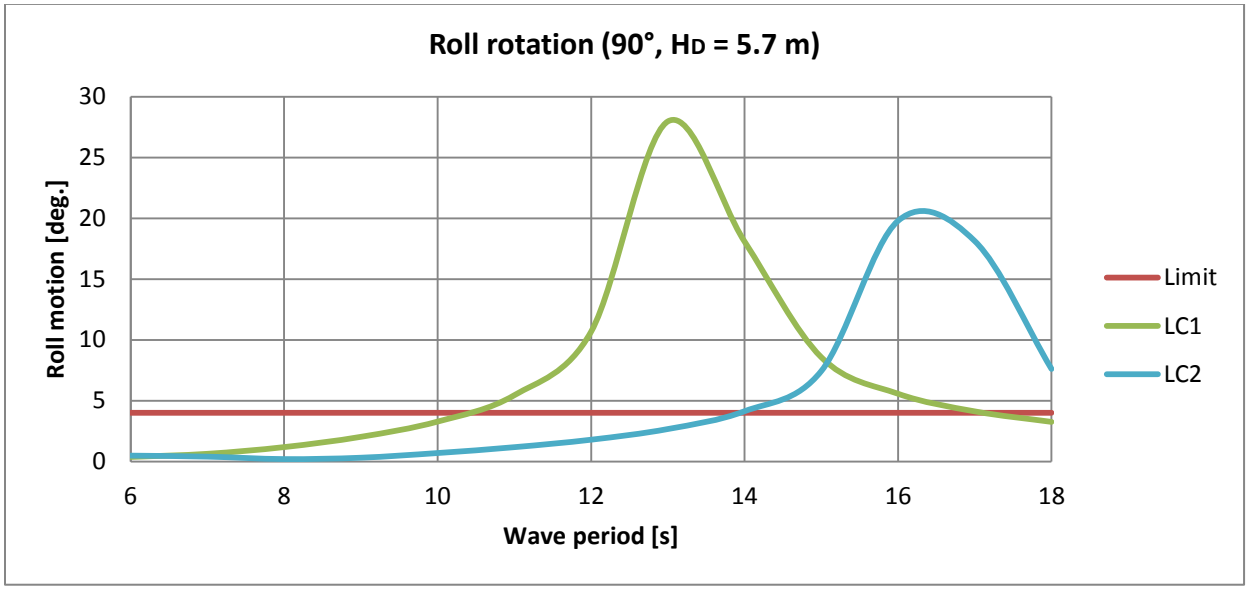

Figure C.0.13: Roll displacement for LC1 and LC2, wave direction 90° and H_D = 5.7 m

C.9 Results for roll rotation for H_D = 7.6 meters

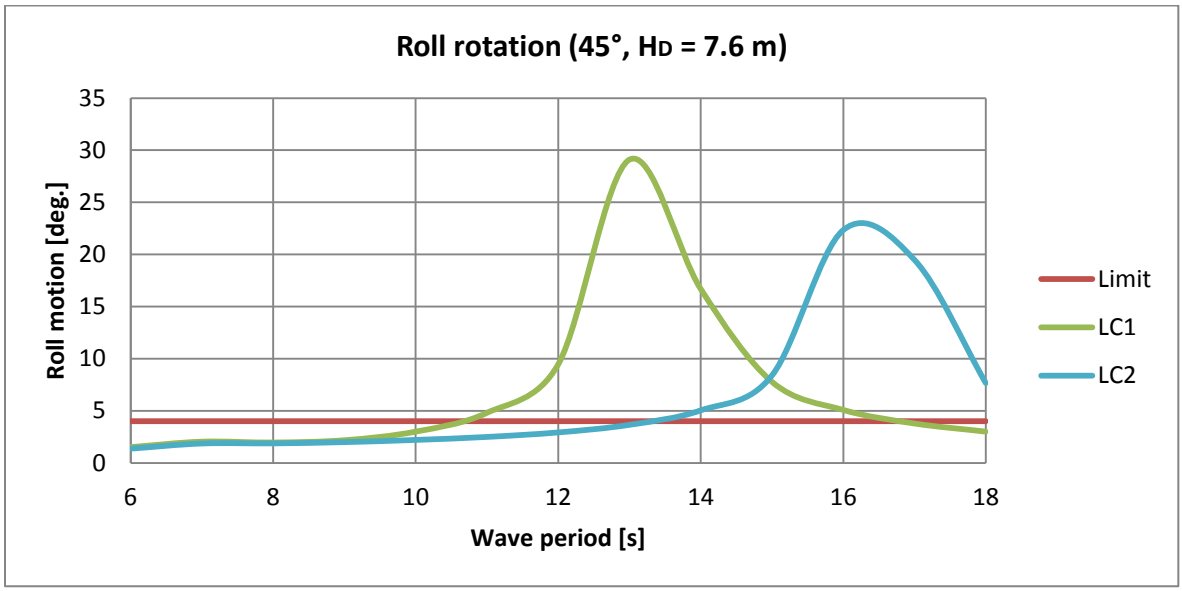

Figure C.0.14: Roll displacement for LC1 and LC2, wave direction 45° and H_D = 7.6 m

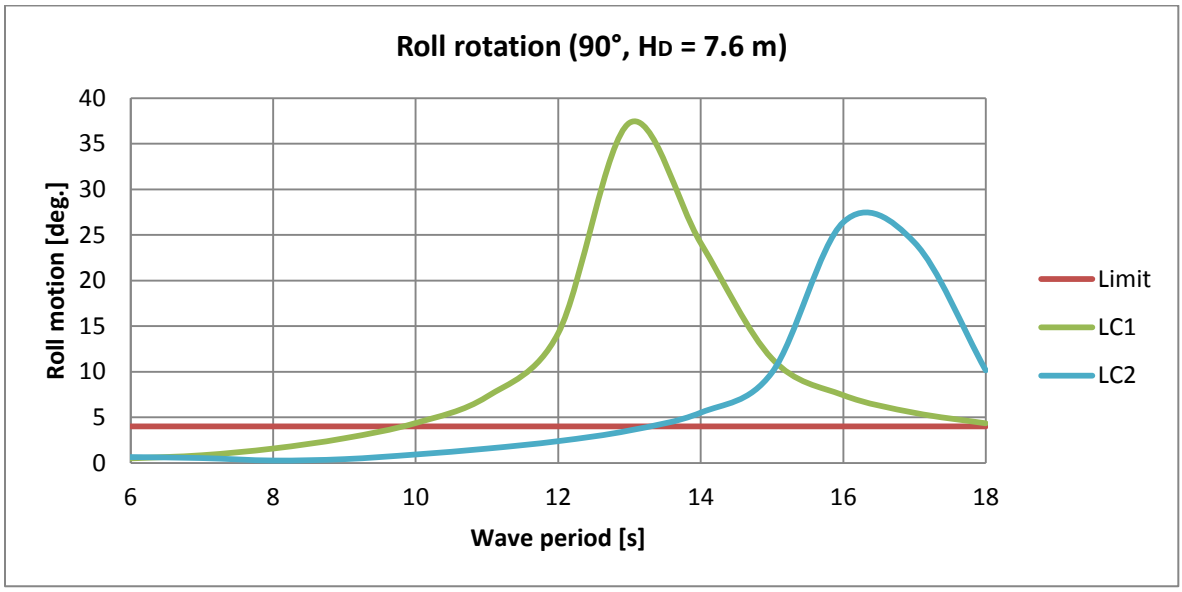

Figure C.0.15: Roll displacement for LC1 and LC2, wave direction 90° and H_D = 7.6 m

C.10 Results for pitch rotation for H_D = 3.8 meters

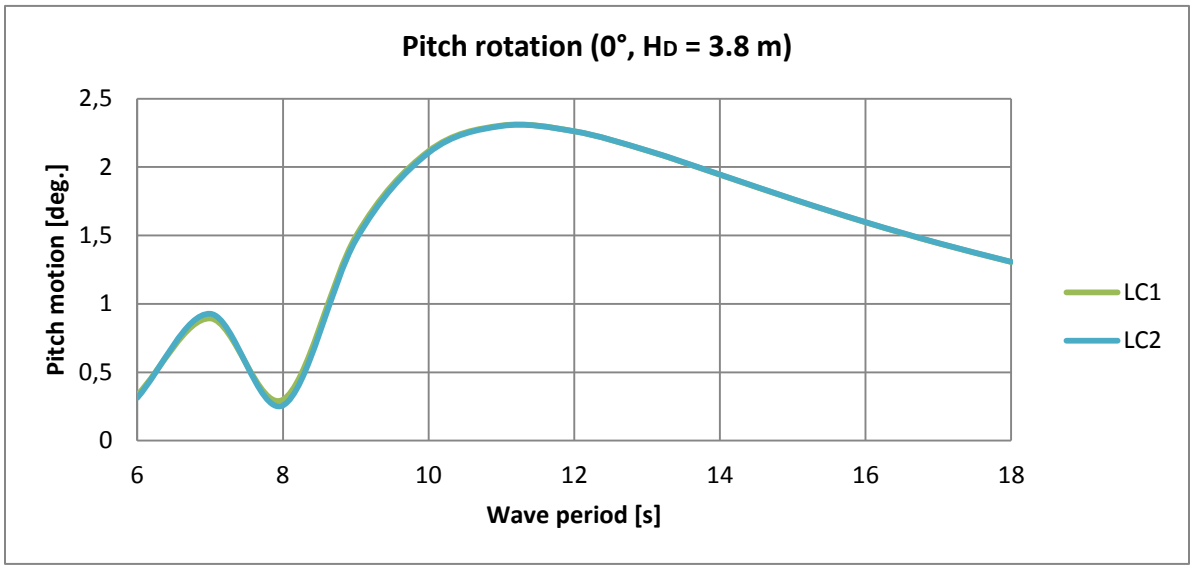

Figure C.0.16: Pitch motion of the vessel for LC1 and LC2, wave direction 0° and H_D = 3.8 m

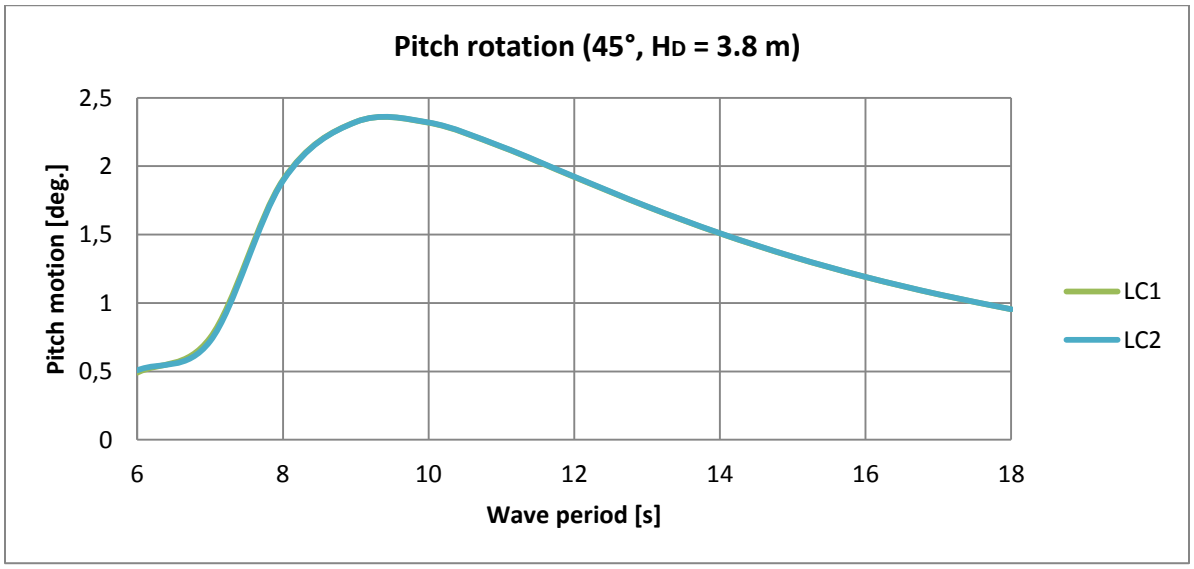

Figure C.0.17: Pitch motion of the vessel for LC1 and LC2, wave direction 45° and H_D = 3.8 m

C.11 Results for pitch rotation for H_D = 5.7 meters

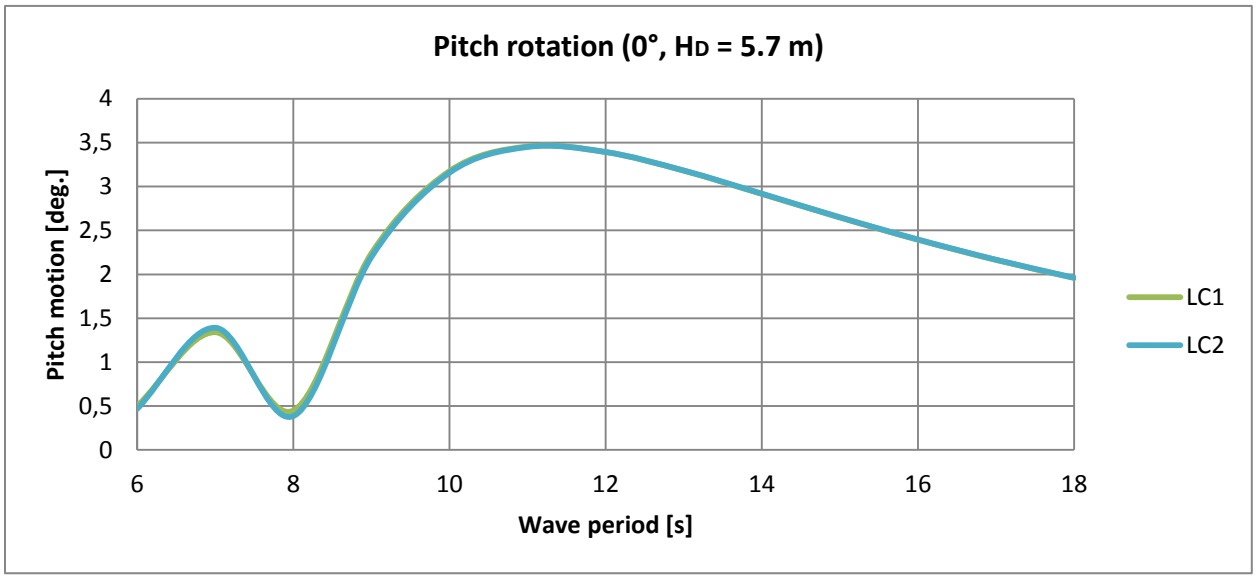

Figure C.0.18: Pitch motion of the vessel for LC1 and LC2, wave direction 0° and H_D = 5.7 m

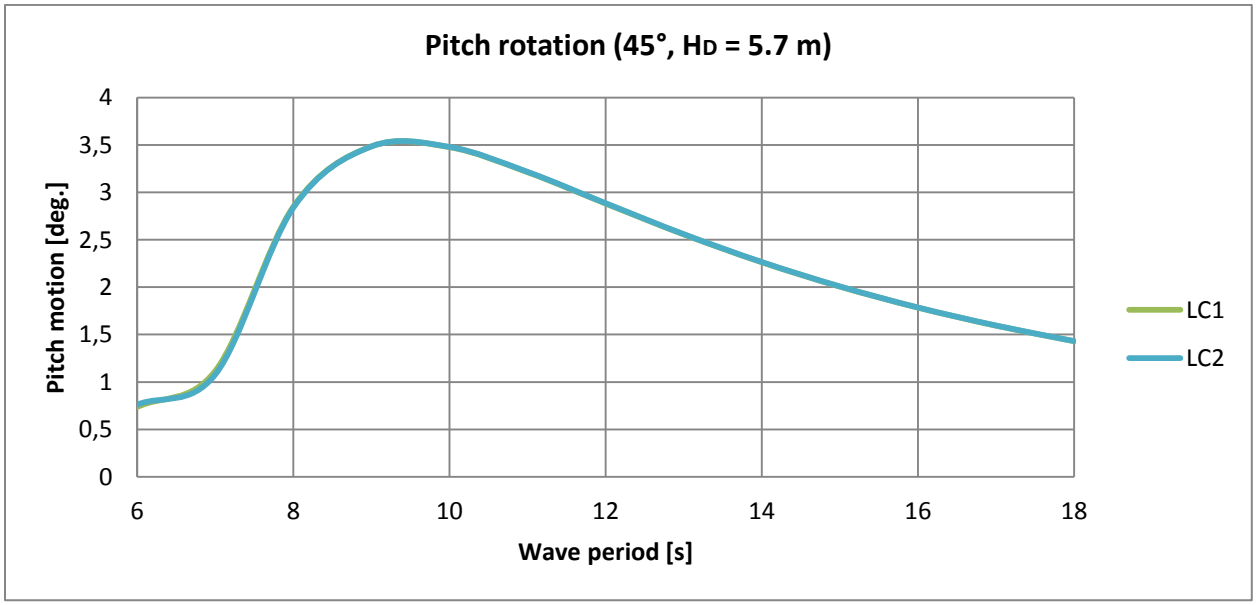

Figure C.0.19: Pitch motion of the vessel for LC1 and LC2, wave direction 45° and H_D = 5.7 m

C.12 Results for pitch rotation for H_D = 7.6 meters

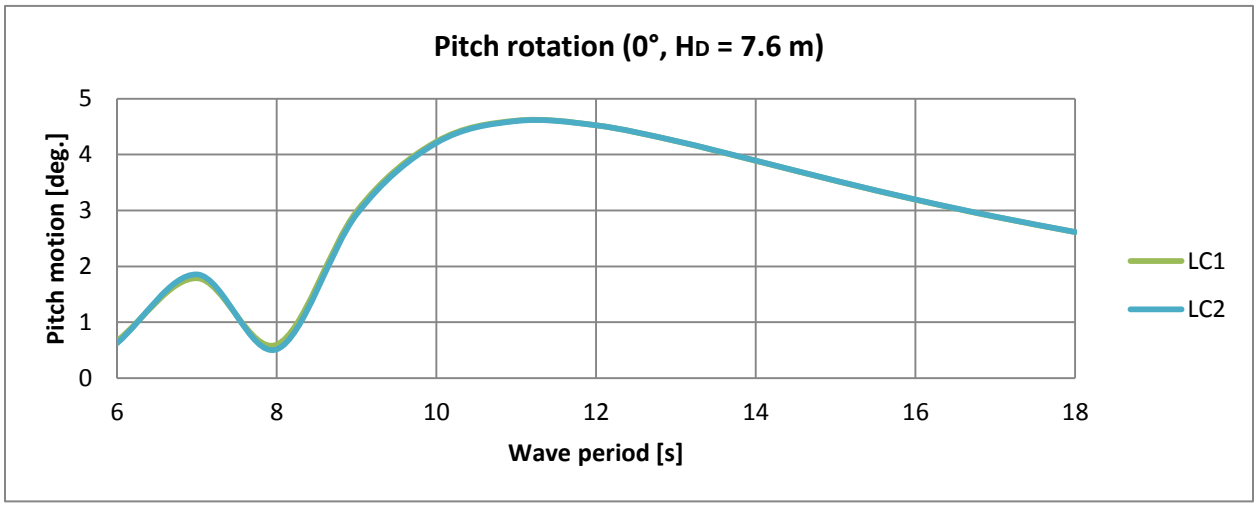

Figure C.0.20: Pitch motion of the vessel for LC1 and LC2, wave direction 0° and H_D = 7.6 m

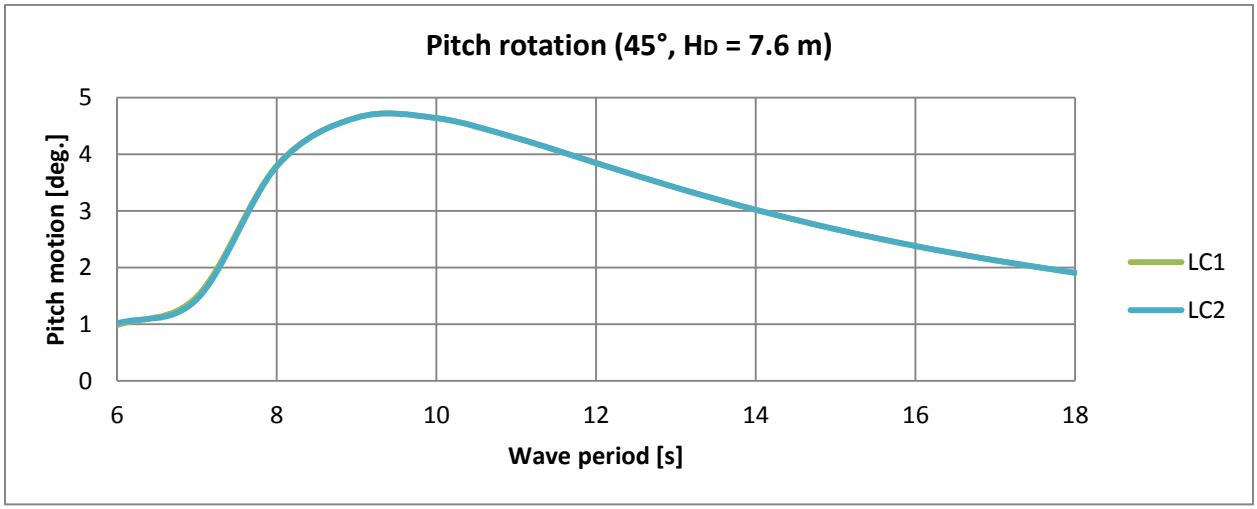

Figure C.0.21: Pitch motion of the vessel for LC1 and LC2, wave direction 45° and H_D = 7.6 m

C.13 Results for top tension for H_D = 3.8 meters

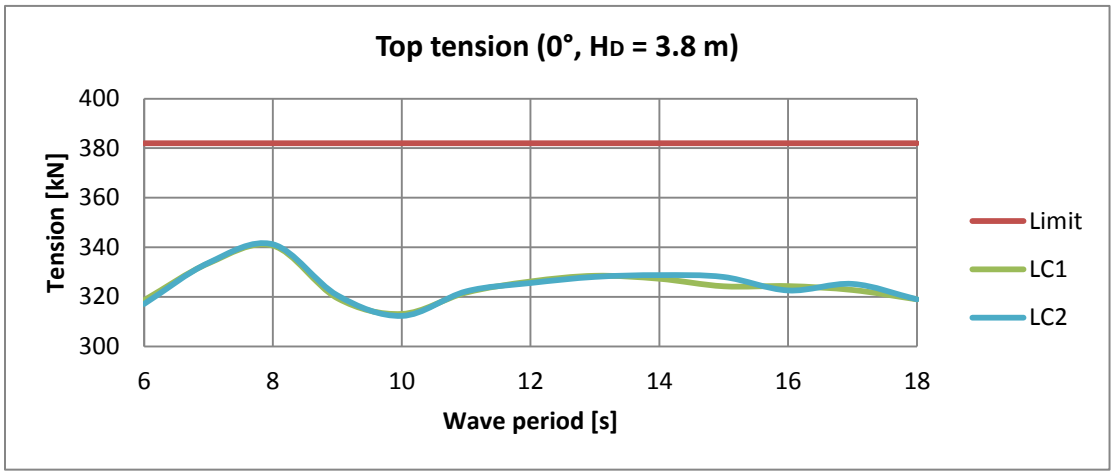

Figure C.0.22: Top tension in flexible flowline for LC1 and LC2, wave direction 0° and H_D = 3.8 m

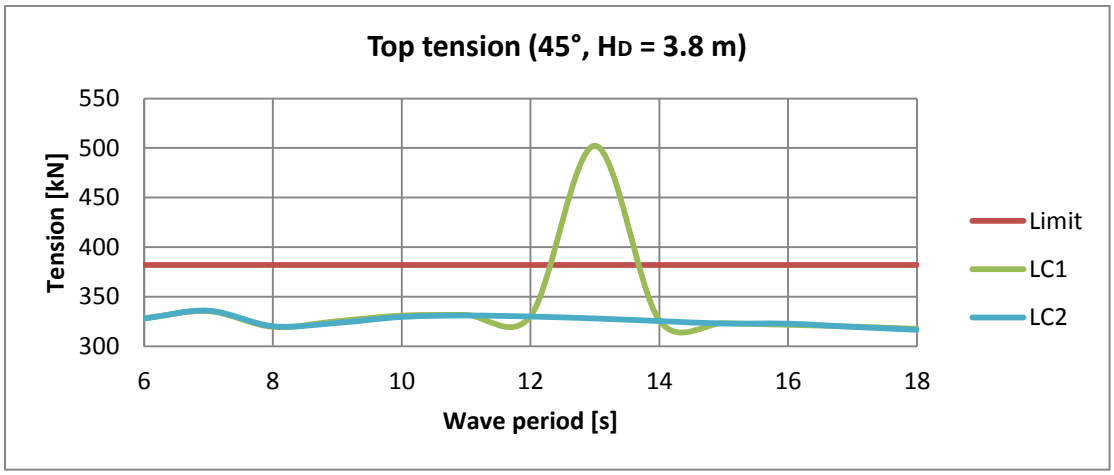

Figure C.0.23: Top tension in flexible flowline for LC1 and LC2, wave direction 45° and H_D = 3.8 m

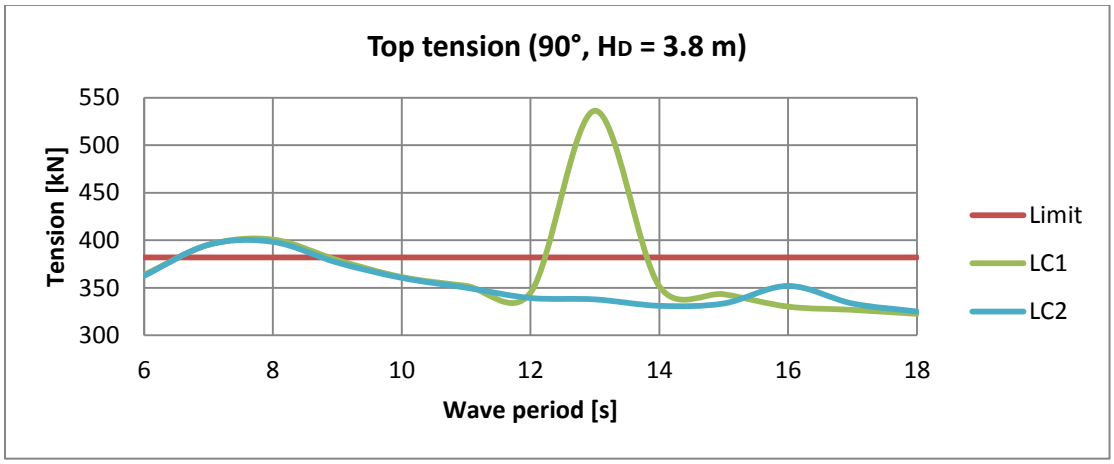

Figure C.0.24: Top tension in flexible flowline for LC1 and LC2, wave direction 90° and H_D = 3.8 m

C.14 Results for top tension for H_D = 5.7 meters

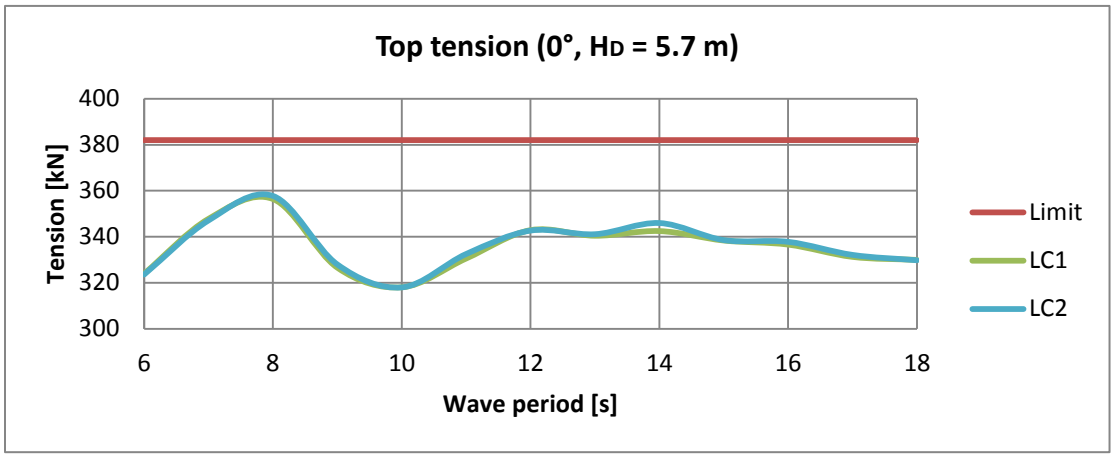

Figure C.0.25: Top tension in flexible flowline for LC1 and LC2, wave direction 0° and H_D = 5.7 m

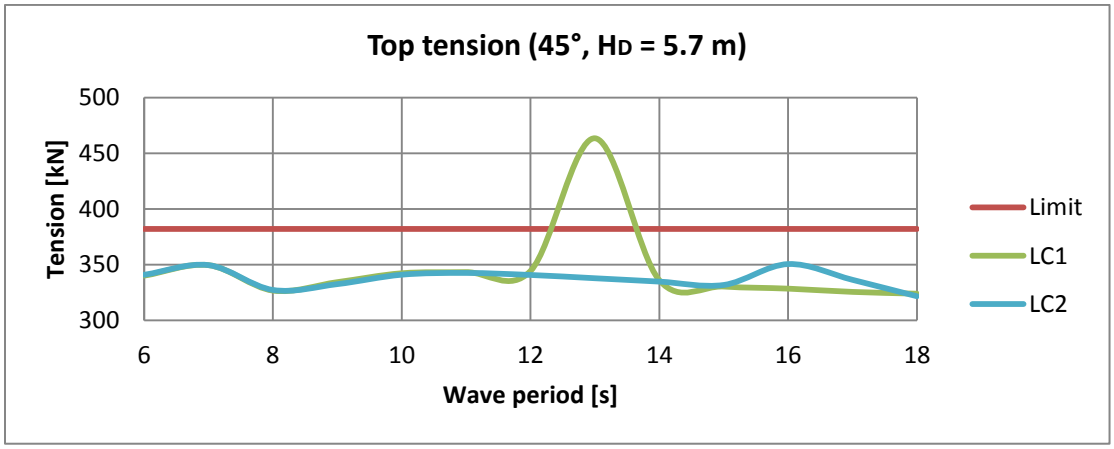

Figure C.0.26: Top tension in flexible flowline for LC1 and LC2, wave direction 45° and H_D = 5.7 m

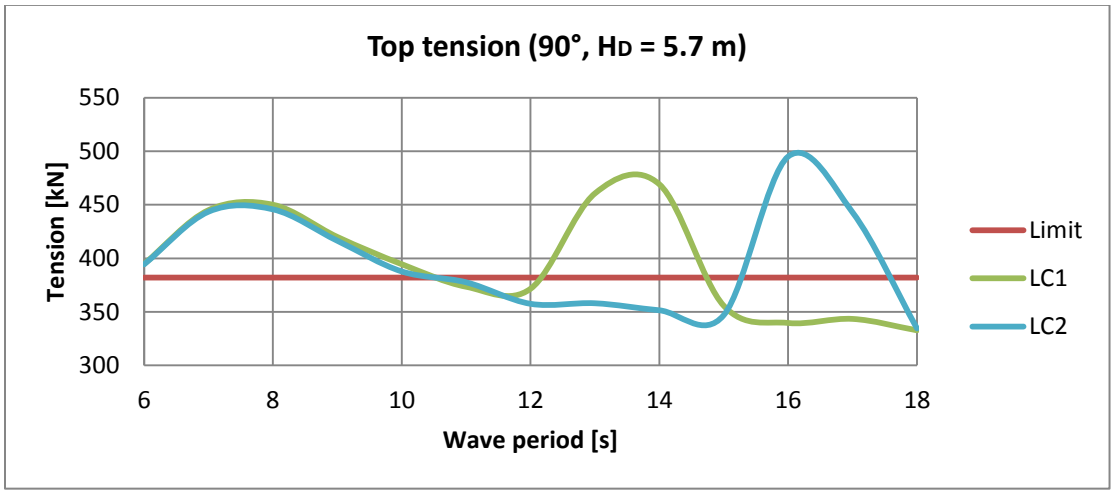

Figure C.0.27: Top tension in flexible flowline for LC1 and LC2, wave direction 90° and H_D = 5.7 m

C.15 Results for top tension for H_D = 7.6 meters

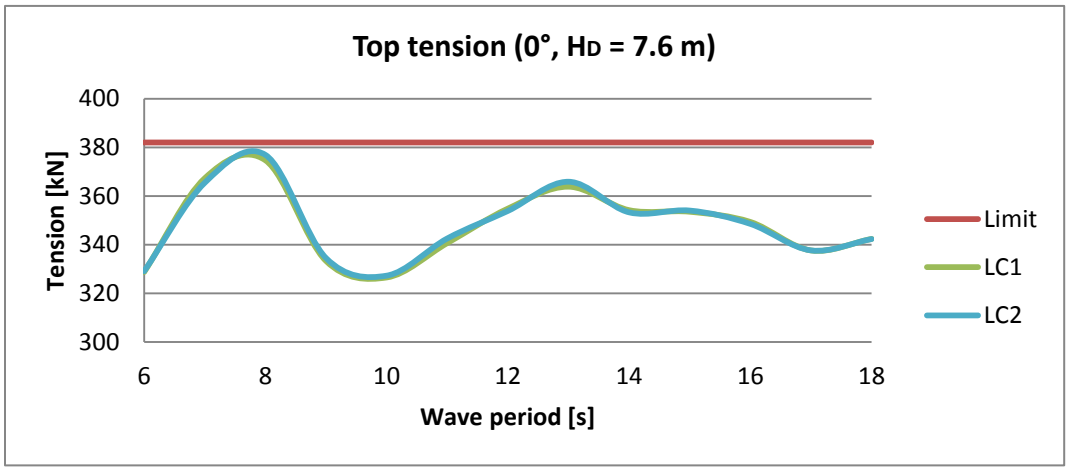

Figure C.0.28: Top tension in flexible flowline for LC1 and LC2, wave direction 0° and H_D = 7.6 m

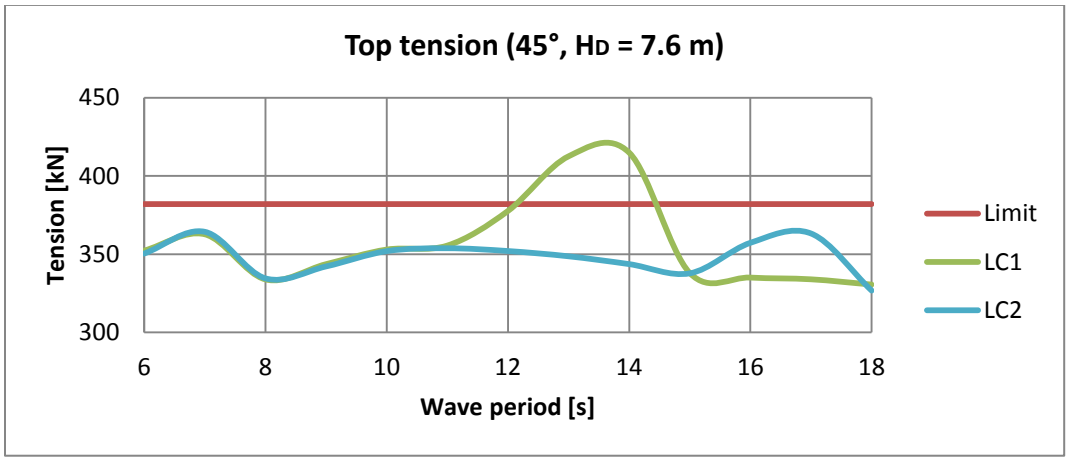

Figure C.0.29: Top tension in flexible flowline for LC1 and LC2, wave direction 45° and H_D = 7.6 m

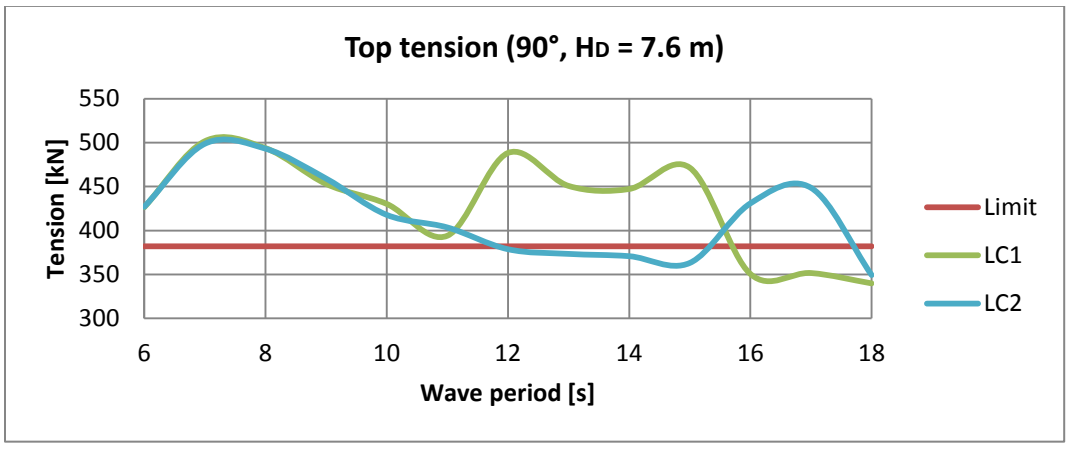

Figure C.0.30: Top tension in flexible flowline for LC1 and LC2, wave direction 90° and H_D = 7.6 m

C.16 Results for the pipe's angle with the vertical for H_D = 3.8 meters

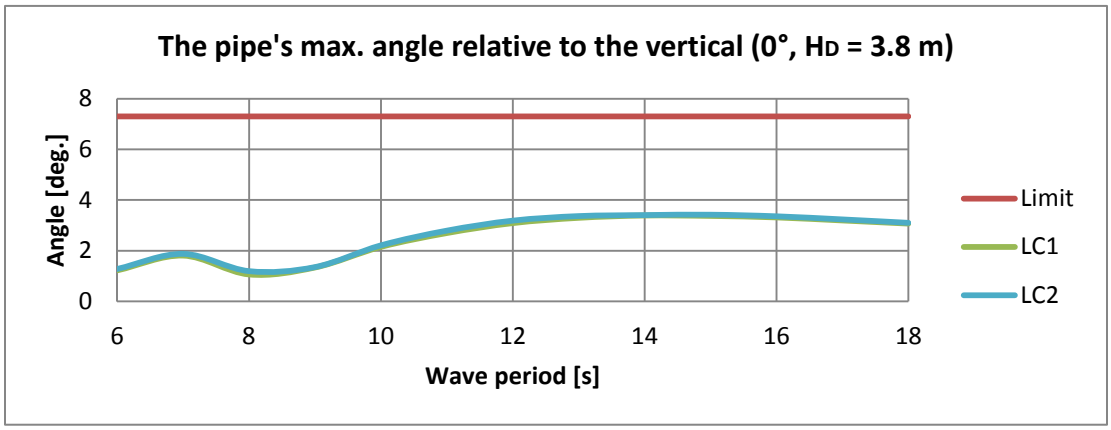

Figure C.0.31: Maximum deflection angle of the flexible flowline from the vertical when going through the moonpool for LC1 and LC2, wave direction 0° and H_D = 3.8 m

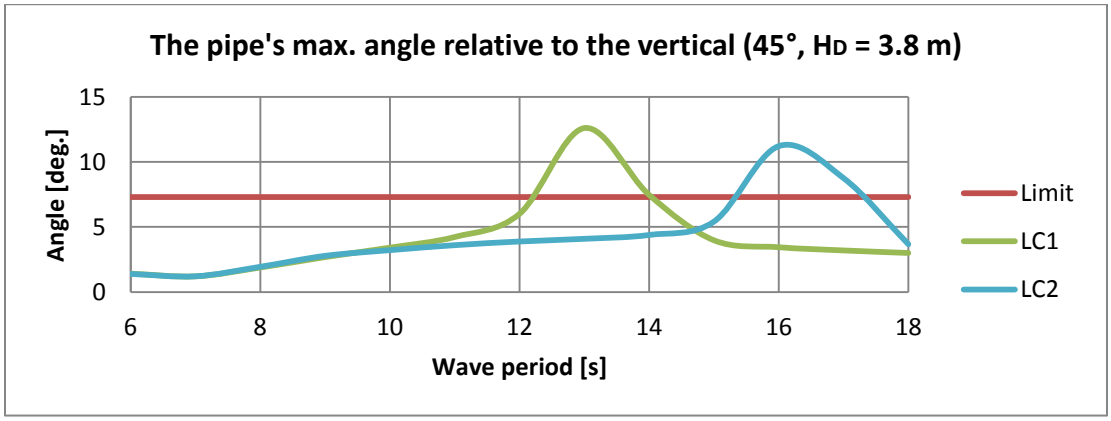

Figure C.0.32: Maximum deflection angle of the flexible flowline from the vertical when going through the moonpool for LC1 and LC2, wave direction 45° and H_D = 3.8 m

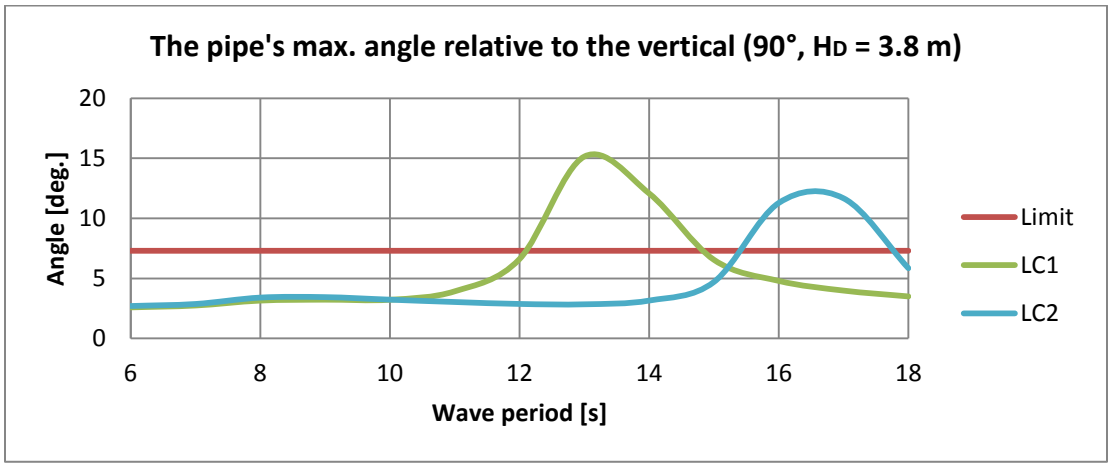

Figure C.0.33: Maximum deflection angle of the flexible flowline from the vertical when going through the moonpool for LC1 and LC2, wave direction 90° and H_D = 3.8 m

C.17 Results for the pipe's angle with the vertical for H_D = 5.7 meters

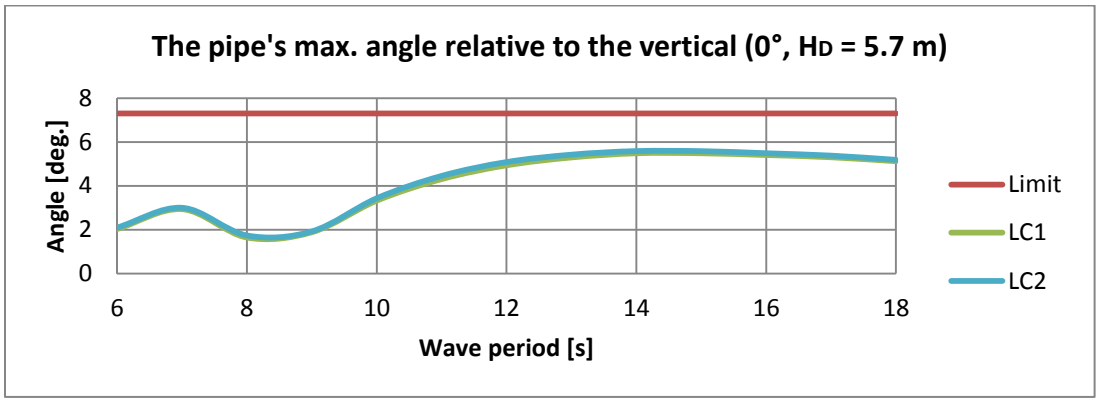

Figure C.0.34: Maximum deflection angle of the flexible flowline from the vertical when going through the moonpool for LC1 and LC2, wave direction 0° and H_D = 5.7 m

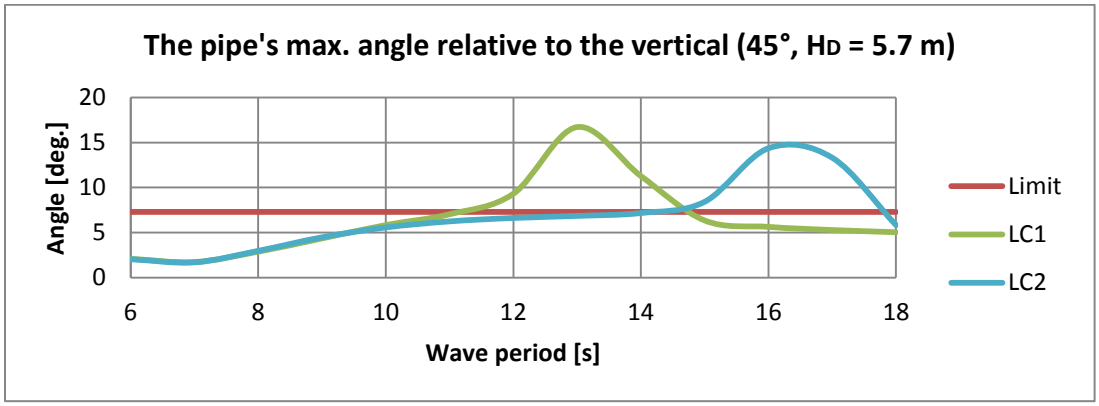

Figure C.0.35: Maximum deflection angle of the flexible flowline from the vertical when going through the moonpool for LC1 and LC2, wave direction 45° and H_D = 5.7 m

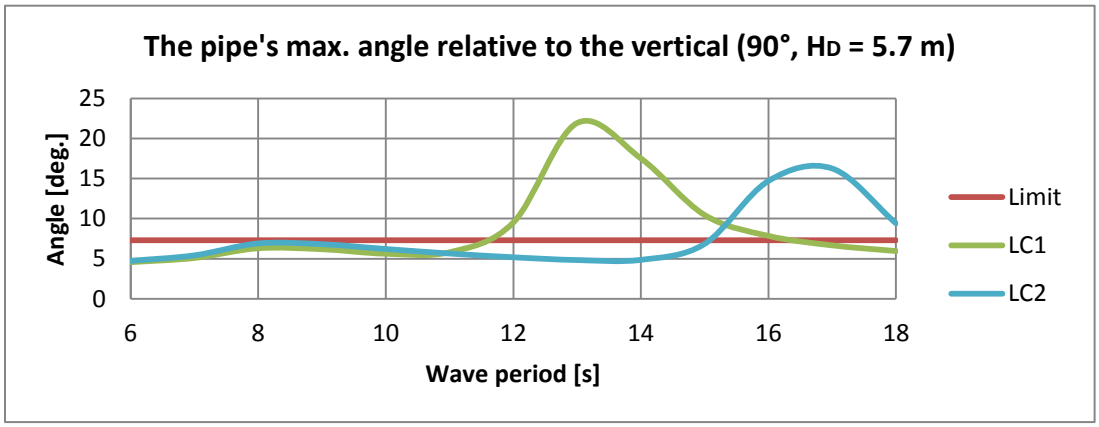

Figure C.0.36: Maximum deflection angle of the flexible flowline from the vertical when going through the moonpool for LC1 and LC2, wave direction 90° and H_D = 5.7 m

C.18 Results for the pipe's angle with the vertical for H_D = 7.6 meters

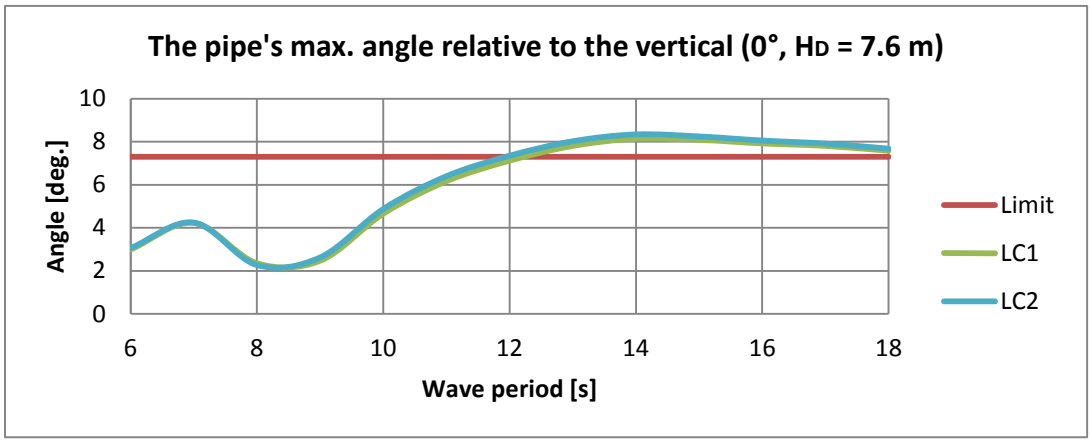

Figure C.0.37: Maximum deflection angle of the flexible flowline from the vertical when going through the moonpool for LC1 and LC2, wave direction 0° and H_D = 7.6 m

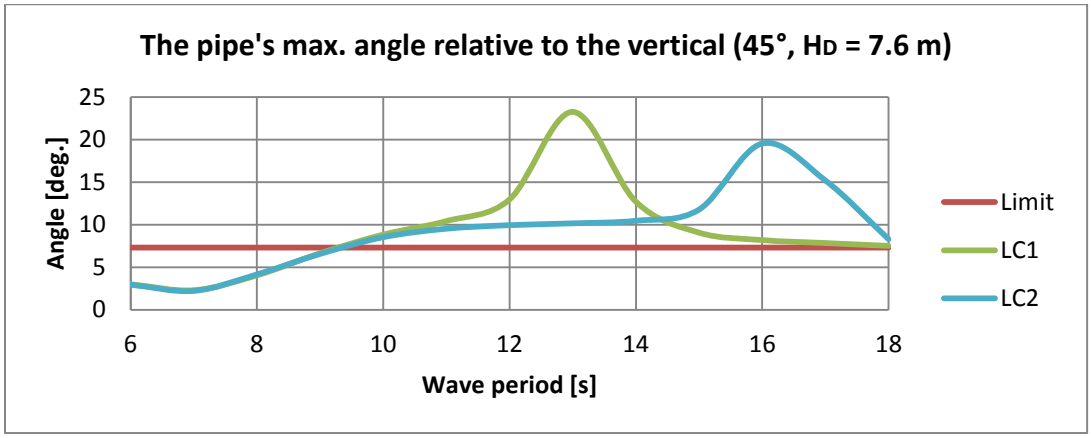

Figure C.0.38: Maximum deflection angle of the flexible flowline from the vertical when going through the moonpool for LC1 and LC2, wave direction 45° and H_D = 7.6 m

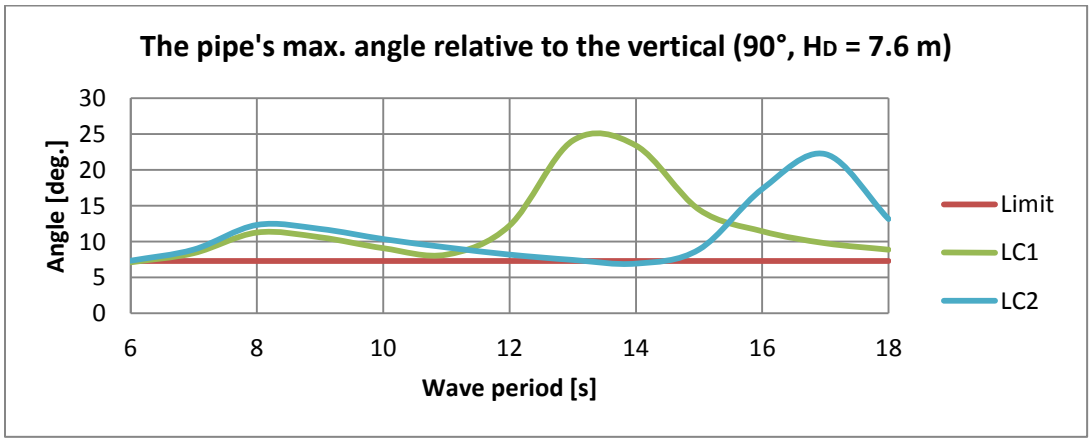

Figure C.0.39: Maximum deflection angle of the flexible flowline from the vertical when going through the moonpool for LC1 and LC2, wave direction 90° and H_D =7.6 m

C.19 Results for compression in sag bend for H_D = 3.8 meters

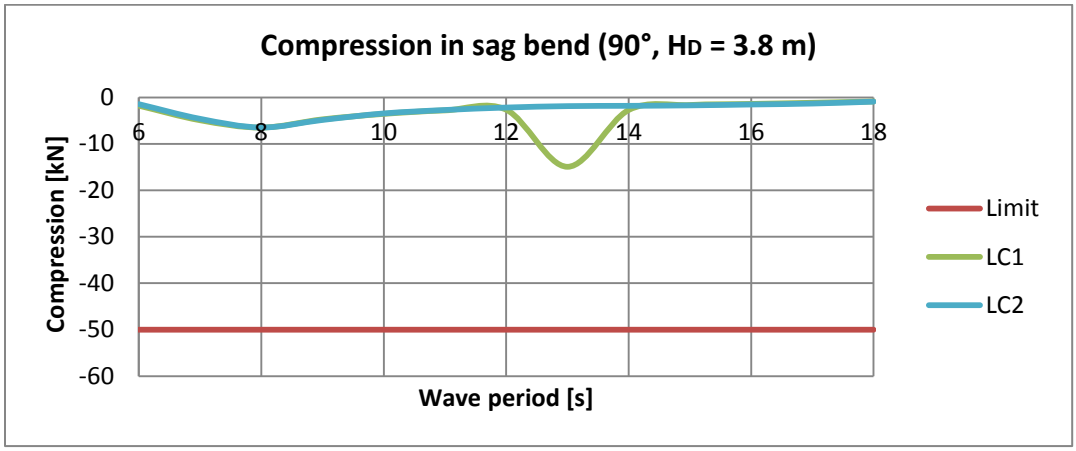

Figure C.0.40: Compression in the sag bend for LC1 and LC2, wave direction 90° and H_D = 3.8 m

C.20 Results for compression in sag bend for H_D = 5.7 meters

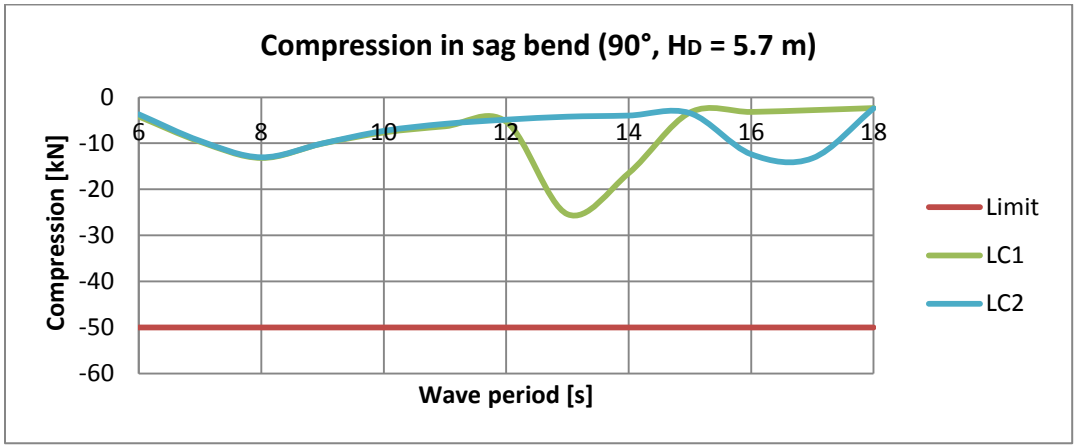

Figure C.0.41: Compression in the sag bend for LC1 and LC2, wave direction 90° and H_D = 5.7 m

C.21 Results for compression in sag bend for H_D = 7.6 meters

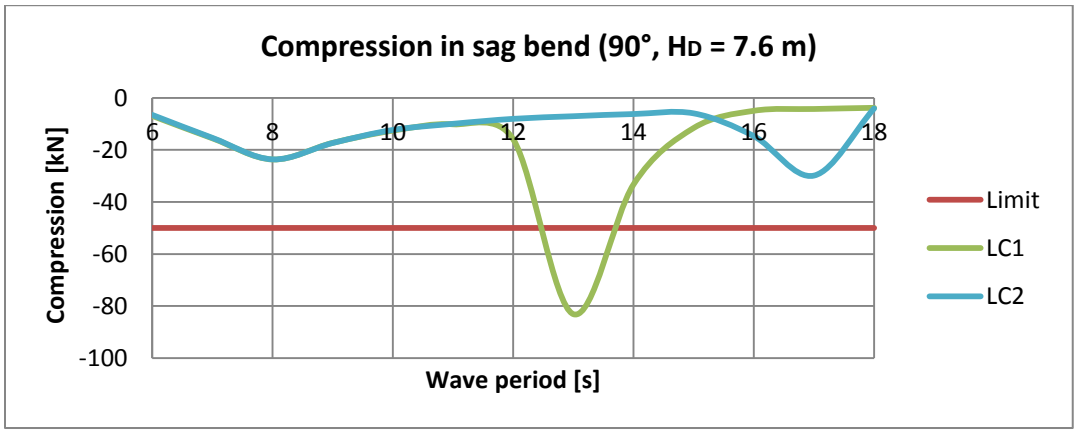

Figure C.0.42: Compression in the sag bend for LC1 and LC2, wave direction 90° and H_D = 7.6 m

C.22 Results for bending radius in sag bend for H_D = 3.8 meters

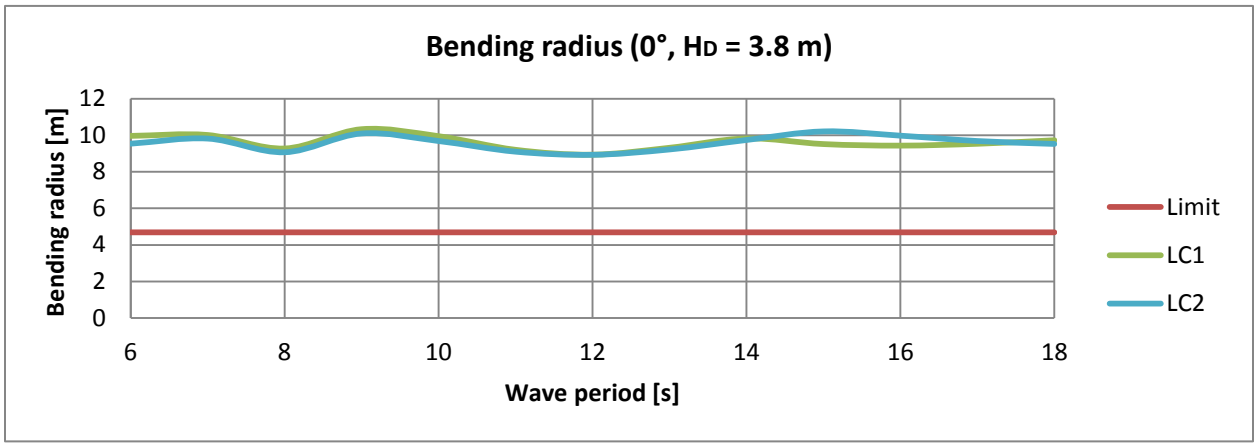

Figure C.0.43: Bending radius for flexible flowline in sag bend for LC1 and LC2, wave direction 0° and H_D = 3.8 m, MBR shown as the red line

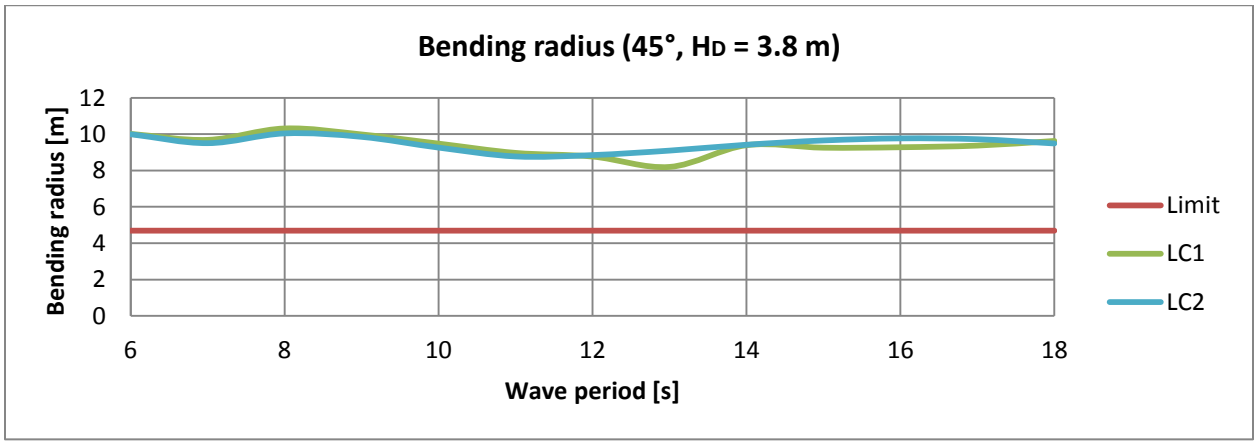

Figure C.0.44: Bending radius for flexible flowline in sag bend for LC1 and LC2, wave direction 45° and H_D = 3.8 m, MBR shown as the red line

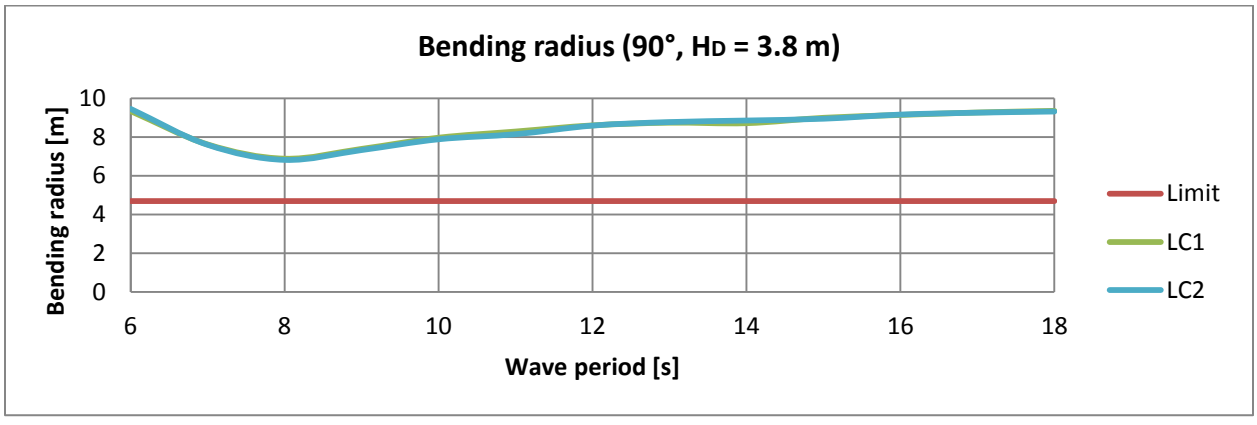

Figure C.0.45: Bending radius for flexible flowline in sag bend for LC1 and LC2, wave direction 90° and H_D = 3.8 m, MBR shown as the red line

C.23 Results for bending radius in sag bend for H_D = 5.7 meters

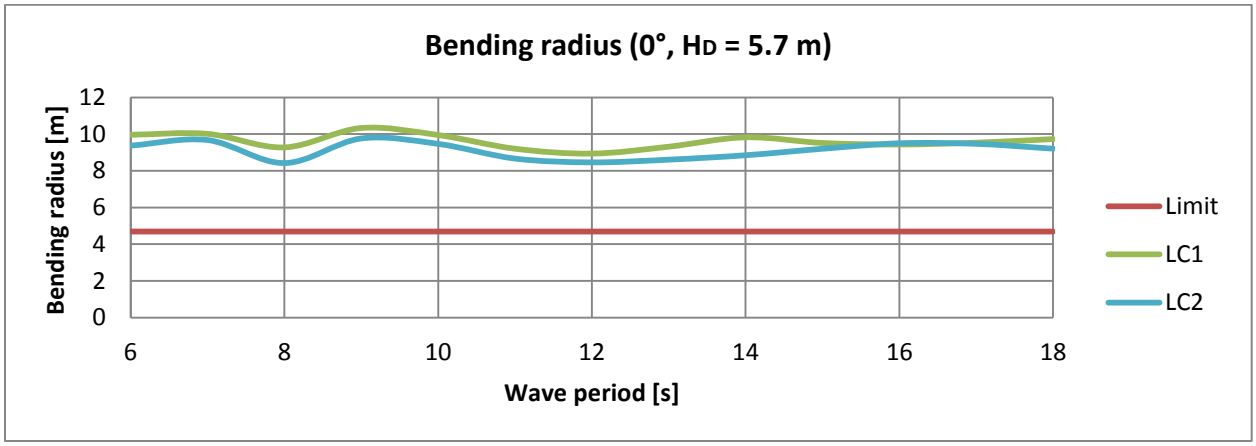

Figure C.0.46: Bending radius for flexible flowline in sag bend for LC1 and LC2, wave direction 0° and H_D = 5.7 m, MBR shown as the red line

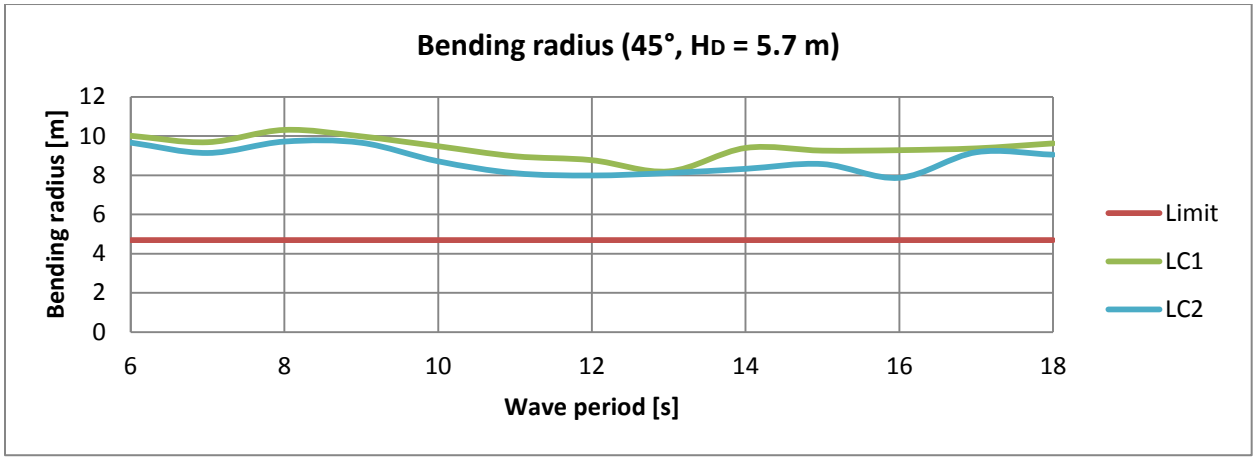

Figure C.0.47: Bending radius for flexible flowline in sag bend for LC1 and LC2, wave direction 45° and H_D = 5.7 m, MBR shown as the red line

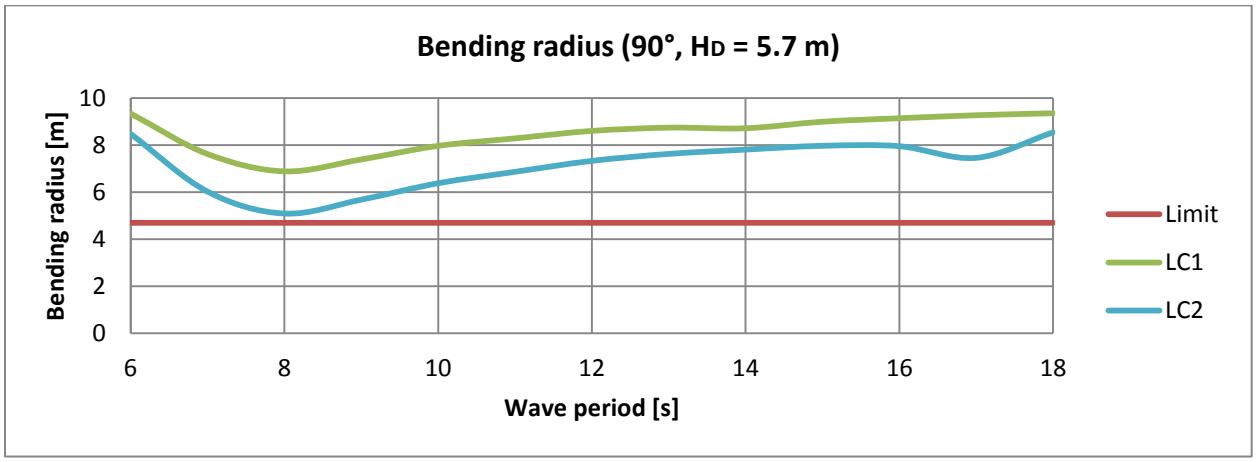

Figure C.0.48: Bending radius for flexible flowline in sag bend for LC1 and LC2, wave direction 90° and H_D = 5.7 m, MBR shown as the red line

C.24 Results for bending radius in sag bend for H_D = 7.6 meters

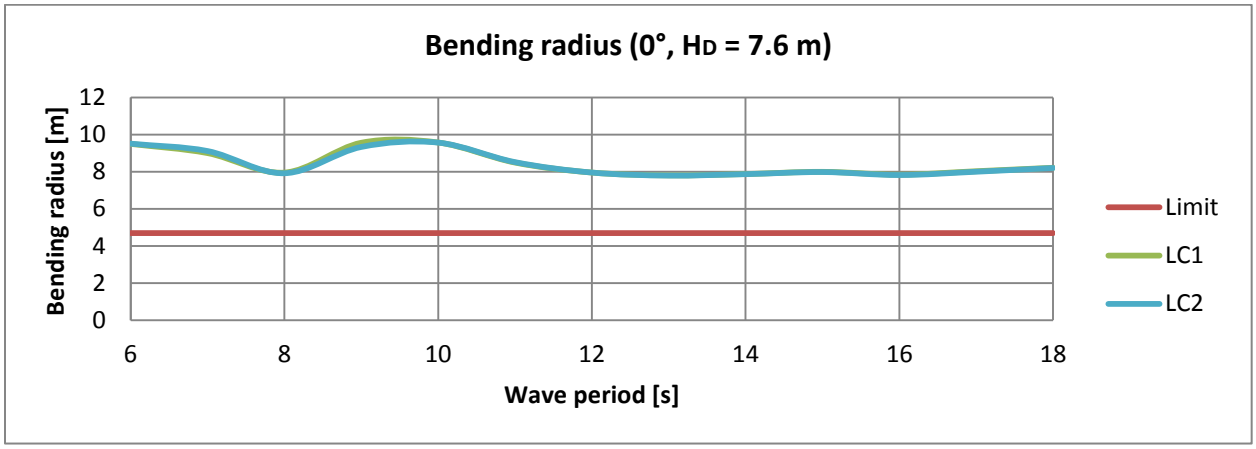

Figure C.0.49: Bending radius for flexible flowline in sag bend for LC1 and LC2, wave direction 0° and H_D = 7.6 m, MBR shown as the red line

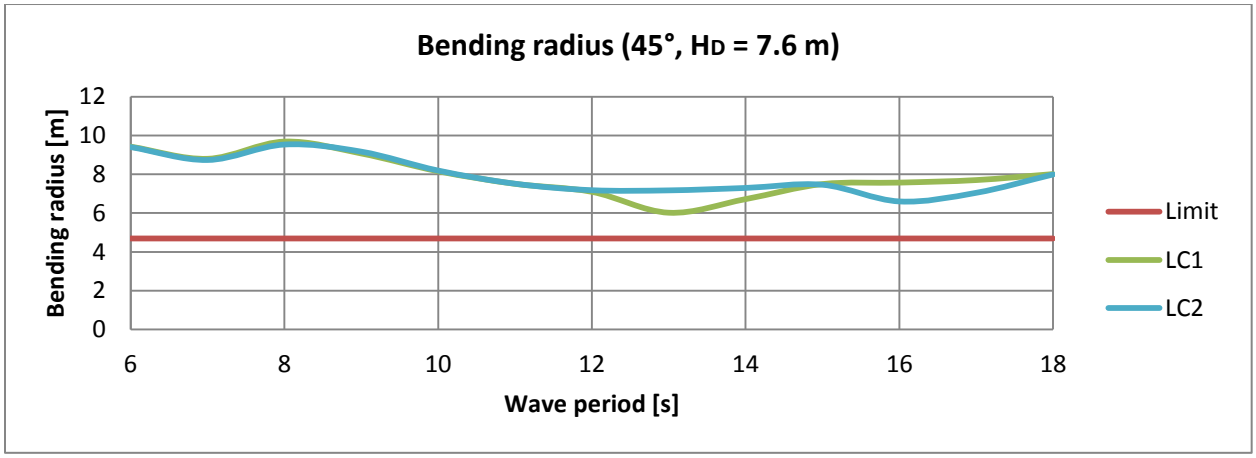

Figure C.0.50: Bending radius for flexible flowline in sag bend for LC1 and LC2, wave direction 45° and H_D = 7.6 m, MBR shown as the red line

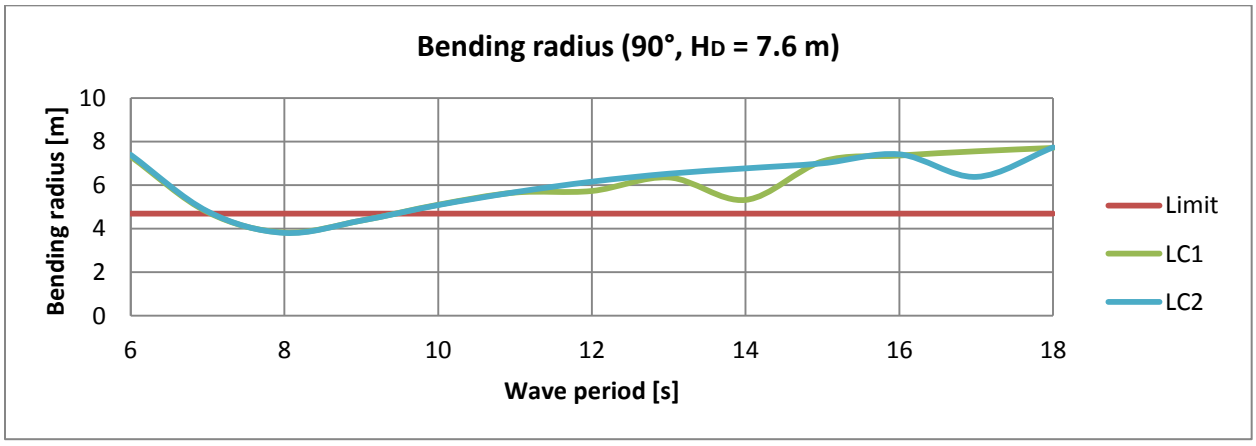

Figure C.0.51: Bending radius for flexible flowline in sag bend for LC1 and LC2, wave direction 90° and H_D = 7.6 m, MBR shown as the red line

C.25 Results for landing of helicopters in daylight for H_D = 3.8 meters

Table C.0.1: Approved (green cells) and non-approved (red cells) wave periods for landing of helicopters for LC1 with H_D = 3.8 m, based on HCA's requirements

Load Case 1, H_D = 3.8 m			
T | Wave direction -->	0°	45°	90°
6			
7			
8			
9			
10			
11			
12			
13			
14			
15			
16			
17			
18			

Table C.0.2: Approved (green cells) and non-approved (red cells) wave periods for landing of helicopters for LC2 with H_D = 3.8 m, based on HCA's requirements

Load Case 2, H_D = 3.8 m			
T | Wave direction -->	0°	45°	90°
6			
7			
8			
9			
10			
11			
12			
13			
14			
15			
16			
17			
18			

C.26 Results for landing of helicopters in daylight for H_D = 5.7 meters

Table C.0.3: Approved (green cells) and non-approved (red cells) wave periods for landing of helicopters for LC1 with H_D = 5.7 m, based on HCA's requirements

Load Case 1, H_D = 5.7 m			
T | Wave direction -->	0°	45°	90°
6			
7			
8			
9			
10			
11			
12			
13			
14			
15			
16			
17			
18			

Table C.0.4: Approved (green cells) and non-approved (red cells) wave periods for landing of helicopters for LC2 with H_D = 5.7 m, based on HCA's requirements

Load Case 2, H_D = 5.7 m			
T | Wave direction -->	0°	45°	90°
6			
7			
8			
9			
10			
11			
12			
13			
14			
15			
16			
17			
18			

C.27 Results for landing of helicopters in daylight for H_D = 7.6 meters

Table C.0.5: Approved (green cells) and non-approved (red cells) wave periods for landing of helicopters for LC1 with H_D = 7.6 m, based on HCA's requirements

Load Case 1, H_D = 7.6 m			
T | Wave direction -->	0°	45°	90°
6			
7			
8			
9			
10			
11			
12			
13			
14			
15			
16			
17			
18			

Table C.0.6: Approved (green cells) and non-approved (red cells) wave periods for landing of helicopters for LC2 with H_D = 7.6 m, based on HCA's requirements

Load Case 2, H_D = 7.6 m			
T | Wave direction -->	0°	45°	90°
6			
7			
8			
9			
10			
11			
12			
13			
14			
15			
16			
17			
18			

C.28 Results for heave rate of helideck for H_D = 3.8 meters

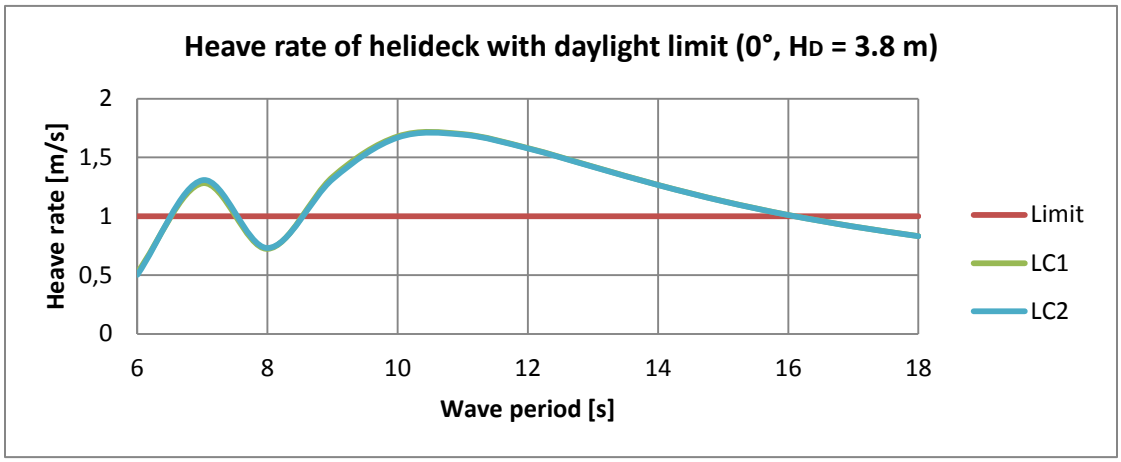

Figure C.0.52: Heave rate of helideck with the daylight limit, for LC1 and LC2, wave direction 0° and H_D = 3.8 m

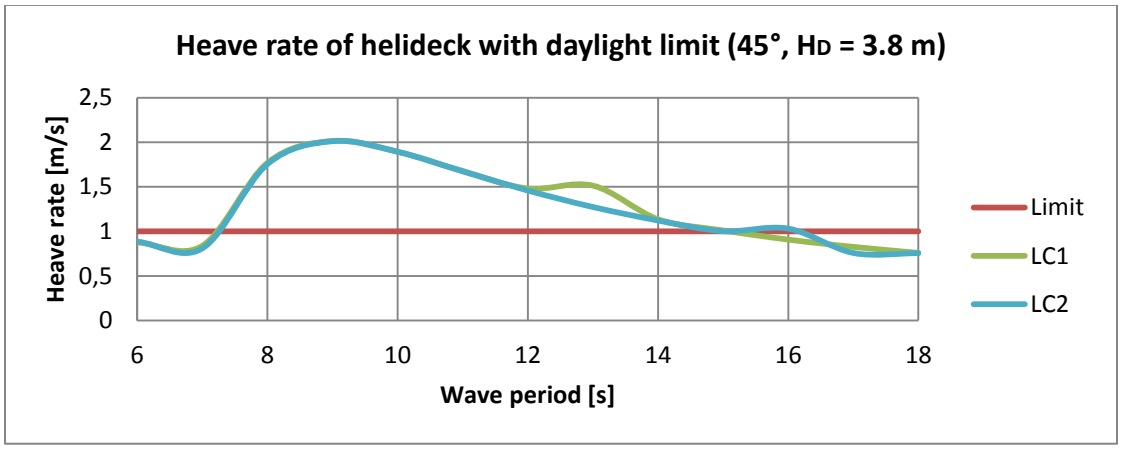

Figure C.0.53: Heave rate of helideck with the daylight limit, for LC1 and LC2, wave direction 45° and H_D = 3.8 m

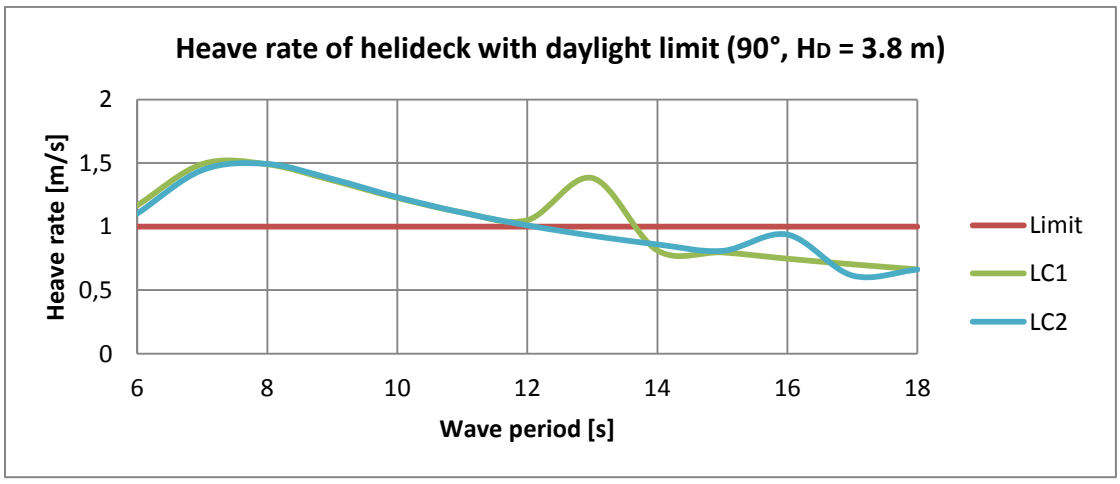

Figure C.0.54: Heave rate of helideck with the daylight limit, for LC1 and LC2, wave direction 90° and H_D = 3.8 m

C.29 Results for heave rate of helideck for H_D = 5.7 meters

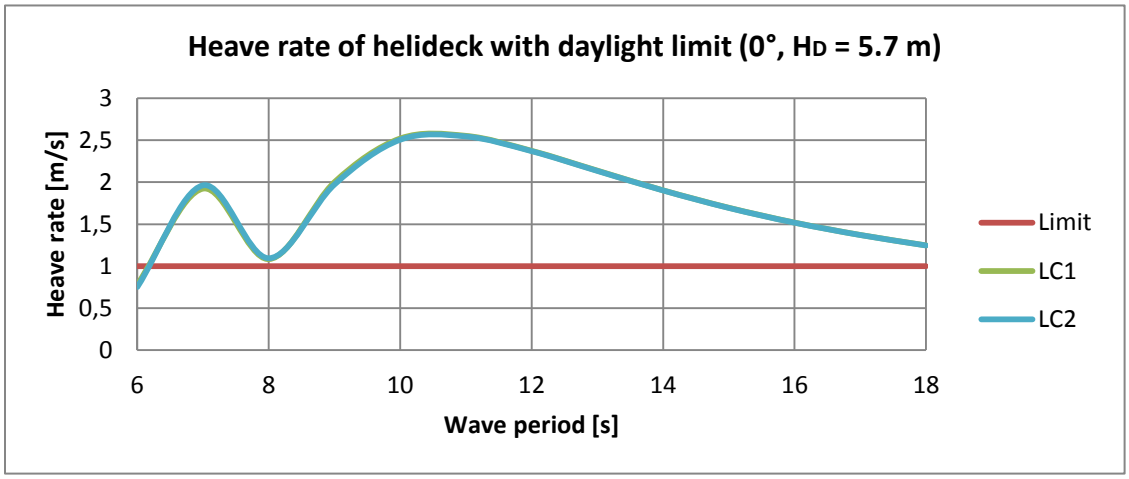

Figure C.0.55: Heave rate of helideck with the daylight limit, for LC1 and LC2, wave direction 0° and H_D = 5.7 m

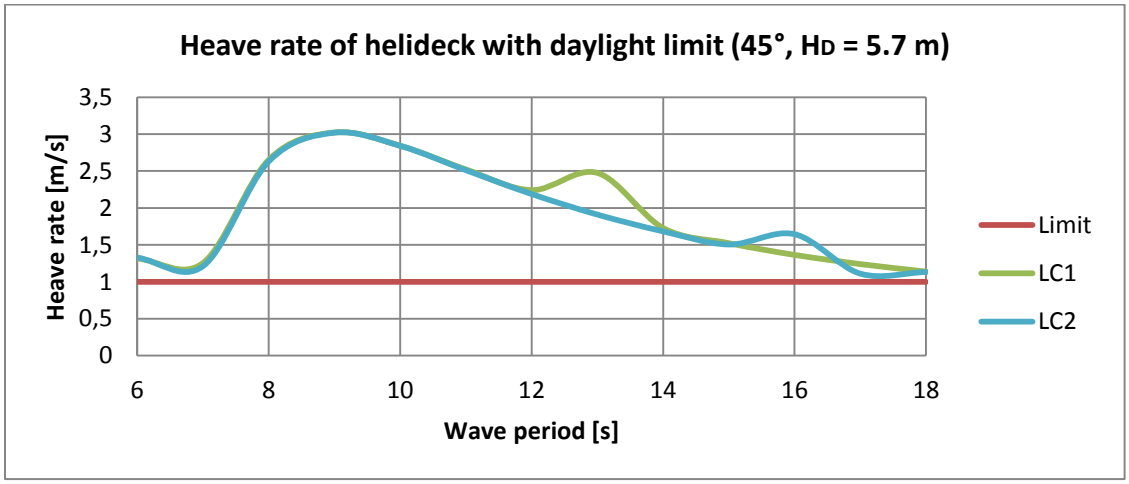

Figure C.0.56: Heave rate of helideck with the daylight limit, for LC1 and LC2, wave direction 45° and H_D = 5.7 m

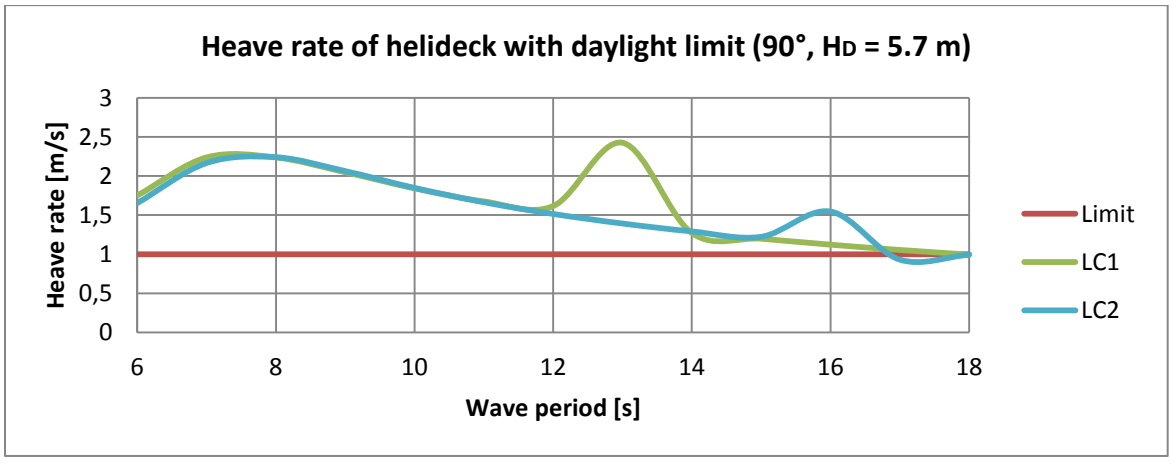

Figure C.0.57: Heave rate of helideck with the daylight limit, for LC1 and LC2, wave direction 90° and H_D = 5.7 m

C.30 Results for heave rate of helideck for H_D = 7.6 meters

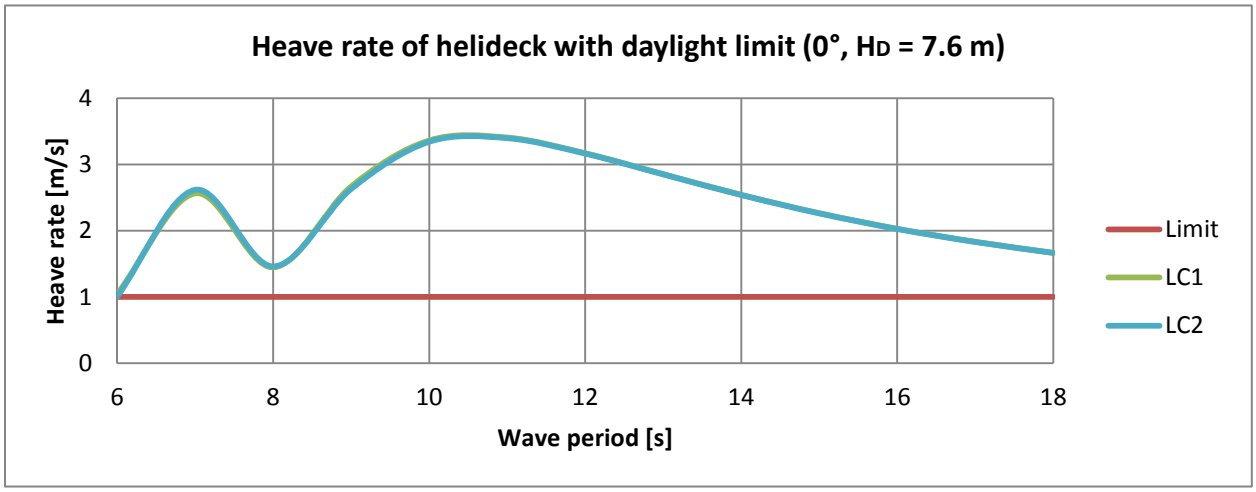

Figure C.0.58: Heave rate of helideck with the daylight limit, for LC1 and LC2, wave direction 0° and H_D = 7.6 m

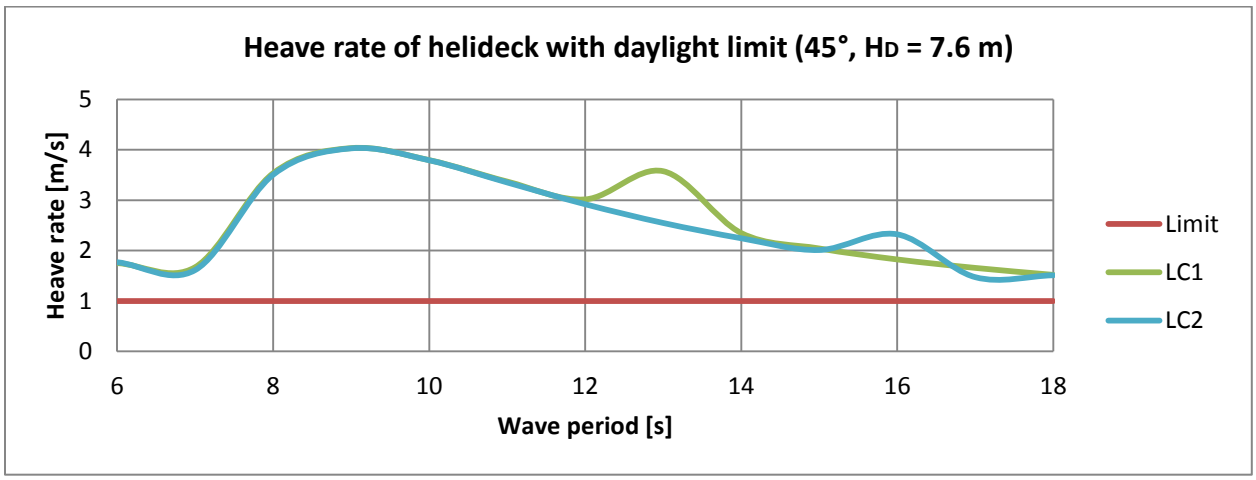

Figure C.0.59: Heave rate of helideck with the daylight limit, for LC1 and LC2, wave direction 45° and H_D = 7.6 m

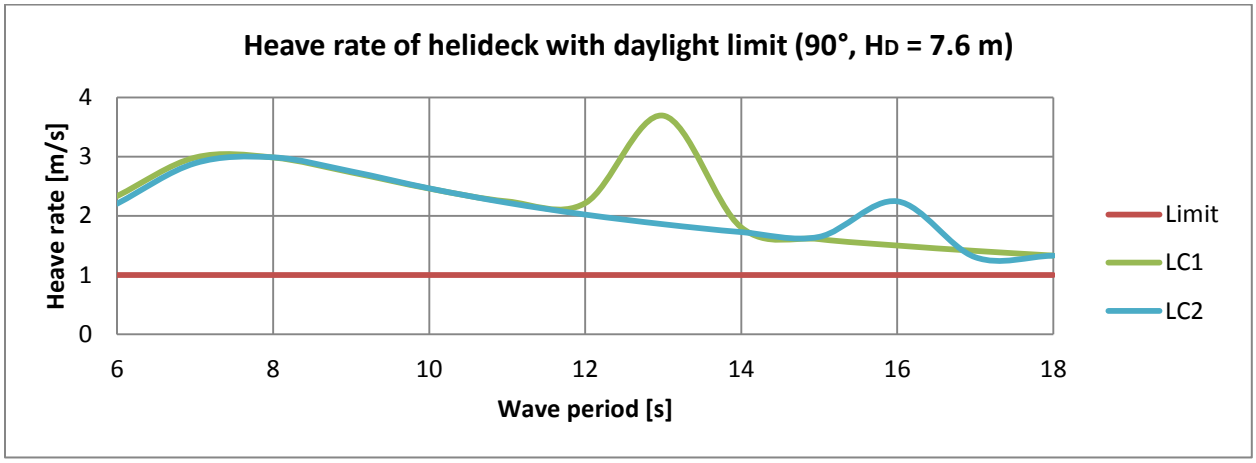

Figure C.0.60: Heave rate of helideck with the daylight limit, for LC1 and LC2, wave direction 90° and H_D = 7.6 m

Appendix D: Helideck monitoring system

The Helideck Monitoring System (HMS) gets input from the MRUs on the vessel to produce helideck motion and weather reports for the helicopters. High grade accelerometers and several gyros do the measurements. The data from the MRUs are processed by the Differential Positioning Sensor (DPS), which also feeds the DP system with data.

The MRUs are specifically designed to measure the roll, pitch, heave and yaw motions. The MRU on the helideck normally measures in the centre of the helideck (Kongsberg Maritime AS, 2013).

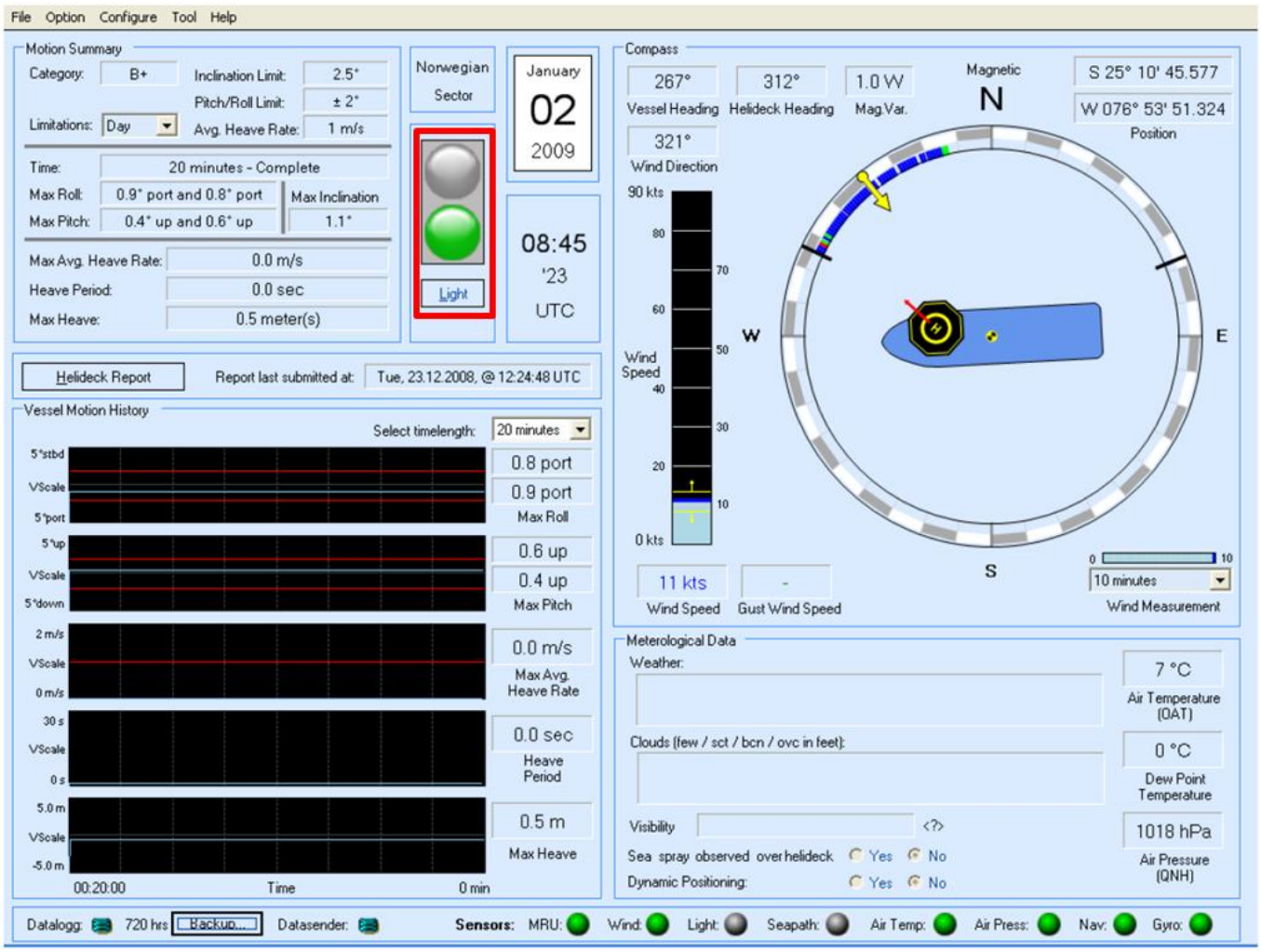

Figure D.0.1: Example of a Helideck Monitoring System on-board a vessel, red square shows if it is red or green light with respect to complying with helideck landing criteria (HCA, Bristow Group, Bond Offshore and CHC, 2010)

The red rectangle in Figure D.0.1 indicates the light which shows if one is complying with helideck landing criteria (ref. chapter 8.5). Green light indicates that the conditions have been steady for at least 20 minutes. The various criteria for landing on the helideck are stated up in the top left corner.

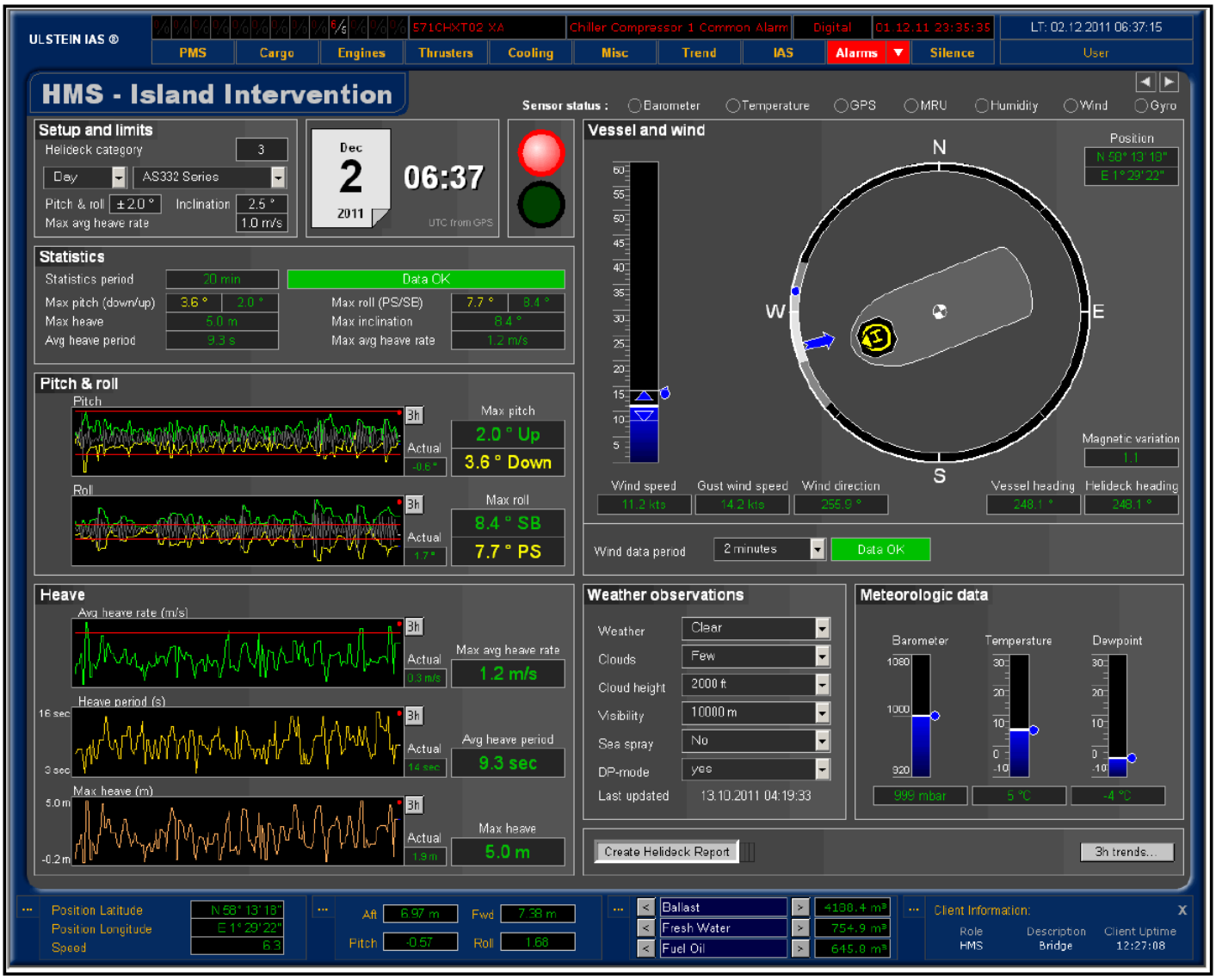

Figure D.0.2: Another example on a HMS, from the vessel Island Intervention (The bridge of Island Intervention, 2011)

From the HMS in Figure D.0.2 one could observe that the light is red which means that the conditions are not satisfying with respect to landing within the helideck criteria from HCA (ref. chapter 8.5). For example is the heave rate limit of 1.0 m/s breached as the maximum average heave rate logged is 1.2 m/s. The same goes for the roll and pitch with a limit of ±2°, but the observations are far above this limit.

The criteria shown in Figures D.0.1 and D.0.2 are for landing in daylight on a helideck with the same certification category as that of Normand Vision (ref. Table 8.4).

Appendix E: New RAOs' loading conditions (Load Case 3 and 4)

These Load Cases are here not presented in the same level of detail as LC1 and LC2, but contain sufficient information for the analysis. Also these new Load Cases have almost full fuel tanks.

E.1: Load Case 3 - Moderately light flexible lay

The total weight of all loads for LC3 is 4711.0 tonnes. So with this deadweight the total displacement of the vessel is ≈ 18131.0 tonnes (as the lightship weight now is adjusted to 13420.0 tonnes, which should be more precise). The calculated value from VERES is however 18760.35 tonnes which is what the RAOs are based on, and is therefore the value that will be used in OrcaFlex. GM = 2.44 meters.

A rough hand calculation, using displacement = 18760.35 tonnes, shows a total displacement volume of ≈ 18303 m^3 due to Archimedes' principle. This loading gives the vessel a mean draught of 6.953 meters with a corresponding estimated freeboard of about 5 meters. For information about the total Centres of Gravity for this Load Case, the reader is referred to Table E.0.5.

Table E.0.1: Overview of liquid loads for Load Case 3 (VARD, 2014)

Liquid loads for Load Case 3	Load value (in tonnes)
Fuel oil (density 850 kg/m^3)	842.4
Fresh water (density 1000 kg/m^3)	294.3
Miscellaneous (lubrication, drain and thruster oil, sewage etc., density 1025 kg/m^3)	326.5
Water ballast (density 1025 kg/m^3)	2487.8
Total liquid loads	*3951.0*

Table E.0.2: Overview of dry loads for Load Case 3 (VARD, 2014)

Dry loads for Load Case 3	Load value (in tonnes)
Crew and stores	100.0
Miscellaneous 1	40.0
Miscellaneous 2	215.0
Pull-down load	80.0
Reel	325.0
Total dry loads	*760.0*

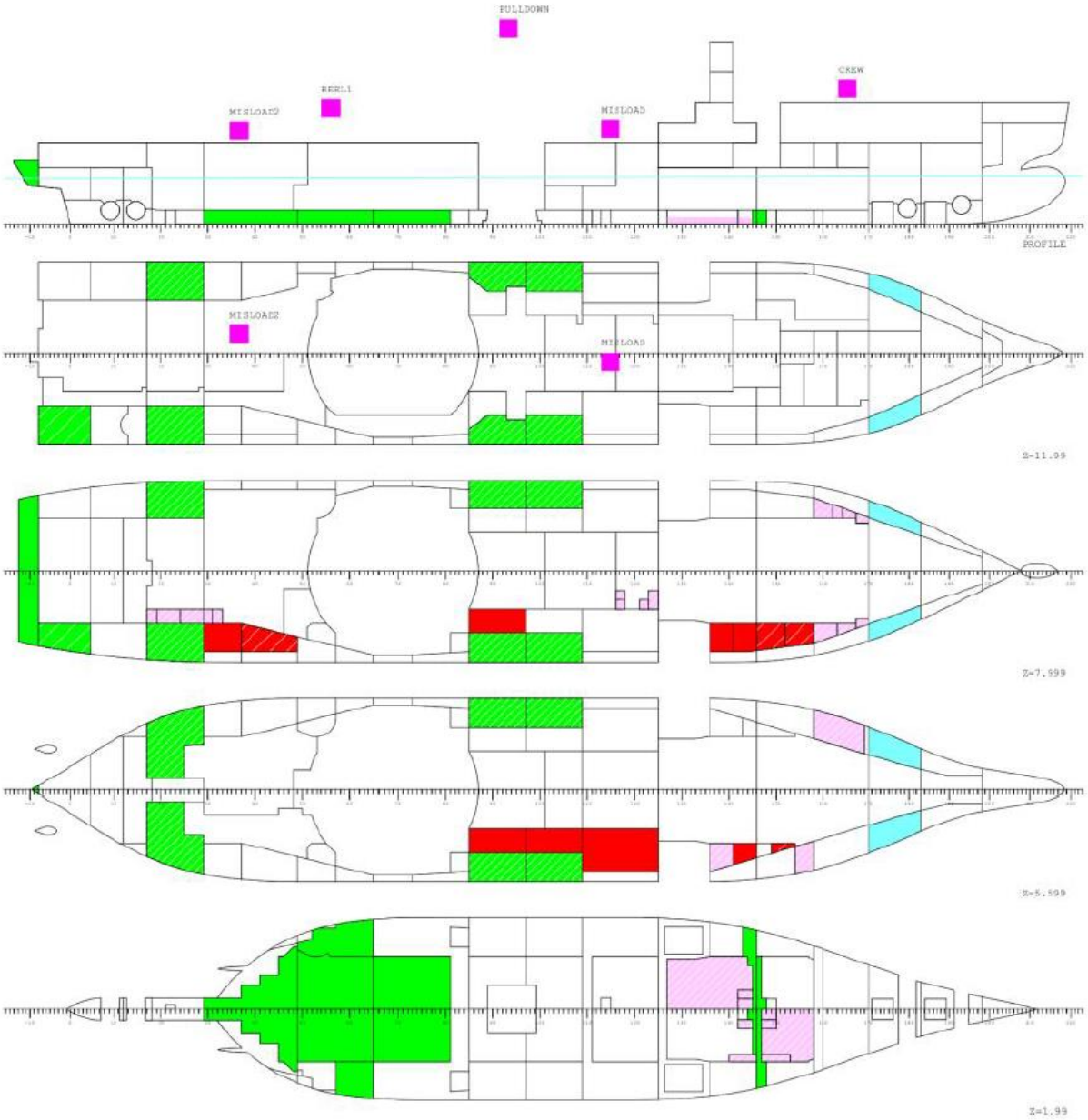

Figure E.0.1: General overview over the load locations on Normand Vision for Load Case 3 (VARD, 2014)

E.2: Load Case 4 – Moderately heavy flexible lay

The total weight of all loads for LC3 is 7844.7 tonnes. So with this deadweight the total displacement of the vessel is ≈ 21264.7 tonnes (as the lightship weight now is adjusted to 13420.0 tonnes, which should be more precise). The calculated value from VERES is however 21983.33 tonnes which is what the RAOs are based on, and is therefore the value that will be used in OrcaFlex. GM = 2.35 meters.

A rough hand calculation, using displacement = 21983.33 tonnes, shows a total displacement volume of ≈ 21447 m^3 due to Archimedes' principle. This loading gives the vessel a mean draught of 7.867 meters with a corresponding estimated freeboard of about 4.1 meters. For information about the total Centres of Gravity for this Load Case, the reader is referred to Table E.0.5.

Table E.0.3: Overview of liquid loads for Load Case 4 (VARD, 2014)

Liquid loads for Load Case 4	Load value (in tonnes)
Fuel oil (density 850 kg/m^3)	842.4
Fresh water (density 1000 kg/m^3)	294.3
Miscellaneous (lubrication, drain and thruster oil, sewage etc., density 1025 kg/m^3)	326.5
Water ballast (density 1025 kg/m^3)	2166.5
Total liquid loads	*3629.7*

Table E.0.4: Overview of dry loads for Load Case 4 (VARD, 2014)

Dry loads for Load Case 4	Load value (in tonnes)
Crew and stores	100.0
Crane	300.0
Miscellaneous 1	40.0
Miscellaneous 2	320.0
Product	2400.0
Pull-down load	80.0
Reel 1	325.0
Reel 2	325.0
Reel 3	325.0
Total dry loads	*4215.0*

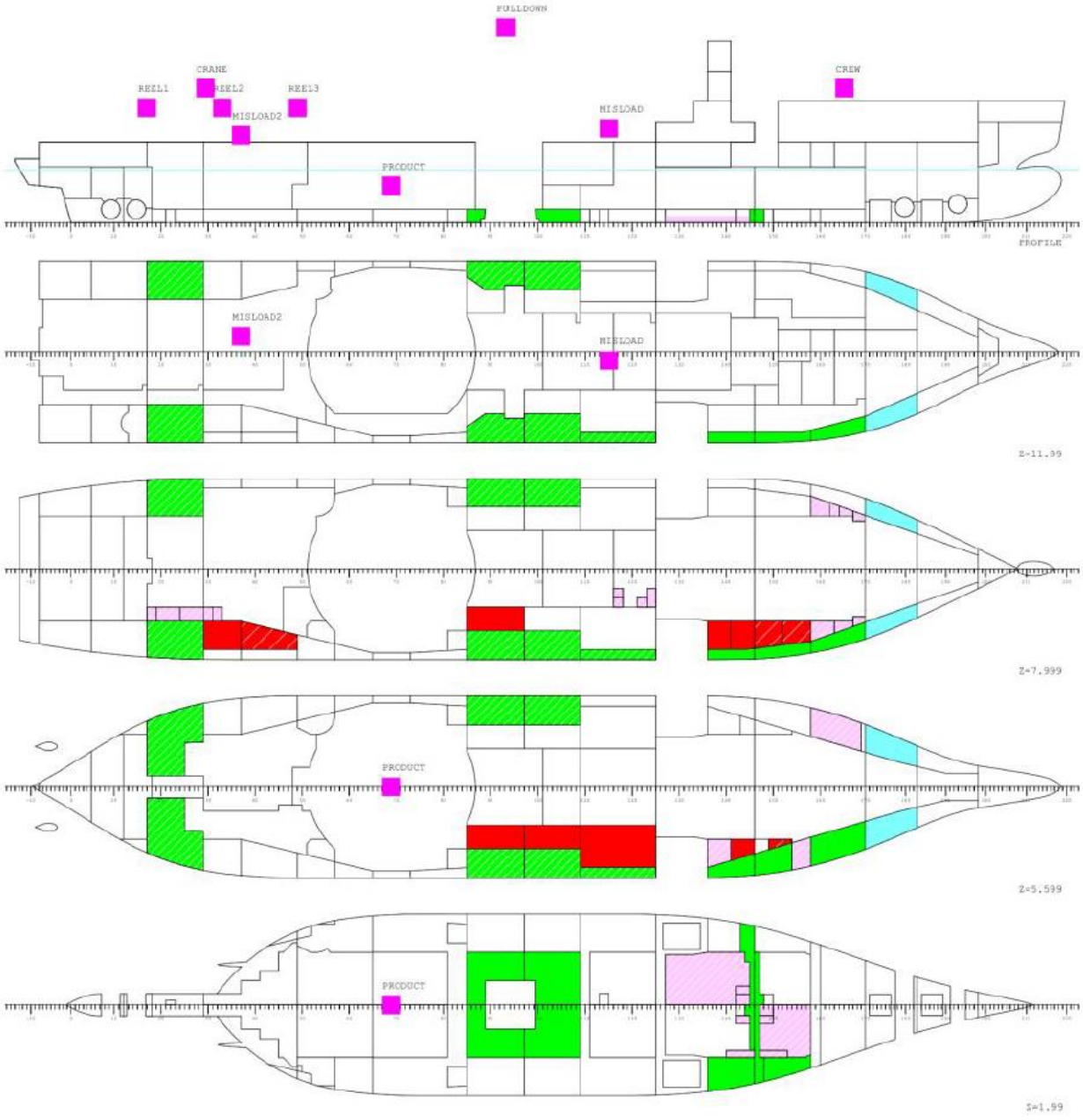

Figure E.0.2: General overview over the load locations on Normand Vision for Load Case 4 (VARD, 2014)

E.3: Adjustment for point of motion

Also for these Load Cases the point of motion must be adjusted as the longitudinal CoG is defined from the zero-frame (ref. Fig. 3.17).
The moonpool center is located at a distance of about 65.2 meters from the "zero-frame".
For convenience the vessel's local coordinate system was chosen to be in the center of the moonpool in the layout model, as shown in sub-chapter 3.8. So then the longitudinal CoG has to be specified from this origin instead, which give a "new/corrected" longitudinal CoG presented in Table E.0.5.

Table E.0.5: Overview over the different CoG and CoB calculated in VERES, "new" longitudinal CoG, as well as the draught and displacement for the two new Load Cases (VARD, 2014)

	CoG, Load Case 3	CoB, Load Case 3	CoG, Load Case 4	CoB, Load Case 4
Longitudinal [m]	69.422	69.422	67.938	67.938
"New" longitudinal [m]	4.222*	N/A	2.738*	N/A
Transverse [m]	0.000*	0.000	0.000*	0.000
Vertical [m]	10.880*	3.814	10.740*	4.338
Mean draught [m]	6.953*		7.867*	
Displacement [tonnes]	18760.35*		21983.33*	

*Used as input in the OrcaFlex model of the vessel

E.4: Roll, heave and pitch RAO graphs for LC3 and LC4

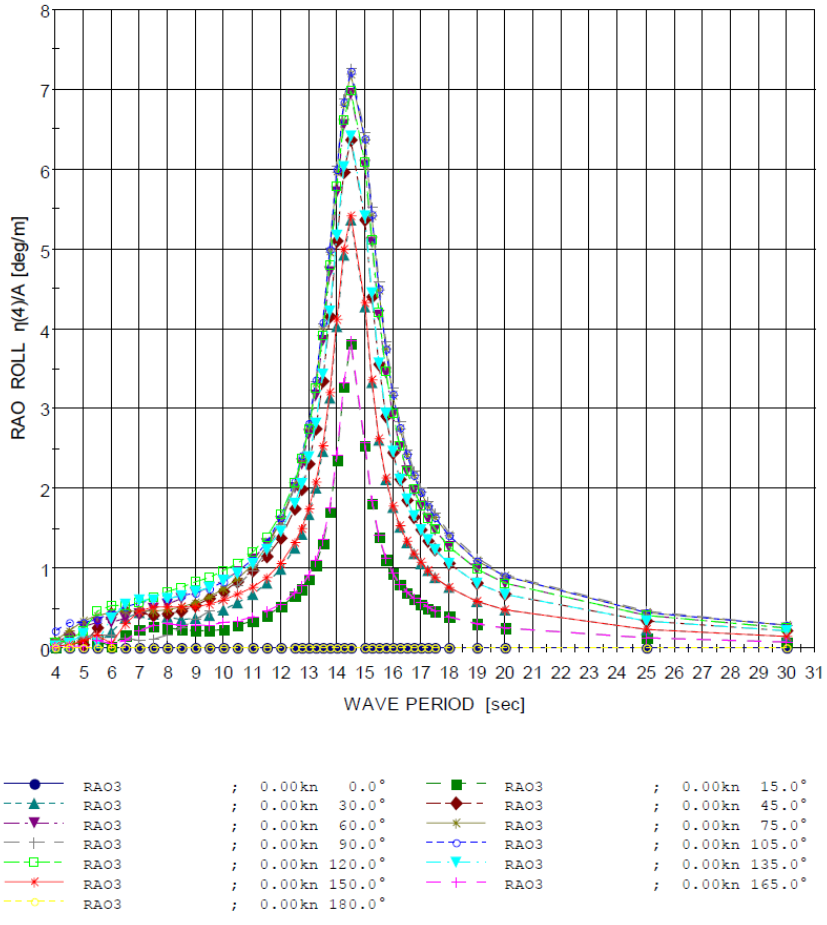

Figure F.0.3: Displacement RAOs for roll motion (LC3) for a range of different wave periods. Wave headings from 0° to 180° with 15° intervals. Based on VERES simulations of Normand Vision (VARD, 2014)

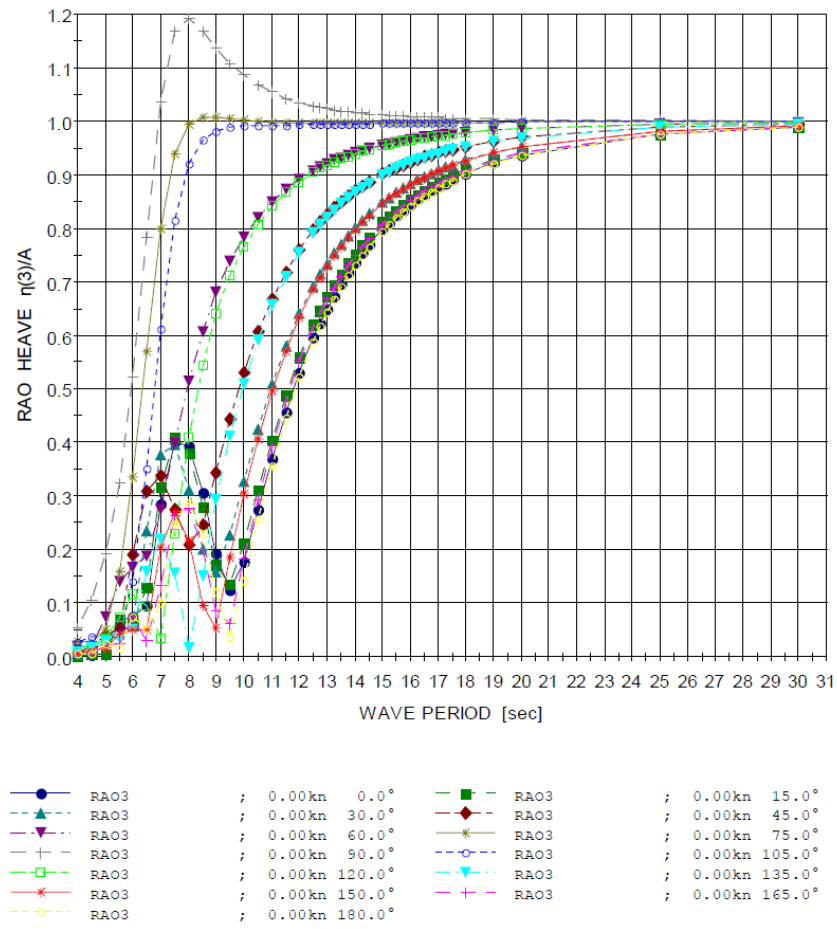

Figure F.0.4: Displacement RAOs for heave motion (LC3) for a range of different wave periods. Wave headings from 0° to 180° with 15° intervals. Based on VERES simulations of Normand Vision (VARD, 2014)

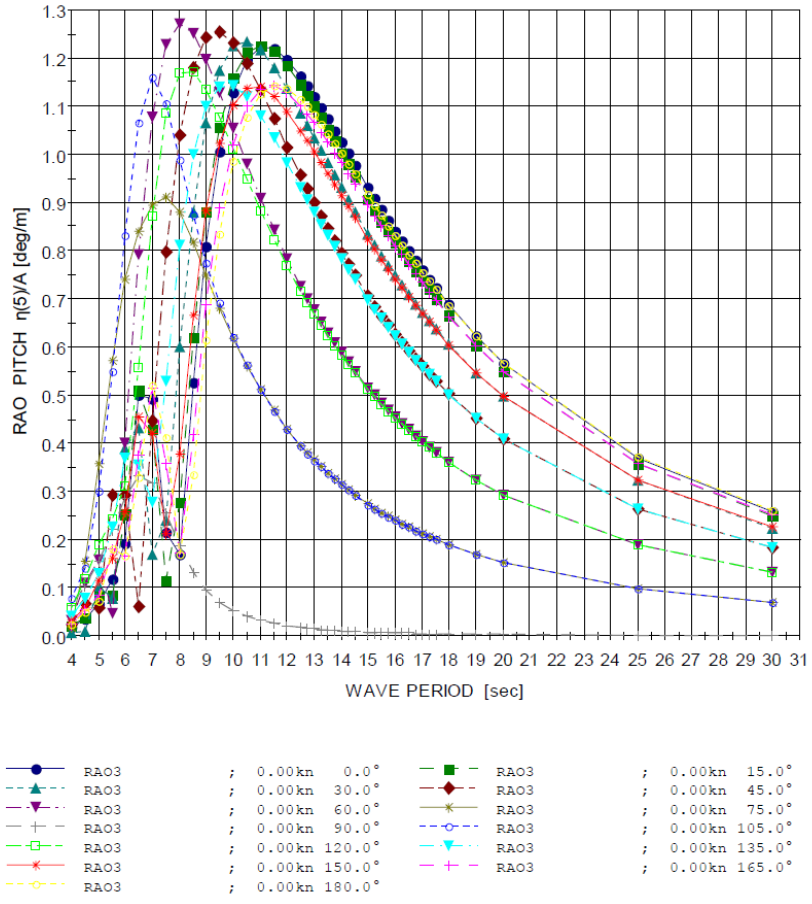

Figure F.0.5: Displacement RAOs for pitch motion (LC3) for a range of different wave periods. Wave headings from 0° to 180° with 15° intervals. Based on VERES simulations of Normand Vision (VARD, 2014)

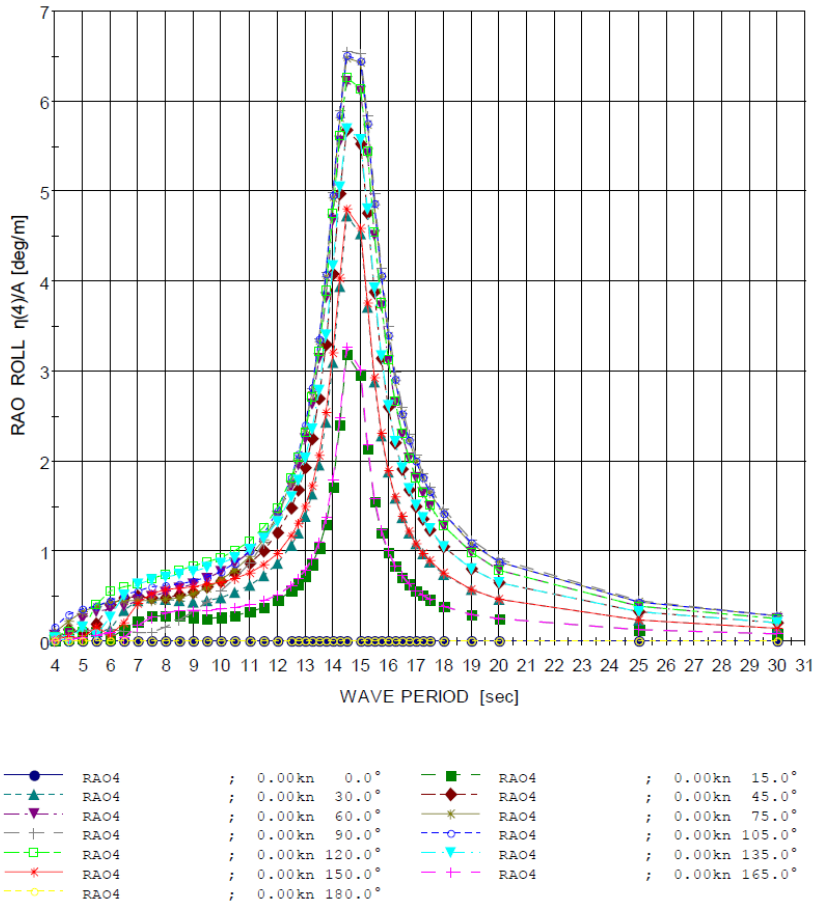

Figure F.0.6: Displacement RAOs for roll motion (LC4) for a range of different wave periods. Wave headings from 0° to 180° with 15° intervals. Based on VERES simulations of Normand Vision (VARD, 2014)

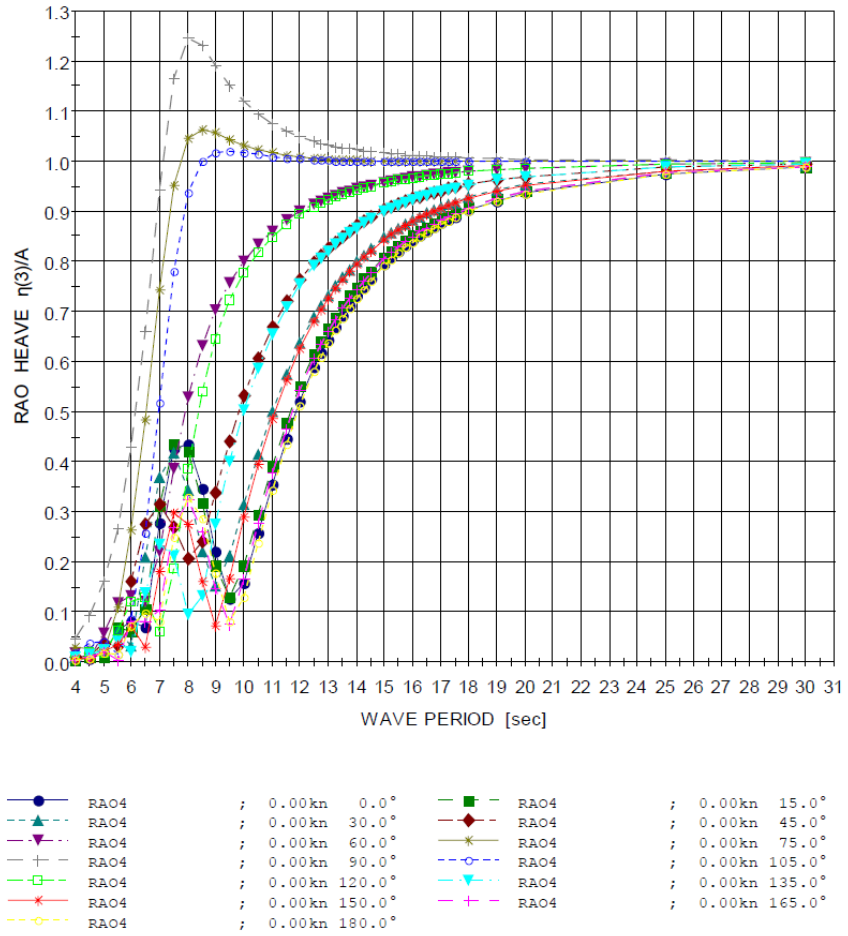

Figure F.0.7: Displacement RAOs for heave motion (LC4) for a range of different wave periods. Wave headings from 0° to 180° with 15° intervals. Based on VERES simulations of Normand Vision (VARD, 2014)

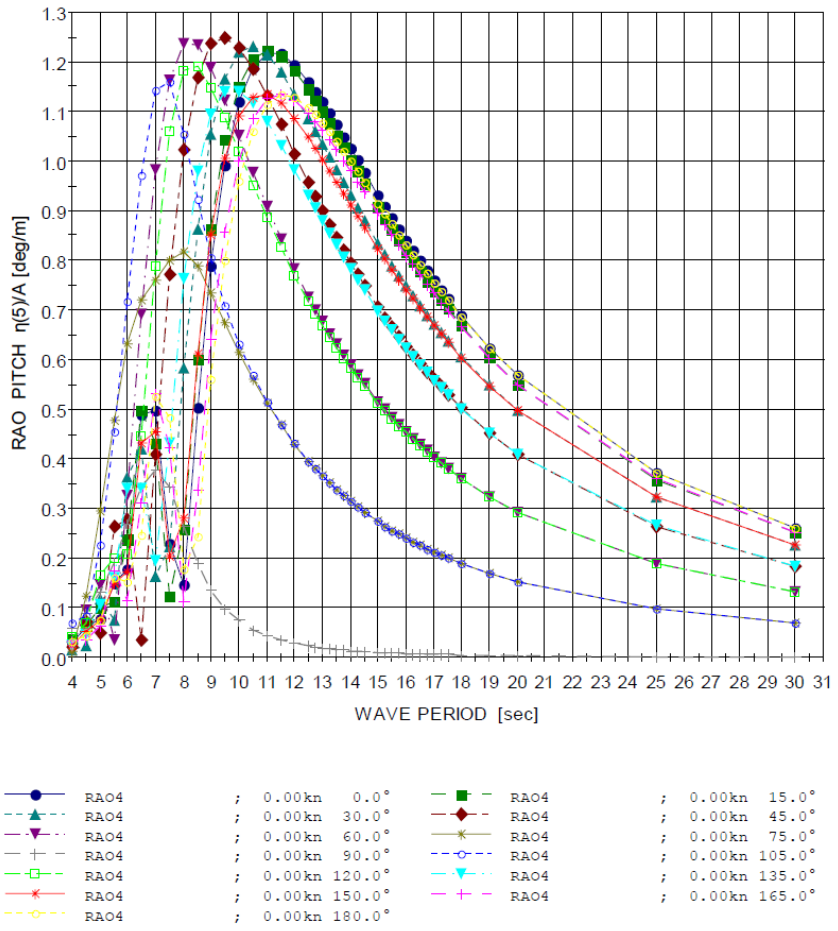

Figure F.0.8: Displacement RAOs for pitch motion (LC4) for a range of different wave periods. Wave headings from 0° to 180° with 15° intervals. Based on VERES simulations of Normand Vision (VARD, 2014)

Appendix F: Results of spot checking of parameters with all Load Cases for H_D = 5.7 meters

The results are presented in the same order as listed in sub-chapter 8.6.

F.1 Comparison of heave acceleration on main deck

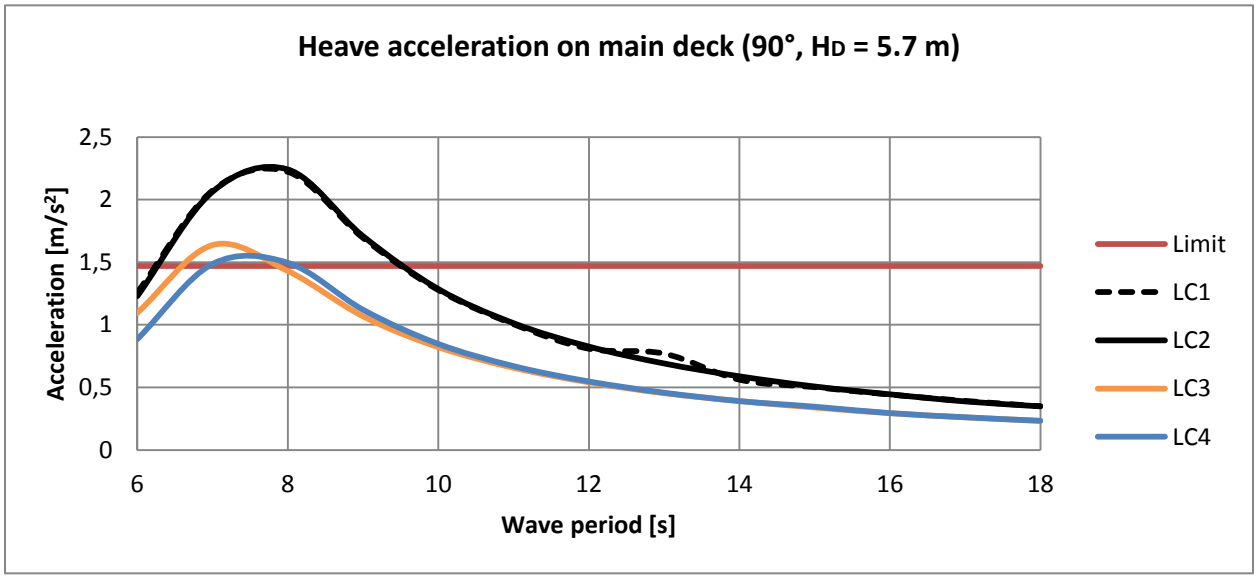

Figure F.0.1: Heave accelerations on main deck for all Load Cases, wave direction 90° and H_D = 5.7 m

F.2 Comparison of lateral acceleration on main deck

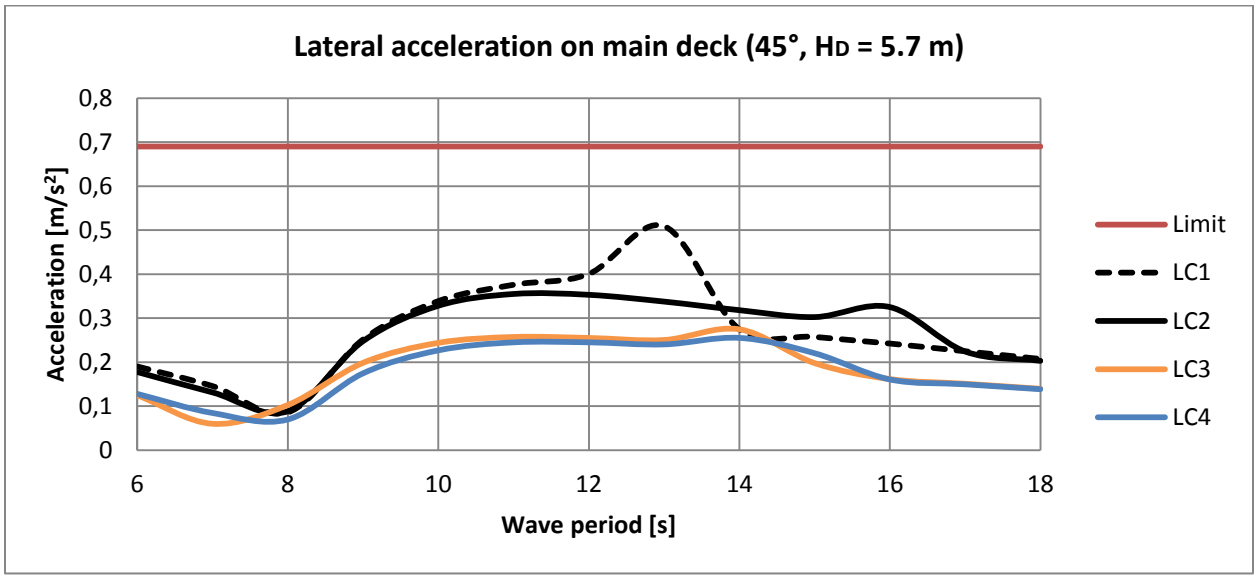

Figure F.0.2: Lateral accelerations on main deck for all Load Cases, wave direction 45° and H_D = 5.7 m

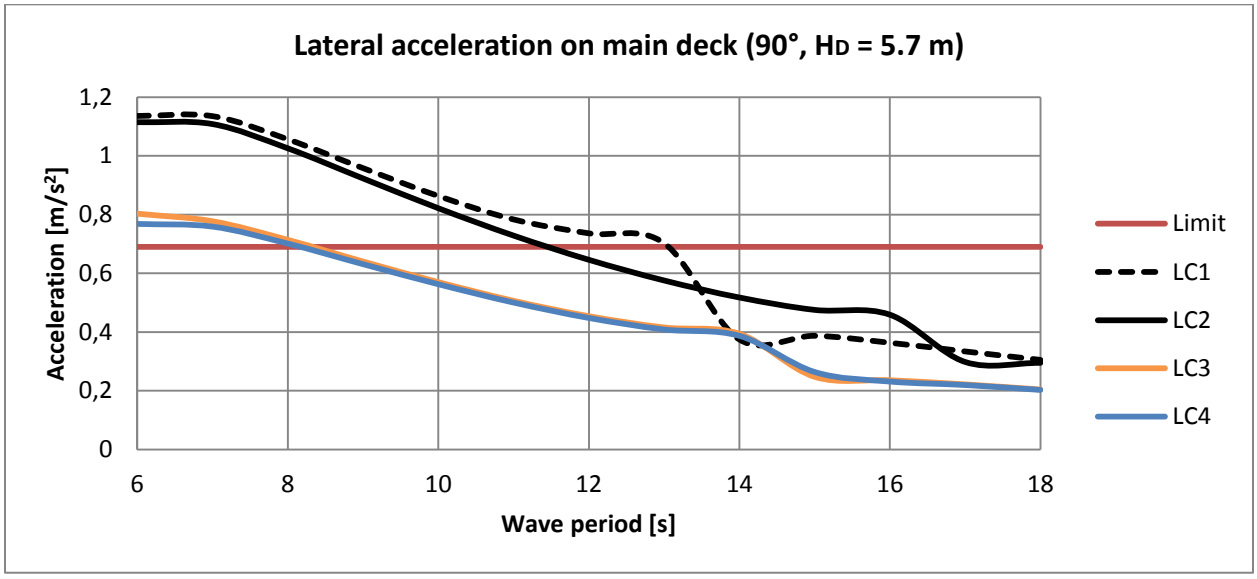

Figure F.0.3: Lateral accelerations on main deck for all Load Cases, wave direction 90° and H_D = 5.7 m

F.3 Comparison of roll rotation

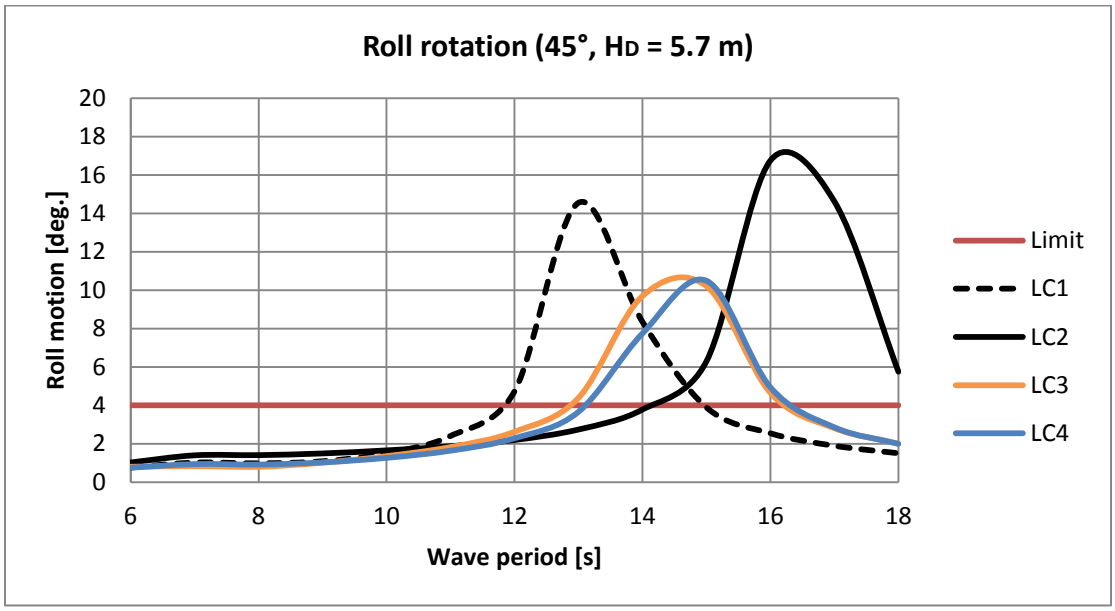

Figure F.0.4: Roll displacement for all Load Cases, wave direction 45° and H_D = 5.7 m

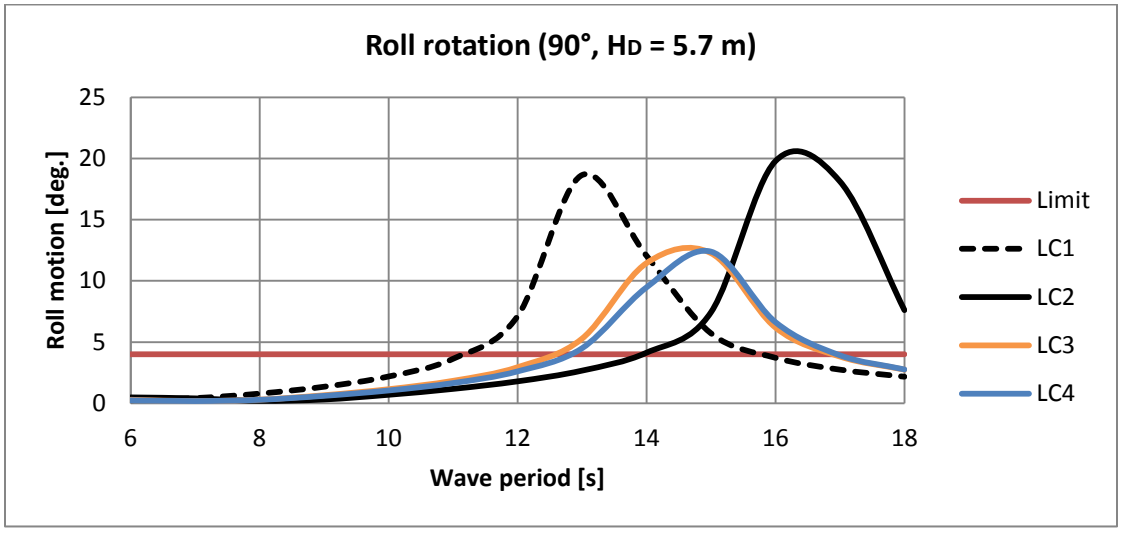

Figure F.0.5: Roll displacement for all Load Cases, wave direction 90° and H_D = 5.7 m

F.4 Comparison of pitch rotation

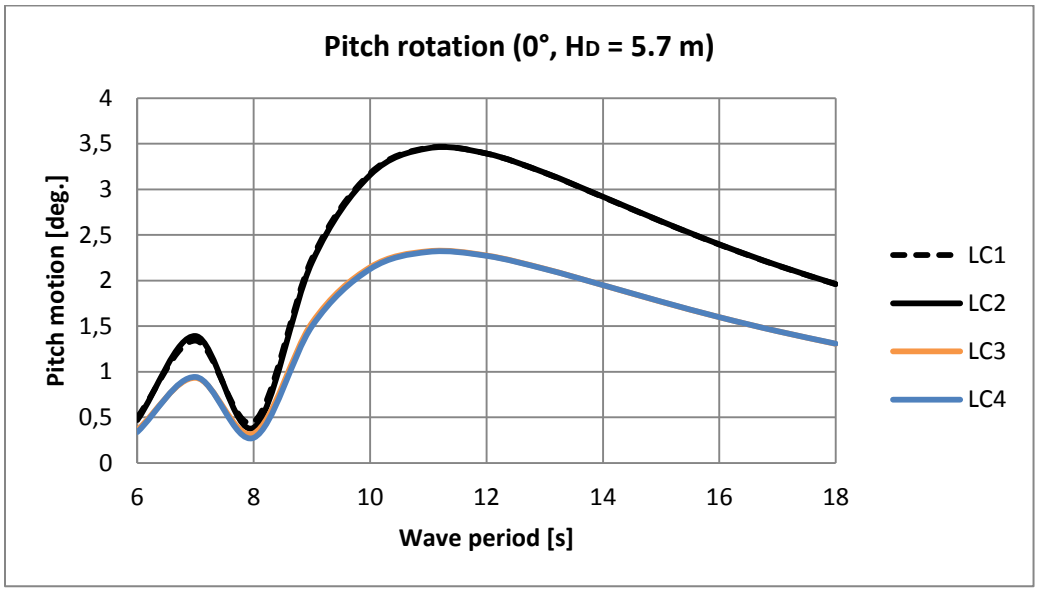

Figure F.0.6: Pitch motion of the vessel for all Load Cases, wave direction 0° and H_D = 5.7 m

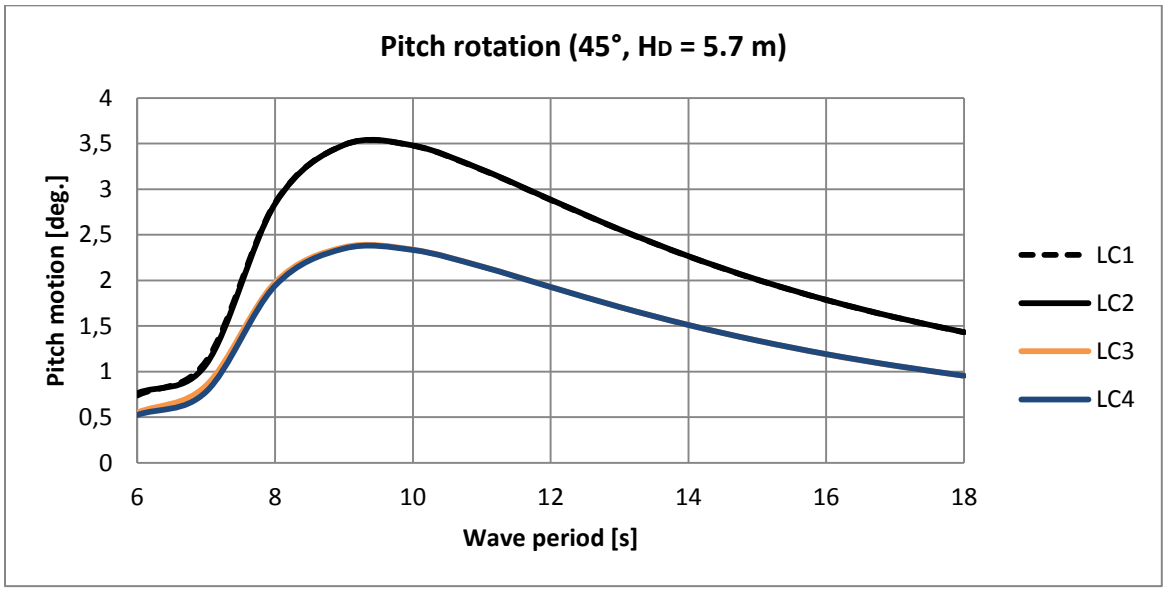

Figure F.0.7: Pitch motion of the vessel for all Load Cases, wave direction 45° and H_D = 5.7 m

F.5 Comparison of top tension

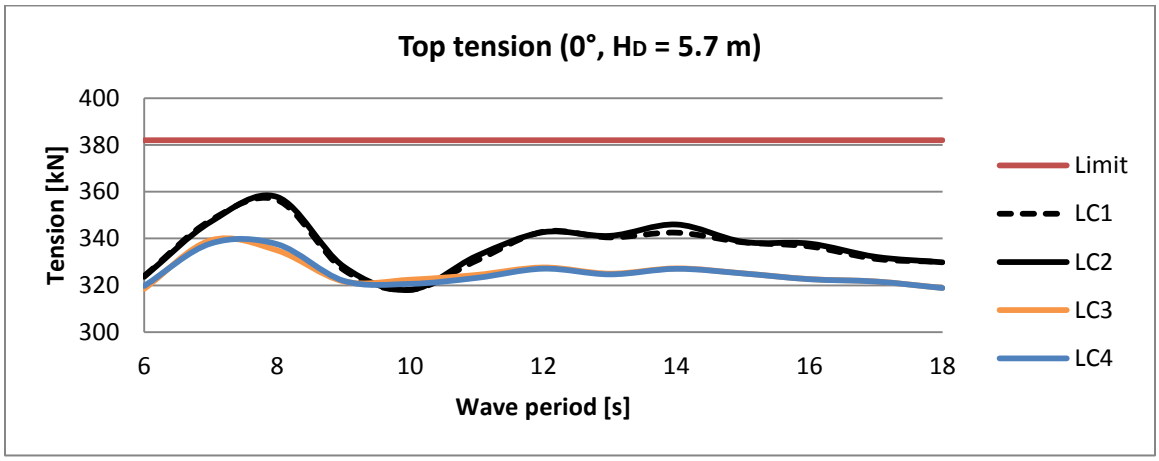

Figure F.0.8: Top tension in flexible flowline for all Load Cases, wave direction 0° and H_D = 5.7 m

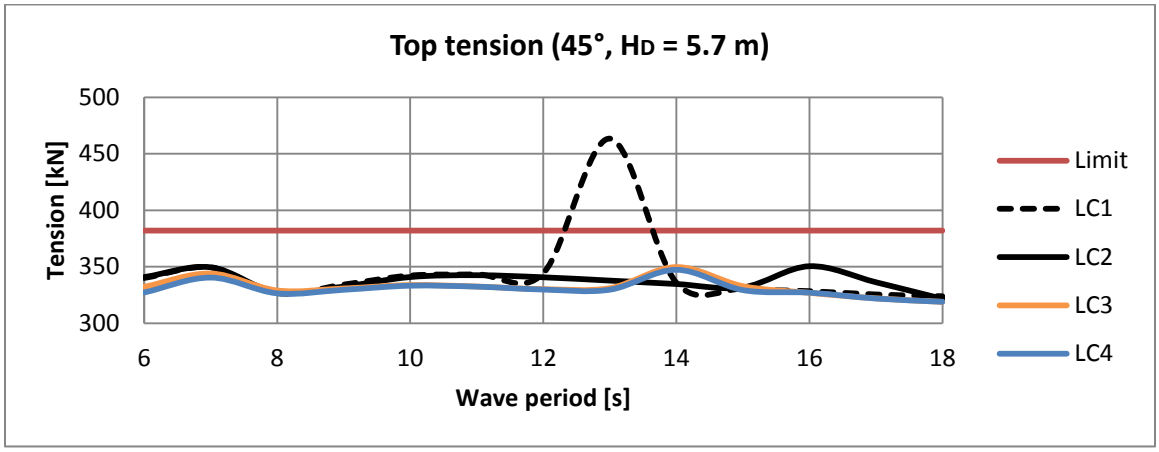

Figure F.0.9: Top tension in flexible flowline for all Load Cases, wave direction 45° and H_D = 5.7 m

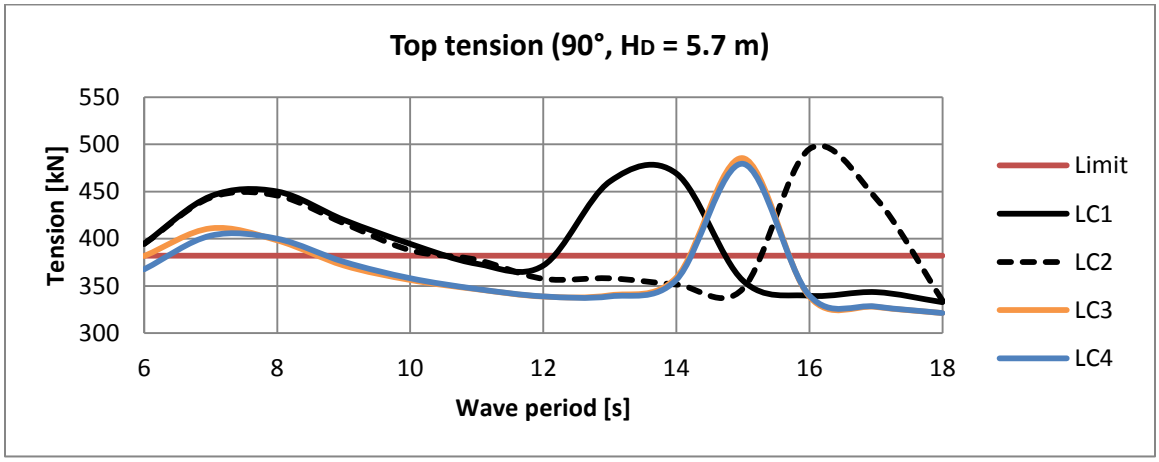

Figure F.0.10: Top tension in flexible flowline for all Load Cases, wave direction 90° and H_D = 5.7 m

F.6 Comparison of the pipe's angle with the vertical

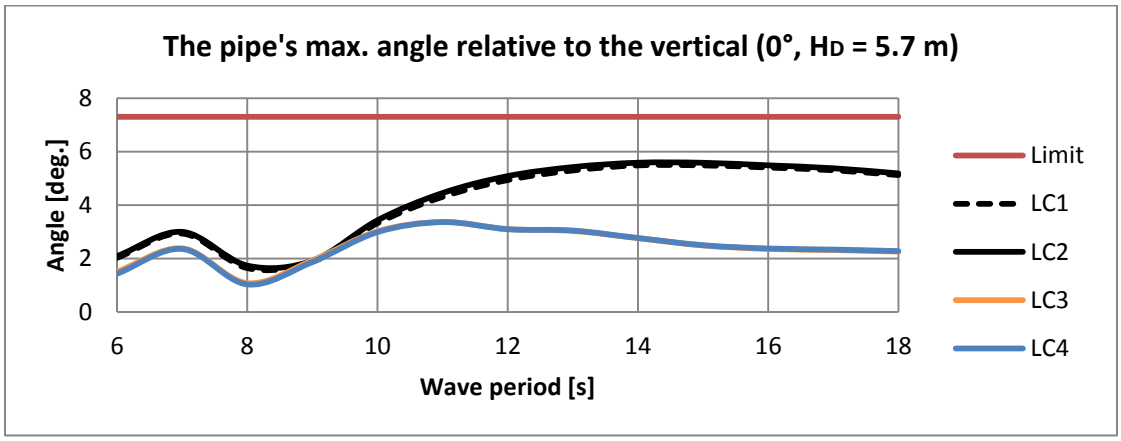

Figure F.0.11: Maximum deflection angle of the flexible flowline from the vertical when going through the moonpool for all Load Cases, wave direction 0° and H_D = 5.7 m

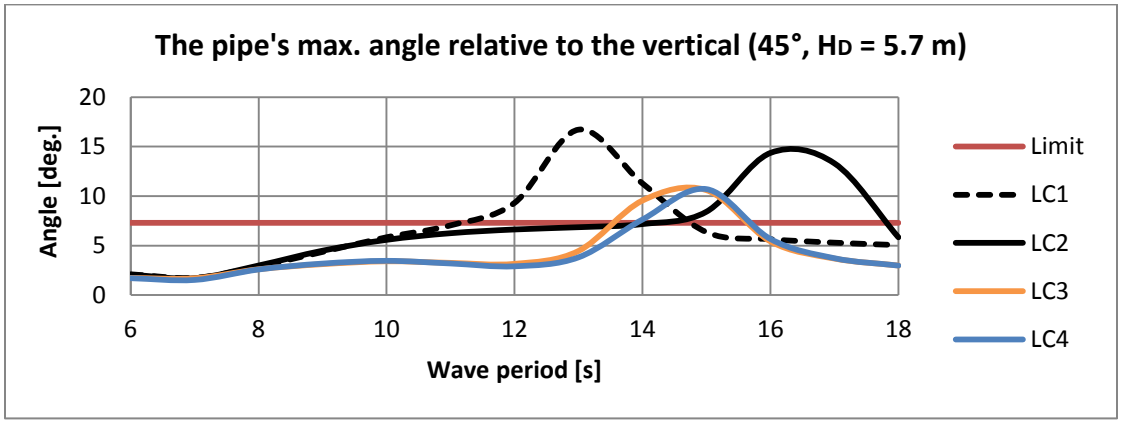

Figure F.0.12: Maximum deflection angle of the flexible flowline from the vertical when going through the moonpool for all Load Cases, wave direction 45° and H_D = 5.7 m

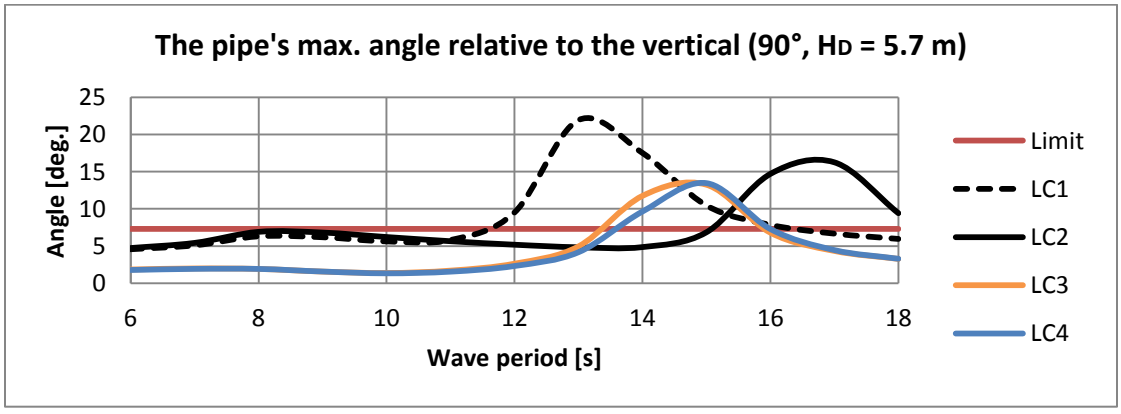

Figure F.0.13: Maximum deflection angle of the flexible flowline from the vertical when going through the moonpool for all Load Cases, wave direction 90° and H_D = 5.7 m

F.7 Comparison of the compression in the sag bend

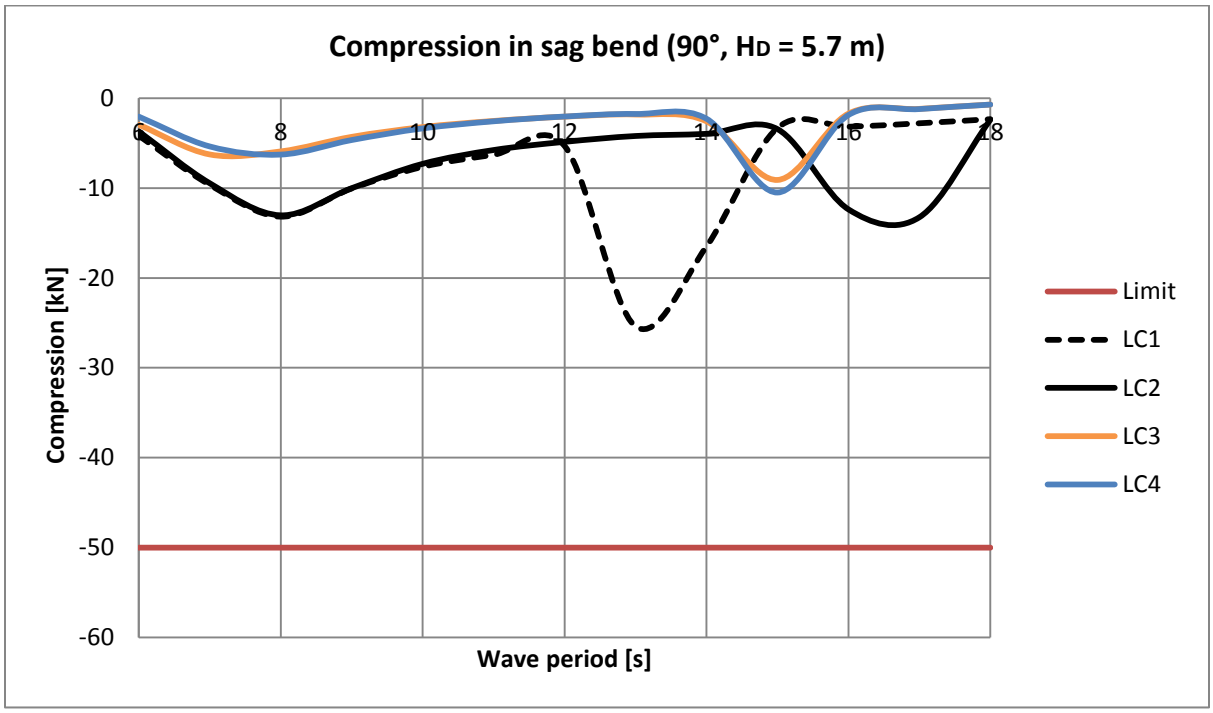

Figure F.0.14: Compression in the sag bend for all Load Cases, wave direction 90° and H_D = 5.7 m

F.8 Comparison of the bending radius in the sag bend

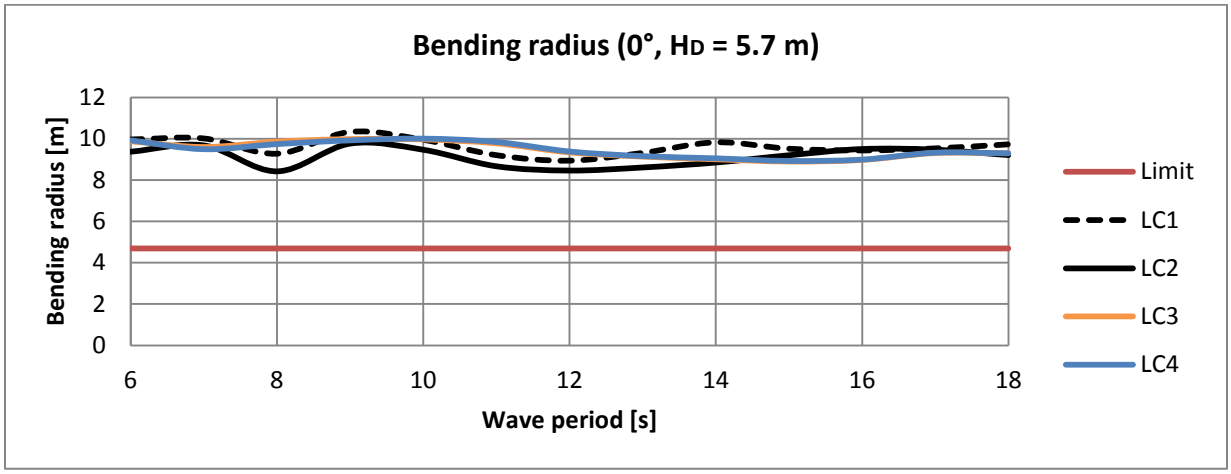

Figure F.0.15: Bending radius for flexible flowline in sag bend for all Load Cases, wave direction 0° and H_D = 5.7 m, MBR shown as the red line

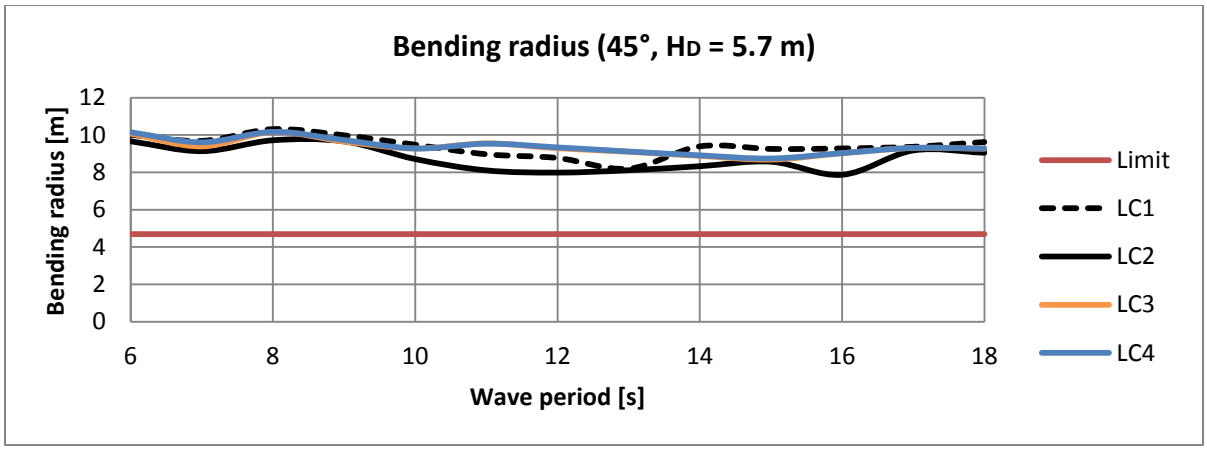

Figure F.0.16: Bending radius for flexible flowline in sag bend for all Load Cases, wave direction 45° and H_D = 5.7 m, MBR shown as the red line

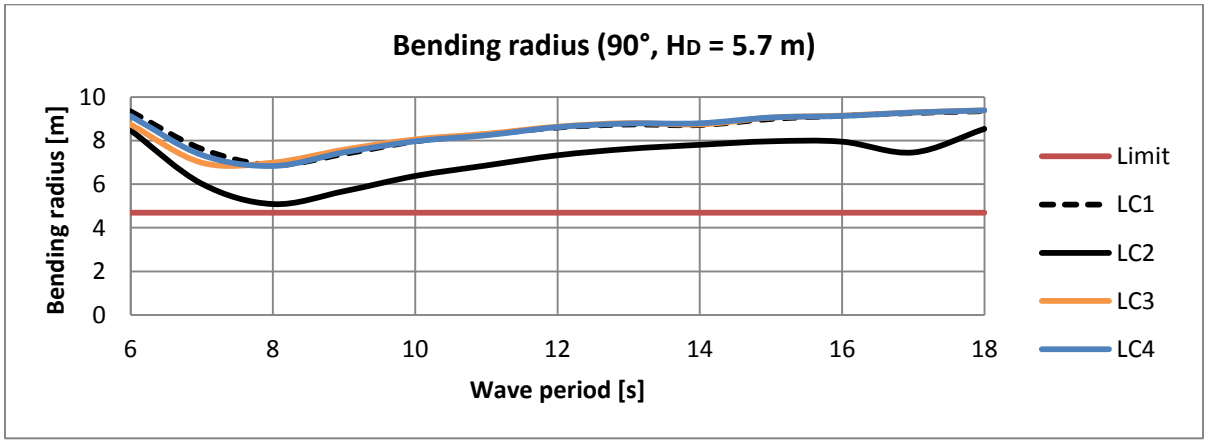

Figure F.0.17: : Bending radius for flexible flowline in sag bend for all Load Cases, wave direction 90° and H_D = 5.7 m, MBR shown as the red line

F.9 Results for landing of helicopters in daylight for Load Case 3 and 4

Table F.0.1: Approved (green cells) and non-approved (red cells) wave periods for landing of helicopter for LC3 with H_D = 5.7 m, based on HCA's requirements

LC3, H_D = 5.7 m			
T | Wave direction -->	0°	45°	90°
6			
7			
8			
9			
10			
11			
12			
13			
14			
15			
16			
17			
18			

Table F.0.2: Approved (green cells) and non-approved (red cells) wave periods for landing of helicopter for LC4 with H_D = 5.7 m, based on HCA's requirements

LC4, H_D = 5.7 m			
T | Wave direction -->	0°	45°	90°
6			
7			
8			
9			
10			
11			
12			
13			
14			
15			
16			
17			
18			

F.10 Comparison of heave rate of the helideck

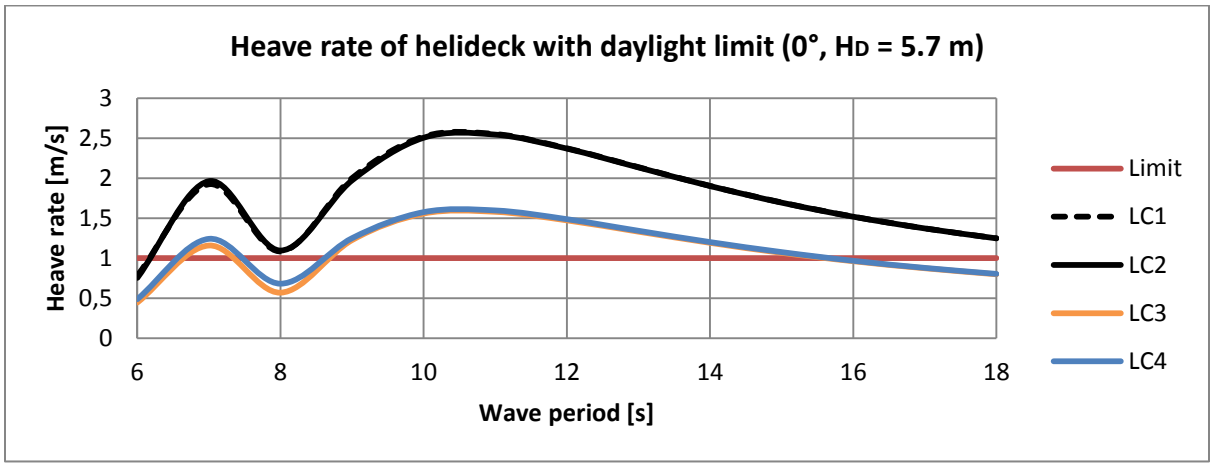

Figure F.0.18: Heave rate of helideck with the daylight limit, all Load Cases, wave direction 0° and H_D = 5.7 m

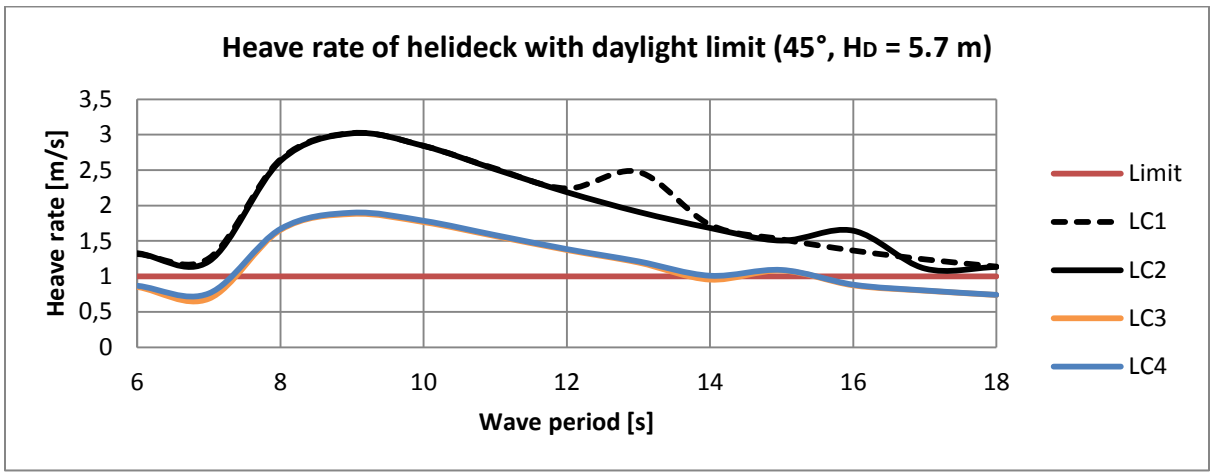

Figure F.0.19: Heave rate of helideck with the daylight limit, all Load Cases, wave direction 45° and H_D = 5.7 m

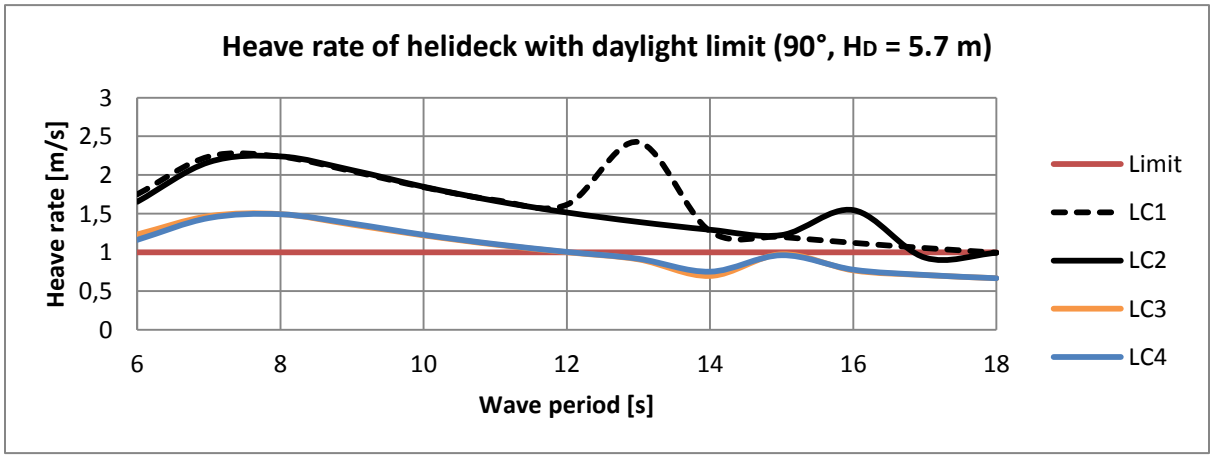

Figure F.0.20: Heave rate of helideck with the daylight limit, all Load Cases, wave direction 90° and H_D = 5.7 m

Appendix G: Relevant metocean data

The Figures G.0.1 – G.0.3 show expected duration of operations limited by significant wave heights of 2, 3 and 4 meters for 24 hours. The figures show the expected mean duration and 10, 50 and 90 percentiles*.
The figures show duration expected for completing a critical operation including waiting time. Duration is measured from the day the operation is ready to start and the start day is assumed to be a random day within the actual month (Mathiesen & Kvingedal, 2010).

*A 90 percentile means that 90 percent of the data are below and 10 percent are above it.

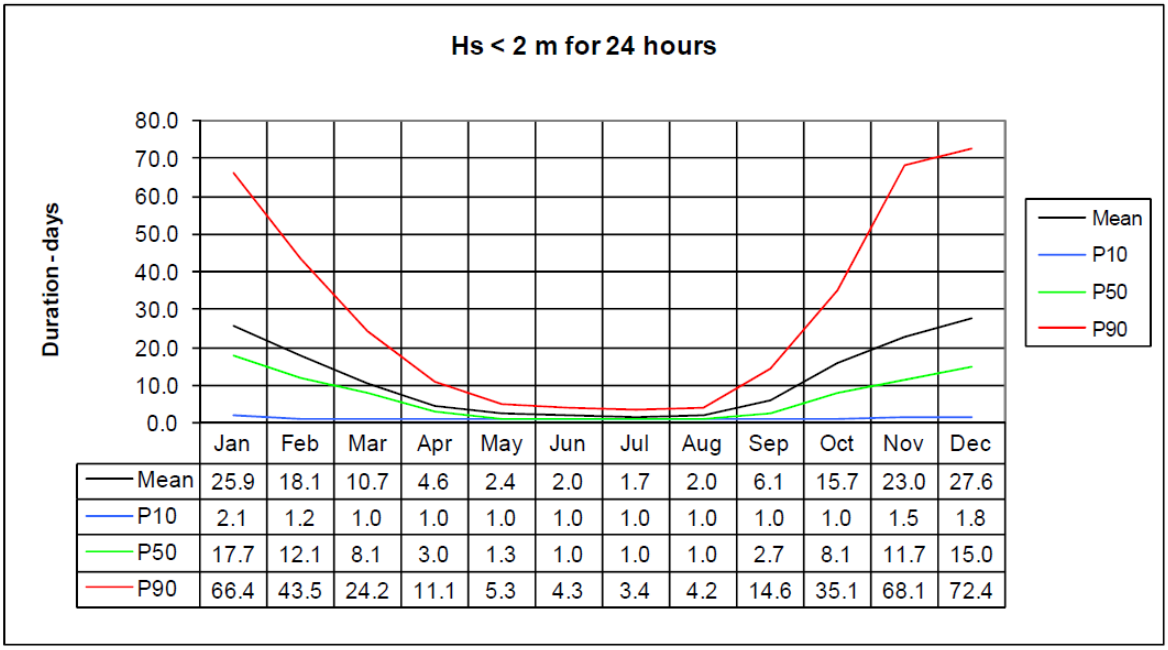

	Jan	Feb	Mar	Apr	May	Jun	Jul	Aug	Sep	Oct	Nov	Dec
Mean	25.9	18.1	10.7	4.6	2.4	2.0	1.7	2.0	6.1	15.7	23.0	27.6
P10	2.1	1.2	1.0	1.0	1.0	1.0	1.0	1.0	1.0	1.0	1.5	1.8
P50	17.7	12.1	8.1	3.0	1.3	1.0	1.0	1.0	2.7	8.1	11.7	15.0
P90	66.4	43.5	24.2	11.1	5.3	4.3	3.4	4.2	14.6	35.1	68.1	72.4

Figure G.0.1: Expected duration, including waiting time, in order to perform operations limited by a significant wave height of 2.0 m for 24 hours (Mathiesen & Kvingedal, 2010)

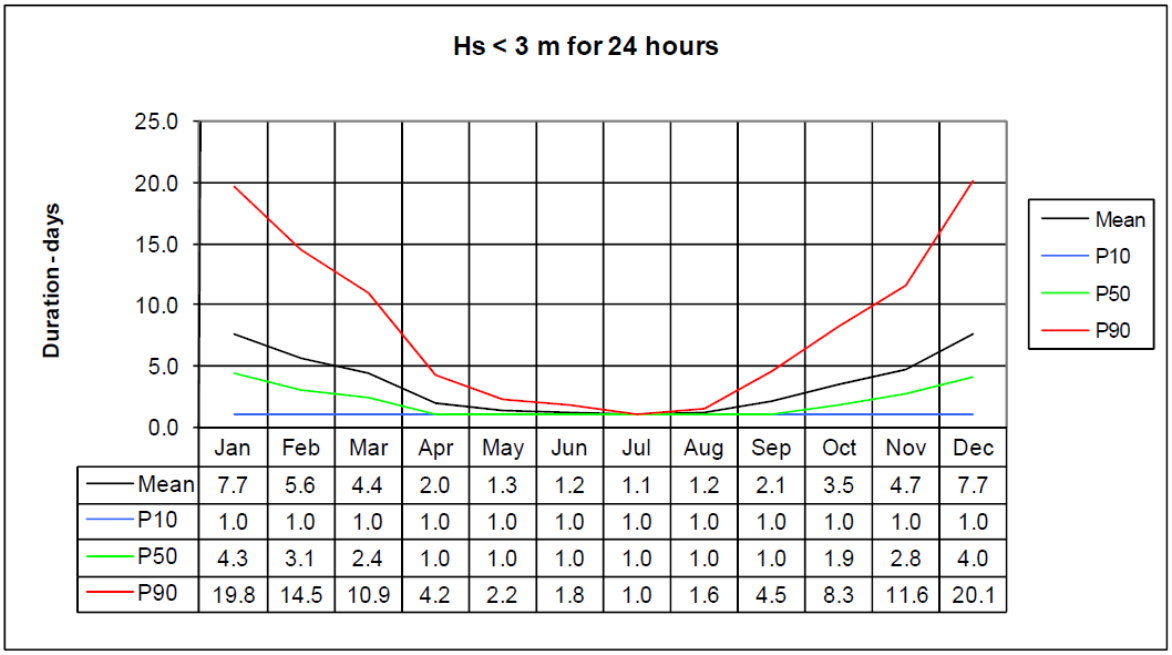

	Jan	Feb	Mar	Apr	May	Jun	Jul	Aug	Sep	Oct	Nov	Dec
Mean	7.7	5.6	4.4	2.0	1.3	1.2	1.1	1.2	2.1	3.5	4.7	7.7
P10	1.0	1.0	1.0	1.0	1.0	1.0	1.0	1.0	1.0	1.0	1.0	1.0
P50	4.3	3.1	2.4	1.0	1.0	1.0	1.0	1.0	1.0	1.9	2.8	4.0
P90	19.8	14.5	10.9	4.2	2.2	1.8	1.0	1.6	4.5	8.3	11.6	20.1

Figure G.0.2: Expected duration, including waiting time, in order to perform operations limited by a significant wave height of 3.0 m for 24 hours (Mathiesen & Kvingedal, 2010)

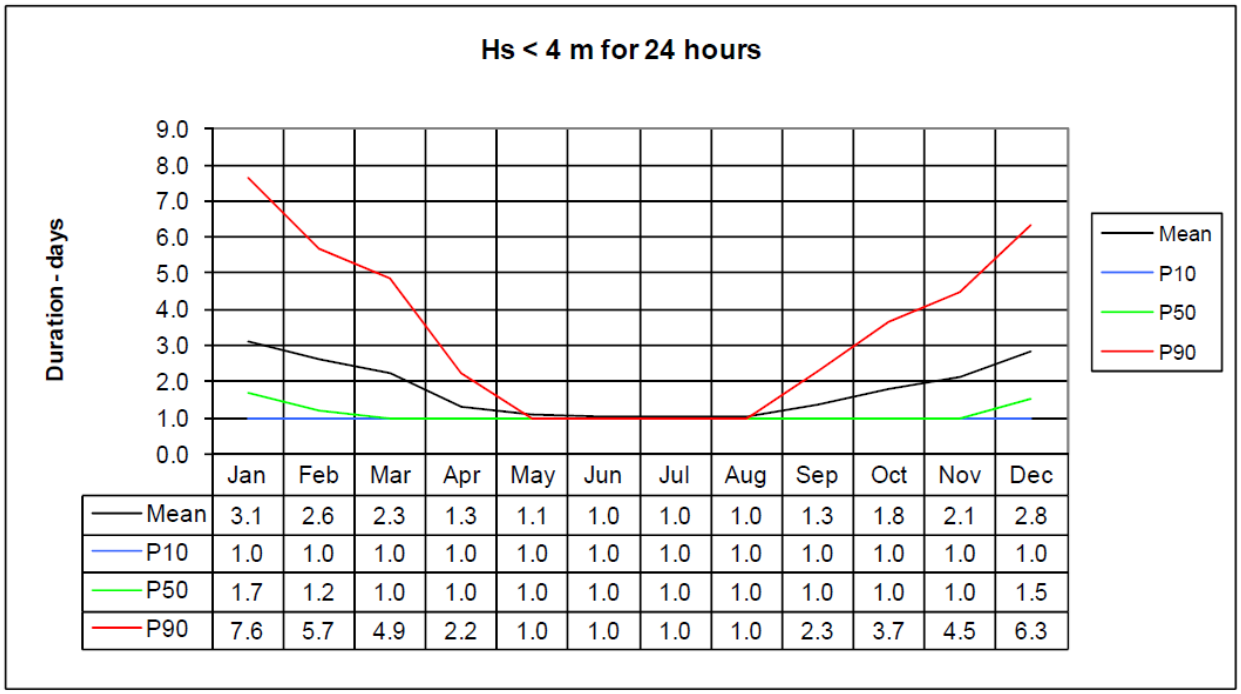

	Jan	Feb	Mar	Apr	May	Jun	Jul	Aug	Sep	Oct	Nov	Dec
Mean	3.1	2.6	2.3	1.3	1.1	1.0	1.0	1.0	1.3	1.8	2.1	2.8
P10	1.0	1.0	1.0	1.0	1.0	1.0	1.0	1.0	1.0	1.0	1.0	1.0
P50	1.7	1.2	1.0	1.0	1.0	1.0	1.0	1.0	1.0	1.0	1.0	1.5
P90	7.6	5.7	4.9	2.2	1.0	1.0	1.0	1.0	2.3	3.7	4.5	6.3

Figure G.0.3: Expected duration, including waiting time, in order to perform operations limited by a significant wave height of 4.0 m for 24 hours (Mathiesen & Kvingedal, 2010)

The scatter diagram (Table G.0.1) is based on measurements by the Norwegian Meteorological Institute. The measurements are from the period 1958 to 2008 and a hindcast model (Wam10) is used to construct the missing data (Mathiesen & Kvingedal, 2010). From the scatter diagram to "distribution diagrams" have been made (ref. Figs. G.0.4 and G.0.5).

Table G.0.1: Expected scatter diagram of significant wave height (H_S) and peak period (T_P) for a period of 100 years at the Snorre field, duration of sea state is 3 hours (Mathiesen & Kvingedal, 2010)

	Spectral peak period (T_p) - (s)																			
H_S (m)	0-3	3-4	4-5	5-6	6-7	7-8	8-9	9-10	10-11	11-12	12-13	13-14	14-15	15-16	16-17	17-18	18-19	19-20	> 20	Sum
0-1	15	289	1350	2836	3669	3493	2718	1847	1143	662	367	197	103	53	27	14	7	4	4	**18798**
1-2	2	139	1599	6403	13260	17844	17941	14730	10472	6709	3983	2235	1204	629	321	161	80	40	38	**97789**
2-3		7	221	1777	6080	11781	15424	15299	12413	8686	5443	3138	1698	876	435	210	99	46	39	**83673**
3-4			12	212	1316	3933	7066	8802	8382	6533	4374	2608	1422	723	348	161	72	31	23	**46015**
4-5				14	177	895	2372	3928	4587	4116	3019	1895	1053	531	248	109	46	19	12	**23022**
5-6				1	16	149	635	1499	2271	2452	2039	1383	798	406	186	79	31	12	6	**11961**
6-7					1	15	117	429	900	1234	1215	922	568	297	136	56	21	7	3	**5922**
7-8						1	14	86	270	501	615	544	370	204	95	38	14	5	2	**2759**
8-9							1	12	59	159	257	278	218	132	64	26	9	3	1	**1218**
9-10								1	9	38	86	120	113	78	41	17	6	2	1	**512**
10-11									1	7	22	42	51	41	25	11	4	1		**206**
11-12										1	4	12	19	19	13	7	3	1		**79**
12-13											1	3	6	8	6	4	2	1		**29**
13-14													1	2	3	2	1			**10**
14-15														1	1	1	1			**4**
15-16																1				**1**
Sum	**17**	**434**	**3182**	**11244**	**24518**	**38111**	**46289**	**46632**	**40507**	**31097**	**21425**	**13377**	**7625**	**3999**	**1950**	**897**	**396**	**171**	**130**	**292000**

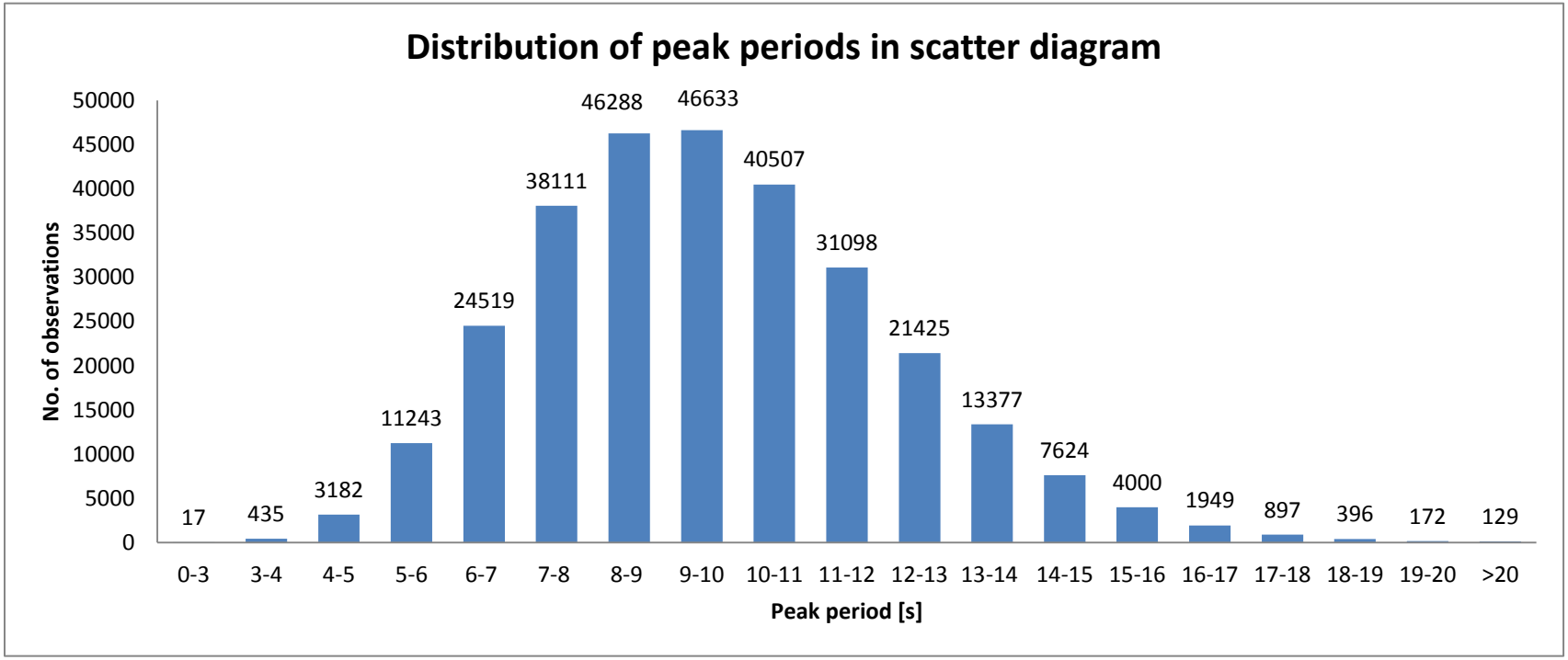

Figure G.0.4: Distribution of the peak periods in scatter diagram presented in Table G.0.1

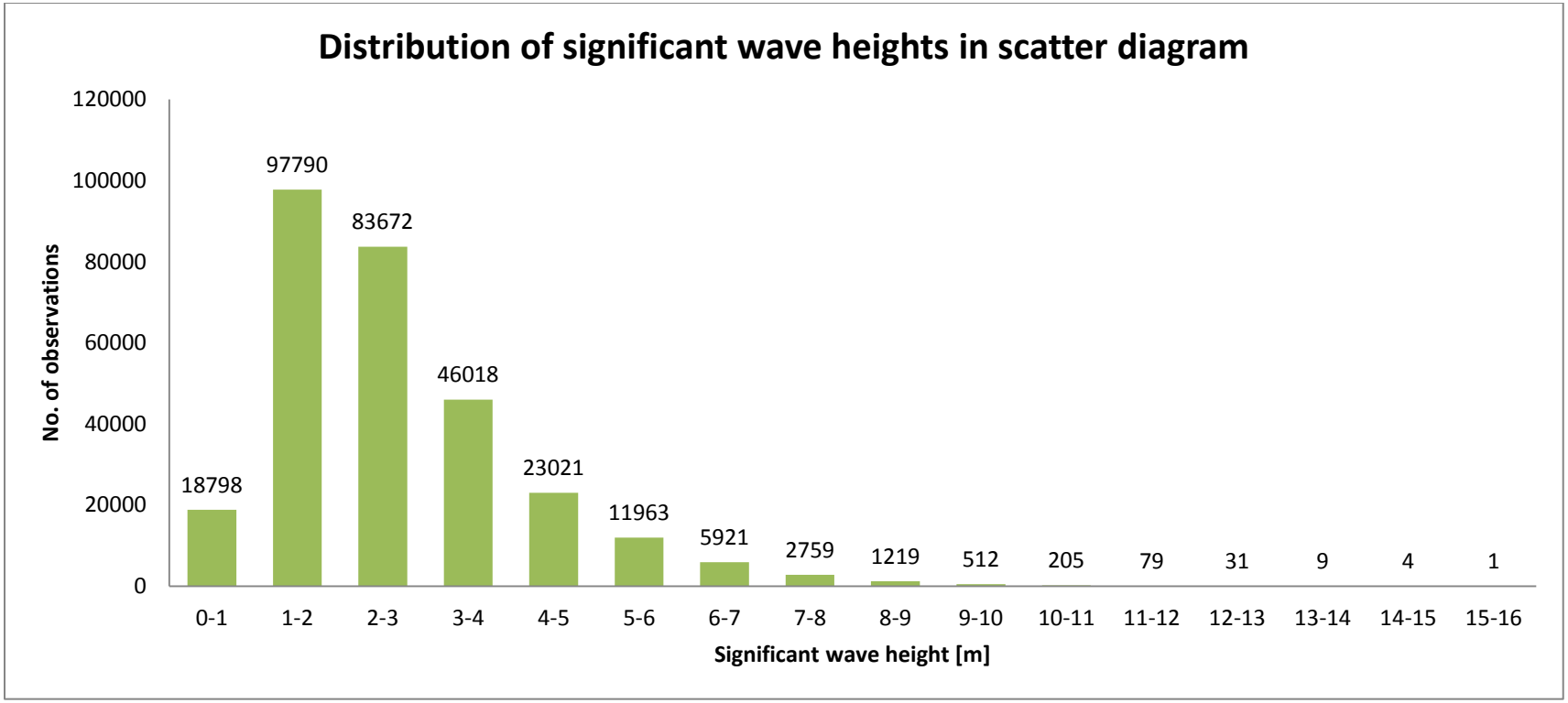

Figure G.0.5: Distribution of the significant wave heights in scatter diagram presented in Table G.0.1

Appendix H: Estimation of water plane area and added mass

The **water plane area** can be estimated from the following simplification as shown in Figure H.0.1.

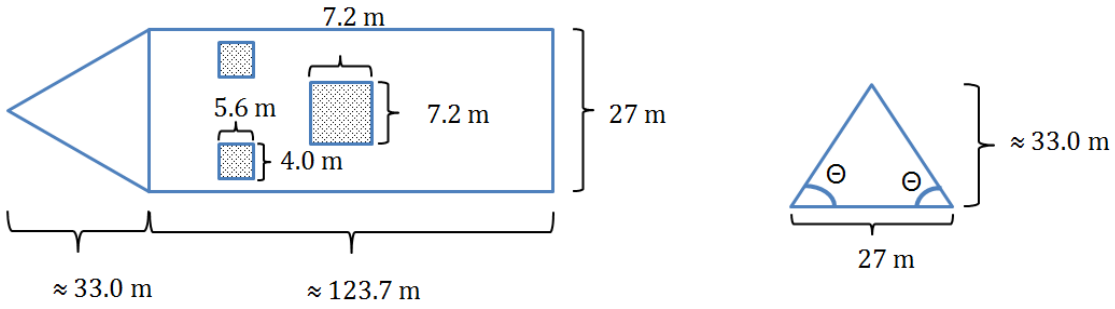

Figure H.0.1: Simplified model of hull in water line for Normand Vision, b = 123.7 m and a = 27 m, θ= 67.8°

The calculation of the estimated water plane area (A) is shown in equation 73.

$$A \approx 27 \cdot (156.7 - 33)m^2 + \frac{27 \cdot 33}{2} m^2 - (7.2)^2\ m^2 - 2 \cdot (5.6 \cdot 4)^2\ m^2 \approx 2755\ m^2 \quad \text{(Eq. 73)}$$

Need also to find the **added mass** for the vessel. According to DNV RP-H103 it may be feasible to use the geometries for flat rectangular and triangular plates from Appendix A in DNV RP-H103 (DNV, 2011). The added mass found should be divided by two according to point 4.6.3.2 in RP-H103, because it is a surface piercing structure. Density used for seawater, ρ = 1025 kg/m^3.

For the triangular part:

$$\theta = tan^{-1}\left(\frac{33\ m}{13.5\ m}\right) \approx 67.8°$$

Giving an added mass coefficient for the triangular part (eq. 74),

$$C_{A\Delta} = \frac{1}{\pi} \cdot (\tan(67.8°))^{1.5} \approx 1.22 \quad \text{(Eq. 74)}$$

This gives an added mass m_{a1} for the triangular part (eq. 75),

$$m_{a1} = \rho C_A V_R = 1025 \frac{kg}{m^3} \cdot 1.22 \cdot \frac{27^3}{3} m^3 \approx 8.2 \cdot 10^6\ kg \quad \text{(Eq. 75)}$$

For the rectangular part:

- b = 123.7 m
- a = 27 m
- b/a ≈ 3.75

Must interpolate (linearly) to get the right added mass coefficient for the rectangular part (eq. 76),

$$C_{A\blacksquare} = 0.840 + (0.872 - 0.840) \cdot \frac{3.75 - 3.17}{4.00 - 3.17} \approx 0.86 \quad \text{(Eq. 76)}$$

Have then the added mass for the rectangular part of the hull (eq. 77),

$$m_{a2} = \rho C_A V_R = 1025 \frac{kg}{m^3} \cdot 0.86 \cdot \frac{\pi}{4} \cdot 27^2 \cdot 123.7\, m^3 \approx 62.4 \cdot 10^6\, kg \quad \text{(Eq. 77)}$$

Have to take into consideration the **added mass of the moonpools' water plugs,** but must first find the added mass (m_{a3} and m_{a4} for the work and ROV moonpools respectively) to subtract from m_{a2} (the rectangular part of the hull's added mass), to not include too much added mass (see eqs. 78 and 79).

Since the work moonpool is quadratic *b/a = 1.0* → C_A = 0.579

$$m_{a3} = \rho C_A V_R = 1025 \frac{kg}{m^3} \cdot 0.579 \cdot \frac{\pi}{4} \cdot 7.2^3\, m^3 \approx 174 \cdot 10^3\, kg \quad \text{(Eq. 78)}$$

Since the two ROV moonpools are not quadratic *b/a = 1.4*, must use linear interpolation → $C_A \approx 0.671$

$$m_{a4} = \rho C_A V_R = 1025 \frac{kg}{m^3} \cdot 0.671 \cdot \frac{\pi}{4} \cdot 5.6^2 \cdot 4\, m^3 \approx 67.8 \cdot 10^3\, kg \quad \text{(Eq. 79)}$$

The formula for the total mass of the water plug (mass of water plug itself plus its added mass) for the vertical movement in the moonpools is given in DNV-RP-H103 (DNV, 2011). Here $D_{draught}$ is the mean draught of the vessel (here the draught for Load Case 2 = 8.303 meters is used), A_{MP} is the cross-sectional area of the moonpool, and the κ–parameter is 0.46 (for rectangular shaped moonpool), see equations 80 (main moonpool) and 81 (ROV moonpool).

$$m_{a5} = \rho A \cdot \left(D_{draught} + \kappa\sqrt{A_{MP}}\right) = 1025 \frac{kg}{m^3} \cdot 7.2^2\, m^2 \left(8.303\, m + 0.46 \cdot \sqrt{7.2^2\, m^2}\right) \approx 617.2 \cdot 10^3\, kg \quad \text{(Eq. 80)}$$

$$m_{a6} = \rho A \cdot \left(D_{draught} + \kappa\sqrt{A_{MP}}\right) = 1025 \frac{kg}{m^3} \cdot 5.6 \cdot 4\, m^2 \left(8.303\, m + 0.46 \cdot \sqrt{5.6 \cdot 4\, m^2}\right) \approx 240.6 \cdot 10^3\, kg \quad \text{(Eq. 81)}$$

Have then the total estimated added mass for the vessel (eq. 82),

$$m_{a,total} = \frac{m_{a1}}{2} + \frac{m_{a2}}{2} - \frac{m_{a3} + 2 \cdot m_{a4}}{2} + m_{a5} + m_{a6} = \frac{8.2 \cdot 10^6 + 62.4 \cdot 10^6 - (174 \cdot 10^3 + 2 \cdot 67.8 \cdot 10^3) kg}{2} + 617.2 \cdot 10^3\, kg + 2 \cdot 240.6 \cdot 10^3\, kg \approx 36.24 \cdot 10^6\, kg \quad \text{(Eq. 82)}$$

Appendix I: Summary tables

Table I.0.1: Summary table with comments for Load Case 1, ref. Figs. in Appendix C

Load Case	H_D [m]	Flowline installation	Manual work on deck	Landing of helicopters
Load Case 1	**3.8**	Mostly unproblematic. Will see some peaks breaking the limits at about 13 seconds for the top tension and deflection angle in 45° and 90° headings. Compression and bending radius are OK.	OK for head seas. Too large roll motion from ≈ 11.5 seconds for 45° and 90° headings. For 90° heading also somewhat high values for heave and lateral acceleration at ≈ 6-8 seconds wave periods. Limited possibilities for manual work for 90° heading.	Night time: Red light. In daylight there is green light for 6, 8 and 17 – 18 seconds for 0° heading. Also green light for 6, 7 and 17 – 18 seconds for 45° heading. Red light for 90° heading.
	5.7	Top tension and deflection angle are OK for head seas. Not OK for 45° and 90° for periods >11 – 15 and 11 – 17 seconds respectively. Still some peaks breaking the top tension limit at about 13 seconds for the top tension and deflection angle in 45° heading. If experiencing beam seas it is not feasible to install the flowline. Compression and bending radius are OK.	OK for head seas. Too much roll from about 11 seconds for 45° heading. Not applicable for manual work with 90° wave heading. Too large heave and lateral acceleration as well as roll motion.	Night time: Red light. Very limited possibilities also at daytime. Green light only for 6 seconds wave period and 0° wave heading.
	7.6	Top tension OK for head seas. Deflection angle too large from about 12 seconds for head seas. Both deflection angle and top tension are too large for 45° heading. Only window is for < 9 seconds. Compression and bending radius are OK for 0° and 45° heading, not for 90°. So there are small possibilities to install flowline in 45° and 90° headings.	OK for head seas. Too much roll from about 11 seconds for 45° heading. Not recommended to do manual work with 90° wave heading. Too large heave and lateral acceleration as well as roll motion (overlapping periods).	Night time: Red light. Daytime: Red light.

Table I.0.2: Summary table with comments for Load Case 2, ref. Figs. in Appendix C

Load Case	H_D [m]	Flowline installation	Manual work on deck	Landing of helicopters
Load Case 2	**3.8**	Mostly unproblematic. No issues for 0° and 45° headings. The only issue is a bit too large top tension for beam seas at about 7-9 seconds wave periods. Compression and bending radius are OK.	Unproblematic for 0° heading. OK for 45 when wave period is < 15 seconds. Mostly OK for beam seas as well. However, too large roll motions occur from ≈ 14 seconds. Also the heave and lateral acceleration are a bit too large from about 6-8 seconds for 90° heading.	Night time: Red light. In daylight there is green light for 6 and 17 – 18 seconds for 0° heading. Also green light for 6 – 7 seconds for 45° heading. Green light also for 45° heading for periods ≥ 13 seconds. Red light for the remaining.
	5.7	Flowline installation is within the limitations for 0° and 45° headings. For beam seas (90°) it is more challenging, but there are an installation window between 11 and 15 seconds. The deflection angle grows too large for periods from 15 seconds. If experiencing beam seas it is not feasible to install the flowline. Compression and bending radius are OK.	Unproblematic for 0° heading. Mostly OK for 45° heading, but see a bit too large roll from about 14 seconds wave period. For 90° only a narrow window for manual work (12 – 13.5 sec.) as the limit is breached for both heave and lateral acceleration, in addition to roll.	Night time: Red light. Very limited possibilities also at daytime. Green light only for 6 seconds wave period and 0° wave heading.
	7.6	Top tension OK for head seas and 45° heading. Top tension is not OK for 90° heading (only small window for 12 – 15 seconds). Deflection angle OK for 6-12 seconds periods for head seas and 6-9 seconds for 45° heading, but is not OK for 90° heading. Compression OK. Bending radius is OK for 0° and 45° headings, not for 90°. So there are small possibilities to install flowline in 45° and 90° headings.	OK for head seas. Too much roll from about 13 seconds for 45° heading. Not recommended to do manual work with 90° wave heading. Too large heave and lateral acceleration as well as roll motion.	Night time: Red light. Daytime: Red light.